UNIVERSITY OF Southampton

University of Southampton Research Repository
ePrints Soton

Copyright © and Moral Rights for this thesis are retained by the author and/or other copyright owners. A copy can be downloaded for personal non-commercial research or study, without prior permission or charge. This thesis cannot be reproduced or quoted extensively from without first obtaining permission in writing from the copyright holder/s. The content must not be changed in any way or sold commercially in any format or medium without the formal permission of the copyright holders.

When referring to this work, full bibliographic details including the author, title, awarding institution and date of the thesis must be given e.g.

AUTHOR (year of submission) "Full thesis title", University of Southampton, name of the University School or Department, PhD Thesis, pagination

http://eprints.soton.ac.uk

UNIVERSITY OF SOUTHAMPTON

FACULTY OF PHYSICAL SCIENCES AND ENGINEERING

Department of Physics and Astronomy

F-Theory Model Building

by

Andrew K Meadowcroft

A thesis submitted in partial fulfillment for the

degree of Doctor of Philosophy

September 2016

UNIVERSITY OF SOUTHAMPTON

Abstract

FACULTY OF PHYSICAL SCIENCES AND ENGINEERING

PHYSICS

Doctor of Philosophy F-Theory Model Building

by Andrew K Meadowcroft

In this thesis we considered non-Abelian monodromy groups in F-theory, based on SU(5) GUTs, with models presented using the V_4, A_4, and D_4 monodromy actions. The role of these symmetries in generating the observed mixing patterns of neutrinos has been considered in the cases of A_4 and D_4 monodromy. An older model based on E_6 is also considered as a candidate model to explain the recent LHC diphoton excess. R-parity violating processes in F-theory have also been considered, and it has been shown that such effects should be considered generic in F-theory without an *ad hoc* R-parity. The strengths of such coupling are discussed in the context of local F-theory Yukawa computations.

Contents

List of Figures

List of Tables

Declaration of Authorship

I, Andrew Meadowcroft , declare that this thesis, entitled 'F-Theory Model Building' and the work presented in it are my own.

I confirm that

- This work was done wholly or mainly while in candidature for a research degree at this university.
- Where I have consulted the published work of others, this is always clearly attributed.
- Where I have quoted the work of others, the source is always given. With the exception of such quotations, this thesis is entirely my own work.
- I have acknowledged all main sources of help.
- Where the thesis is based on work done by myself jointly with others, I have made clear exactly what was done by others and what I have contributed myself.
- Work contained in this thesis has previously been published in references [1–4]. The work in [5] is currently being considered for publication.

Signed:

Date:

Acknowledgements

I would like to thank my long-suffering parents for putting up with my grumpiness, without whom I would quite literally be nothing! Thank you too to Nayra, who has ensured that I am a lot better travelled than when we first met on the roof, as well as all the hours spent giving me something to think about besides work. I hope we have many adventures yet to come.

I would also like to thank the many people who stepped onto the badminton court with me for countless hours of entertainment, especially the players of the Eagles men's second team for making our matches special – John your shots were almost as good as your shorts. I would also like to thank all the doppelkopf players for the many hours wasted together playing cards, with a special thanks to Tobi for teaching us the game – not to mention the many, many drinks we shared. A special thanks also to Marc, for proof reading parts of this thesis, putting up with me as a friend and housemate, badminton, cards, and more besides. Thanks also to my many other officemates for the interesting conversations and the afternoon coffee breaks.

I should like to offer a special thank you to George Leontaris for his many invaluable contributions to our work, as well as the many entertaining hours of meetings during our time working together and his hospitality in Ioannina. Thanks also to Miguel Crispim Romão and Athanasios Karozas for the many discussions and for their contributions to this research. Most importantly perhaps, I would like to thank my supervisor, Steve King. Without whose encouragement and supervision this work would not have been possible. I secretly like remaking plots.

Chapter 1

Introduction

1.1 Overview

The two pinnacles of modern fundamental physics are the Standard Model (SM) and General Relativity (GR), which between them provide stunningly accurate predictions of the dynamics of the universe. With the detection of gravitational waves [6], a major prediction of GR has finally been confirmed. Likewise, the detection of a particle consistent with the Higgs boson [7, 8] is the last predicted fundamental particle of the SM.

So far, these two theories have not been compromised by evidence, standing up to the scrutiny of experiment, notwithstanding the discovery of neutrino oscillations. One might then ask: why go beyond? What is left for theorists to try to explain that is not already adequately understood within these frameworks?

As far as the SM is concerned, there is a degree of arbitrariness about it as a model. For example, there are three generations of matter, with experiments indicating that there should not be a fourth, which are identical but for their masses. The SM makes no prediction for these masses, and the number of generations itself is seemingly arbitrary. All in all, the SM has nineteen free parameters, all of which are input by hand with no predictive mechanism provided. This is only made worse by the detection of neutrino oscillations, which indicate that neutrinos have mass, indicating that a further seven free parameters are required, bringing the total to twenty six.

The discovery that neutrinos have mass also opens up another avenue of thought regarding right-handed neutrinos. Specifically, neutrinos having mass indicates that there must be right-handed neutrinos, which could form both Dirac and Majorana mass terms. There is also the potentially connected issue that the masses of the neutrinos, while not known absolutely, must be much smaller than those of the other fermions we see. In particular, the top quark appears to be about thirteen orders of magnitude[1] heavier than the neutrino mass scale, which seems unnatural and bizarre.

The SM also suffers from a "hierarchy" problem, wherein the Higgs mass has quadratic divergences associated with loop-corrections. These divergences can be renormalised, however the bare mass of the Higgs boson must then be the same order as the cutoff in the loop momentum. If the scale of new physics is the Planck scale, this leads to a bare mass that is fifteen orders of magnitude greater than the physical mass! This is what is known as fine-tuning and is generally frowned upon since it is tantamount to tweaking the parameters to be "just right".

Setting this aside, there are some other more pressing issues to consider. Firstly, cosmological observations indicate that the baryonic matter of the universe, which is described by the SM, only comprises $\sim$5% of the universe. The vast majority of the energy of the universe is wrapped up in two sources: dark matter ($\sim$ 25%) and dark energy ($\sim$ 70%). Dark matter, which only seems to interact gravitationally, is indirectly observed by the behaviour of the rotations of galaxies, which cannot be accounted for by visible matter. Dark energy on the other hand seems to be some fundamental property of space itself, driving an acceleration of the expansion of the universe.

In terms of how to address the points raised here, there are numerous candidates. Supersymmetry, a proposed relation between fermions and bosons, could offer a solution to the hierarchy problem, while also potentially featuring dark matter candidates. Supersymmetry also appeals to theorists because it forms natural partnerships with both Grand Unified Theories (GUTs) and string theories.

[1] $m_{top} \sim 10,000,000,000,000 \times m_{\nu}$

GUTs [9] provide a strong aesthetic appeal, since they take the unification of the electroweak symmetry in the SM a step further, proposing that the entire SM gauge group could merely be the shards of some higher, broken symmetry. Such symmetries include SU(5) [9], SU(5)×U(1) [10], SO(10) [11], and E_6 [12], with each making different predictions. In the case of SU(5), the unification can explain why the charges of the SM particles are quantised, such that the proton and the electron have equal but opposite charges. GUT groups can also be realised in string theories, which provide a description of quantum gravity. One manifestation of string theory that has attracted much interest in recent years is F-theory, which will be the central topic of this thesis.

F-theory [13] is a twelve dimensional formulation of Type IIB string theory, featuring an elliptic fibration, which can lead to GUT groups being realised as subgroups of a maximum parent symmetry of E_8 [14]. A great deal of work has gone into the development of F-theory model building [15–21]. Development of global compactifications have been discussed in the literature [22–29], with attention also being given to calculation of Yukawa couplings based on overlap integrals at points of enhanced symmetry in the internal manifold [30–39]. There have also been other works [40–46] that consider Mordell-Weil U(1)s in F-theory, due to the elliptic fibration properties.

In lieu of global constructions, the so-called semi-local approach has offered a promising way to realise the popular GUT groups in an F-theory set-up [1–3, 14,47–56]. This has allowed consideration of baryon and lepton number violation [3, 26, 38, 56, 57], flavour/family symmetries [1–3, 50, 51, 58, 59], as well as the aforementioned GUT constructions.

This thesis will focus on SU(5) GUTs in F-theory, with a particular interest in how the discrete symmetries that may arise from the E_8 point in the geometry affect the particle physics of the theory. For the remainder of this first chapter, an overview of some concepts pertaining to the Standard Model and to extensions of it are presented. In chapter 2, a review of some concepts in semi-local F-theory is presented, along with the work published in [1], which discusses Klein

monodromy actions in F-theory, as well as a geometric form of R-parity. Chapter 3 presents a model from [2], which focuses on neutrino mixing effects arising from an SU(5) $\times$ A_4 type model in F-theory, where we find that it is possible to explain the large mixing and small masses of the neutrino sector. Chapter 5, based on [3], discusses the framework of an SU(5)$\times D_4$ construction, which, using the geometric parity, can produce novel results for baryon and lepton number violating processes. The model presented is free from proton decay, but exhibits neutron-antineutron oscillations, which would be an interesting experimental signature of the model. In chapter 6, we discuss an apparent excess in diphoton production, indicating a $\sim$ 750GeV scalar or pseudoscalar, seen at the Large Hadron Collider (LHC) experiments ATLAS and CMS. Presented in [4], it was shown that this excess would be consistent with bulk exotics shown to arise in E_6 embeddings of SU(5) GUTs, originally developed in [52–54]. Chapter 7 presents an analysis of R-parity violating couplings, based on [5]. Making use of techniques previously used to calculate Yukawa couplings, the strength of R-parity violating couplings are estimated, with regions of single R-parity violating couplings identified in the parameter space. The findings are then summarised and discussed in the concluding chapter.

1.2 The Standard Model

Of the four known fundamental forces of nature, three – the strong nuclear, weak nuclear, and electromagnetic interactions – are encapsulated in the Standard Model (SM) of particle physics. The model, centred on the gauge symmetry $SU(3)_c \times SU(2)_L \times U(1)_Y$, includes vector bosons to mediate each force, three copies of each of the quarks and leptons, and a scalar field – the Higgs field – to break the electroweak part of the model and give masses to the weak bosons.

The known fundamental particles are classified as either bosons or fermions, depending on whether they have integer or half integer spin, depending on their representation under the Lorentz group. The bosons are associated to the three forces in the SM, with eight gluons associated to the strong force, three massive

bosons for the weak force ($W^{\pm}$ & Z^0), and the photon of electromagnetism. These spin-1 particles arise naturally from enforcing local invariance of the symmetries of the SM.

The fermions are then subdivided into quarks and leptons, depending on whether or not they interact with the strong force. Each generation of quarks then has an $\mathrm{SU}(2)_L$ doublet made up of a left-handed, up-type quark and a left-handed, down-type quark, and right-handed, up- and down-type quarks. The lepton of each generation comprise an $\mathrm{SU}(2)_L$ doublet with a neutrino and a charged lepton, and a right-handed, charged lepton. Crucially, there are no right-handed neutrinos in the vanilla version of the SM, since a right-handed neutrino would be an absolute singlet of the SM. The only possible interaction would be through Yukawa couplings with the Higgs field, however neutrinos were thought to be massless particles until the measurement of neutrino oscillations, so the right-handed particle must be added.

The remainder of this section comprises discussion of some fundamental concepts associated with the SM, while the following sections within this chapter will be dedicated to concept that extend the SM – Beyond the Standard Model (BSM) physics – such as supersymmetry, unification, and string theory.

1.2.1 The Dirac Equation

The Dirac equation is a relativistic generalisation of the Schrödinger equation, which unlike the Klein-Gordon equation can accommodate the half integer spin of fermions such as the electron. Unlike the Schrödinger equation, the Dirac equation is a first order differential equation in both time and spatial coordinates:

$$(i\gamma^{\mu}\partial_{\mu} - m)\Psi_D = 0\,. \tag{1.1}$$

In the Dirac representation (or basis), the matrices γ^μ are related to the Pauli matrices as:

$$\gamma^0 = \begin{pmatrix} I & 0 \\ 0 & -I \end{pmatrix}, \ \gamma^i = \begin{pmatrix} 0 & \sigma^i \\ -\sigma^i & 0 \end{pmatrix}. \tag{1.2}$$

In this notation, Ψ_D has a four component structure, which means there are four solutions to the equation. These give rise to a description of particles and antiparticles, each with two different spin states available.

An alternative basis for the Dirac equation is the so-called Weyl (or chiral) basis, which differentiates the notations for left-handed and right-handed components of the Dirac equation - i.e. separating the components based on their spin properties. In such a basis, we write

$$\Psi_D = \begin{pmatrix} \xi_\alpha \\ \chi^{\dagger\dot{\alpha}} \end{pmatrix}, \tag{1.3}$$

where $\alpha, \dot{\alpha} = 1, 2$ and the ξ_α is left-handed spinor and $\chi^{\dagger\dot{\alpha}}$ is right-handed. Hermitian conjugation maps a left(right)-handed spinor to a right(left)-handed spinor. In this basis, γ^μ is instead written as

$$\gamma^0 = \begin{pmatrix} 0 & I \\ I & 0 \end{pmatrix}, \ \gamma^i = \begin{pmatrix} 0 & \sigma^i \\ -\sigma^i & 0 \end{pmatrix}. \tag{1.4}$$

We may introduce two projection operators to project out left- or right-handed components of the Dirac equation,

$$P_{L/R} = \frac{1}{2}(1 \mp \gamma_5) \tag{1.5}$$

$$\gamma^5 = -i\gamma^0\gamma^1\gamma^2\gamma^3 = \begin{pmatrix} -I & 0 \\ 0 & I \end{pmatrix}. \tag{1.6}$$

It is trivial to see that applying P_L to Ψ_D returns only the left-handed component ξ_α and likewise for the right-handed component and P_R.

Writing Equation (1.1) in terms of left-handed and right-handed Weyl spinors,

$$\mathcal{L}_D = i\xi^\dagger\overline{\sigma^\mu}\partial_\mu\xi + i\chi^\dagger\sigma^\mu\partial_\mu\chi - m(\xi\chi + \xi^\dagger\chi^\dagger), \tag{1.7}$$

where contracted spinor indices are dropped by convention. We have introduced $(\sigma^\mu)_{\alpha\dot{\alpha}} = (I, \sigma)_{\alpha\dot{\alpha}}$ and $(\overline{\sigma}^\mu)^{\dot{\alpha}\alpha} = (I, -\sigma)^{\dot{\alpha}\alpha}$. This new form of the Dirac equation shows that mass terms introduce a mixing between the left-handed and right-handed components, such that in the massless limit the equation decouples into left and right-handed currents.

1.2.2 Abelian Gauge Symmetries

The Dirac equation, as discussed in the previous section, can be derived using the Euler-Lagrange equation as applied to the Dirac Lagrangian density,

$$\mathcal{L} = \overline{\Psi}_D(i\gamma^\mu\partial_\mu - m)\Psi_D. \tag{1.8}$$

Equation (1.8) is invariant under a global $U(1)$ symmetry (a complex phase transformation):

$$\Psi \to \mathrm{e}^{-i\alpha}\Psi\,, \tag{1.9}$$

where α is a real number with no dependence on coordinates. However, this is clearly not the most general complex phase transformation, since we could easily extend the concept such that $\alpha \to \alpha(x)$ - a local phase. The Dirac Lagrangian is not invariant under such a local phase transformation without modification. In order to keep invariance, we must introduce the covariant derivative D_μ, so that we make the replacement:

$$\partial_\mu \to D_\mu = \partial_\mu + ieA_\mu. \tag{1.10}$$

The field A_μ is a vector field that transforms as:

$$A_\mu \to A_\mu - \frac{1}{e}\partial_\mu \alpha. \tag{1.11}$$

The introduction of this new field ensures the Lagrangian is invariant under the local phase transformation, while also accommodating the gauge kinetic and interacting terms containing the gauge field A_μ,

$$\mathcal{L} = \overline{\Psi}(i\gamma^\mu \partial_\mu - m)\Psi + e\overline{\Psi}\gamma^\mu A_\mu \Psi - \frac{1}{4}F^{\mu\nu}F_{\mu\nu}, \tag{1.12}$$

where the so-called field strength tensor, $F_{\mu\nu}$, is

$$F_{\mu\nu} = \partial_\mu A_\nu - \partial_\nu A_\mu \,. \tag{1.13}$$

If we take the new vector field A_μ to be a physical field, then we may interpret this new field as the photon that mediates the electromagnetic force. Thus, by enforcing a local symmetry, we have found a natural requirement for a so-called gauge field. It is also interesting to note that under the transformation properties of the gauge field, a mass term ($\sim m^2 A^\mu A_\mu$) would be forbidden since it would spoil the invariance of the Lagrangian.

1.2.3 Non-Abelian Gauge Symmetries

The group of local phase transformations considered in the previous section, identified with the electromagnetic force, is the Abelian group $U(1)$. Let us consider a case where we enforce a similar property set with non-Abelian transformations, corresponding to an SU(N) group. The Dirac Lagrangian for each of the N components of the wavefunction $\Psi = (\psi_1, \ldots, \psi_N)^T$, will be the same as the Lagrangian of Equation (1.8). A general SU(N) transformation,

$$\Psi \to e^{i\alpha_a T^a}\Psi \,, \tag{1.14}$$

is parameterized by a phase and an $N \times N$ matrix, T^a, which are the generators of the group, obeying the commutation relation

$$\left[T^a, T^b\right] = i f_{abc} T^c \,. \tag{1.15}$$

Provided we consider α to be a local phase, the free Lagrangian is not immediately invariant under this action. In order to preserve this symmetry, once again a covariant derivative must be introduced,

$$\partial_\mu \to D_\mu = \partial_\mu + i g T_a G^a_\mu. \tag{1.16}$$

Under the group action the vector field, G^a_μ, must transform as

$$G^a_\mu \to G^a_\mu - \frac{1}{g}\partial_\mu \alpha^a - f_{abc}\alpha^b G^c_\mu \,. \tag{1.17}$$

Note the extra factor dependent upon the structure constants of the SU(N) group, which arises from the need to balance the transformation of the interaction term, $g\overline{\Psi}\gamma_\mu T^a \Psi G^\mu_a$. The full Lagrangian of a non-Abelian gauge theory, including the gauge kinetic term is

$$\mathcal{L} = \overline{\Psi}(i\gamma^\mu \partial_\mu - m)\Psi - g\overline{\Psi}\gamma_\mu T^a \Psi G^\mu_a - \frac{1}{4} G^a_{\mu\nu} G^{\mu\nu}_a \,, \tag{1.18}$$

where the field strength tensor is similar to that of Equation (1.13), but with a factor arising due to the non-Abelian nature of the symmetry:

$$G^a_{\mu\nu} = \partial_\mu G^a_\nu - \partial_\nu G^a_\mu - g f_{abc} G^b_\mu G^c_\nu \,. \tag{1.19}$$

An interesting side effect of enforcing local invariance of this symmetry is that the gauge kinetic term necessarily has these extra, non-Abelian terms. These terms give new interaction properties to the field G^a_μ, causing it to couple to itself. Specifically there will be three-point and four-point interaction vertices. This type of symmetry can be used to describe the strong and weak nuclear forces.

1.2.4 Electroweak Symmetry Breaking

The Standard Model gauge group is invariant under $SU(3)_c \times SU(2)_L \times U(1)_Y$. However, the physical spectrum of particles does not correspond to such a symmetry, and the vector bosons of the weak force are massive. This is due to the presence of a scalar field, called the Higgs field, which breaks the $SU(2)_L \times U(1)_Y$ part of the symmetry group to $U(1)_{EM}$, giving masses to three vector bosons.

Let us consider a spin-0 (scalar) field that couples to the electroweak part of the Standard Model. Considering only the pure gauge electroweak terms , this would have a Lagrangian with two gauge kinetic parts (one each for $SU(2)_L$ and $U(1)_Y$), a potential for the new scalar field, and a scalar kinetic term:

$$\mathcal{L} = -\frac{1}{4} W^a_{\mu\nu} W_a^{\mu\nu} - \frac{1}{4} F^{\mu\nu} F_{\mu\nu} + (D_\mu \Phi)^\dagger D^\mu \Phi - V(\Phi), \tag{1.20}$$

where the field strength tensor $F_{\mu\nu}$ is defined as in Equation (1.13), and $W^a_{\mu\nu}$ as in Equation (1.19) - with suggestive notational change to use W. In order to comply with gauge invariance under both the Abelian $U(1)$ and non-Abelian SU(2) symmetries, the covariant derivative takes parts from both Equation (1.10) and Equation (1.16):

$$D_\mu = \partial_\mu + i\frac{g'}{2} B_\mu + i\frac{g}{2} \sigma_a W^a_\mu. \tag{1.21}$$

The scalar potential is taken to be of the form

$$V(\Phi) = \mu^2 \Phi^\dagger \Phi + \lambda (\Phi^\dagger \Phi)^2 \,, \tag{1.22}$$

which will take different forms depending on the signs of μ^2 and λ. Let us take ϕ to be a general complex field,

$$\Phi(x) = \frac{1}{\sqrt{2}} \begin{pmatrix} \phi_1(x) + i\phi_2(x) \\ \phi_3(x) + i\phi_4(x) \end{pmatrix}, \tag{1.23}$$

then we can find the minimum of the scalar potential by taking its derivative and

setting it equal to zero,

$$\frac{-\mu^2}{\lambda} = \phi_1^2 + \phi_2^2 + \phi_3^2 + \phi_4^2. \tag{1.24}$$

If $\mu^2 < 0$ and $\lambda > 0$ this potential will have a set of minima that are together SU(2) invariant. This potential is often referred to as a "Mexican hat" potential and, if one sits at the centre of such a potential, one would see the rotational symmetry of it. If we select one of the vacua however, this symmetry will be broken - as if one were to sit at a point in the brim of the hat rather than at the point of rotational symmetry. A simple choice of vacuum alignment with $\phi_1 = \phi_2 = \phi_4 = 0$ and $\phi_3^2 = v^2 = \frac{-\mu}{\lambda}$ achieves this symmetry breaking. We can expand about this vacuum using a local field $h(x)$,

$$\Phi(x) = \frac{1}{\sqrt{2}} \begin{pmatrix} 0 \\ v + h(x) \end{pmatrix}, \tag{1.25}$$

which will give the scalar field $h(x)$ a mass, due to the potential part of the Lagrangian. However, this scalar field will also interact with the vector fields via the covariant derivative. Consider the four massless fields B_μ and W_μ^a and their interaction with ϕ, which gives rise to a term

$$\begin{aligned} \left| (i\frac{g'}{2} B_\mu + i\frac{g}{2}\sigma_a W_\mu^a)\Phi \right|^2 &= \frac{1}{8} \left| \begin{pmatrix} g'B_\mu + gW_\mu^3 & gW_\mu^1 - igW_\mu^2 \\ gW_\mu^1 + igW_\mu^2 & g'B_\mu - gW_\mu^3 \end{pmatrix} \begin{pmatrix} 0 \\ v \end{pmatrix} \right|^2 \\ &= \frac{g^2 v^2}{8}(W_\mu^1 W^{1\,\mu} + W_\mu^2 W^{2\,\mu}) + \frac{v^2}{8}(g'B_\mu - gW_\mu^3)(g'B^\mu - gW^{3\,\mu}). \end{aligned} \tag{1.26}$$

The first part of this term shows that there should be two vector fields with identical masses. Making a redefinition $\sqrt{2}W^\pm = (W^1 \mp iW^2)$ and knowing that such a mass term is of the form $\frac{1}{2}M^2 W^+ W^-$, these bosons have masses

$$M_W = \frac{gv}{2}\,. \tag{1.27}$$

The remaining part can be seen as the mixing of the two fields B_μ and W_μ^3 in an

off-diagonal basis. However, examination of the mass mixing matrix reveals that one eigenvalue is zero, so that we may define two new fields in the diagonal basis:

$$A_\mu = \frac{g' W_\mu^3 + g B_\mu}{\sqrt{g'^2 + g^2}} \tag{1.28}$$

$$Z_\mu = \frac{g W_\mu^3 - g' B_\mu}{\sqrt{g'^2 + g^2}} \tag{1.29}$$

The new field A_μ will be massless, corresponding to the photon, while the Z_μ field will be a neutral, massive boson mediating neutral current processes of the weak force. The mass of this neutral vector boson will be different to the mass of the $W^\pm$ bosons due to the mixing between B_μ and W_μ^3. Its mass will arise from a term like $\frac{1}{2} M_Z^2 Z^\mu Z_\mu$, which means the mass is

$$M_Z = \frac{v}{2}\sqrt{g'^2 + g^2}. \tag{1.30}$$

The ratio of the masses M_Z and M_W or the ratio of g and g' can be equivalently related to some mixing angle θ_W to parameterise the inequality of the two masses (couplings):

$$\frac{M_W}{M_Z} = \cos\theta_W \ \ , \ \ \frac{g'}{g} = \tan\theta_W \, . \tag{1.31}$$

1.2.5 Yukawa Couplings

The Higgs field responsible for electroweak symmetry breaking is not confined to coupling to the gauge fields of the electroweak sector. It also couples to fermionic fields, which in the electroweak part of the Standard Model are comprised of left-handed doublets of $\mathrm{SU}(2)_L$ and right-handed $\mathrm{SU}(2)_L$ singlets. A consequence of this is that the usual explicit mass term for the fermionic fields, $m\overline{\psi}\psi$, would violate $\mathrm{SU}(2)_L$ gauge invariance and so is not allowed. The couplings between the Higgs field and these fermionic fields are called Yukawa couplings, with the full Yukawa part of the Standard Model Lagrangian comprised of three pieces,

$$\mathcal{L}_Y = Y_u Q_L^\dagger \Phi^c u_R + Y_d Q_L^\dagger \Phi d_R + Y_e L^\dagger \Phi e_R + \text{hermitian conjugate}, \tag{1.32}$$

where the left-handed $\mathrm{SU}(2)_L$ doublets Q_L and L refer to the quark doublet and lepton doublet and Φ^c is a new field related to the original Higgs field,

$$Q_L = \begin{pmatrix} u_L \\ d_L \end{pmatrix}, \quad L = \begin{pmatrix} \nu_L \\ e_L \end{pmatrix}, \quad \Phi^c = i\sigma^2\Phi^* \tag{1.33}$$

and the u_R, d_R, and e_R fields are the right-handed up-type quark, down-type quark, and charged lepton respectively. The $Y_{u,d,e}$ are 3×3 matrices, due to the three generations described by the Standard Model, and as such there will in general be mixing between generations.

With the choice of vacuum alignment in Equation (1.25), each of the terms in the Yukawa sector generates a mass,

$$y_u^{ij}(Q_L^\dagger \Phi^c u_R)^\dagger = \frac{y_u^{ij}}{\sqrt{2}} u_R^j \begin{pmatrix} v + h(x) & 0 \end{pmatrix} \begin{pmatrix} u_L^i \\ d_L^i \end{pmatrix} = \frac{y_u^{ij} v}{\sqrt{2}} u_L^i u_R^j + \frac{y_u^{ij}}{\sqrt{2}} h u_L^i u_R^j \tag{1.34}$$

which is identified as $m_u^{ij} = \frac{y_u^{ij} v}{\sqrt{2}}$. There is also a coupling between the Higgs field and the left- and right-handed quark fields, which can be measured in collider experiments. However, since $y_u^{ij} = \sqrt{2} m_u^{ij}/v$, for lighter generations this will be a small coupling and hence hard to measure. On the other hand, due to its large mass, the top quark couples strongly to the Higgs.

1.2.6 Neutrinos

In the "vanilla" Standard Model, neutrinos are massless, since there are no right-handed neutrinos, which would be absolute singlets of the Standard Model. However, neutrino oscillation measurements have revealed that at least two of the three generations of neutrino must have a mass. The absolute value of this mass is not known, with the lightest neutrino still possibly massless, but the total mass of the neutrino sector is known to be very small – $m_\nu \sim 10^{-6} m_e$. The ordering of the neutrino mass hierarchy is also unknown, since the mass squared differences are the measured quantity, meaning that while we may know the difference between the masses of each generation of neutrino, we do not know in which order

they are arranged.

The mechanism of this mass generation is also unknown, since neutrinos can be Majorana, allowing for two possible mass terms,

$$\mathcal{L}_\nu = m_D \overline{\nu_L} \nu_R + M_R \overline{\nu_R^c} \nu_R + \text{hermitian conjugate}, \tag{1.35}$$

with m_D and M_R both matrices. It is important to appreciate that a term of the form $M_L \overline{\nu_L} \nu_L^c$ must be zero in the standard model, since the presence of such a term would interfere with electroweak processes – ν_L interacts with the $W^\pm$ and Z^0 bosons, while ν_R does not.

Though it is not known whether or not neutrinos are Majorana in nature, the possibility leads to an explanation for their comparatively small masses via the so-called *seesaw* mechanism. In this mechanism, the right-handed neutrino is taken to have a large Majorana mass, while the Dirac mass is comparable to the charged lepton sector. Inserting the Higgs vacuum choice, Equation (1.25), to give a dimensionful Dirac mass, Equation (1.35) can be expressed by a mixing matrix between Dirac masses and Majorana masses:

$$\begin{pmatrix} \overline{\nu_L} & \overline{\nu_R^c} \end{pmatrix} \begin{pmatrix} 0 & m_D \\ m_D^T & M \end{pmatrix} \begin{pmatrix} \nu_L^c \\ \nu_R \end{pmatrix} + \text{h.c.}, \tag{1.36}$$

which has two eigenvalues. In the limit where $M \gg m_D$, these two eigenvalues of mass are approximately M and m_D^2/M, the latter of which would correspond to the light effective mass of the neutrinos. For a good review of neutrino mass generation see [60].

1.2.7 Anomalies

An important property that must be considered regarding the SM is that of gauge anomalies, or rather their cancellation. While a current may be conserved at tree-level, when one includes loops corrections due to quantum effects, it is possible that that current may no longer be conserved - this is what we mean by

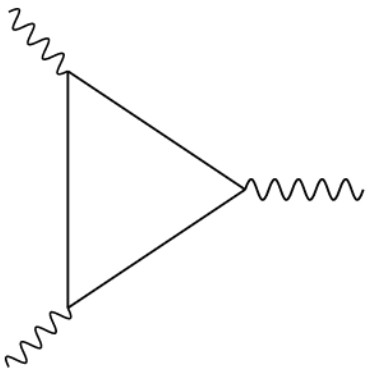

Figure 1.1: Gauge anomalous diagrams arise at vertices of the type shown here, where external vector fields are coupled by fermion loops. Here, each external leg may be any gauge boson of the theory, while the internal propagators are due to all fermionic fields to which those bosons couple. A consistent gauge symmetry must have a total of zero anomalous contributions, which is true of the standard model.

an anomaly.[2]

Because the electroweak sector of the SM couples differently for left-handed and right-handed fields, it is possible that an anomaly could occur for the model. In order to check this, one must consider the one-loop triangle diagrams for three boson vertices of the type shown in Figure 1.1, with each external boson one of the three SM gauge fields. There is also a gravitational anomaly associated with two gravitons and a photon.

Each diagram has a contribution proportional to the trace of the generators (t^a) over the fermionic fields allowed in the triangle shown in Figure 1.1,

$$\mathcal{A}^{abc} \propto \mathrm{Tr}(\gamma^5 t^a \{t^b, t^c\}). \tag{1.37}$$

Some triangle diagrams can immediately be eliminated, since they are left-right symmetric, for example a three-gluon diagram or any diagram involving only a single gluon. It transpires that if one considers all the possible diagrams, each in turn can be shown to vanish. As such, the anomalies of the SM all cancel

[2] A famous example of this is the Adler-Bell-Jackiw anomaly [61,62], also known as the chiral anomaly, which is a non-gauge anomaly. We shall not discuss this in this thesis.

perfectly, which insures that the currents associated with the gauge fields are conserved at the quantum level of the theory.[3]

There is, however, a caveat of this perfect cancellation, which is that it requires that quarks and leptons necessarily come in complete families. Put another way, this implies that the number of each type of fermionic field is the same in the SM:

$$n(e_L) = n(\nu_L) = n(e_R) = n(u_L) = n(d_L) = n(u_R) = n(d_R). \tag{1.38}$$

This in itself is an interesting result for the SM, since it essentially requires some relationship between the numbers of quarks and leptons in the theory in order to remove anomalous effects.

1.3 Supersymmetry

The SM is invariant under the Poincaré symmetry group, a generalization of Lorentz symmetry, which ensures compatibility with special relativity. This group covers transformations of the form

$$x^\mu \to \Lambda^\mu_\nu x^\nu + a^\mu, \tag{1.39}$$

which leave the line element invariant ($g_{\mu\nu}x^\mu x^\nu$), with the transformation Λ leaving the Minkowski metric invariant: $\Lambda^\mu_\sigma \eta_{\mu\nu}\Lambda^\nu_\tau = \eta_{\sigma\tau}$. The generators of this group are those of the space-time translations, P_μ, and those of Lorentz boosts and rotations, $M_{\mu\nu}$, which have the commutation relations

$$[M_{\mu\nu}, M_{\tau\sigma}] = i(\eta_{\eta\tau}M_{\nu\sigma} + \eta_{\nu\sigma}M_{\mu\tau} - \eta_{\nu\tau}M_{\mu\sigma} - \eta_{\mu\sigma}M_{\nu\tau}), \tag{1.40}$$

$$[M_{\mu\nu}, P_\sigma] = i(\eta_{\nu\sigma}P_\mu - \eta_{\mu\sigma}P_\nu), \tag{1.41}$$

$$[P_\mu, P_\nu] = 0. \tag{1.42}$$

[3]Put another way this is a statement that unitarity is not violated by the quantum theory.

One may also define the Pauli-Ljubanski vector,

$$W_\mu = \frac{1}{2}\epsilon_{\mu\nu\sigma\tau}P^\nu M^{\sigma\tau}, \tag{1.43}$$

which commutes with both P_μ and $M_{\mu\nu}$. The Casimirs[4] of the Poincaré can then be identified as P^2 and W^2, which allows the classification of all physical states in terms of the eigenvalues of these two operators.

The Coleman-Mandula theorem [63] posits that, in short, there are no extensions to the Poincaré symmetry that are not trivial, internal symmetries. However, there is one known symmetry that can evade this no-go theorem: supersymmetry. Supersymmetry (SUSY) adds a set of fermionic generators to those of the Poincaré group, which are allowed by the Coleman-Mandula theorem since the generators are fermionic.

These new generators alter the spin of particles, turning a fermionic state into a bosonic state and visa versa, with the generators having half-integer spin. These new generators are written in terms of a left-handed Weyl spinor, $Q_{\alpha=1,2}$, and its hermitian conjugate, which add the extra relations

$$\begin{aligned}
&\{Q_\alpha, Q_\beta\} = \{\overline{Q}_{\dot{\alpha}}, \overline{Q}_{\dot{\beta}}\} = [Q_\alpha, P_\mu] = 0, \\
&\{Q_\alpha, \overline{Q}_{\dot{\beta}}\} = 2\sigma^\mu_{\alpha\dot{\beta}}P_\mu, \\
&[Q_\alpha, M_{\mu\nu}] = i(\sigma_{\mu\nu})^\beta_\alpha Q_\beta.
\end{aligned} \tag{1.44}$$

to the Poincaré algebra, to create a larger superalgebra.

There are some interesting and important properties immediately evident from the commutation relations of the combined operators of SUSY. Firstly, the new, spin-altering operators commute with the generators of any gauge symmetries, which implies that states that are acted upon by the new operators will have the same gauge quantum numbers as the original state. Also, since these new operators commute with P^2, the masses of states acted upon by the SUSY operators will be unchanged. As such, the so-called superpartners of any state

[4]Casimirs are operators that commute with all the generators of a group

in a supersymmetric theory should be identical to the original state barring the change in spin. The consequences of this are profound, since, assuming SUSY is unbroken, every particle would have a corresponding partner with spin differing by $\frac{1}{2}$. Clearly, this is not seen in nature, however, if SUSY is broken and provided it happens above the TeV scale, then SUSY may still have a role to play. The details of SUSY breaking shall not be discussed in this thesis.

It is natural to consider a framework wherein the particles and the corresponding superpartners are combined into supermultiplets. This framework can be subcategorised into two subclasses of supermultiplet: the chiral supermultiplet and the vector supermultiplet. Both cases are subject to the requirement that the number of bosonic degrees of freedom is equal to the fermionic degrees of freedom in a given supermultiplet.

The chiral supermultiplet[5] contains a spin-$\frac{1}{2}$ Weyl fermion, which has two degrees of freedom due to the possible chiralities. Consequently, there must be a complex scalar field (two bosonic degrees of freedom) corresponding to the superpartner of the Weyl fermion. Since the representations within this supermultiplet transform differently under gauge interactions for left-handed and right-handed components, this would contain the SM fermions and their superpartners, which are known as sfermions.

The vector supermultiplet contains a spin-1 vector boson field, which is massless and thus again has two degrees of freedom. A subtlety is that the superpartner must be a spin-$\frac{1}{2}$ Weyl fermion and not spin-$\frac{3}{2}$, in order to be renormalisable. The fermions in this supermultiplet cannot correspond to those of the SM however, as they are found in the adjoint representation, which is its own conjugate and so left- and right-handed fields do not transform differently. These new particles are known as gauginos.

It is necessary to note that the degrees of freedom discussed here referred to on-shell fields, which is only sufficient for the classical case. If one requires consideration of off-shell properties, then the matter becomes less straight-forward, since an off-shell fermionic field has four degrees of freedom, while a complex

[5]The chiral supermultiplet is sometimes referred to as the scalar or matter supermultiplet.

	ϕ	ψ	F
Spin	0	$\frac{1}{2}$	0
On-shell d.o.f.	2	2	0
Off-shell d.o.f.	2	4	2

(a) Chiral supermultiplet

	A_μ	λ_μ	D_μ
Spin	1	$\frac{1}{2}$	1
On-shell d.o.f.	2	2	0
Off-shell d.o.f.	3	4	1

(b) Vector supermultiplet

Table 1.1: The chiral and vector supermultiplets are generalisations of the standard model fields to group together fields with the same quantum numbers but with different spin. Each supermultiplet also includes an auxiliary field to account for degrees of freedom when considering off-shell physics.

scalar field still has only two. As such, in the case of the chiral supermultiplet, one must introduce an auxiliary scalar field, usually denoted F, that has two degrees of freedom off-shell, but none on-shell. Similarly in the case of the vector supermultiplet, the bosonic field has only three degrees of freedom off-shell, so a bosonic auxiliary field must be added that has the remaining degree of freedom in the off-shell case - which is usually labeled D. The supermultiplet contents are summarised in Table 1.1. The auxiliary fields must feature in any supersymmetric Lagrangian, however they will not have kinetic terms and are not physical fields, but merely keeping track of the degrees of freedom correctly.

1.3.1 The Hierarchy problem

While not one of the original motivations of SUSY, it is often touted by advocates of the theory that SUSY can solve the gauge hierarchy problem. This references a perceived fine-tuning issue of the SM, wherein the Higgs mass term is quadratically divergent, so that the correction due to fermion loops (in particular the top quark loop) is sensitive to the cutoff in the momentum loop integral,

$$\Delta\mu^2 \sim \lambda_{top}\Lambda^2. \tag{1.45}$$

While the correction is renormalisable, the bare mass of the Higgs boson must be of the same order as the cutoff, which may be at a high scale. For example, if $\lambda \sim 10^{16}$GeV (the GUT scale, which will be discussed in the next section), then in order to have a Higgs mass at the 125GeV observed value, one would

required cancellations down twenty eight orders of magnitude - a spectacular case of fine-tuning!

In order to avoid this problem, one might set the cutoff to be at a lower scale, which then anticipates some new physics arising at that cutoff. However, SUSY offers a novel solution to the problem by means of symmetry arguments to protect the Higgs mass from quadratic divergences.

Introducing scalar partners of the SM fermions, with the same masses and gauge representations, gives new couplings to the Higgs field (ϕ),

$$\mathcal{L} = -\lambda_f \overline{f} f \phi - \lambda_s |S|^2 |\phi|^2, \tag{1.46}$$

where $\lambda_{f,s}$ are dimensionless couplings and f and S are fermioninc and scalar fields respectively. If one calculates the contributions of these couplings to the one loop correction of the Higgs mass squared, one finds that the contributions are of opposite sign. In fact, provided $\lambda_s = |\lambda_f|^2$, this cancellation would be exact, removing the quadratic divergences at all order in perturbation theory. Such a relation in couplings is required in SUSY.

While this seems to be a great improvement, it is worth considering that the new leading order correction to the Higgs mass squared is proportional to the mass of the scalar particle, and as such the mass of the superpartner cannot be much higher than the TeV scale without creating a replica hierarchy problem.

1.3.2 The Minimal Supersymmetric Standard Model

Extending the SM to include supersymmetry essentially requires extending every field to be a supermultiplet. For example, the left-handed quark doublet of the SM, $Q = (u_L\, d_L)$, must be extended to also include $(\tilde{u}_L\, \tilde{d}_L)$ in the new chiral supermultiplet. This is essentially a straightforward notational extension, which is succinctly summarised in Table 1.2. We use the notation of [64], where $\overline{u}$ (and also $\overline{d}$ or $\overline{e}$) refers to a supermultiplet containing the left-handed Weyl spinors $\tilde{u}_R^*$ and $u_R^\dagger$, rather than conjugation. This allows us to write the so-called Minimal Supersymmetric Standard Model (MSSM) in a compact form.

	spin-0	spin-$\frac{1}{2}$	Gauge rep.
$\hat{Q}$	$(\tilde{u}_L\, \tilde{d}_L)$	$(u_L\, d_L)$	$(3,2)_{1/6}$
$\hat{u}$	$\tilde{u}_R^*$	$u_R^\dagger$	$(\overline{3},1)_{-2/3}$
$\hat{d}$	$\tilde{d}_R^*$	$d_R^\dagger$	$(\overline{3},1)_{1/3}$
$\hat{L}$	$(\tilde{\nu}_L\, \tilde{e}_L)$	$(\nu_L\, e_L)$	$(1,2)_{-1/2}$
$\hat{e}$	$\tilde{e}_R^*$	$e_R^\dagger$	$(1,1)_1$
$\hat{H}_u$	$(H_u^+\, H_u^0)$	$(\tilde{H}_u^+\, \tilde{H}_u^0)$	$(1,2)_{1/2}$
$\hat{H}_d$	$(H_d^0\, H_d^-)$	$(\tilde{H}_d^0\, \tilde{H}_d^-)$	$(1,2)_{-1/2}$

(a) Chiral supermultiplets of the MSSM

	spin-$\frac{1}{2}$	spin-1	Gauge rep.
G	$\tilde{g}$	g	$(8,1)_0$
W	$\tilde{W}^\pm\, \tilde{W}^0$	$W^\pm\, W^0$	$(1,3)_0$
B	$\tilde{B}^0$	B^0	$(1,1)_0$

(b) Vector supermultiplets of the MSSM

Table 1.2: The chiral and vector supermultiplets required in the minimal supersymmetric extension of the standard model.

In the MSSM, it is clearly necessary that the Higgs field be embedded in a chiral supermultiplet, with a superpartner referred to as a higgsino. However, it is also required that there be two Higgs fields rather than the minimal one of the SM. The principle reasons for this are twofold. Firstly, if one wishes to write down Yukawa couplings for the up and down quarks, then Higgs fields with hypercharge of $+\frac{1}{2}$ and $-\frac{1}{2}$ are respectively required in order to write down a SM-invariant coupling. Secondly, and in a somewhat related vein, the addition of supersymmetry can spoil the anomaly cancellation of the SM. The SM anomaly cancellation conditions $\mathrm{Tr}(T_3^2 Y) = \mathrm{Tr}(Y^3) = 0$, where the trace is over the fermions of the theory, would no longer be satisfied if a higgsino with hypercharges of $+\frac{1}{2}$ or $-\frac{1}{2}$ were added. However, adding a higgsino with each hypercharge value will restore anomaly cancellation.

This extension of the SM to the MSSM literally doubles the number of particles in the theory. However, as of writing this thesis, no SUSY partners have been observed. Most obviously perhaps, the new particles must have masses equal to those of the SM particles they share supermultiplets with. This lack of observation implies that SUSY, if it exists, must be a broken symmetry like that of the electroweak theory. While we will not discuss the details of SUSY breaking, this

breaking should not be too far above the TeV scale in order to leave SUSY with any hope of reducing the gauge hierarchy problem.

Setting problems of SUSY breaking to one side, one may write down the superpotential for the MSSM,

$$W = \hat{u}Y_u\hat{Q}\hat{H}_u - \hat{d}Y_d\hat{Q}\hat{H}_d - \hat{e}Y_e\hat{L}\hat{H}_d + \mu\hat{H}_d\hat{H}_u + \lambda\hat{L}\hat{L}\hat{e} + \lambda'\hat{Q}\hat{L}\hat{d} + \lambda''\hat{u}\hat{u}\hat{d} + \beta\hat{L}\hat{H}_u\,, \tag{1.47}$$

where $Y_{u,d,e}$ are Yukawa matrices, and we denote here the fact that these are superfields with $\hat{X}$ for each field X – we shall suppress this notation in the rest of this thesis. These terms are sufficient to have Yukawas for the quarks and charged leptons, as well as a mass for the Higgs boson. However, there are additional terms corresponding to baryon and lepton number violation. The trilinear λ, λ', and λ'' couplings correspond to a large number of processes, with the most constraining being proton decay. While no single trilinear coupling can lead to proton decay at dangerous rates, combinations of couplings are generally considered to be dangerous. As such, it is usual to introduce some form of R-parity or R-symmetry to forbid these couplings. This amounts to applying a Z_2 symmetry between SM and SUSY particles - $+$ and $-$ labels respectively - which is sufficient to remove the dangerous terms from the superpotential[6]. This may in some sense be considered an *ad hoc* assignment, though such mechanisms can be motivated in string theory.

1.4 Unification and SU(5)

The SM gauge group, $SU(3)_c \times SU(2)_L \times U(1)_Y$, features the unification of the electromagnetic and weak nuclear forces. Considering this, a set of aesthetically pleasing extensions of the SM can be found by extending this principle, with the aspiration of a grand unification of the SM in some larger group. This notion of beauty is lead further by considering the running of the SM coupling to high

[6]Other options for assignments exist that can remove the dangerous operators in a similar manner. For example assigning Higgs supermultiplets $+$ and quarks and leptons $-$ will forbid all these terms. One could also attempt a more exotic and interesting assignment, for example using some $Z_{N\neq 2}$ discrete symmetry.

energies, which appear to show a point of near-intersection at some high scale.

The first attempt at such a model was an SU(5) model, proposed by Georgi and Glashow [9] , which constitutes the smallest group with the SM as a subgroup.[7] This SU(5) construction shall form the basis of the models presented in the subsequent chapters. As such, presented here is an introduction to this construction. The main competitor GUT groups are $SO(10)$ and E_6, however these shall not be discussed in any detail here, though in short they offer more complete unifications, in particular with embeddings for right-handed neutrinos in unified representations.

1.4.1 Matter representations

The fundamental representation of any SU(N) group has dimension N. Considering the case of an SU(5) group with the SM embedded within it, the fundamental representation is a 5-dimensional one, with two options for embedding SM fermion representations,

$$5 \to (3,1)_{-1/3} \oplus (1,2)_{1/2}, \tag{1.48}$$

$$5 \to (3,1)_{2/3} \oplus (1,2)_{1/2}. \tag{1.49}$$

The second of these two embeddings is not a viable option, since the hypercharge generator would not be traceless - a requirement of SU(N) generators. As such, the first option should be taken, which implies the embedding of d_L^c and L into a fundamental representation of the GUT group, with the former as a colour triplet and the latter as an SU(2) doublet. The matter will be embedded in the antifundamental representation however, in order to pair the representations

[7] Any group hoping to be a candidate unification group must have rank of at least 4 to be able to contain the standard model gauge group.

correctly with those of the SM matter,

$$\overline{5} = \begin{pmatrix} d^c_{red} \\ d^c_{green} \\ d^c_{blue} \\ e \\ -\nu_e \end{pmatrix} = \begin{pmatrix} \mathbf{d^c} \\ L \end{pmatrix}. \tag{1.50}$$

It is an interesting feature that the charge operator, Q, must be traceless by requirement as an SU(5) operator. As such, the sum of its eigenvalues must vanish. Considering the fundamental representation embedding above, the sum of the charges adds up to zero in this way. This is the realisation of charge quantisation for the down-type quark and electron in the SU(5) model.

This clearly does not include the entire SM fermionic sector, the rest of which must be embedded into some higher dimensional representation. The next largest SU(5) representations are the symmetric and antisymmetric representations,

$$5 \otimes 5 = 10_a \oplus 15_s, \tag{1.51}$$

where 10_a is antisymmetric and 15_s is symmetric. If we take the fundamental representation as above,

$$5 = (3,1)_{-1/3} \oplus (1,2)_{1/2},$$

then we may construct the representations for an antisymmetric representation of the GUT group,

$$5 \otimes 5 = \underbrace{(3,2)_{1/6} \oplus (\overline{3},1)_{-2/3} \oplus (1,1)_1}_{10_a} \oplus \underbrace{(3,2)_{1/6} \oplus (6,1)_{-2/3} \oplus (1,3)_1}_{15_s}. \tag{1.52}$$

The representations within the antisymmetric part of the tensor product are exactly the required representations for the remaining SM fermions, $Q_L = (u_L,\, d_L)$,

u_L^c, and e_L^c. The full embedding is then

$$10 = \frac{1}{\sqrt{2}} \begin{pmatrix} 0 & u_r^c & -u_g^c & -u_b & -d_b \\ -u_r^c & 0 & u_b^c & -u_g & -d_g \\ u_g & -u_b^c & 0 & -u_r & -d_g \\ u_b & u_g & u_r & 0 & -e^c \\ d_b & d_g & d_r & e^c & 0 \end{pmatrix}. \tag{1.53}$$

Here, charge quantisation is ensured because the antisymmetric representation embedding is formed by the tensor product of two fundamental representations. Thus charge quantisation is unambiguously a feature of SU(5) GUTS. The full fermionic content of the SU(5) model is a 10 and a $\overline{5}$ for each of the three generations of the standard model.

Anomaly cancellation in SU(5)

As we have briefly discussed, the SM is an anomaly-free theory, a property that is also shared by SU(5). We shall briefly justify this statement. For any given fermion representation (R) of SU(N), the anomaly of that representation is proportional to a trace over the generators [65],

$$\mathrm{Tr}(\{T_R^a, T_R^b\} T_R^c) = \frac{1}{2} A(R) d^{abc}, \tag{1.54}$$

where A(R) is independent of the generator choice and d^{abc} is related to the commutation properties of the SU(N) group[8]. One is free to choose any three generators to calculate $A(R)$, so let us choose Q. Referring to the embedding in Equation (1.50), the antifundamental representation the anomaly is

$$A(\overline{5}) = \mathrm{Tr}(Q^3) = 3(\frac{1}{3})^3 + (-1)^3 = -\frac{8}{9}. \tag{1.55}$$

[8] d^{abc} is known as the third order antisymmetric invariant of SU(N)

While Equation (1.53) gives an anomaly contribution

$$A(10) = 3(-\frac{2}{3})^3 + 3(\frac{2}{3})^3 + 3(-\frac{1}{3})^3 + (1)^3 = \frac{8}{9}. \tag{1.56}$$

Since the anomaly contributions combine additively, these two contributions cancel each other perfectly. Consequently, one can conclude that provided there are equal numbers of (complete) antifundamental and antisymmetric representations,

$$n(\overline{5}) = n(10), \tag{1.57}$$

then the SU(5) model remains anomaly free.

1.4.2 Gauge representations

The SM gauge sector is comprised of bosons in the adjoint representations of their respective gauge groups. In order to embed these representations into an SU(5) GUT group, they should be set within the adjoint of this new gauge group, which has a degree of 24. This can easily accommodate the SM gauge bosons, however, when decomposing from SU(5) to $SU(3)_c \times SU(2)_L \times U(1)_Y$, there appear to be extra representations,

$$24 \rightarrow (8,1)_0 \oplus (1,3)_0 \oplus (1,1)_0 \oplus (3,2)_{-\frac{5}{6}} \oplus (\overline{3},2)_{\frac{5}{6}} \tag{1.58}$$

the physics of which must be considered. Looking at the representations involved, these new gauge bosons must violate baryon and lepton number, hence facilitating proton decay - see Section 1.4.4. The generators of SU(5) can be categorised in terms of the generators of the SM gauge group and extra generators. The SU(3) and SU(2) generators are embedded on the block diagonal upper three-by-three

and lower two-by-two,

$$L^{1,\ldots,8} = \frac{1}{2}\begin{pmatrix} & & & 0 & 0 \\ & \lambda^{1,\ldots,8} & & 0 & 0 \\ & & & 0 & 0 \\ 0 & 0 & 0 & 0 & 0 \\ 0 & 0 & 0 & 0 & 0 \end{pmatrix}, \quad L^{9,10,11} = \frac{1}{2}\begin{pmatrix} & & & 0 & 0 \\ & 0 & & 0 & 0 \\ & & & 0 & 0 \\ 0 & 0 & 0 & \multicolumn{2}{c}{\multirow{2}{*}{$\sigma^{1,2,3}$}} \\ 0 & 0 & 0 & & \end{pmatrix}, \tag{1.59}$$

where $\lambda^{1,\ldots,8}$ are the generators of SU(3) and $\sigma^{1,2,3}$ are those of SU(2). The hypercharge generator is assigned to the diagonal matrix,

$$L^{12} = \frac{1}{2\sqrt{15}}\text{diag}(-2,-2,-2,3,3). \tag{1.60}$$

In the SM, the electric charge operator is given as the linear combination of the hypercharge generator and the T_3 ,

$$Q = T_3 + Y. \tag{1.61}$$

However, the generators of SU(5) must satisfy the requirement that $\text{Tr}(L^i L^j) = \delta_{ij}/2$. Consequently, $\text{Tr}(Q^2) = \text{Tr}(T_3^2) + \text{Tr}(Y^2)$ should equal one. If one takes the hypercharge assignments of Equation (1.50), $Q = \frac{1}{3}\text{diag}(1,1,1,-3,0)$ and hence $\text{Tr}(Q^2) = \frac{4}{3}$ and the relation does not hold. This can be rectified if instead the relation is

$$Q = T_3 + \sqrt{\frac{5}{3}}Y, \tag{1.62}$$

introducing a new normalisation.

The remaining twelve generators are then all the combinations of the follow-

ing[9]

$$L^{13,15,17\ldots} = \frac{1}{2}\begin{pmatrix} & & & 1 & 0 \\ & 0 & & 0 & 0 \\ & & & 0 & 0 \\ 1 & 0 & 0 & & \\ 0 & 0 & 0 & 0 & \end{pmatrix}, \quad L^{14,16,18\ldots} = \frac{1}{2}\begin{pmatrix} & & & i & 0 \\ & 0 & & 0 & 0 \\ & & & 0 & 0 \\ -i & 0 & 0 & & \\ 0 & 0 & 0 & 0 & \end{pmatrix}. \tag{1.63}$$

The gauge field of the unified field theory is then a linear combination of the form,

$$A_\mu = \sqrt{2}\sum_{a=1}^{24} A_\mu^a L_a = \begin{pmatrix} G_1^1 - \frac{2B}{\sqrt{30}} & G_2^1 & G_3^1 & \overline{X}^1 & \overline{Y}^1 \\ G_1^2 & G_2^2 - \frac{2B}{\sqrt{30}} & G_3^2 & \overline{X}^2 & \overline{Y}^2 \\ G_1^3 & G_2^3 & G_3^3 - \frac{2B}{\sqrt{30}} & \overline{X}^3 & \overline{Y}^3 \\ X_1 & X_2 & X_3 & \frac{3B}{\sqrt{30}} + \frac{W_3}{\sqrt{2}} & \frac{W_1+iW_2}{\sqrt{2}} \\ Y_1 & Y_2 & Y_3 & \frac{W_1-iW_2}{\sqrt{2}} & \frac{3B}{\sqrt{30}} - \frac{W_3}{\sqrt{2}} \end{pmatrix}. \tag{1.64}$$

By analogy with the $W^\pm$ bosons of the electroweak sector, the fields X_i and Y_i are defined

$$\begin{aligned} X_\mu^1 &= \tfrac{A_\mu^{13}+iA_\mu^{14}}{\sqrt{2}}, \quad X_\mu^2 = \tfrac{A_\mu^{15}+iA_\mu^{16}}{\sqrt{2}}, \quad X_\mu^3 = \tfrac{A_\mu^{17}+iA_\mu^{18}}{\sqrt{2}}, \\ Y_\mu^1 &= \tfrac{A_\mu^{19}+iA_\mu^{20}}{\sqrt{2}}, \quad Y_\mu^2 = \tfrac{A_\mu^{21}+iA_\mu^{22}}{\sqrt{2}}, \quad Y_\mu^3 = \tfrac{A_\mu^{23}+iA_\mu^{24}}{\sqrt{2}}, \end{aligned} \tag{1.65}$$

making explicit the symmetry properties of the new bosons. This has an analogy with the quark doublet representations of the antisymmetric representation. These new bosons have charges under both SU(3) and SU(2), while also having charges $Q = 4/3$ and $Q = 1/3$ for X_μ and Y_μ respectively. The principal effect of the addition of these bosons is the emergence of baryon and lepton number violating processes, including proton decay.

[9]Six of the generators are the combinations of 1s reflected over the main diagonal, with the remaining six being $\pm i$s about the main diagonal.

1.4.3 Breaking SU(5)

It is almost a trivial statement that observed physics is not consistent with an unbroken SU(5) GUT, which means the SU(5) symmetry, if it is manifest in nature, must be broken analogously to the electroweak symmetry breaking in the SM. As such, any breaking of the symmetries in a model of this type must be a multi-step, multi-scale process. The first such stage must be the breaking of SU(5) to $SU(3)_c \times SU(2)_L \times U(1)_Y$ at some high scale, which will give the X_μ and Y_μ bosons masses at that scale. The second is the usual Higgs mechanism, which breaks the electroweak part of the SM to $U(1)_{em}$.

In order to achieve a breaking of SU(5), one can introduce an adjoint representation Higgs, constructed by taking the tensor product of a fundamental and an anti-fundamental representation, $5 \otimes \overline{5} = 24 \oplus 1$. This Higgs field must get a non-zero vacuum expectation value in the direction of the hypercharge generator, which will keep the SM part of the GUT group intact, while giving a mass to the X_μ and Y_μ part of the spectrum. We denote such a field as a 5×5 matrix,

$$\phi_b^a = \begin{pmatrix} H_1^1 - \frac{2}{\sqrt{30}}H_B & H_2^1 & H_3^1 & \overline{H}_X^1 & \overline{H}_Y^1 \\ H_1^2 & H_2^2 - \frac{2}{\sqrt{30}}H_B & H_3^2 & \overline{H}_X^2 & \overline{H}_Y^2 \\ H_1^3 & H_2^3 & H_3^3 - \frac{2}{\sqrt{30}}H_B & \overline{H}_X^3 & \overline{H}_Y^3 \\ H_X^1 & H_X^2 & H_X^3 & \frac{3}{\sqrt{30}}H_B + \frac{H^0}{\sqrt{2}} & H^+ \\ H_Y^1 & H_Y^2 & H_Y^3 & H^- & \frac{3}{\sqrt{30}}H_B - \frac{H^0}{\sqrt{2}} \end{pmatrix}, \tag{1.66}$$

where the fields, H, mirror the representations of the adjoint fields of Equation (1.64). We also introduce a Higgs field that will correspond to the electroweak Higgs, which must be in the fundamental representation,

$$H^a = \begin{pmatrix} D^1 \\ D^2 \\ D^3 \\ h^+ \\ h^0 \end{pmatrix}. \tag{1.67}$$

The Lagrangian of the Higgs sector is comprised of all possible invariants that can be written with these two fields,

$$\mathcal{L} = (D_\mu H)^\dagger_a (D^\mu H)^a + \frac{1}{2}(D_\mu \phi)^a_b (D^\mu \phi)^b_a - V(\phi, H), \tag{1.68}$$

where the covariant derivatives are

$$\begin{aligned}(D_\mu H)^a &= \left(\partial_\mu \delta^a_b - \frac{ig}{\sqrt{2}}(A_\mu)^a_b\right) H^b, \\ (D_\mu \phi)^a_b &= \left(\partial_\mu \delta^a_c \delta^d_b - \frac{ig}{\sqrt{2}}(A_\mu)^a_c \delta^d_b + \frac{ig}{\sqrt{2}}(A_\mu)^d_b \delta^a_c\right) \phi^c_d \\ &= \partial \phi^a_b - \frac{ig}{\sqrt{2}}[A_\mu, \phi]^a_b.\end{aligned} \tag{1.69}$$

The potential is comprised of a total of nine terms, arising from the ϕ-only, H-only, and mixed terms,

$$\begin{aligned}V(\phi, H) = &- \frac{\mu^2}{2}\mathrm{Tr}(\phi^2) + \frac{a}{4}[\mathrm{Tr}(\phi^2)]^2 + \frac{b}{4}\mathrm{Tr}(\phi^4) + \frac{c}{3}\mathrm{Tr}(\phi^3) \\ &- \frac{\nu^2}{2} H^\dagger H + \frac{\lambda}{4}(H^\dagger H)^2 \\ &+ \alpha (H^\dagger H)\mathrm{Tr}(\phi^2) + \beta H^\dagger \phi^2 H + \gamma H^\dagger \phi H.\end{aligned} \tag{1.70}$$

This potential is usually simplified by imposing a Z_2 symmetry[10] on ϕ, eliminating the c and γ terms. This will be sufficient to break both the GUT symmetry and the electroweak sector when the appropriate vacuum expectations are selected for ϕ and H, provided $\mu, \nu > 0$.

Let us consider only the GUT breaking portion of this process. This breaking will be triggered by the imposition of a vacuum expectation in the H_B and H_0 fields,

$$\begin{aligned}\langle H_B \rangle &= -\frac{\sqrt{30}}{2} v, \\ \langle H^0 \rangle &= -\frac{\epsilon v}{\sqrt{2}},\end{aligned} \tag{1.71}$$

where v is the scale of the GUT breaking and epsilon is a number parameterising the relative size of the two vacuum expectations, which we shall set to zero for

[10] We impose that all terms must be invariant under $\phi \to -\phi$

simplifications sake[11]. If one solves for the minimum of this potential, one finds that the vacuum expectation is solved for

$$v^2 = \frac{4\mu^2}{30a + 7b}, \tag{1.72}$$

provided that $30a+7b > 0$ and, of course, $\mu^2 > 0$. The consequence of this breaking is that the X_μ and Y_μ bosons must get masses to account for the Goldstone bosons unleashed by the twelve degrees of freedom left over after accounting for the unbroken $SU(3)_c \times SU(2)_L \times U(1)_Y$ subgroup after breaking SU(5). Using Equation (1.69) and Equation (1.68), along with the vacuum alignment of the adjoint Higgs,

$$\langle \phi \rangle = v \times \mathrm{diag}(1, 1, 1, -\frac{3}{2}, -\frac{3}{2}), \tag{1.73}$$

the masses can be shown to be proportional to the vacuum expectation of the GUT breaking,

$$M_X^2 = M_Y^2 = \frac{25}{8} g^2 v^2. \tag{1.74}$$

This will naturally keep these extra bosons at a high scale, provided GUT breaking occurs well above the electroweak scale.

The second stage of the symmetry breaking will be triggered at the electroweak scale, with a vacuum expectation being given to the fundamental Higgs,

$$\langle H^a \rangle = \begin{pmatrix} 0 \\ 0 \\ 0 \\ 0 \\ v_{ew} \end{pmatrix}. \tag{1.75}$$

This will trigger a mass for the SM Higgs boson in the usual way, however it will leave the colour triplet of $D_{1,2,3}$ massless. These colour triplets mediate proton decay and so must gain a large mass in order to suppress this process. Such a mass can only come from the mixed part of the potential - cross terms between

[11] It can be shown [9] that ϵ must necessarily be small - i.e. $\epsilon \ll 1$.

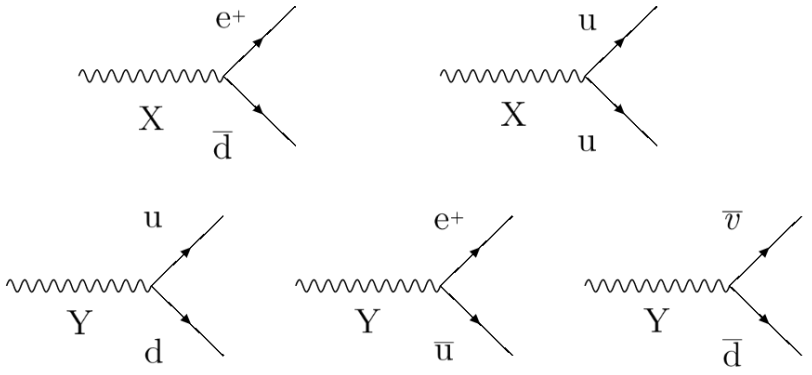

Figure 1.2: Baryon and lepton number violating vertices arising from the gauge sector or the SU(5) GUT model.

ϕ_b^a and H^a. Inserting the vacuum expectation of Equation (1.73), the cross term part of the potential gives GUT scale masses to both the SU(2) and SU(3) part of the fundamental Higgs,

$$V(\phi, H) = v^2 \left(\frac{15}{2}\alpha + \beta\right) D^\dagger D + v^2 \left(\frac{15}{2}\alpha + \frac{9}{4}\beta\right) h^\dagger h. \tag{1.76}$$

While solving the problem of a light D_i spectrum, this creates a new issue: the SM Higgs will now have a GUT scale mass too. The only way to avoid this problem is to insist upon a delicate cancellation of terms (fine-tuning) to force the term to vanish. This is realised if

$$\alpha = -\frac{9}{30}\beta. \tag{1.77}$$

The fine-tuning of this doublet-triplet splitting is unappealing due to the requirement that the free parameters be related in a very specific manner, and as such reduces the appeal of the classical SU(5) model.

1.4.4 SU(5) GUTs and proton decay

In the SU(5) model, the extra gauge bosons arising from the unified adjoint representation cause baryon and lepton number violation, which together can allow proton decay via dimension-6 operators. The interactions, arising from the

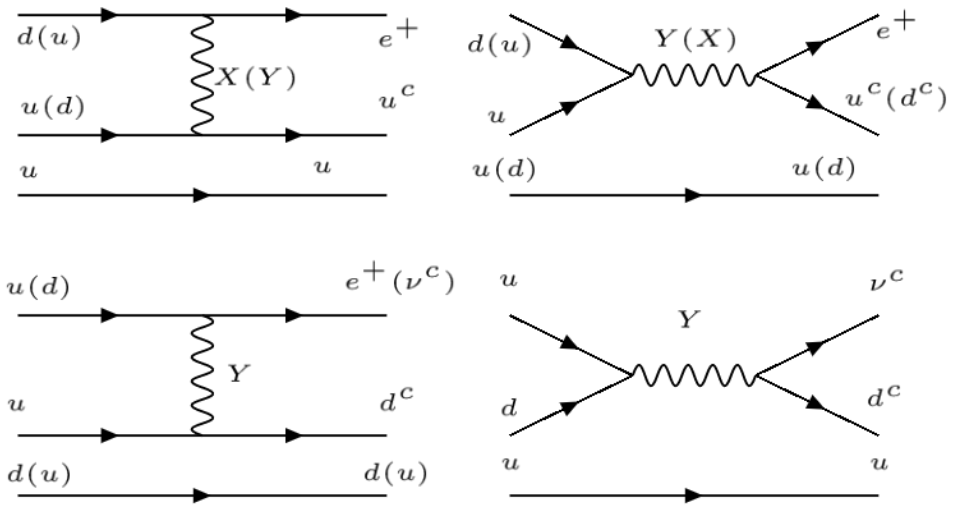

Figure 1.3: Feynman diagrams of proton decay processes arising from the additional gauge bosons of the SU(5) model.

kinetic parts of the Lagrangian,

$$\mathcal{L} = i\overline{\psi}^a_{\overline{5}}\gamma^\mu(D_\mu\psi_{\overline{5}})_a + i\overline{\psi}^a_{10}b\gamma^\mu(D_\mu\psi_{10})_{ab}, \tag{1.78}$$

give rise to five new couplings, which are shown in Figure 1.2. In an unbroken GUT scenario, with the X_μ and Y_μ fields massless, these vertices would cause proton decay to be rampant[12]. However, assuming the SU(5) group is broken to the SM gauge group, the decay rate of the proton would be suppressed by the scale of the GUT breaking. Provided this scale is high enough, the propagator for the X_μ/Y_μ is inversely proportional to the mass squared. The decay can be either to a charged meson and an antineutrino ($p \to \pi^+\overline{\nu}$), or to a neutral meson and a positron ($p \to \pi^0 e^+$), as shown in the graphs of Figure 1.3.

Considering the processes illustrated by Figure 1.3, the proton lifetime is then $\tau_p \sim \frac{M_X^4}{g^4 m_p^5}$. Experimentally, the proton lifetime is constrained to be $\tau_p > 5 \times 10^{33}$years [66], which means, the GUT scale must be $\sim 10^{15}$GeV.

[12]The neutron could also decay via similar processes

1.4.5 Yukawa couplings

Because the fermionic matter content of the SM is embedded into two representations of the SU(5) GUT , the Yukawa couplings arise from two different SU(5) invariants,

$$\mathcal{L} = \overline{\psi}^i_{\overline{5}} Y_5 (\psi_{10})_{ij} (H^*)^j + \frac{1}{4} \epsilon_{ijklm} \psi^{ij}_{10} Y_{10} \psi^{kl}_{10} H^m, \tag{1.79}$$

where $Y_{5,10}$ are 3×3 matrices corresponding to the three generation copies. Note that due to the choice of representation for the matter fields, the fermions do not couple to the adjoint representation Higgs field, ϕ, thus preventing them from acquiring a mass at the GUT scale.

Upon breaking of the electroweak symmetry of the SM, the quarks and charged leptons will get masses through the usual coupling to the Higgs. However, the masses of the down-type quarks and the charged leptons will be inextricably intertwined due to their shared GUT representation,

$$\mathcal{L} = d^c Y_5 Q h^* + L Y_5 e^c h^* + u^c (Y_{10} + Y_{10}^T) Q h. \tag{1.80}$$

In fact, at the GUT scale, the masses of the charged leptons are exactly equal to their generational counterpart down-type quarks,

$$m_d = m_e, \;\; m_s = m_\mu, \;\; m_b = m_\tau. \tag{1.81}$$

This relationship is affected by the running of the Yukawa couplings with the energy scale, however even with this taken into account the mass relations cannot be compatible with experiment. Thus a minimal SU(5) has unrealistic mass relations between quarks and leptons. A common extension often taken is to add a Higgs field in the 45 representation of SU(5), which changes the relations to be more realistic,

$$m_d = 3 m_e, \;\; m_s = \frac{1}{3} m_\mu, \;\; m_b = m_\tau. \tag{1.82}$$

1.4.6 Supersymmetric SU(5)

A key motivation of the SU(5) GUT was the apparent unification of SM couplings at some high scale. However, if one runs the SM couplings up to this high scale, the unification of couplings does not occur. This is a clear elephant-in-the-room situation for the SU(5) theory. A possible solution to this shortcoming is the introduction of SUSY to the SU(5) GUT model. In fact, it transpires that if one does this, with all superpartners having TeV scale masses, then the couplings of the SM now unify, albeit at the higher scale of $\sim 10^{16}$GeV. This fact alone is a very persuasive argument for supersymmeterising SU(5).

The principal modification to the spectrum of the SUSY version of SU(5) is that now we must have an H_u and an H_d representation - 5_{H_u} and $\overline{5}_{H_d}$ respectively. The superpotential terms equivalent to Equation (1.79) is then

$$W = \overline{5}_M Y_5 10_M \overline{5}_{H_d} + 10_M Y_{10} 10_M 5_{H_u}. \tag{1.83}$$

The drawback of adding SUSY to the model is the addition of extra operators that can mediate proton decay. While the X_μ and Y_μ mediated processes are dimension-6 operators, the new operators will be dimension-4 and -5. Imposition of an R-parity or R-symmetry can remove the dimension-4 operators, which would otherwise be the most dangerous to proton stability. This imposition is often an *ad hoc* process in many models, though F-theory may provide tools for motivating such a mechanism.

The dimension-5 operators are a different matter, since they arise from the colour triplet part of the Higgs multiplets. The processes are of the type shown in Figure 1.4, which after integrating out the triplet Higgs will have a cross-section inversely proportional to the mass of the triplets. It will also be suppressed by the mass of the superpartners, so that the lifetime of the proton due to this process is

$$\tau_p \sim \frac{M_D^2 M_{\tilde{Z}}}{m_p^5} \left(\frac{m_W^2}{m_u m_s} \right)^2. \tag{1.84}$$

Since $M_D \sim M_X$, the main constraint is the mass of the SUSY partner, which

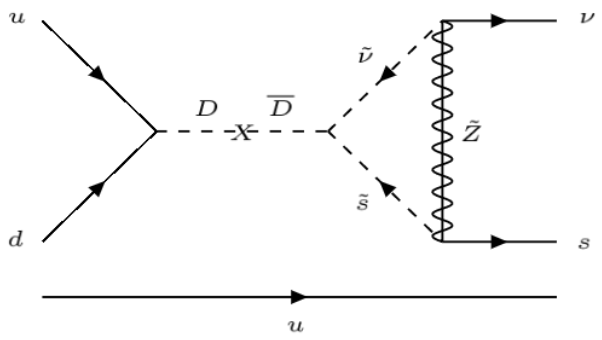

Figure 1.4: Proton decay to kaons, via colour triplet partners of the Higgs field arising from supersymmetrising SU(5) GUTS.

must be sufficiently large to ensure proton decay is suppressed. This process is highly constrained by experiment, with the distinguishing feature, compared to dimension-6 processes, being the presence of kaons in the final state rather than pions. In the SUSY SU(5), due to the raised GUT scale, this dimension-5 process will totally dominate the dimension-6, which will be even more suppressed than in the vanilla SU(5) GUT.

1.5 String Theory

The SM provides an accurate, quantum mechanical description of three of the fundamental interactions known in nature. However, it makes no predictions regarding gravity, which is still the domain of the classical theory of General Relativity (GR). While GR is extremely successful at describing the large scale phenomena of the universe, including the recent discovery of gravitational waves [6], it falls down when in the regime in which quantum effects take hold. A popular candidate to fill the metaphorical void of quantum gravity is string theory.

Historically speaking, string theory was originally devised as a candidate description of the strong nuclear force. As it transpires, QCD emerged as a successful theory of this interaction, while string theory was plagued by tachyons and seemingly unnatural spin-2 states. Hence, for a time, string theory was abandoned. However, it was later realised that the spin-2 state could be interpreted

as a gravtion, which is the force carrier of gravity in the quantum mechanical picture.

The basic premise of string theory is to replace point-like particles by extended, one-dimensional objects, which we call strings. Depending on the boundary conditions specified for a given string, it may be either an open or closed string. While a closed string simply has periodic (or anti-periodic) boundary conditions, the open string can have either Neumann or Dirichlet boundary conditions, corresponding to a free string or a string with ends fixed to higher-dimensional objects. These higher-dimensional objects are referred to as Dp-branes[13], an important class of objects we shall discuss in this section.

The first significant string theory constructed was only able to describe bosons. This bosonic string theory requires a 26-dimensional spacetime to be consistent. Later attempts yielded so-called superstring theories, able to describe fermionic matter as well. These were referred to as simply Type I, Type IIA, and Type IIB superstring theories, while later still two extra string theories called Heterotic strings were also developed - $E_8 \times E_8$ and $SO(32)$.

An interesting property of these string theories is that, under certain transformations, the types of string are related by "dualities". This indicates that they are all in some sense part of a broader, encompassing theory. Though we shall note delve into this topic beyond this remark, it is worth mentioning that Type IIB string theory is dual to itself under S-duality, which leads to F-theory.

1.5.1 Gauge symmetries

To discuss some key concepts related to F-theory, let us consider Type IIB string theory, since it is closely related to F-theory. Type IIB string theory has both closed and open strings, with the former corresponding to the graviton and the latter SM particles. If we set aside the closed strings and focus on the non-gravity part of the theory, the open strings must be paired with Dp-branes if they are to have Dirichlet boundary conditions.

In general, a string in an N-dimensional spacetime will have p Neumann

[13]More properly they are Dirichlet branes of dimension p.

boundary conditions and $N-p$ Dirichlet boundary conditions[14], with the time coordinate being taken to Neumann. The Lorentz symmetry group of full spacetime is $SO(1,N-1)$, while this may be decomposed based on the boundary conditions,

$$SO(1,N-1) \rightarrow SO(1,p)_{brane} \times SO(1,N-p-1)_{spacetime}. \tag{1.85}$$

Considering a string with both ends attached to the same Dp-brane, upon performing a mode expansion and quantising the operators, the spatial wavefunction is found to depend only on the brane coordinate - not the dimensions in which the string is free to propagate [67]. It can be shown [67] that the first excited state of the mode expansion includes a spin-1 component, which can be associated to a U(1) gauge field on the brane. There are also scalars under the Lorentz group of the brane, which instead are vectors under the spacetime Lorentz group.

The presences of a gauge field on the brane proves to be a useful property. Let us then also consider the case where N such branes share the same spacetime positions. In such a case a string attached to this "stack" of branes can attach each of its ends to any of the N branes – a total of N^2 combinations. Clearly in this case the U(1) associated to each individual brane becomes a part of a large symmetry group – $\mathrm{U}(1)^N \rightarrow \mathrm{U}(N)$ – giving rise to an adjoint representation field, which is associated to a gauge field. This point is illustrated by Figure 1.5 in the simple example of two branes stacking to form one brane with a U(2) gauge field, with the four combinations of string attachments becoming one.

A second interesting case arises when a string has ends attached to two different (separated) stacks. In this case, the representation must be a bi-fundamental of the two gauge theories realised on those stacks. For example, a U(3) stack intersecting a U(2) stack would allow a string with one end fixed to each stack so that it is in the fundamental representation of each – a very useful property since fermions in the SM have SU(3) and SU(2) representations.

[14]This is trivial since the string must have a boundary condition in every dimension. Thus is must either have a Neumann or Dirichlet boundary condition for each dimension

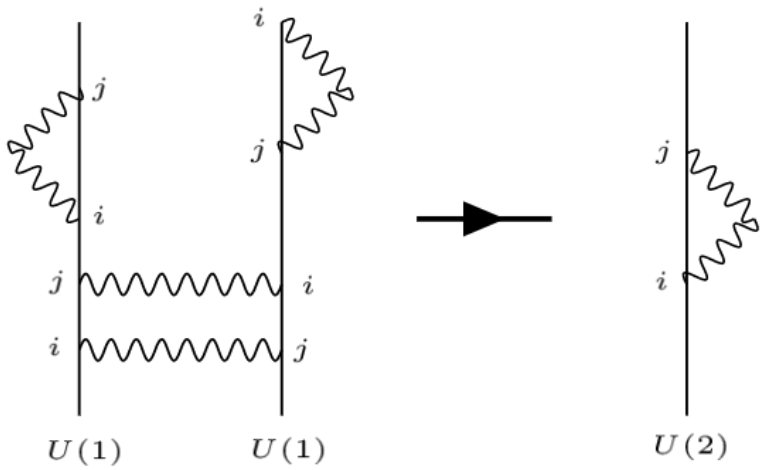

Figure 1.5: In the case where two branes are separated, a string may have ends attached to the branes in four different combinations. However, when the two branes stack these four attachments are not distinguishable and instead we have extra gauge degrees of freedom - we take two U(1) branes and end up with one U(2) brane.

1.5.2 SU(5) and brane intersections

Much of the work in this thesis is centred on SU(5) models in F-theory, which is realised on a so-called GUT surface – a D7-brane with SU(5) gauge properties. In Type IIB string theory, we could consider a stack of 5 D7-branes, giving a U(5) gauge group, however let us consider the SU(5) subgroup of this, $\mathrm{U}(5) \rightarrow \mathrm{SU}(5) \times \mathrm{U}(1)$. The representation supported on the GUT surface is the adjoint of the group, which does not accommodate the representations in an SU(5) GUT - the $\overline{5}$ and 10 representations.

In order to realise the required representations, let us consider the symmetry enhancement if a further D7-brane, intersects the GUT surface. The symmetry can be enhanced to SU(6), so that at the intersection point there is an adjoint representation of that group – Figure 1.6 shows this enhancement of the gauge group where brane stacks intersect one another. Decomposing this,

$$\begin{gathered} \mathrm{SU}(6) \rightarrow \mathrm{SU}(5) \times \mathrm{U}(1) \\ 35 \rightarrow (24,0)+(1,0)+(\overline{5},6)+(5,-6), \end{gathered} \tag{1.86}$$

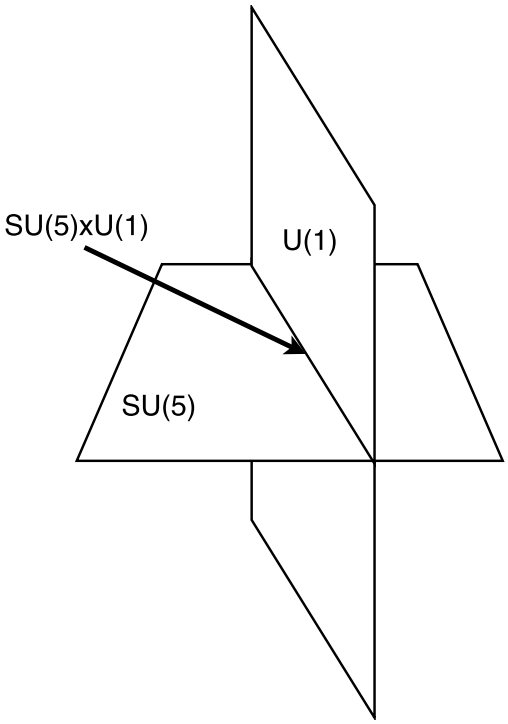

Figure 1.6: Pictorial representation of a brane housing an SU(5) GUT symmetry with an intersecting brane enhancing the symmetry at the intersection point to SU(5)×U(1).

one can see that the fundamental representation is realised at the intersection point. Another possible enhancement that can be seen from group theory leads to an embedding of the antisymmetric representation in the group SO(10),

$$\begin{aligned} \mathrm{SO}(10) &\to \mathrm{SU}(5) \times \mathrm{U}(1) \\ 45 &\to (24,0) + (1,0) + (\overline{10},-4) + (10,4), \end{aligned} \tag{1.87}$$

which means that an SU(5) embedding can be facilitated by branes.

In fact, one may extend this logic further to describe Yukawa couplings in such a framework, since two branes intersecting on the GUT surface may further enhance the symmetry at their point of intersection. Firstly, the down-type quark

and charged lepton couplings would arise from a point of SO(12) in the geometry,

$$\begin{aligned} \mathrm{SO}(12) &\to \mathrm{SU}(5) \times \mathrm{U}(1)_a \times \mathrm{U}(1)_b \\ 66 &\to (24,0,0) + (1,0,0) \\ &+(\overline{10},-4,0) + (10,4,0) \\ &+(\overline{5},-2,2) + (5,2,2) + (\overline{5},-,2,-2) + (5,2,-2). \end{aligned} \tag{1.88}$$

The SU(5) Yukawa coupling is of the type $10 \times \overline{5} \times \overline{5}$, which can be picked out with the representations $(10,4,0)$, $(\overline{5},-2,2)$, and $(\overline{5},-,2,-2)$. There is of course a subtlety in this, since we are actually dealing with a U(5) brane and must account for the remaining U(1). In the case of the down-type/charged lepton this is not an issue, since the $\overline{5}$ has -1 charge, while the 10 has charge 2 – hence they cancel the charge.

The up-type Yukawa cannot be identified in a point of SO(12), so instead we examine another enhancement, E_6,

$$\begin{aligned} \mathrm{E}_6 &\to \mathrm{SU}(5) \times \mathrm{U}(1)_a \times \mathrm{U}(1)_b \\ 78 &\to (24,0,0) + (1,0,0) + (1,0,0) \\ &+(\overline{10},-4,0) + (10,4,0) + (\overline{10},1,3) + (10,-1,-3) \\ &+(\overline{5},3,-3) + (5,-3,3) + (1,-5,-3) + (1,5,3). \end{aligned} \tag{1.89}$$

Here the up-type Yukawa is due to the $(10,4,0)$, $(10,-1,-3)$, and $(5,-3,3)$ representations. However, when we consider the aforementioned $\mathrm{U}(5) \to \mathrm{SU}(5) \times \mathrm{U}(1)$ problem, the coupling clearly will not be allowed. This problem can be avoided in F-theory, as we will discuss in the next chapter.

Chapter 2

F-theory and the MSSM from SU(5) with Klein Monodromy

F-Theory [13] is a 12 dimensional formulation of Type IIB string theory, with the internal dimensions classified as a complex Calabi-Yau four-fold elliptically fibred over a threefold base [68]. There is a well studied correspondence between the singularities of elliptically fibred spaces and the gauge groups to which they relate. This is an intriguing feature for theorists, since it facilitates popular GUT groups [15, 18–20, 22, 55, 59, 69–71] such as SU(5), $SO(10)$ or E_6, with a maximum symmetry enhancement of the exceptional group E_8 [14]. As such, in F-Theory one realises the GUT group on a D7-brane, which wraps a four-complex-dimensional surface, $S_{\rm GUT}$. The intersections of other D7-branes with this surface (and each other) dictates where matter is localised – so-called matter curves. Where these matter curves intersect the symmetry is further enhanced and Yukawa coupling can be realised. Using a local approach one can calculate Yukawa couplings using overlap integrals over the relevant wavefunctions [30–39], while a global approach, requiring knowledge of the full compactification of the Calabi-Yau fourfold, is required to have a complete understanding of the physics of a particular construction [22–29].

In this thesis, the so-called semi-local [14, 47, 49]approach will be used, which allows decoupling of the full geometry while still preserving some mechanism for

studying the properties of the GUT surface. In this approach, the GUT surface is taken to fall from a theory with a point of E_8 [14], which is the largest non-Abelian symmetry allowed by this elliptic fibration. This E_8 is broken by an adjoint representation Higgs field to the relevant GUT group, for example, if we consider an SU(5) GUT group, the adjoint of E_8 decomposes in to an SU(5) associated to the GUT group and a commutant group[1], which is also SU(5),

$$\begin{gathered} E_8 \to SU(5)_{\text{GUT}} \times SU(5)_{\perp}, \\ 248 \to (24,1) \oplus (1,24) \oplus (10,5) \oplus (\overline{5},10) \oplus (5,\overline{10}) \oplus (\overline{10},\overline{5}). \end{gathered} \tag{2.1}$$

All matter representations and all Yukawa couplings are assumed to descend from this symmetry point, so the matter representations must arise when the D7-branes associated with the U(1)s of the perpendicular SU(5) intersect the GUT surface, which corresponds to an enhancement of the symmetry at that intersection point. This symmetry enhancement is associated with degeneration of the elliptic fibre associated with F-theory. A powerful property of this picture is that the topological properties of the internal space are converted to constraints on the effective field theory model in a direct manner. Moreover, in these constructions it is possible to implement a flux mechanism that breaks the symmetry and generates chirality in the spectrum.

2.1 Elliptic fibration in F-theory

The elliptic fibration of F-theory reduces the eight extra dimensions of the theory, a complex Calabi-Yau four-fold, to a six dimensional base space and two dimensions corresponding to the elliptic fibre. The latter is a torus at all points in this base space, with modulus

$$\tau = C_0 + ie^{-\phi}. \tag{2.2}$$

[1]The commutant of a group M in some parent group P, M' say, is the set of all elements in the parent group that commute with the elements of M.

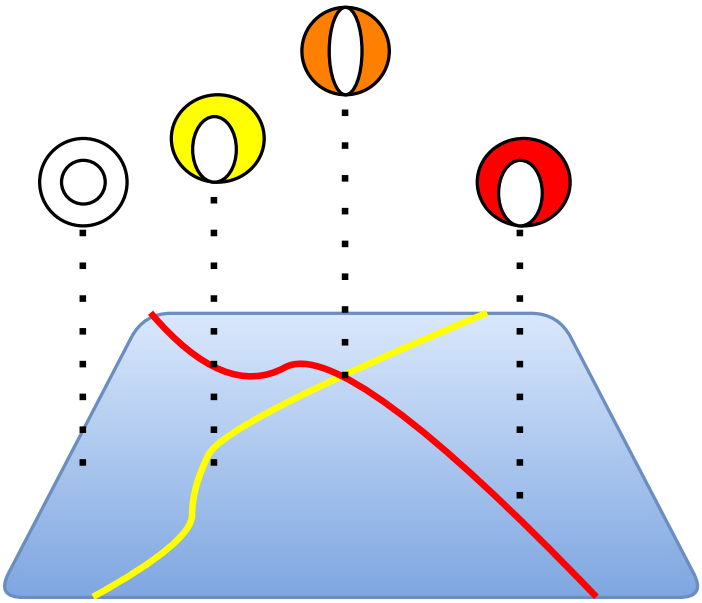

Figure 2.1: A pictorial representation of a Calabi-Yau fourfold, which exhibits elliptic fibration over a threefold base, B_3. The fibration is manifest as a 2-Torus at every point in the base, as shown. The modulus of the torus at each point is related to the axio-dilaton profile, $\tau = C_0 + i/g_s$. Where the fibre degenerates, the presence of a D7-brane orthogonal to the base is indicated. Where those D7-branes intersect, the fibre may degenerate further.

This torus corresponds to the properties of the axion (C_0) and the dilaton ($\phi = \ln g_s$), both of which are scalars in the bosonic part of the theory [72]. The profile of this axio-dilaton is affected by the presence of D7-branes, which means the geometric dimensions of the torus fibre keep track of the behaviour of τ in the base space.

In this thesis we will be assuming that there exists a GUT surface in the internal manifold, which is associated to a holomorphic divisor residing inside the threefold base, B_3. If we designate with z the 'normal' direction to this GUT surface, the GUT divisor is the zero limit of the holomorphic section z in B_3, i.e. at $z \to 0$. The elliptic fibration on B_3 is described by the Weierstrass equation,

$$y^2 = x^3 + f(z)x + g(z), \tag{2.3}$$

where x and y are complex coordinates on the GUT surface (S_{GUT}) and z is a complex coordinate, which as mentioned is normal to S_{GUT}. The functions f and g are eighth and twelfth degree polynomials in z respectively. The form of this

equation and its discriminant,

$$\Delta = 4f^3 + 27g^2, \tag{2.4}$$

determine the type of singularities present in the geometry – where the discriminant has a zero, the fibre degenerates. Due to the work of Kodaira [73, 74], we have a full classification of the ADE gauge groups supported by the singularities of a particular space. By performing a process known as Tate's algorithm [75], which entails enforcing vanishing of the discriminant to various orders in z, we may recast the Weierstrass equation in the so called Tate form. If we begin by expanding f and g as

$$f(z) = \sum_i f_i z^i\,, \;\; g(z) = \sum_j g_j z^j\,, \tag{2.5}$$

and enforce that the z^0 coefficient of Δ vanishes,

$$\begin{aligned}
&\Delta = 4(f_0 + f_1 z + \dots f_8 z^8)^3 + 27(g_0 + g_1 z + \dots g_{12} z^{12})^2, \\
&\Delta = (4f_0^3 + 27g_0^2) + (12 f_0^2 f_1 + 54 g_0 g_1) z \\
&+ (12(f_0 f_1^2 + f_0^2 f_2) + 27(g_1^2 + g_0 g_2)) z^2 + O(z^3).
\end{aligned} \tag{2.6}$$

Clearly, the vanishing of the z^0 coefficient is satisfied by $f_0 = -\frac{t^2}{3}$ and $g_0 = \frac{2t^3}{27}$. This, along with the coordinate shift $x \to x + \frac{t}{3}$, changes the Weierstrass equation to

$$y^2 = x^3 + t x^2 + x(f_1 z + \dots) + (\tilde{g}_1 z + \tilde{g}_2 z^2 \dots), \tag{2.7}$$

where $\tilde{g}_i = \frac{f_i t}{3} + g_i$. It transpires that setting $\tilde{g}_1 = \frac{f_1 t}{3} + g_1$ is sufficient to make the z^1 coefficient of Δ vanish. This process can be continued order-wise, to give full classification of the singularities, while the Weierstrass equation can then be written in Tate form,

$$y^2 + \alpha_1 x y + \alpha_3 y = x^3 + \alpha_2 x^2 + \alpha_4 x + \alpha_6\,. \tag{2.8}$$

Type	Group	α_1	α_2	α_3	α_4	α_6	Δ
I_0	0	0	0	0	0	0	0
I_0	-	0	0	1	1	1	1
I_0	-	0	0	1	1	2	2
I^S_{2n}	SU($2n$)	0	1	n	n	2n	2n
I^S_{2n+1}	SU($2n+1$)	0	1	n	n+1	2n+1	2n+1
I^{*S}_1	$SO(10)$	1	1	2	3	5	7
IV^{*S}	E_6	1	2	3	3	5	8
III^{*S}	E_7	1	2	3	3	5	9
II^S	E_8	1	2	3	4	5	10

Table 2.1: The vanishing orders of each of the coefficients of Equation (2.8) in terms of the coordinate z for various various interesting gauge groups to be realised in an elliptically fibred space. The gauge groups are supported by specific types of singular fibre, as classified by Kodaira. See [76] [75].

The α_n coefficients in this equation and their vanishing order determine the singularity of the surface. For example, an SU(5) singularity would correspond to [47, 49, 58]:

$$\alpha_1 = -b_5,\ \alpha_2 = b_4 z,\ \alpha_3 = -b_3 z^2,\ \alpha_4 = b_2 z^3,\ \alpha_6 = b_0 z^5\,. \tag{2.9}$$

Table 2.1 outlines the conditions required for some of the more interesting groups to be realised in the geometry.

The Tate form of the Weierstrass equation will correspond to an SU(5) singularity if the conditions of Equation (2.9) are enforced. This gives a relatively complicated polynomial in the coordinates of the space:

$$y^2 = x^3 + b_0 z^5 + b_2 x z^3 + b_3 y z^2 + b_4 x^2 z + b_5 x y\,. \tag{2.10}$$

However, using homogeneous complex coordinates, $z \to U$, $x \to V^2$, and $y \to V^3$, the Weierstrass equation becomes

$$b_0 U^5 + b_2 V^2 U^3 + b_3 V^3 U^2 + b_4 V^4 U + b_5 V^5 = 0. \tag{2.11}$$

We may then locally select some affine parameter, $s = U/V$, so that the above equation reduces to a fifth order polynomial in s, the roots of which are identified

as the roots of $SU(5)_\perp$, t_i:

$$C_5 = b_5 + b_4 s + b_3 s^2 + b_2 s^3 + b_1 s^4 + b_0 s^5 \propto \prod_{i=1}^{5} (s + t_i)\,, \tag{2.12}$$

where the homologies of the coefficients in the above equation are given by:

$$[b_k] = \eta - k c_1 \tag{2.13}$$

$$\eta = 6c_1 - t \tag{2.14}$$

where c_1 and t are the first Chern classes of the Tangent and Normal bundles respectively. This equation accounts for the antisymmetric representation of the GUT group, while an equation to characterise the fundamental representation should be a tenth order polynomial with roots $t_i + t_j$ as stated above. By consistency with Equation (2.12), this can be written in terms of the coefficients of the equation for the antisymmetric representation. The defining equation is the zeroth order part of that polynomial, which can be shown to be:

$$P_5 = b_3^2 b_4 - b_2 b_3 b_5 + b_0 b_5^2 \propto \prod_{i>j} (t_i + t_j). \tag{2.15}$$

These two equations are sufficient to describe the matter content of an SU(5) GUT model in F-theory, however the exact matter content is influenced by monodromy actions on the roots, which we shall discuss in Section 2.2.

2.2 Monodromy

The perpendicular group left over after isolating the GUT group within the parent E_8 theory will cause various points of symmetry enhancement on the GUT surface. For example, in the SU(5) case we shall consider, the model essentially has four $U(1)$s intersecting the SU(5) GUT surface at various points,

$$E_8 \to SU(5)_{GUT} \times SU(5)_\perp \to SU(5)_{GUT} \times U(1)^4\,. \tag{2.16}$$

The assumed E_8 point of enhancement is broken by a Higgs field in the adjoint of the group, which has a coordinate dependent vacuum expectation value. The roots of the field, t_i, are such that on the GUT surface, they are identified with the roots of the fundamental representation of the perpendicular group – $SU(5)_\perp$ [17]. At local points on the surface, these roots may vanish leading to an enhancement of the symmetry – akin to a restoration towards the full E_8, which would occur if all roots vanished simultaneous on the GUT surface. However, the charges associated to these enhancements must cancel out in the low energy theory, such as for Yukawa couplings.

We shall focus on Yukawa couplings, which are formed in the usual way for an SU(5) GUT theory, with the additional constraint that the 10s have charges t_i and the $\bar{5}$/5s have charge t_i+t_j. This extra property arises from the perpendicular group charges, such that one can identify the weights of the perpendicular group as :

$$\begin{aligned}
&\Sigma_{10} \,:\, t_i = 0, \\
&\Sigma_{\bar{5}} \,:\, t_i + t_j = 0,\ i \neq j \\
&\Sigma_{1} \,:\, \pm(t_i - t_j) = 0,\ i \neq j.
\end{aligned}$$

With this in mind, the top quark and the bottom/tau Yukawa couplings are of the form:

$$\begin{aligned}
\text{top type Yukawas: } & 10_{t_i} \cdot 10_{t_j} \cdot 5_{-t_k - t_l} \\
\text{with: } & k \neq l \\
\text{bottom/tau type Yukawas: } & 10_{t_i} \cdot \bar{5}_{t_j + t_k} \cdot \bar{5}_{t_l + t_m} \\
\text{with: } & j \neq k \ \text{ and } \ l \neq m
\end{aligned}$$

In order for the top quark to have a tree-level, renormalisable coupling, the diagonal term in the matrix ($10_{t_i} \cdot 10_{t_i} \cdot 5_{-t_j - t_k}$ with $j \neq k$) must have no residual charge under the perpendicular $U(1)$s. Clearly there is no way to achieve this as

$j \neq k$ for the 5 carrying the Higgs. As a consequence we seem to be unable to write down any terms to give a renormalisable top, which is a phenomenologically undesirable feature.

However, in general not all the roots are independent and there will be some monodromy action(s) relating two or more roots. An enlightening yet simple example (following the presentation in [72]) is the minimal monodromy action, which is Z_2. Suppose that two of the roots of the spectral cover found in Equation (2.12) cannot be factorised within the same field as the original coefficients of the equation[2], i.e.

$$C_5 = b_5+b_4 s+b_3 s^2+b_2 s^3+b_1 s^4+b_0 s^5 = (a_1+a_2 s+a_3 s^2)(a_4+a_5 s)(a_6+a_7 s)(a_8+a_9 s)\,. \tag{2.17}$$

The quadratic part of this equation has two roots,

$$r_1 = \frac{-a_2+\sqrt{a_2^2-4a_1a_3}}{2a_3},\; r_2 = \frac{-a_2-\sqrt{a_2^2-4a_1a_3}}{2a_3}, \tag{2.18}$$

which are identical, up to the sign in front of the discriminant. Let $w = a_2^2-4a_1a_3$, then it we may also write, without loss of generality, $w = e^{i\theta}|w|$, which is invariant under $\theta \to \theta + 2\pi$. However, since we deal with $\sqrt{w} = e^{i\theta/2}\sqrt{|w|}$, the roots $r_{1,2}$ are not invariant, but instead interchange $r_1 \leftrightarrow r_2$, implying that the D7-branes associated to those roots are interchangeable under this action. In terms of the top quark coupling, the consequence is that the charge of the 5 carrying the up-type Higgs may have charge $(-t_j - t_k) \to -2t_j$, where the two roots are directly identified.The top quark Yukawa coupling then becomes:

$$10_{t_i} \cdot 10_{t_i} \cdot 5_{-t_i-t_j} \to 10_{t_i} \cdot 10_{t_i} \cdot 5_{-2t_i}\,, \tag{2.19}$$

which is trivially invariant under the perpendicular $U(1)$s allowing a renormalisable top Yukawa.

This example is the simplest and minimal monodromy choice available, how-

[2]Note that due to tracelessness of SU(5), $b_1 = 0$

ever there are a large number of monodromy options. Since we do not have any knowledge of the global geometry, we must select any monodromy groups for our model by hand. In the case of an SU(5) theory, the monodromy group can range from the simple Z_2 case already discussed to the Weyl group of the five weights, S_5. The latter is one of the many non-Abelian monodromy groups, which until the work of [50] had been largely ignored in favour of Abelian alternatives.

When one implements an SU(5) GUT group, the monodromy group could be any subgroup of S_5. In terms of the spectral cover equation, depending on the geometry of the manifold, C_5 will decompose into several factors

$$C_5 = \prod_j C_j, \tag{2.20}$$

where the C_j factors will be non-factorisable.

In this section we shall follow the work published in [1], and consider the case of a Klein Group monodromy $V_4 = Z_2 \times Z_2$ [14, 49, 55, 56, 77]. Interestingly, with this particular spectral cover, there are two ways to implement the monodromy action, depending on whether V_4 is a transitive or non-transitive subgroup of S_4. A significant part of the present chapter will be devoted to the viability of the corresponding two kinds of effective models.

For each of the Klein group monodromies, the implied the splitting of the spectral cover is $C_5 \to C_4 \times C_1$ and $C_5 \to C_2 \times C_2' \times C_1$, for the transitive and non-transitive cases respectively. Assuming the splitting $C_5 \to C_4 \times C_1$, the permutation takes place between the four roots, say $t_{1,2,3,4}$, and the corresponding Weyl group is S_4. Notwithstanding, under specific geometries to be discussed in the subsequent sections, the monodromy may be described by the Klein group $V_4 \in S_4$. The second case, implying the spectral cover factorisation $C_4 \to C_2 \times C_2'$, has two non-trivial identifications acting on the pairs (t_1, t_2) and (t_3, t_4). It transpires that the two scenarios give rise to different properties at the spectral cover level, which are the communicated down to any model one might construct. We will analyse the basic features of these two spectral cover factorisations in the remainder of this chapter.

Cycles	S_4 cycles	Trans. A_4	Trans. V_4
4	(1234), (1243), (1324), (1342), (1423), (1432)	No	No
3	(123), (124), (132), (134), (142), (143), (234), (243)	Yes	No
2+2	(12)(34), (13)(24), (14)(23)	Yes	Yes
2	(12), (13), (14), (23), (24), (34)	No	No
1	e	Yes	Yes

Table 2.2: A summary of the permutation cycles of S_4, categorised by cycle size and whether or not those cycles are contained within the transitive subgroups A_4 and V_4. This also shows that V_4 is necessarily a transitive subgroup of A_4, since it contains all the $2+2$-cycles of A_4 and the identity only.

2.2.1 S_4 Subgroups and Monodromy Actions

The group of all permutations of four elements, S_4, has a total of 24 elements.[3] These include 2,3,4 and 2+2-cycles, all of which are listed in Table 2.2. These cycles form a total of 30 subgroups of S_4, shown in Figure 2.2. Of these there are those subgroups that are transitive subgroups of S_4: the whole group, A_4, D_4, Z_4 and the Klein group.

We focus now on compactification geometries consistent with the Klein group monodromy $V_4 = Z_2 \times Z_2$. We observe that there are three non-transitive V_4 subgroups within S_4 and only one transitive subgroup. This transitive Klein group is the subgroup of the A_4 subgroup. Considering Table 2.2, one can see that A_4 is the group of all even permutations of four elements and the transitive V_4 is that group excluding 3-cycles. The significance of this is that in the case of Galois theory, to be discussed in Section 2.3, the transitive subgroups A_4 and V_4 are necessarily irreducible quartic polynomials, while the non-transitive V_4 subgroups of S_4 should be reducible.

In terms of group elements, the Klein group that is transitive in S_4 has the elements:

$$\{(1), (12)(34), (13)(24), (14)(23)\} \tag{2.21}$$

which are the 2+2-cycles shown in Table 2.2 along with the identity. On the other hand, the non-transitive Klein groups within S_4 are isomorphic to the subgroup

[3]The order of an S_N group is given by $N!$

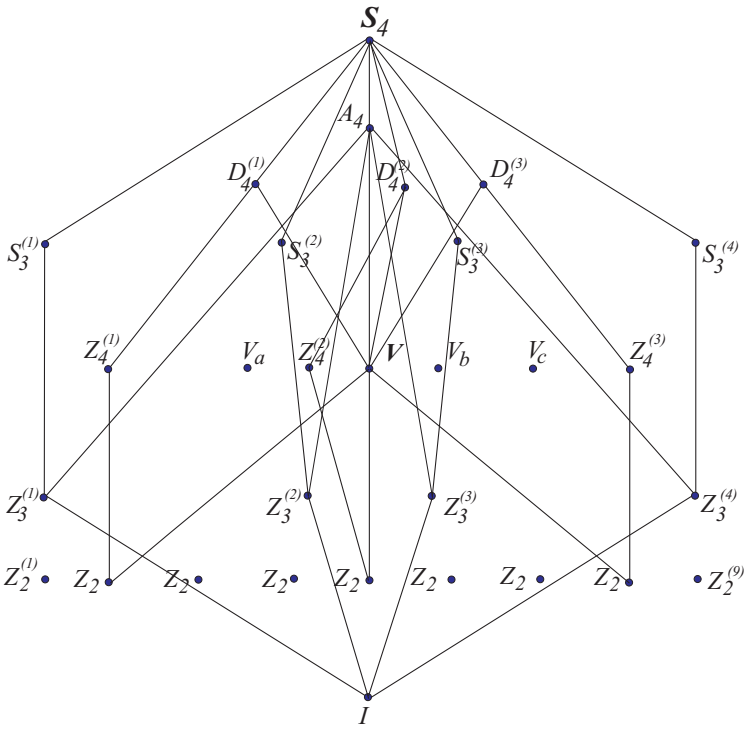

Figure 2.2: Pictorial summary of the subgroups of S_4, the group of all permutations of four elements - representative of the symmetries of a cube.

containing the elements:

$$V_4 = \{(1), (12), (34), (12)(34)\} \tag{2.22}$$

The distinction here is that the group elements are not all within one cycle, since we have two 2-cycles and one 2+2-cycle. These types of subgroup must lead to a factorisation of the quartic polynomial, as we shall discuss in Section 2.3. Referring to Figure 2.2, these Klein groups are the nodes disconnected from the web, while the central V_4 is the transitive group.

2.2.2 Spectral cover factorisation

In this section we will discuss the two possible factorisations of the spectral surface compatible with a Klein Group monodromy, in accordance with the previous analysis. In particular, we shall be examining the implications of a monodromy action that is a subgroup of S_4 - the most general monodromy action relating four weights. In particular we shall be interested in a chain of subgroups, which

we shall treat as a problem in Galois theory:

$$S_4 \to A_4 \to V_4 \tag{2.23}$$

The C_4 spectral cover

This set of monodromy actions require the spectral cover of Equation (2.12) to split into a linear part and a quartic part:

$$\begin{gathered} C_5 \to C_4 \times C_1 \\ C_5 \to (a_5 s^4 + a_4 s^3 + a_3 s^2 + a_2 s + a_1)(a_6 + a_7 s). \end{gathered} \tag{2.24}$$

The $b_1 = 0$ condition must be enforced for SU(5) tracelessness. This can be solved by consistency with Equation (2.24),

$$b_1 = a_5 a_6 + a_4 a_7 = 0\,. \tag{2.25}$$

Let us introduce a new section a_0, enabling one to write a general solution of the form:

$$\begin{aligned} a_4 &= \pm a_0 a_6 \\ a_5 &= \mp a_0 a_7. \end{aligned}$$

Upon making this substitution, the defining equations for the matter curves are:

$$C_5 \; := a_1 a_6 \tag{2.26}$$

$$C_{10} := (a_2^2 a_7 + a_2 a_3 a_6 \mp a_0 a_1 a_6^2)(a_3 a_6^2 + (a_2 a_6 + a_1 a_7) a_7) \tag{2.27}$$

which is the most general, pertaining to an S_4 monodromy action on the roots. By consistency between Equation (2.24) and Equation (2.12), we can calculate

that the homologies of the coefficients are:

$$[a_i] = \eta - (i-6)c_1 - \chi,\ i = 1,2,3,4,5, \tag{2.28}$$

$$[a_6] = \chi,\ [a_7] = c_1 + \chi, \tag{2.29}$$

$$[a_0] = \eta - 2(c_1 + \chi). \tag{2.30}$$

The $C_2 \times C_2' \times C_1$ case

If the V_4 actions are not derived as transitive subgroups of S_4, then the Klein group is isomorphic to:

$$V_4 :\ \{(1), (12), (12)(34), (34)\}. \tag{2.31}$$

This is not contained in A_4, but is admissible from the spectral cover in the form of a monodromy $C_5 \to C_2 \times C_2' \times C_1$.

Then, the $\mathbf{10} \in SU(5)$ GUT ($\in SU(5)_\perp$) spectral cover reads

$$C_5 : (a_1 + a_2 s + a_3 s^2)(a_4 + a_5 s + a_6 s^2)(a_7 + a_8 s) \tag{2.32}$$

We may now match the coefficients of this polynomial in each order in s to the ones of the spectral cover with the b_k coefficients:

$$\begin{aligned} b_0 &= a_{368} \\ b_1 &= a_{367} + a_{358} + a_{268} \\ b_2 &= a_{357} + a_{267} + a_{348} + a_{258} + a_{168} \\ b_3 &= a_{347} + a_{257} + a_{167} + a_{248} + a_{158} \\ b_4 &= a_{247} + a_{157} + a_{148} \\ b_5 &= a_{147} \end{aligned} \tag{2.33}$$

following the notation $a_{ijk} = a_i a_j a_k$ in [49]. In order to find the homology classes of the new coefficients a_i, we match the coefficients of the above polynomial in each order in s to the ones of Equation (2.12) such that we get relations of the

form $b_k = b_k(a_i)$.

Comparing to the homologies of the unsplit spectral cover, a solution for the above can be found for the homologies of a_i. Notice, though, that we have 6 well defined homology classes for b_j with only 8 a_i coefficients, therefore the homologies of a_i are defined up to two homology classes:

$$\begin{aligned} [a_{n=1,2,3}] &= \chi_1 + (n-3)c_1, \\ [a_{n=4,5,6}] &= \chi_2 + (n-6)c_1, \\ [a_{n=7,8}] &= \eta + (n-8)c_1 - \chi_1 - \chi_2. \end{aligned} \tag{2.34}$$

We have to enforce the $SU(5)$ tracelessness condition, $b_1 = 0$. An Ansatz for the solution was put forward in [49],

$$\begin{aligned} a_2 &= -c(a_6 a_7 + a_5 a_8) \\ a_3 &= c a_6 a_8, \end{aligned} \tag{2.35}$$

which introduces a new section, c, whose homology class is completely defined by

$$[c] = -\eta + 2\chi_1. \tag{2.36}$$

With this ansatz for the solution of the splitting of spectral cover, P_{10} reads

$$P_{10} = a_1 a_4 a_7, \tag{2.37}$$

while the P_5 splits into

$$P_5 = a_5(a_6 a_7 + a_5 a_8)(a_6 a_7^2 + a_8(a_5 a_7 + a_4 a_8))(a_1 - a_5 a_7 c), \tag{2.38}$$

$$(a_1^2 - a_1(a_5 a_7 + 2a_4 a_8)c + a_4(a_6 a_7^2 + a_8(a_5 a_7 + a_4 a_8))c^2). \tag{2.39}$$

An extended analysis of this interesting case will be presented in the subsequent sections.

2.3 A little bit of Galois theory

So far, we have outlined the properties of the most general spectral cover with a monodromy action acting on four of the roots of the perpendicular SU(5) group. This monodromy action is the Weyl group S_4, however a subgroup is equally admissible as the action. Transitive subgroups are subject to the theorems of Galois theory, which will allow us to determine what properties the coefficients of the quartic factor of Equation (2.24) must have in order to have roots with a particular symmetry [47]- [3]. In this paper we shall focus on the Klein group, $V_4 \cong Z_2 \times Z_2$. As already mentioned, the transitive V_4 subgroup of S_4 is contained within the A_4 subgroup of S_4, and so shall share some of the same requirements on the coefficients.

While Galois theory is a field with an extensive literature to appreciate, in the current work we need only reference a handful of key theorems. We shall omit proofs for these theorems as they are readily available in the literature and are not required for the purpose at hand.

Theorem 1. *Let K be a field with characteristic different than 2, and let $f(X)$ be a separable, polynomial in $K(X)$ of degree n.*

- *If $f(X)$ is irreducible in $K(X)$ then its Galois group over K has order divisible by n.*
- *The polynomial $f(X)$ is* irreducible *in $K(X)$* if and only if *its Galois group over K is a transitive subgroup of S_n.*

This first theorem offers the key point that any polynomial of degree n, that has non-degenerate roots, but cannot be factorised into polynomials of lower order with coefficients remaining in the same field must necessarily have a Galois group relating the roots that is S_n or a transitive subgroup thereof.

Theorem 2. *Let K be a field with characteristic different than 2, and let $f(X)$ be a separable, polynomial in $K(X)$ of degree n. Then the Galois group of $f(X)$ over K is a subgroup of A_n* if and only if *the discriminant of f is a square in K.*

As already stated, we are interested specifically in transitive V_4 subgroups. Theorem 2 gives us the requirement for a Galois group that is A_4 or its transitive subgroup V_4 - both of which are transitive in S_4. Note that no condition imposed on the coefficients of the spectral cover should split the polynomial ($C_4 \to C_2 \times C_2$), due to Theorem 1. We also know by Theorem 2 that both V_4 and A_4 occur when the discriminant of the polynomial is a square, so we necessarily require another mechanism to distinguish the two.

2.3.1 The Cubic Resolvent

The so-called Cubic Resolvent, is an expression for a cubic polynomial in terms of the roots of the original quartic polynomial we are attempting to classify. The roots of the cubic resolvent are defined to be,

$$x_1 = (t_1t_2 + t_3t_4),\ x_2 = (t_1t_3 + t_2t_4),\ x_3 = (t_1t_4 + t_2t_3) \tag{2.40}$$

and one can see that under any permutation of S_4 these roots transform between one another. However, in the event that the polynomial has roots with a Galois group relation that is a subgroup of S_4, the roots need not all lie within the same orbit. The resolvent itself is defined trivially as:

$$(x-(t_1t_2+t_3t_4))(x-(t_1t_3+t_1t_4))(x-(t_1t_4+t_3t_2)) = g_3x^3+g_2x^2+g_1x+g_0 \tag{2.41}$$

The coefficients of this equation can be determined by relating of the roots to the original $\mathcal{C}_4$ coefficients. This resulting polynomial is:

$$g(x) = a_5^3x^3 - a_3a_5^2x^2 + (a_2a_4 - 4a_1a_5)\,a_5x - a_2^2a_5 + 4a_1a_3a_5 - a_1a_4^2 \tag{2.42}$$

Note that this may be further simplified by making the identification $y = a_5x$.

$$g(y) = y^3 - a_3y^2 + (a_2a_4 - 4a_1a_5)\,y - a_2^2a_5 + 4a_1a_3a_5 - a_1a_4^2 \tag{2.43}$$

Group	Discriminant	Cubic Resolvent
S_4	$\Delta \neq \delta^2$	Irreducible
A_4	$\Delta = \delta^2$	Irreducible
D_4/Z_4	$\Delta \neq \delta^2$	Reducible
V_4	$\Delta = \delta^2$	Reducible

Table 2.3: A summary of the conditions on the partially symmetric polynomials of the roots and their corresponding Galois group.

If the cubic resolvent is factorisable in the field K, then the Galois group does not contain any three cycles. For example, if the Galois group is V_4, then the roots will transform only under the 2+2-cycles:

$$V_4 \subset A_4 = \{(1), (12)(34), (13)(24), (14)(23)\}\,. \tag{2.44}$$

Each of these actions leaves the first of the roots in Equation (2.40) invariant, thus implying that the cubic resolvent is reducible in this case. If the Galois group were A_4, the 3-cycles present in the group would interchange all three roots, so the cubic resolvent is necessarily irreducible. This leads us to a third theorem, which classifies all the Galois groups of an irreducible quartic polynomial (see also Table 2.3).

Theorem 3. *The Galois group of a quartic polynomial $f(x) \in K$, can be described in terms of whether or not the discriminant of f is a square in K and whether or not the cubic resolvent of f is reducible in K.*

2.4 Klein monodromy and the origin of matter parity

In this section we will analyse a class of four-dimensional effective models obtained under the assumption that the compactification geometry induces a $Z_2 \times Z_2$ monodromy. As we have seen in the previous section, there are two distinct ways to realise this scenario, which depends on whether the corresponding Klein group is transitive or non-transitive.

There are significant differences in the phenomenological implications of these models since in a factorised spectral surface matter and Higgs are associated with

different irreducible components [4].

In the present work we will choose to explore the rather promising case where the monodromy Klein group is non-transitive. In other words, this essentially means that the spectral cover admits a $C_2 \times C_2' \times C_1$ factorisation. The case of a transitive Klein group is more involved and it is not easy to obtain a viable effective model.

Hence, turning our attention to the non-transitive case, the basic structure of the model obtained in this case corresponds to one of those initially presented in [14] and subsequently elaborated by other authors [49]- [55]. This model possesses several phenomenologically interesting features and we consider it is worth elaborating it further.

2.4.1 Analysis of the $Z_2 \times Z_2$ model

To set the stage, we first present a short review of the basic characteristics of the model following mainly the notation of [49]. The $Z_2 \times Z_2$ monodromy case implies a $2 + 2 + 1$ splitting of the spectral fifth-degree polynomial which has already been given in Equation (2.32). Under the action Equation (2.31), for each element, either x_2 and x_3 roots defined in Equation (2.40) are exchanged or the roots are unchanged.

The effective model is characterised by three distinct 10 matter curves, and five 5 matter curves. The matter curves, along with their charges under the perpendicular surviving $U(1)$ and their homology classes are presented in table 2.4.

Knowing the homology classes associated to each curve allows us to determine the spectrum of the theory through the units of Abelian fluxes that pierce the matter curves. Namely, by turning on a flux in the $U(1)_X$ directions, we can endow our spectrum with chirality and break the perpendicular group. In order

[4] Further phenomenological issues concerning proton decay and unbroken $U(1)$ factors beyond a local spectral cover can be found in [26, 56].

Curve	$U(1)$ Charge	Defining Equation	Homology Class
10_1	t_1	a_1	$-2c_1 + \chi_1$
10_3	t_3	a_4	$-2c_1 + \chi_2$
10_5	t_5	a_7	$\eta - c_1 - \chi_1 - \chi_2$
5_1	$-2t_1$	$a_6a_7 + a_5a_8$	$\eta - c_1 - \chi_1$
5_{13}	$-t_1 - t_3$	$a_1^2 - a_1(a_5a_7 + 2a_4a_8)c + \ldots$	$-4c_1 + 2\chi_1$
5_{15}	$-t_1 - t_5$	$a_1 - a_5a_7c$	$-2c_1 + \chi_1$
5_{35}	$-t_3 - t_5$	$a_6a_7^2 + a_8(a_5a_7 + a_4a_8)$	$2\eta - 2c_1 - 2\chi_1 - \chi_2$
5_3	$-2t_3$	a_5	$-c_1 + \chi_2$

Table 2.4: Matter curves and their charges and homology classes

to retain an anomaly free spectrum we need to allow for

$$\sum M_5 + \sum M_{10} = 0, \tag{2.45}$$

where M_5 (M_{10}) denote $U(1)_X$ flux units piercing a certain 5 (10) matter curve.

A non-trivial flux can also be turned on along the Hypercharge. This will allow us to split GUT irreducible representations, which will provide a solution for the doublet-triplet splitting problem. In order for the Hypercharge to remain unbroken, the flux configuration should not allow for a Green-Schwarz mass, which is accomplished by

$$F_Y \cdot c_1 = 0,\ F_Y \cdot \eta = 0, \tag{2.46}$$

where F_Y is the hypercharge flux and the dot notation indicates the intersection, with the flux restricting trivially upon the tangent and normal bundles [48].

For the new, unspecified, homology classes, χ_1 and χ_2 we let the flux units piercing them to be

$$F_Y \cdot \chi_1 = N_1,\ F_Y \cdot \chi_2 = N_2, \tag{2.47}$$

where N_1 and N_2 are flux units, and are free parameters of the theory.

For a fiveplet, 5 one can use the above construction to split the doublet and

Curve	Weight	N_Y	N_X	Spectrum
10_1	t_1	N_1	M_{10_1}	$M_{10_1}Q + (M_{10_1} - N_1)u^c + (M_{10_1} + N_1)e^c$
10_3	t_3	N_2	M_{10_3}	$M_{10_3}Q + (M_{10_3} - N_2)u^c + (M_{10_3} + N_2)e^c$
10_5	t_5	$-N$	M_{10_5}	$M_{10_5}Q + (M_{10_5} + N)u^c + (M_{10_5} - N)e^c$
5_1	$-2t_1$	$-N_1$	M_{5_1}	$M_{5_1}\overline{d^c} + (M_{5_1} - N_1)\overline{L}$
5_{13}	$-t_1 - t_3$	$2N_1$	$M_{5_{13}}$	$M_{5_{13}}\overline{d^c} + (M_{5_{13}} + 2N_1)\overline{L}$
5_{15}	$-t_1 - t_5$	N_1	$M_{5_{15}}$	$M_{5_{15}}\overline{d^c} + (M_{5_{15}} + N_1)\overline{L}$
5_{35}	$-t_3 - t_5$	$-N_1 - N$	$M_{5_{35}}$	$M_{5_{35}}\overline{d^c} + (M_{5_{35}} - 2N_1 - N_2)\overline{L}$
5_3	$-2t_3$	N_2	M_{5_3}	$M_{5_3}\overline{d^c} + (M_{5_3} + N_2)\overline{L}$

Table 2.5: Matter curve spectrum. Note that $N = N_1 + N_2$ has been used as short hand.

triplet representations

$$n(3,1)_{-1/3} - n(\overline{3},1)_{1/3} = M_5, \tag{2.48}$$

$$n(1,2)_{1/2} - n(1,2)_{-1/2} = M_5 + N, \tag{2.49}$$

where the states are presented in the SM basis. For a 10 we have

$$n(3,2)_{1/6} - n(\overline{3},2)_{-1/6} = M_{10}, \tag{2.50}$$

$$n(\overline{3},1)_{-2/3} - n(3,1)_{2/3} = M_{10} - N, \tag{2.51}$$

$$n(1,1)_1 - n(1,1)_{-1} = M_{10} + N. \tag{2.52}$$

In the end, given a value for each M_5, M_{10}, N_1, N_2 the spectrum of the theory is fully defined as can be seen in Table 2.5

2.4.2 Matter Parity

Some major issues in supersymmetric GUT model building, including operators leading to fast proton decay and other flavour processes at unacceptable rates, are usually solved by introducing the concept of R-parity. In early F-theory model building [49,51], such matter parity symmetries where introduced by hand. Here, in the present approach, the conjecture is that as in the case of the GUT symmetries which are associated with the manifold singularities, R-parity can also be attributed to the geometric properties of the manifold.

In this work we concentrate on models with matter being distributed on dif-

ferent matter curves in contrast to the models where all three families reside on a single curve. In such models the Higgs field, H_u, is accommodated on a suitable curve so that a tree-level coupling for the up-quark fermion mass matrix is ensured. Similarly, we may require at most one tree level coupling for down-type quarks. Because of $U(1)$ symmetries left over under some chosen monodromy action, all other mass entries are generated at higher orders. However, despite the existence of $U(1)$ symmetries, it is possible that other trilinear (tree-level) couplings among the fermion fields themselves are still allowed in the effective superpotential. In the present $2+2+1$ spectral cover splitting for example, we can see that more than one down-quark type trilinear coupling exists, since any of the following $10_1(\bar{5}_{13}\bar{5}_{35}+\bar{5}_{15}\bar{5}_3)$, $10_3(\bar{5}_{13}\bar{5}_{15}+\bar{5}_1\bar{5}_{35})$ and $10_5(\bar{5}_1\bar{5}_3+\bar{5}_{13}\bar{5}_{13})$ are invariant under all symmetries. A similar picture emerges for the up-quark sector. Such terms are also present in $2+1+1+1$ as well as other splittings as can be easily checked. Assigning the Higgs in the appropriate fiveplet, one of the above terms may account for the quark mass of the third generation. Of course, we might seek appropriate flux parameters to eliminate chiral states on the unwanted fiveplets involved in the remaining terms, but this is not always possible. In such cases additional restrictions are required and a possible solution to this drawback is the concept of R-parity.

In an F-theory framework, we can think of three different ways to introduce R-parity in the model: As a first approach, we may impose, *ad hoc* , a Z_2 symmetry on the grounds of the desired low energy phenomenology. As has already been said, this has been suggested in early F-theory constructions. However, inasmuch as F-theory gauge symmetries are intimately connected to geometric properties, it would be desirable that R-parity has also a geometric origin. A second possibility, then, is to seek such a symmetry within the properties of the spectral cover. Finally, a third way to deal with the annihilation of the perilous Yukawa couplings is to introduce new symmetries emerging from specific elliptic fibrations possessing rational sections. Indeed, these imply the existence of new $U(1)$ symmetries [40] of the Mordell-Weil type, beyond those embedded in the

non-Abelian part. Such symmetries may prevent undesirable terms.

Given the fact that the GUT symmetries in F-theory are associated with geometric singularities, in the present work we think it is also worth exploring the possibility that R-parity may be of a similar nature. Of course, imposing R-parity in a bottom up approach is always possible, however, we will follow the second path and attempt to describe R-parity from geometric symmetries associated with the spectral cover. Such a conjecture might also look *ad hoc* but in the following we will try to give a kind of 'evidence' of this correlation.

It was proposed [58], that in local F-Theory constructions there are geometric discrete symmetries of the spectral cover that manifest on the final field theory. In F-theory the relevant data originate form the geometric properties of the Calabi-Yau four-fold and the G_4-flux. For example, for a surface of the type $S = \mathbb{P}^2$, it was shown in [58] that a Z_2 transformation acting on S generates also a Z_2 transformation on spinors. If this transformation is a symmetry of the specific geometric configuration, it should also be a symmetry of the spectral surface and this is indeed the case.

To be more precise, we analyse this in some detail for the $SU(5)$ group where the spectral surface is described by the equation $\sum_{k=0}^{5} b_k s^{5-k} = 0$. We consider the GUT divisor S_{GUT} and three open patches S, T, U covering S_{GUT}; we define a phase $\phi_N = \frac{2\pi}{N}$ and a map σ_N such that

$$\sigma_N : [S : T : U] \ \rightarrow \ [e^{i\phi_N} S : e^{i\phi_N} T : U]$$

For a Z_2 symmetry discussed in [58] one requires a Z_2 background configuration, with a Z_2 action so that the mapping is

$$\sigma_2 : [S : T : U] \rightarrow [-S : -T : U] \text{ or } [S : T : -U]$$

To see if this is a symmetry of the local geometry for a given divisor, we take local coordinates for the three trivialization patches. These can be defined as $(t_1, u_1) = (T/S, U/S)$, $(s_2, u_2) = (S/T, U/T)$ and $(s_3, t_3) = (S/U, T/U)$. Assuming that

$\sigma_2(p)$, is the map of a point p under σ_2 transformation the corresponding local coordinates are mapped according to

$$\begin{aligned}(t_1, u_1, \xi_s)|_{\sigma_2(p)} &= (t_1, -u_1, -\xi_s)|_p, \\ (s_2, u_2, \xi_t)|_{\sigma_2(p)} &= (s_2, -u_2, -\xi_t)|_p, \\ (s_3, t_3, \xi_u)|_{\sigma_2(p)} &= (-s_3, -t_3, \xi_u)|_p.\end{aligned} \tag{2.53}$$

This is an $SU(3)$ rotation on the three complex coordinates, which acts on the spinors in the same way. Hence, starting from a Z_2 symmetry of the threefold we conclude that a Z_2 transformation is also induced on the spinors. The required discrete symmetry must be a symmetry of the local geometry. This can happen if the defining equation of the spectral surface is left invariant under the corresponding discrete transformation. Consequently we expect non-trivial constraints on the polynomial coefficients b_k, which carry the information of local geometry. In order to extract these constraints we focus on a single trivialization patch and take s to be the coordinate along the fiber. Under the mapping of points $p \to \sigma(p)$ we consider the phase transformation

$$s(\sigma(p)) = s(p)\, e^{i\phi}, \;\; b_k(\sigma(p)) \;=\; b_k(p)\, e^{i(\chi-(6-k)\phi)}.$$

Under this action, each term in the spectral cover equation transforms the same way

$$b_k s^{5-k} \to e^{i(\chi-\phi)} b_k s^{5-k}$$

It can be readily observed that a non-trivial solution accommodates a Z_N symmetry for $\phi = \frac{2\pi}{N}$. Thus, for $N = 2$, we have $\phi = \pi$ and the transformation reduces to

$$s \to -s, \; b_k \to (-1)^k e^{i\chi}\, b_k. \tag{2.54}$$

Further, we may assume that this symmetry is communicated from the $\mathcal{C}_5$ theory to the split spectral cover geometry. On matter curves GUT symmetry is

enhanced while their geometric description is given by the defining equations. Clearly, the properties of their coefficients are determined from b_k's. Our conjecture is that the R-parity is determined in analogy with the bulk surface fields. In this respect, for a Z_2 choice, to all fields residing on a specific matter curve, we assign either even or odd parity in accordance with the property of its corresponding defining equation.

Returning to the present construction, for curves accommodating MSSM chiral matter we will assume that R-parity is defined by the corresponding 'parity' of its defining equation, which is fixed through its relation with the $\mathcal{C}_5$ coefficients. Thus the chiral matter fields on the same matter curve must necessarily have the same parity, since it is a symmetry arising from the matter curve itself. For the specific models of this work, we can use [55] the equations relating

$$b_k \propto a_l a_m a_n, \text{ with } l+m+n=17 \tag{2.55}$$

to find the transformation rules of the a_k such that the spectral cover equation respects the symmetry of Equation (2.55). Consistency with Equation (2.55) implies that the coefficients a_n should transform as

$$a_n \to e^{i\psi_n} e^{i(11/3-n)\phi} a_n. \tag{2.56}$$

We now note that the above transformations can be achieved by a Z_N symmetry if $\phi = 3\frac{2\pi}{N}$. In that case one can find, by looking at the Equation (2.33) for $b_k \propto a_l a_m a_n$ that we have

$$\psi_1 = \psi_2 = \psi_3 \tag{2.57}$$

$$\psi_4 = \psi_5 = \psi_6 \tag{2.58}$$

$$\psi_7 = \psi_8 \tag{2.59}$$

meaning that there are three distinct cycles, and

$$\chi = \psi_1 + \psi_4 + \psi_7. \tag{2.60}$$

Furthermore, the section c introduced to split the matter conditions (2.35) has to transform as

$$c \to e^{i\phi_c} c, \tag{2.61}$$

with

$$\phi_c = \psi_3 - \psi_6 - \psi_7 + \left(-\frac{11}{3} + 11\right)\phi \quad , \quad \phi_c = \psi_2 - \psi_5 - \psi_8 + \left(-\frac{11}{3} + 11\right)\phi. \tag{2.62}$$

We can now deduce what would be the matter parity assignments for Z_2 with $\phi = 3(2\pi/2)$. Let $p(x)$ be the parity of a section (or products of sections), x. We notice that there are relations between the parities of different coefficients, for example one can easily find

$$\frac{p(a_1)}{p(a_2)} = -1 \tag{2.63}$$

amongst others, which allow us to find that all parity assignments depend only on three independent parities

$$p(a_1) = i \tag{2.64}$$

$$p(a_4) = j \tag{2.65}$$

$$p(a_7) = k \tag{2.66}$$

$$p(c) = ijk, \tag{2.67}$$

where we notice that $i^2 = j^2 = k^2 = +$. The parities for each matter curve – both in form of a function of i, j, k and all possible assignments – can are presented in the Table 2.6.

As such, models from $Z_2 \times Z_2$ are completely specified by the information present in Table 2.7.

Curve	Charge	Parity	All possible assignments							
10_1	t_1	i	$+$	$-$	$+$	$-$	$+$	$-$	$+$	$-$
10_3	t_3	j	$+$	$+$	$-$	$-$	$+$	$+$	$-$	$-$
10_5	t_5	k	$+$	$+$	$+$	$+$	$-$	$-$	$-$	$-$
5_1	$-2t_1$	jk	$+$	$+$	$-$	$-$	$-$	$-$	$+$	$+$
5_{13}	$-t_1-t_3$	$+$	$+$	$+$	$+$	$+$	$+$	$+$	$+$	$+$
5_{15}	$-t_1-t_5$	i	$+$	$-$	$+$	$-$	$+$	$-$	$+$	$-$
5_{35}	$-t_3-t_5$	j	$+$	$+$	$-$	$-$	$+$	$+$	$-$	$-$
5_3	$-2t_3$	$-j$	$-$	$-$	$+$	$+$	$-$	$-$	$+$	$+$

Table 2.6: All possible matter parity assignments

Curve	Charge	Matter Parity	Spectrum
10_1	t_1	i	$M_{10_1}Q+(M_{10_1}-N_1)u^c+(M_{10_1}+N_1)e^c$
10_3	t_3	j	$M_{10_3}Q+(M_{10_3}-N_2)u^c+(M_{10_3}+N_2)e^c$
10_5	t_5	k	$M_{10_5}Q+(M_{10_5}+N_1+N_2)u^c+(M_{10_5}-N_1-N_2)e^c$
5_1	$-2t_1$	jk	$M_{5_1}\overline{d^c}+(M_{5_1}-N_1)\overline{L}$
5_{13}	$-t_1-t_3$	$+$	$M_{5_{13}}\overline{d^c}+(M_{5_{13}}+2N_1)\overline{L}$
5_{15}	$-t_1-t_5$	i	$M_{5_{15}}\overline{d^c}+(M_{5_{15}}+N_1)\overline{L}$
5_{35}	$-t_3-t_5$	j	$M_{5_{35}}\overline{d^c}+(M_{5_{35}}-2N_1-N_2)\overline{L}$
5_3	$-2t_3$	$-j$	$M_{5_3}\overline{d^c}+(M_{5_3}+N_2)\overline{L}$

Table 2.7: All the relevant information for model building with $Z_2\times Z_2$ monodromy

2.4.3 The Singlets

In the context of F-theory GUTs, the local geometry cannot tell us everything about the singlets of the theory, however using the spectral cover formalism it is possible to be consistent in our discussion of these fields. For the singlets on the GUT surface we start by looking at the splitting equation for singlet states, P_0. For $SU(5)$ these are found to be

$$\begin{aligned}P_0 = {} & 3125b_5^4b_0^4+256b_4^5b_0^3-3750b_2b_3b_5^3b_0^3+2000b_2b_4^2b_5^2b_0^3+2250b_3^2\\ & b_4b_5^2b_0^3-1600b_3b_4^3b_5b_0^3-128b_2^2b_4^4b_0^2+144b_2b_3^2b_4^3b_0^2-27b_3^4b_4^2b_0^2+825\\ & b_2^2b_3^2b_5^2b_0^2-900b_2^3b_4b_5^2b_0^2+108b_3^5b_5b_0^2+560b_2^2\\ & b_3b_4^2b_5b_0^2-630b_2b_3^3b_4b_5b_0^2+16b_2^4b_4^3b_0-4b_2^3b_3^2b_4^2b_0+108b_2^5b_5^2b_0\\ & +16b_2^3b_3^3b_5b_0-72b_2^4b_3b_4b_5b_0\end{aligned} \tag{2.68}$$

Applying the solution for the $Z_2\times Z_2$ monodromy from Eq.(2.34,2.35) the

above splits into 13 factors as follows

$$P_0 = a_6^2 a_8^2 c \left(a_5^2 - 4a_4 a_6\right) \left(a_8(a_4 a_8 - a_5 a_7) + a_6 a_7^2\right)^2$$
$$\left(c(a_5 a_8 + a_6 a_7)^2 - 4a_1 a_6 a_8\right) \left(a_1 a_8 + a_7 c(a_5 a_8 + 2a_6 a_7)\right)^2$$
$$\left(a_1^2 a_6 + a_1 c\left(-2a_4 a_6 a_8 + 2a_5^2 a_8 + a_5 a_6 a_7\right) + a_4 c^2\left(a_6 a_8(a_4 a_8 + 3a_5 a_7) + 2a_5^2 a_8^2 + a_6^2 a_7^2\right)\right)^2 \tag{2.69}$$

Their homologies and geometric parities can be founded by applying the results from the previous section, and are presented in Table 2.8. Note that three of the factors arising must have a charge of zero, indicating that they are not localised on the GUT surface.

Equation	Power	Charge	Homology Class	Matter Parity
a_6	2	$\pm(t_1 - t_3)$	χ_2	j
a_8	2	$\pm(t_1 - t_5)$	$\eta - \chi_1 - \chi_2$	$-k$
c	1	0	$-\eta + 2\chi_1$	ijk
$a_5^2 - \ldots$	1	0	$-2c_1 + \chi_2$	$+$
$a_8(a_4 a_8 - \ldots$	2	$\pm(t_3 - t_5)$	$2\eta - 2c_1 - 2\chi_1 - \chi_2$	j
$c(a_5 a_8 + \ldots$	1	0	$\eta - 2c_1$	ijk
$(a_1 a_8 + \ldots$	2	$\pm(t_1 - t_5)$	$\eta - 2c_1 - \chi_2$	$-ik$
$(a_1^2 a_6 + \ldots$	2	$\pm(t_1 - t_3)$	$-4c_1 + 2\chi_1 + \chi_2$	j

Table 2.8: Defining equations, multiplicity, homologies, matter parity, and perpendicular charges of singlet factors

2.4.4 Application of Geometric Matter Parity

We study now the implementation of the explicit $Z_2 \times Z_2$ monodromy model presented in [49] alongside the matter parity proposed above. The model under consideration is defined by the flux data

$$N_1 = M_{5_{15}} = M_{5_{35}} = 0, \tag{2.70}$$
$$N_2 = M_{10_3} = M_{5_1} = 1 = -M_{10_5} = -M_{5_3}, \tag{2.71}$$
$$M_{10_1} = 3 = -M_{5_{13}}, \tag{2.72}$$

which leads to the spectrum presented in Table 2.9 alongside all possible geometric parities.

Curve	Charge	Spectrum	All possible assignments							
10_1	t_1	$3Q + 3u^c + 3e^c$	+	−	+	−	+	−	+	−
10_3	t_3	$Q + 2e^c$	+	+	−	−	+	+	−	−
10_5	t_5	$-Q - 2e^c$	+	+	+	+	−	−	−	−
5_1	$-2t_1$	$D_u + H_u$	+	+	−	−	−	−	+	+
5_{13}	$-t_1 - t_3$	$-3\overline{d^c} - 3\overline{L}$	+	+	+	+	+	+	+	+
5_{15}	$-t_1 - t_5$	0	+	−	+	−	+	−	+	−
5_{35}	$-t_3 - t_5$	$-\overline{H}_d$	+	+	−	−	+	+	−	−
5_3	$-2t_3$	$-\overline{D}_d$	−	−	+	+	−	−	+	+

Table 2.9: Spectrum and allowed geometric parities for the $Z_2 \times Z_2$ monodromy model

Name	Charge	All possible assignments							
θ_1	$\pm(t_1 - t_3)$	+	+	−	−	+	+	−	−
θ_2	$\pm(t_1 - t_5)$	−	−	−	−	+	+	+	+
θ_3	0	+	−	−	+	−	+	+	−
θ_4	0	+	+	+	+	+	+	+	+
θ_5	$\pm(t_3 - t_5)$	+	+	−	−	+	+	−	−
θ_6	0	+	−	−	+	−	+	+	−
θ_7	$\pm(t_1 - t_5)$	−	+	−	+	+	−	+	−
θ_8	$\pm(t_1 - t_3)$	+	+	−	−	+	+	−	−

Table 2.10: Singlet curves and their perpendicular charges and geometric parity. Note that singlets with zero charge are necessarily not localised on the GUT surface.

Inspecting Table 2.9 one can arrive at some conclusions. For example, looking at the spectrum from each curve it's immediate that all matter is contained in 10_1 and 5_{13}, while the Higgs fields come from 5_1 and 5_{35}, and the rest of the states are exotics that come in vector-like pairs. Immediately we see that there will be R-Parity violating terms since 5_{13} has positive parity.

In order to fully describe the model one also has to take into account the singlets, whose perpendicular charges and all possible geometric parities can be seen in Table 2.10, where the charge conjugated partner is included in the same row - i.e. θ_i has the same parity as $\overline{\theta}_i$.

Note that not all the factors of Equation (2.69) appear to be singlets incident

at points on the GUT divisor. In particular, the fields associated to the factors c, $a_5^2 - \ldots$ and $c(a_5 a_8 + \ldots$ are uncharged under the perpendicular group weights. As such these cannot be incident upon the GUT surface and we shall not consider them to participate in any couplings for the rest of this work.

Of the possible combinations $\{i, j, k\}$ for the geometric parity assignments, the only choices that allow for a tree-level top quark mass are:

$$\begin{aligned} \{i, j, k\} &= \{+, +, +\} \\ \{i, j, k\} &= \{-, +, +\} \\ \{i, j, k\} &= \{+, -, -\} \\ \{i, j, k\} &= \{-, -, -\} \end{aligned} \tag{2.73}$$

The option that most closely resembles the R-parity imposed in the model [49] corresponds to the choice $i = -$, $j = k = +$. However, if R-parity has a geometric origin the parity assignments of matter curves cannot be arbitrarily chosen. Using the Mathematica package presented in [78], it is straight forward to produce the spectrum of operators up to an arbitrary mass dimension. One can readily observe that its implementation allows a number of operators that could cause Bilinear R-Parity Violation (BRPV) at unacceptably high rates. For example, the lowest order operators are:

$$H_u L\theta_1,\ H_u L\theta_5,\ H_u L\theta_1\theta_4,\ H_u L\theta_4\theta_8,\ H_u L\overline{\theta}_3\theta_4 \tag{2.74}$$

with higher order operators also present, amplifying the scale of the problem. In order to avoid problems, we must forbid vacuum expectations for a number of singlets. This does not immediately appear to be a model killing issue, however we must look to the exotic masses. Considering the Higgs triplets $D_{u/d}$, the only

mass terms are:

$$D_u D_d \theta_1 \theta_1 \theta_3,\ D_u D_d \theta_1 \theta_1 \theta_6,\ D_u D_d \theta_1 \theta_2 \overline{\theta}_5,\ D_u D_d \theta_1 \theta_3 \theta_8,$$
$$D_u D_d \theta_1 \theta_6 \theta_8,\ D_u D_d \theta_2 \overline{\theta}_5 \theta_8,\ D_u D_d \theta_3 \theta_8 \theta_8,\ D_u D_d \theta_6 \theta_8 \theta_8 \tag{2.75}$$

As can be seen each of these terms contains θ_1 or θ_8. Since these are required to have no vacuum expectation value, it follows that the Higgs triplets cannot become massive. Since this is a highly disfavoured feature, we must rule out this model.

It transpires that in a similar way, all the models with this flux assignment must be ruled out when we apply this geometric parity. This is due to the tension between BRPV terms and exotic masses, which seem to always be at odds in models with this novel parity. This motivates one to search for models without any exotics, as these models will not have any constraining features coming from exotic masses, and we shall analyse one such model in the subsequence.

2.5 Deriving the MSSM with the seesaw mechanism

The parameter space of models is very large, given the number of reasonable combinations of fluxes, multiplicities and choices of geometric parities. There are a number of ways to narrow the parameter space of any search, for example requiring that there be no exotics present in the spectrum, or contriving there to be only one tree-level Yukawa coupling to enable a heavy top quark. Furthermore, the observed large hierarchy of the up-quark mass spectrum emerges naturally from a rank one mass matrix and this means that the associated gauge invariant term $10_{t_i} 10_{t_j} 5_{-t_i - t_j}$ can account for it only under a monodromy action such that two matter curves are identified $t_i = t_j$.

We note however that in general monodromies allow more than one tree-level coupling in the superpotential and therefore it is necessary to implement some form of R-parity or matter parity in F-theory GUT models. For example in [49, 51], the authors add such a parity by hand, protecting the models they

Curve	Charge	Matter Parity	Spectrum
10_1	t_1	$-$	$Q_3 + Q_2 + u_3^c + 3e^c$
10_3	t_3	$+$	$-$
10_5	t_5	$-$	$Q_1 + u_2^c + u_1^c$
5_1	$-2t_1$	$-$	$-\overline{L}_1$
5_{13}	$-t_1 - t_3$	$+$	$2H_u$
5_{15}	$-t_1 - t_5$	$-$	$-\overline{d}_2^c - \overline{d}_1^c - \overline{L}_2$
5_{35}	$-t_3 - t_5$	$+$	$-2\overline{H}_d$
5_3	$-2t_3$	$-$	$-\overline{d}_3^c - \overline{L}_3$
$1_{15} = \theta_7$	$t_1 - t_5$	$-$	N_R^a
$1_{51} = \overline{\theta}_7$	$t_5 - t_1$	$-$	N_R^b

Table 2.11: Matter content for a model with the standard matter parity arising from a geometric parity assignment.

present from dangerous operators allowed in supersymmetric SU(5) GUTs - for example trilinear R-parity violating terms.

Let us make a choice for the flux parameters and phases that enables the implementation of a standard matter parity:

$$\begin{aligned} &\{N_1 = 1, N_2 = 0\} \\ &M_{10_1} = -M_{5_{13}} = 2 \\ &M_{10_5} = -M_{5_3} = 1 \\ &M_{10_3} = M_{5_1} = M_{5_{15}} = M_{5_{35}} = 0 \\ &i = -j = k = - \end{aligned} \tag{2.76}$$

The matter spectrum of this model is summarised in Table 2.11. With this choice, Table 2.10 will select the column with only the singlets θ_7 and $\overline{\theta}_7$ having a negative matter parity. Provided this singlet does not acquire a vacuum expectation it will then be impossible for Bilinear R-parity violating terms due to the nature of the parity assignments. This will also conveniently give us candidates for right-handed neutrinos, θ_7 and $\overline{\theta}_7$.

2.5.1 Yukawas

Having written down a spectrum that has the phenomenologically preferred R-parity, we must now examine the allowed couplings of the model. The model only allows Yukawa couplings to arise at non-renormalisable levels, however the resulting couplings give rise to rank three mass matrices. This is because the perpendicular group charges must be canceled out in any Yukawa couplings. For example, the Yukawa arising from $10_1 \cdot 10_1 \cdot 5_{13}$ has a charge $t_1 - t_3$, which may be canceled by the $\theta_{1/8}$ singlets. Consider the Yukawas of the Top sector,

$$\begin{aligned} 10_1 \cdot 10_1 \cdot 5_{13} \cdot (\overline{\theta}_1 + \overline{\theta}_8) &\rightarrow (Q_3 + Q_2) u_3 H_u (\overline{\theta}_1 + \overline{\theta}_8) \\ 10_1 \cdot 10_5 \cdot 5_{13} \cdot \theta_5 &\rightarrow ((Q_3 + Q_2)(u_1 + u_2) + Q_1 u_3) H_u \theta_5 \\ 10_5 \cdot 10_5 \cdot 5_{13} \cdot \theta_2 \cdot \theta_5 &\rightarrow Q_1 (u_1 + u_2) H_u \theta_2 \theta_5 \end{aligned} \tag{2.77}$$

where the numbers indicate generations (1, 2 and 3). The resulting mass matrix should be rank three, however the terms will not all be created equally and the rank theorem [35] should lead to suppression of operators arising from the same matter curve combination[5]:

$$M_{u,c,t} \sim v_u \begin{pmatrix} \epsilon\theta_2\theta_5 & \theta_2\theta_5 & \theta_5 \\ \epsilon^2\theta_5 & \epsilon\theta_5 & \epsilon(\overline{\theta}_1 + \overline{\theta}_8) \\ \epsilon\theta_5 & \theta_5 & \overline{\theta}_1 + \overline{\theta}_8 \end{pmatrix} \tag{2.78}$$

where each element of the matrix has some arbitrary coupling constant. We use here ϵ to denote suppression due to the effects of the Rank Theorem [35] for Yukawas arising from the same GUT operators. The lightest generation will have the lightest mass due to an extra GUT scale suppression arising from the second singlet involved in the Yukawa. There are a large number of corrections at higher orders in singlet VEVs, which we have not included here for brevity. These corrections will also be less significant compared to the lowest order contributions.

[5] The rank theorem of [35] states that for multiple generations of matter on the same matter curve, only one generation gets a yukawa coupling at leading order. We refer the reader to [35] for the details, however in short one can expect the remaining generations to be suppressed, naturally giving a hierarchical structure.

In a similar way, the Down-type Yukawa couplings arise as non-renormalisable operators, coming from four different combinations. The operators for this sector often exploit the tracelessness of SU(5), so that the sum of the GUT charges must vanish. The leading order Yukawa operators,

$$\begin{aligned} 10_1 \cdot \overline{5}_3 \cdot \overline{5}_{35} \cdot (\theta_1 + \theta_8) &\to (Q_3 + Q_2) d_3 H_d (\theta_1 + \theta_8) \\ 10_1 \cdot \overline{5}_{15} \cdot \overline{5}_{35} \cdot \theta_5 &\to (Q_3 + Q_2)(d_1 + d_2) H_d \theta_5 \\ 10_5 \cdot \overline{5}_3 \cdot \overline{5}_{35} \cdot (\theta_1 + \theta_8)\theta_2 &\to Q_1 d_3 H_u (\theta_1 + \theta_8)\theta_2 \\ 10_5 \cdot \overline{5}_{15} \cdot \overline{5}_{35} \cdot \theta_2 \cdot \theta_5 &\to Q_1 (d_1 + d_2) H_u \theta_2 \theta_5 \end{aligned} \tag{2.79}$$

The resulting mass matrix will, like in the Top sector, be a rank three matrix, with a similar form:

$$M_{d,s,b} \sim v_d \begin{pmatrix} \epsilon\theta_2\theta_5 & \theta_2\theta_5 & (\theta_1 + \theta_8)\theta_2 \\ \epsilon^2\theta_5 & \epsilon\theta_5 & \epsilon(\theta_1 + \theta_8) \\ \epsilon\theta_5 & \theta_5 & \theta_1 + \theta_8 \end{pmatrix} \tag{2.80}$$

The structure of the Top and Bottom sectors appears to be quite similar in this model, which should provide a suitable hierarchy to both sectors.

The Charged Leptons will have a different structure to the Bottom-type quarks in this model, due primarily to the fact the e_i^c matter is localised on one GUT tenplet. The Lepton doublets however all reside on different $\overline{5}$ representations, which will fill out the matrix in a non-trivial way, with the operators:

$$\begin{aligned} 10_1 \cdot \overline{5}_3 \cdot \overline{5}_{35} \cdot (\overline{\theta}_1 + \overline{\theta}_8) &\to L_3 (e_1^c + e_2^c + e_3^c) H_d (\overline{\theta}_1 + \overline{\theta}_8) \\ 10_1 \cdot \overline{5}_{15} \cdot \overline{5}_{35} \cdot \theta_5 &\to L_2 (e_1^c + e_2^c + e_3^c) H_d \theta_5 \\ 10_1 \cdot \overline{5}_1 \cdot \overline{5}_{35} \cdot (\theta_1 + \theta_8) &\to L_1 (e_1^c + e_2^c + e_3^c) H_d (\theta_1 + \theta_8) \end{aligned} \tag{2.81}$$

The mass matrix for the Charged Lepton sector will be subject to suppressions arising due to the effects discussed above.

2.5.2 Neutrino Masses

The spectrum contains two singlets that do not have vacuum expectation values, which protects the model from certain classes of dangerous operators. These singlets, $\theta_7/\overline{\theta}_7$, also serve as candidates for right-handed neutrinos. Let us make the assignment $\theta_7 = N_R^a$ and $\overline{\theta}_7 = N_R^b$. This gives Dirac masses from two sources, the first of which involve all lepton doublets and N_R^a:

$$\begin{aligned} \overline{5}_3 \cdot 5_{13} \cdot \theta_7 \cdot \overline{\theta}_5 &\to L_3 N_R^a H_u \overline{\theta}_5 \\ \overline{5}_{15} \cdot 5_{13} \cdot \theta_7 \cdot (\overline{\theta}_1 + \overline{\theta}_8) &\to L_2 N_R^a H_u (\overline{\theta}_1 + \overline{\theta}_8) \\ \overline{5}_1 \cdot 5_{13} \cdot \theta_7 \cdot (\overline{\theta}_1 + \overline{\theta}_8) \cdot \theta_2 &\to L_1 N_R^a H_u (\overline{\theta}_1 + \overline{\theta}_8)\theta_2 \end{aligned} \tag{2.82}$$

This generates a hierarchy for neutrinos, however the effect will be mitigated by the operators arising from the N_R^b singlet:

$$\begin{aligned} \overline{5}_3 \cdot 5_{13} \cdot \overline{\theta}_7 \cdot (\overline{\theta}_1 + \overline{\theta}_8) \cdot \theta_2 &\to L_3 N_R^b H_u (\overline{\theta}_1 + \overline{\theta}_8)\theta_2 \\ \overline{5}_{15} \cdot 5_{13} \cdot \overline{\theta}_7 \cdot \theta_2 \cdot \theta_5 &\to L_2 N_R^b H_u \theta_2 \theta_5 \\ \overline{5}_1 \cdot 5_{13} \cdot \overline{\theta}_7 \cdot \theta_5 &\to L_1 N_R^b H_u \theta_5 \end{aligned} \tag{2.83}$$

If all these Dirac mass operators are present in the low energy spectrum, then the neutrino sector should have masses that mix greatly. This is compatible with our understanding of neutrinos from experiments, which requires large mixing angles compared to the other sectors.

A light mass scale for the neutrinos can be generated using the seesaw mechanism [79], which requires large right-handed Majorana masses to generate light physical left-handed Majorana neutrino mass at low values. The singlets involved in this scenario has perpendicular charges that must be canceled out, as with the quark and charged lepton operators. Fortunately, this can be achieved, in part due to the presence of $\theta_2/\overline{\theta}_2$, which have the same charge combinations as $N_R^{a,b}$. The leading contribution to the mass term will come from the off diagonal $\theta_7\overline{\theta}_7$

term, however there are diagonal contributions:

$$\frac{\langle\theta_2\rangle^2}{\Lambda}\overline{\theta}_7^2 \;+\; \frac{\langle\overline{\theta}_2\rangle^2}{\Lambda}\theta_7^2 \;+\; M\theta_7\overline{\theta}_7 \tag{2.84}$$

Two right-handed neutrinos are sufficient to generate the appropriate physical light masses for the neutrinos required by experimental constraints [80, 81].

2.5.3 Other Features

An interesting property of this model is the requirement of extra Higgs fields. Due to the flux factors, under doublet-triplet splitting it is necessary to have two copies of the up and down-type Higgs. This insures that the model is free of Higgs colour triplets, D_u/D_d in the massless spectrum, while also allowing the designation of + parity to Higgs matter curves. As a consequence of this, the μ-term for the Higgs mass would seem to give four Higgs operators of the same mass: $M_{ij}H_u^iH_d^j$, with $i,j=1,2$. However, since for both the up and down-types there are two copies on the matter curve, we can call upon the rank theorem [35]. Consider the operator for the μ-term:

$$5_{13}\cdot\overline{5}_{35}\cdot\theta_2 \to M_{ij}H_u^iH_d^j \to M\begin{pmatrix}\epsilon_h^2 & \epsilon_h\\ \epsilon_h & 1\end{pmatrix}\begin{pmatrix}H_u^1\\ H_u^2\end{pmatrix}\begin{pmatrix}H_d^1 & H_d^2\end{pmatrix} \tag{2.85}$$

This operator will give a mass that is naturally large for one generation of the Higgs, while the second mass should be suppressed due to non-perturbative effects. This is parameterised by ϵ_h, which is required to be sufficiently small as to allow a Higgs to be present at the electroweak scale, while the leading order Higgsl must be heavy enough to remain at a reasonably high scale and not prevent unification. Thus we should have a light Higgs boson as well as a heavier copy that is as of yet undetected.

The spectrum is free of the Higgs colour triplets D_u/D_d, however we must still consider operators of the types $QQQL$ and $d^cu^cu^ce^c$, since the colour triplets may appear in the spectrum at the string scale. Of these types of operator, most are forbidden at leading order due to the charges of the perpendicular group.

However, one operator is allowed and we must consider this process:

$$10_1 10_1 10_5 \overline{5}_3 \rightarrow (Q_3 + Q_2)(Q_3 + Q_2)Q_1 L_3 + (u_2^c + u_1^c)u_3^c d_3^c (e_1^c + e_2^c + e_3^c) \quad (2.86)$$

None of the operators arising are solely first generation matter, however due to mixing they may contribute to any proton decay rate. The model in question only has one of each type of Higgs matter curve, which means any colour triplet partners must respect the perpendicular charges of those curves. The result of this requirement is that the vertex between the initial quarks and the D_u colour triplet must also include a singlet to balance the charge, with the same requirement for the final vertex. The resulting operator should be suppressed by some high scale where the colour triplets are appearing in the spectrum - Λ_s. The most dangerous contribution of this operator can be assume to be the $Q_2 Q_1 Q_2 L_3$ component, which will mix most strongly with the lightest generation. It can be estimated that, given the quark mixing and the mixing structure of the charged Leptons in particular, the suppression scale should be in the region $\sim 10^{4-6}\Lambda_s$. This estimate seems to place the suppression of proton decay at too small a value, though not wildly inconsistent.

However, if we consider Figure 2.3, we can see that while the external legs of this process give an overall adherence to the charges of the perpendicular group charges, the vertices require singlet contributions. For example, the first vertex is $Q_2 Q_1 D_u \theta_5$, which is non-renormalisable and we cannot write down a series of renormalisable operators to mediate this effective operator. This is because the combination of perpendicular group and GUT charges constrain heavily the operators we can write down, which means proton decay can be seen to be suppressed here by the dynamics as well as the symmetries required by the F-theory formalism. The full determination of the coupling strengths of any process of this type in F-theory should be found through computing the overlap integral of the wavefunctions involved [38], and this will be discussed in upcoming work on R-parity violating processes.

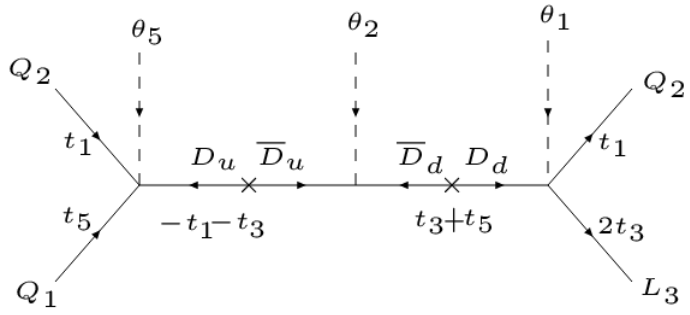

Figure 2.3: Proton Decay graph

2.6 Conclusions

We have revisited a class of $SU(5)$ SUSY GUT models which arise in the context of the spectral cover with Klein Group monodromy $V_4 = Z_2 \times Z_2$. By investigating the symmetry structures of the spectral cover equation and the defining equations of the mater curves it is possible to understand the F-theory geometric origin of matter parity, which has hitherto been just assumed in an *ad hoc* way. In particular, we have shown how the simplest Z_2 matter parities can be realised via the new geometric symmetries respected by the spectral cover. By exploiting the various ways that these symmetries can be assigned, there are a large number of possible variants.

We have identified a rather minimal example of this kind, where the low energy effective theory below the GUT scale is just the MSSM with no exotics and standard matter parity. Furthermore, by deriving general properties of the singlet sector, consistent with string vacua, including the D and F-flatness conditions, we were able to identify two singlets, which provide suitable candidates for a two right-handed neutrinos. We were thus able to derive the MSSM extended by a two right-handed neutrino seesaw mechanism. We also computed all baryon and lepton number violating operators emerging from higher non-renormalisable operators and found all dangerous operators to be forbidden.

Chapter 3

A_4 as a monodromy group and family symmetry in F-theory

In the literature, there are a great many works that utilise the extra U(1)s of F-theory, along with Abelian Z_N monodromies to construct models with realistic quark and lepton mass hierarchies – for example [47, 49, 58]. While it is gratifying that such symmetries can arise from a string derived model, where the parameter space is subject to constraints from the first principles of the theory, the possibility of having only continuous Abelian family symmetry in F-theory represents a very restrictive choice. By contrast, other string theories have a rich group structure embodying both continuous and discrete symmetries at the same time [82]- [83]. It may be regarded as something of a drawback of the F-theory approach that the family symmetry is constrained to be a product of $U(1)$ symmetries. Indeed the results of the neutrino oscillation experiments are in agreement with an almost maximal atmospheric mixing angle θ_{23}, a large solar mixing θ_{12}, and a non-vanishing but smaller reactor angle θ_{13}, all of which could be explained by an underlying non-Abelian discrete family symmetry (for recent reviews see for example [84–86]).

Recently, discrete symmetries in F-theory have been considered [50] on an elliptically fibered space with an $SU(5)$ GUT singularity, where the effective theory is invariant under a more general non-Abelian finite group. They considered all

possible monodromies that induce an additional discrete (family-type) symmetry on the model. For the $SU(5)$ GUT minimal unification scenario in particular, the accompanying discrete family group could be any subgroup of the S_5 permutation symmetry, and the spectral cover geometries with monodromies associated to the finite symmetries S_4, A_4 and their transitive subgroups, including the dihedral group D_4 and $Z_2 \times Z_2$, were discussed. However a detailed analysis was only presented for the $Z_2 \times Z_2$ case, while other cases such as A_4 were not fully developed into a realistic model.

In this chapter we extend the analysis in [50] in order to construct realistic models based on the case of A_4, combined with $SU(5)$ GUT, comparing our results to existing field theory models based on these groups. We provide an explicit calculation to support the emergence of the family symmetry as from the discrete monodromies. We shall discuss the conditions for the transition of S_4 to A_4 discrete family symmetry "escorting" the $SU(5)$ GUT and propose a discrete version of the doublet-triplet splitting mechanism for A_4, before constructing a realistic model which is analysed in detail.

Considering the case of an A_4 monodromy, we must consider that the spectral cover equation, C_5, should be separable in the following two factors as in Equation (2.27).

This implies the 'breaking' of the $SU(5)_\perp$ to the monodromy group S_4, (or one of its subgroups such as A_4), described by the fourth degree polynomial

$$C_4 : \qquad \sum_{k=1}^{5} a_k s^{k-1} = 0 \tag{3.1}$$

and a $U(1)$ associated with the linear part. New and old polynomial coefficients satisfy simple relations $b_k = b_k(a_i)$ which can be easily extracted comparing by consistency of Equation (2.27) with the unsplit spectral cover. Table 3.1 summarizes the relations between the coefficients of the unfactorised spectral cover and the a_j coefficients for the cases under consideration in the present work.

The homologies of the coefficients b_i are given in terms of the first Chern class

b_i	a_j coefficients for 4+1	a_j coefficients for 3+2	a_j coefficients for 3+1+1
b_0	a_5a_7	a_4a_7	$a_4a_6a_8$
b_1	$a_5a_6 + a_4a_7$	$a_4a_6 + a_3a_7$	$a_4a_6a_7 + a_4a_5a_8 + a_3a_6a_8$
b_2	$a_4a_6 + a_3a_7$	$a_4a_5 + a_3a_6 + a_2a_7$	$a_4a_5a_7 + a_3a_5a_8 + a_3a_6a_7 + a_2a_6a_8$
b_3	$a_3a_6 + a_2a_7$	$a_3a_5 + a_2a_6 + a_1a_7$	$a_3a_5a_7 + a_2a_5a_8 + a_2a_6a_7 + a_1a_6a_8$
b_4	$a_2a_6 + a_1a_7$	$a_2a_5 + a_1a_6$	$a_2a_5a_7 + a_1a_6a_7 + a_1a_5a_8$
b_5	a_1a_6	a_1a_5	$a_1a_5a_7$

Table 3.1: table showing the relations $b_i = b_i(a_j)$ between coefficients of the spectral cover equation under various decompositions from the unfactorised equation.

of the tangent bundle (c_1) and of the normal bundle ($-t$), which can be found in Equation (2.13).

We may use these to calculate the homologies $[a_j]$ of our a_j coefficients, since if $b_i = a_j a_k \ldots$ then $[b_i] = [a_j] + [a_k] + \ldots$, allowing us to rearrange for the required homologies. Note that since we have in general more a_j coefficients than our fully determined b_i coefficients, the homologies of the new coefficients cannot be fully determined. For example, if we factorise in a $3 + 1 + 1$ arrangement, we must have 3 unknown parameters, which we call $\chi_{k=1,2,3}$. In the following sections we will examine in detail the predictions of the A_4 model.

3.1 A_4 models in F-theory

We assume that the spectral cover equation factorises to a quartic polynomial and a linear part, as shown in Equation (2.24). The homologies of the new coefficients may be derived from the original b_i coefficients. Referring to Table 3.1, we can see that the homologies for this factorisation are easily calculable, up to some arbitrariness of one of the coefficients - we have seven a_j and only six b_i. We choose $[a_6] = \chi$ in order to make this tractable. It can then be shown that the homologies are those of Equation (2.28).

After referring to Table 3.1, we see that $P_{10} = a_1 a_6 = 0$. Therefore there are two tenplet matter curves, whose homologies are given by those of a_1 and a_6. We shall assume at this point that these are the only two distinct curves, though a_1 appears to be associated with S_4 (or a subgroup) and hence should be reducible in terms of representations of the monodromy group, since a quadruplet is not an

Curve	Equation	Homology	Hyperflux - N	Multiplicity
10_a	a_1	$\eta - 5c_1 - \chi$	$-N$	M_{10_a}
10_b	a_6	χ	$+N$	M_{10_b}
5_c	$a_2^2 a_7 + a_2 a_3 a_6 \mp a_0 a_1 a_6^2$	$2\eta - 7c_1 - \chi$	$-N$	M_{5_c}
5_d	$a_3 a_6^2 + (a_2 a_6 + a_1 a_7) a_7$	$\eta - 3c_1 + \chi$	$+N$	M_{5_d}

Table 3.2: table of matter curves, their homologies, charges and multiplicities.

irreducible representation of S_4. Similarly, for the fiveplets, we have the defining equation as in Equation (2.27), which gives two coefficients.

The homologies of these curves are calculated from those of the b_i coefficients and are presented in Table 3.2. We may also impose flux restrictions if we define:

$$\begin{aligned} \mathcal{F}_Y \cdot \chi &= N \,, \\ \mathcal{F}_Y \cdot c_1 = \mathcal{F}_Y \cdot \eta &= 0 \,, \end{aligned} \tag{3.2}$$

where $N \in \mathbb{Z}$ and $\mathcal{F}_Y$ is the hypercharge flux.

Considering equation (2.24), we see that $b_5/b_0 = t_1 t_2 t_3 t_4 t_5$, so there are at most five ten-curves, one for each of the weights. Under S_4 and it's subgroups, four of these are identified, which corroborates with the two matter curves seen in Table 3.1. As such we identify $t_{i=1,2,3,4}$ with this monodromy group and the coefficient a_1 and leave t_5 to be associated to a_6.

Similarly, we have at most ten five-curves when $s = 0$, given in the form $t_i + t_j$ with $i \neq j$. Examining the equations for the two five curves that are manifest in this model after application of our monodromy, the quadruplet involving $t_i + t_5$ forms the curve labeled 5_d, while the remaining sextet - $t_i + t_j$ with $i, j \neq 5$ - sits on the 5_c curve.

3.1.1 The discriminant

The above considerations apply equally to both the S_4 and A_4 discrete groups. From the effective model point of view, all the useful information is encoded in the properties of the polynomial coefficients a_k and if we wish to distinguish these two models further assumptions for the latter coefficients have to be made. Indeed, if we assume that in the above polynomial, the coefficients belong to a certain

field $a_k \in \mathcal{F}$, without imposing any additional specific restrictions on a_k, the roots exhibit an S_4 symmetry. If, as desired, the symmetry acting on roots is the subgroup A_4 the coefficients a_k must respect certain conditions. Such constraints emerge from the study of partially symmetric functions of roots. In the present case in particular, we recall that the A_4 discrete symmetry is associated only to even permutations of the four roots t_i. Further, we note now that the partially symmetric function

$$\delta = (t_1 - t_2)(t_1 - t_3)(t_1 - t_4)(t_2 - t_3)(t_2 - t_4)(t_3 - t_4)$$

is invariant only under the even permutations of roots. The quantity δ is the square root of the discriminant,

$$\Delta = \delta^2 \tag{3.3}$$

and as such δ should be written as a function of the polynomial coefficients $a_k \in \mathcal{F}$ so that $\delta \in \mathcal{F}$ too. The discriminant is computed by standard formulae and is found to be

$$\begin{aligned}\Delta(a_k) = {} & 256a_1^3a_5^3 - \left(27a_2^4 - 144a_1a_3a_2^2 + 192a_1^2a_4a_2 + 128a_1^2a_3^2\right)a_5^2 \\ & - 2\left(2\left(a_2^2 - 4a_1a_3\right)a_3^3 - \left(9a_2^2 - 40a_1a_3\right)a_2a_4a_3 + 3\left(a_2^2 - 24a_1a_3\right)a_1a_4^2\right)a_5 \\ & - a_4^2\left(4a_4a_2^3 + a_3^2a_2^2 - 18a_1a_3a_4a_2 + \left(4a_3^3 + 27a_1a_4^2\right)a_1\right).\end{aligned} \tag{3.4}$$

In order to examine the implications of (3.3) we write the discriminant as a polynomial of the coefficient a_3 [50]

$$\Delta \equiv g(a_3) = \sum_{n=0}^{4} c_n a_3^n \tag{3.5}$$

where the c_n are functions of the remaining coefficients $a_k,\ k \neq 3$ and can be easily computed by comparison with (3.4). We may equivalently demand that

$g(a_3)$ is a square of a second degree polynomial

$$g(a_3) = (\kappa a_3^2 + \lambda a_3 + \mu)^2$$

A necessary condition that the polynomial $g(a_3)$ is a square, is its own discriminant Δ_g to be zero. One finds

$$\Delta_g \propto D_1^2 D_2^3$$

where

$$\begin{aligned} D_1 &= a_2^2 a_5 - a_1 a_4^2 \\ D_2 &= \left(27 a_1^2 a_4 - a_2^3\right) a_4^3 - 6 a_1 a_2^2 a_5 a_4^2 + 3 a_2 \left(9 a_2^3 - 256 a_1^2 a_4\right) a_5^2 + 4096 a_1^3 a_5^3 \end{aligned} \tag{3.6}$$

We observe that there are two ways to eliminate the discriminant of the polynomial, either putting $D_1 = 0$ or by demanding $D_2 = 0$ [50].

In the first case, we can achieve $\Delta = \delta^2$ if we solve the constraint $D_1 = 0$ as follows

$$\begin{aligned} a_2^2 &= 2 a_1 a_3 \\ a_4^2 &= 2 a_3 a_5 \end{aligned} \tag{3.7}$$

Substituting the solutions (3.7) in the discriminant we find

$$\Delta \;=\; \delta^2 \;=\; \left[a_2 a_4 \left(a_3^2 - 2\, a_2 a_4\right) \left(a_3^2 - a_2 a_4\right) / a_3^3\right]^2 \tag{3.8}$$

The above constitute the necessary conditions to obtain the reduction of the symmetry [50] down to the Klein group $V \sim Z_2 \times Z_2$. On the other hand, the second condition $D_2 = 0$, implies a non-trivial relation among the coefficients

$$(a_2^2 a_5 - a_4^2 a_1)^2 \;=\; \left(\frac{a_2 a_4 - 16 a_1 a_5}{3}\right)^3 \tag{3.9}$$

Plugging in the $b_1 = 0$ solution, the constraint (3.9) take the form

$$(a_2^2 a_7 + a_0 a_1 a_6^2)^2 \quad = \quad a_0 \left(\frac{a_2 a_6 + 16 a_1 a_7}{3} \right)^3 \tag{3.10}$$

which is just the condition on the polynomial coefficients to obtain the transition $S_4 \to A_4$.

3.1.2 Towards an $SU(5) \times A_4$ model

Using the previous analysis, in this section we will present a specific example based on the $SU(5) \times A_4 \times U(1)$ symmetry. We will make specific choices of the flux parameters and derive the spectrum and its superpotential, focusing in particular on the neutrino sector.

It can be shown that if we assume an A_4 monodromy any quadruplet is reducible to a triplet and singlet representation, while the sextet of the fives reduces to two triplets (details can be found in the appendix).

Singlet-Triplet Splitting Mechanism

It is known from group theory and a physical understanding of the group that the four roots forming the basis under A_4 may be reduced to a singlet and triplet. As such we might suppose intuitively that the quartic curve of A_4 decomposes into two curves - a singlet and a triplet of A_4.

As a mechanism for this we consider an analogy to the breaking of the $SU(5)_{GUT}$ group by $U(1)_Y$. We then postulate a mechanism to facilitate Singlet-Triplet splitting in a similar vein. Switching on a flux in some direction of the perpendicular group, we propose that the singlet and triplet of A_4 will split to form two curves. This flux should be proportional to one of the generators of A_4, so that the broken group commutes with it. If we choose to switch on $U(1)_s$ flux in the direction of the singlet of A_4, then the discrete symmetry will remain unbroken by this choice.

Continuing our previous analogy, this would split the curve as follows:

$$(10,4) = \begin{cases} (10,1) = M + N_s \\ \\ (10,3) = M \end{cases} . \tag{3.11}$$

The homologies of the new curves are not immediately known. However, they can be constrained by the previously known homologies given in Table 3.2. The coefficient describing the curve should be expressed as the product of two coefficients, one describing each of the new curves - $a_i = c_1 c_2$. As such, the homologies of the new curves will be determined by $[a_i] = [c_1] + [c_2]$.

If we assign the $U(1)$ flux parameters by hand, we can set the constraints on the homologies of our new curves. For example, for the curve given in Table 3.2 as 10_a would decompose into two curves - 10_1 and 10_2, say. Assigning the flux parameter, N, to the 10_2 curve, we constrain the homologies of the two new curves as follows:

$$\begin{aligned} [10_1] =& a\eta + bc_1 \\ [10_2] =& c\eta + dc_1 - \chi \\ \text{Where: } & a + c = 1 \text{ and } b + d = -5\,. \end{aligned}$$

Similar constraints may also be placed on the five-curves after decomposition.

Using our procedure, we can postulate that the charge N will be associated to the singlet curve by the mechanism of a flux in the singlet direction. This protects the overall charge of N in the theory. With the fiveplet curves it is not immediately clear how to apply this since the sextet of A_4 can be shown to factorise into two triplets. Closer examination points to the necessity to cancel anomalies. As such the curves carrying H_u and H_d must both have the same charge under N. This will insure that they cancel anomalies correctly. These motivating ideas have been applied in Table 3.3.

GUT-group doublet-triplet splitting

Initially massless states residing on the matter curves comprise complete vector multiplets. Chirality is generated by switching on appropriate fluxes. At the $SU(5)$ level, we assume the existence of M_5 fiveplets and M_{10} tenplets. The multiplicities are not entirely independent, since we require anomaly cancellation,[1] which amounts to the requirement that $\sum_i M_{5_i} + \sum_j M_{10_j} = 0$. Next, turning on the hypercharge flux, under the $SU(5)$ symmetry breaking the 10 and $5, \bar{5}$ representations split into different numbers of Standard Model multiplets [88]. Assuming N units of hyperflux piercing a given matter curve, the fiveplets split according to:

$$\begin{aligned} n(3,1)_{-1/3} - n(\bar{3},1)_{+1/3} &= M_5 \,, \\ n(1,2)_{+1/2} - n(1,2)_{-1/2} &= M_5 + N \,, \end{aligned} \tag{3.12}$$

Similarly, the M_{10} tenplets decompose under the influence of N hyperflux units to the following SM-representations:

$$\begin{aligned} n(3,2)_{+1/6} - n(\bar{3},2)_{-1/6} &= M_{10} \,, \\ n(\bar{3},1)_{-2/3} - n(3,1)_{+2/3} &= M_{10} - N \,, \\ n(1,1)_{+1} - n(1,1)_{-1} &= M_{10} + N \,. \end{aligned} \tag{3.13}$$

Using the relations for the multiplicities of our matter states, we can construct a model with the spectrum parametrised in terms of a few integers in a manner presented in Table 3.3.

In order to curtail the number of possible couplings and suppress operators surplus to requirement, we also call on the services of an R-symmetry. This is commonly found in supersymmetric models, and requires that all couplings have a total R-symmetry of 2. Curves carrying SM-like fermions are taken to have $R = 1$, with all other curves $R = 0$. The existence of such symmetries relies on an *ad hoc* assumption that such a symmetry exists, most likely through a geometric property of the internal manifold. Similar assumptions are found in the literature,

[1] For a discussion in relaxing some of the anomaly cancellation conditions and related issues see [87].

Curve	Rep.	N_Y	M	Matter content	R
10_1	$(10,3)_0$	0	M_{T1}	$3\left[M_{T1}Q_L + u_L^c(M_{T1} - N_Y) + e_L^c(M_{T1} + N_Y)\right]$	1
10_2	$(10,1)_0$	$-N$	M_{T2}	$M_{T2}Q_L + u_L^c(M_{T2} - N_Y) + e_L^c(M_{T2} + N_Y)$	1
10_3	$(10,1)_{t_5}$	$+N$	M_{T3}	$M_{T3}Q_L + u_L^c(M_{T3} - N_Y) + e_L^c(M_{T3} + N_Y)$	1
5_1	$(5,3)_0$	0	M_{F1}	$3\left[M_{F1}\bar{d}_L^c + (M_{F1} + N_Y)\bar{L}\right]$	1
5_2	$(5,3)_0$	$-N$	M_{F2}	$3\left[M_{F2}\bar{D} + (M_{F2} + N_Y)\bar{H}_d)\right]$	0
5_3	$(5,3)_{t_5}$	$+N$	M_{F3}	$3\left[M_{F3}D + (M_{F3} + N_Y)H_u\right]$	0
5_4	$(5,1)_{t_5}$	0	M_{F4}	$M_{F4}\bar{d}_L^c + (M_{F4} + N_Y)\bar{L}$	1

Table 3.3: Table showing the possible matter content for an $SU(5)_{\rm GUT} \times A_4 \times U(1)_\perp$, where it is assumed the reducible representation of the monodromy group may split the matter curves. The curves are also assumed to have an R-symmetry

for example [48,49], where the authors use add an R-parity to make their models safe from bilinear and trilinear baryon/lepton number violating terms. In this instance the choice of an R-symmetry could introduce an axion, which may also serve as a dark matter candidate.

3.2 A simple model: $N = 0$

Any realistic model based on this table must contain at least 3 generations of quark matter (10_{M_i}), 3 generations of leptonic matter ($\bar{5}_{M_i}$), and one each of 5_{H_u} and 5_{H_d}. We shall attempt to construct a model with these properties using simple choices for our free variables.

In order to build a simple model, let us first choose the simple case where N=0, then we make the following assignments:

$$\begin{aligned} M_{T1} = M_{F4} = 0 \\ M_{T2} = 1 \\ M_{T3} = 2 \\ M_{F1} = M_{F2} = -M_{F3} = -1 \end{aligned} \tag{3.14}$$

Note that it does not immediately appear possible to select a matter arrangement that provides a renormalisable top-coupling, since we will be required to use our GUT-singlets to cancel residual t_5 charges in our couplings, at the cost of renormalisability.

Curve	$SU(5) \times A_4 \times U(1)$	M	Matter content	R-Symmetry
10_1	$(10,3)_0$	0	-	1
$10_2 = T_3$	$(10,1)_0$	1	$Q_L + u_L^c + e_L^c$	1
$10_3 = T$	$(10,1)_{t_5}$	2	$2Q_L + 2u_L^c + 2e_L^c$	1
$\bar{5}_1 = F$	$(\bar{5},3)_0$	1	$3L + 3d_L^c$	1
$\bar{5}_2 = H_d$	$(\bar{5},3)_0$	1	$3\bar{D} + 3H_d$	0
$5_3 = H_u$	$(5,3)_{t_5}$	1	$3D + 3H_u$	0
5_4	$(5,1)_{t_5}$	0	-	1
θ_a	$(1,3)_{-t_5}$	-	Flavons	0
θ_b	$(1,1)_{-t_5}$	-	Flavon	0
θ_c	$(1,3)_0$	-	ν_R	1
θ_d	$(1,3)_0$	-	Flavons	0
$\theta_{a'}$	$(1,3)_{t_5}$	-	-	0
$\theta_{b'}$	$(1,1)_{t_5}$	-	-	0

Table 3.4: Table of Matter content in $N = 0$ model

3.2.1 Basis

The bases of the triplets are such that triplet products, $3_a \times 3_b = 1+1'+1''+3_1+3_2$, behave as:

$$1 = a_1b_2 + a_2b_2 + a_3b_3$$

$$1' = a_1b_2 + \omega a_2b_2 + \omega^2 a_3b_3$$

$$1'' = a_1b_2 + \omega^2 a_2b_2 + \omega a_3b_3$$

$$3_1 = (a_2b_3,\, a_3b_1,\, a_1b_2)^{\mathrm{T}}$$

$$3_2 = (a_3b_2,\, a_1b_3,\, a_2b_1)^{\mathrm{T}}$$

where $3_a = (a_1,\, a_2,\, a_3)^{\mathrm{T}}$ and $3_b = (b_1,\, b_2,\, b_3)^{\mathrm{T}}$. This has been demonstrated in the Appendix A.1, where we show that the quadruplet of weights decomposes to a singlet and triplet in this basis. Note that all couplings must of course produce singlets of A_4 by use of these triplet products where appropriate.

3.2.2 Top-type quarks

The Top-type quarks admit a total of six mass terms, as shown in Table 3.5. The third generation has only one valid Yukawa coupling - $T_3 \cdot T_3 \cdot H_u \cdot \theta_a$. Using the

Coupling type	Generations	Full coupling
Top-type	Third generation	$T_3 \cdot T_3 \cdot H_u \cdot \theta_a$
	Third-First/Second generation	$T \cdot T_3 \cdot H_u \cdot \theta_a \cdot \theta_b$
		$T \cdot T_3 \cdot H_u \cdot (\theta_a)^2$
	First/Second generation	$T \cdot T \cdot H_u \cdot \theta_a \cdot (\theta_b)^2$
		$T \cdot T \cdot H_u \cdot (\theta_a)^2 \cdot \theta_b$
		$T \cdot T \cdot H_u \cdot (\theta_a)^3$
Bottom-type /Charged Leptons	Third generation	$F \cdot H_d \cdot T_3$
		$F \cdot H_d \cdot T_3 \cdot \theta_d$
	First/Second generation	$F \cdot H_d \cdot T \cdot \theta_b$
		$F \cdot H_d \cdot T \cdot \theta_a$
		$F \cdot H_d \cdot T \cdot \theta_a \cdot \theta_d$
		$F \cdot H_d \cdot T \cdot \theta_b \cdot \theta_d$
Neutrinos	Dirac-type mass	$\theta_c \cdot F \cdot H_u \cdot \theta_a$
		$\theta_c \cdot F \cdot H_u \cdot \theta_a \cdot \theta_d$
		$\theta_c \cdot F \cdot H_u \cdot \theta_b$
		$\theta_c \cdot F \cdot H_u \cdot \theta_b \cdot \theta_d$
	Right-handed neutrinos	$M\theta_c \cdot \theta_c$
		$(\theta_d)^n \cdot \theta_c \cdot \theta_c$

Table 3.5: Table of all mass operators for $N = 0$ model.

above algebra, we find that this coupling is:

$$\begin{aligned}(1 \times 1) \times (3 \times 3) &\to 1 \times 1 \\ &\to 1 \\ (T_3 \times T_3) \times H_u \times \theta_a &\to (T_3 \times T_3) v_i a_i \\ i &= 1, 2, 3\end{aligned}$$

With the choice of vacuum expectation values (VEVs):

$$\begin{aligned}\langle H_u \rangle &= (v, 0, 0)^{\mathrm{T}} \\ \langle \theta_a \rangle &= (a, 0, 0)^{\mathrm{T}} \\ \langle \theta_b \rangle &= b\end{aligned} \tag{3.15}$$

this will give the Top quark it's mass, $m_t = yva$. The choice is partly motivated by A_4 algebra, as the VEV will preserve the S-generators. This choice of VEVs will also kill off the operators $T \cdot T_3 \cdot H_u \cdot (\theta_a)^2$ and $T \cdot T \cdot H_u \cdot (\theta_a)^2 \cdot \theta_b$, which can be seen by applying the algebra above.

The full algebra of the contributions from the remaining operators is included in Appendix A.2. Under the already assigned VEVs, the remaining operators contribute to give the overall mass matrix for the Top-type quarks:

$$m_{u,c,t} = va \begin{pmatrix} y_3 b^2 + y_4 a^2 & y_3 b^2 + y_4 a^2 & y_2 b \\ y_3 b^2 + y_4 a^2 & y_3 b^2 + y_4 a^2 & y_2 b \\ y_2 b & y_2 b & y_1 \end{pmatrix} \tag{3.16}$$

This matrix is clearly hierarchical with the third generation dominating the hierarchy, since the couplings should be suppressed by the higher order nature of the operators involved. Due to the rank theorem [35], the two lighter generations can only have one massive eigenvalue. However, corrections due to instantons and non-commutative fluxes are known as mechanisms to recover a light mass for the first generation [35] [33].

3.2.3 Charged Leptons

The Charged Lepton and Bottom-type quark masses come from the same GUT operators. Unlike the Top-type quarks, these masses will involve SM-fermionic matter that lives on curves that are triplets under A_4. It will be possible to avoid unwanted relations between these generations using the ten-curves, which are strictly singlets of the monodromy group. The operators, as per Table 3.5, are computed in full in Appendix A.2. Since we wish to have a reasonably hierarchical structure, we shall require that the dominating terms be in the third generation. This is best served by selecting the VEV $\langle H_d \rangle = (0, 0, v)^{\mathrm{T}}$. Taking the lowest order of operator to dominate each element, since we have non-renormalisable operators, we see that we have then:

$$m_{e,\mu,\tau} = v \begin{pmatrix} y_7 d_2 b + y_{11} d_3 a & y_7 d_2 b + y_{11} d_3 a & y_3 d_2 \\ y_5 a & y_5 a & y_2 d_1 \\ y_4 b & y_4 b & y_1 \end{pmatrix}. \tag{3.17}$$

We should again be able to use the Rank Theorem to argue that while the first

generation should not get a mass by this mechanism, the mass may be generated by other effects [35] [33]. We also expect there might be small corrections due to the higher order contributions, though we shall not consider these here.

The bottom-type quarks in $SU(5)$ have the same masses as the charged leptons, with the exact relation between the Yukawa matrices being due to a transpose. However this fact is known to be inconsistent with experiment. In general, when renormalization group running effects are taken into account, the problem can be evaded only for the third generation. Indeed, the mass relation $m_b = m_\tau$ at M_{GUT} can be made consistent with the low energy measured ratio m_b/m_τ for suitable values of $\tan\beta$. In field theory $SU(5)$ GUTs the successful Georgi-Jarlskog GUT relation $m_s/m_\mu = 1/3$ can be obtained from a term involving the representations $\bar{5} \cdot 10 \cdot 45$ but in the F-theory context this is not possible due to the absence of the 45 representation. Nevertheless, the order one Yukawa coefficients may be different because the intersection points need not be at the same enhanced symmetry point. The final structure of the mass matrices is revealed when flux and other threshold effects are taken into account. These issues will not be discussed further here and a more detailed exposition may be found in [30], with other useful discussion to be found in [34].

3.2.4 Neutrino sector

Neutrinos are unique in the realms of currently known matter in that they may have both Dirac and Majorana mass terms. The couplings for these must involve an $SU(5)$ singlet to account for the required right-handed neutrinos, which we might suppose is $\theta_c = (1,3)_0$. It is evident from Table 3.5 that the Dirac mass is formed of a handful of couplings at different orders in operators. We also have a Majorana operator for the right-handed neutrinos, which will be subject to corrections due to the θ_d singlet, which we assign the most general VEV, $\langle\theta_d\rangle = (d_1, d_2, d_3)^{\mathrm{T}}$.

If we now analyze the operators for the neutrino sector in brief, the two leading order contribution are from the $\theta_c \cdot F \cdot H_u \cdot \theta_a$ and $\theta_c \cdot F \cdot H_u \cdot \theta_b$ operators. With the

VEV alignments $\langle\theta_a\rangle = (a,0,0)^{\mathrm{T}}$ and $\langle H_u\rangle = (v,0,0)^{\mathrm{T}}$, we have a total matrix for these contributions that displays strong mixing between the second and third generations:

$$m = \begin{pmatrix} y_0 va & 0 & 0 \\ 0 & y_1 va & y_9 bv \\ 0 & y_8 bv & y_1 va \end{pmatrix}, \tag{3.18}$$

where $y_0 = y_1 + y_2 + y_3$. The higher order operators, $\theta_c \cdot F \cdot H_u \cdot \theta_a \cdot \theta_d$ and $\theta_c \cdot F \cdot H_u \cdot \theta_b \cdot \theta_d$, will serve to add corrections to this matrix, which may be necessary to generate mixing outside the already evident large 2-3 mixing from the lowest order operators. If we consider the $\theta_c \cdot F \cdot H_u \cdot \theta_b \cdot \theta_d$ operator,

$$\theta_c \cdot F \cdot H_u \cdot \theta_d \cdot \theta_b \to \begin{pmatrix} 0 & z_3 v d_2 b & z_2 v d_3 b \\ z_1 v d_2 b & 0 & 0 \\ z_4 v d_3 b & 0 & 0 \end{pmatrix}. \tag{3.19}$$

We use z_i coefficients to denote the suppression expected to affect these couplings due to renormalisability requirements. We need only concern ourselves with the combinations that add contributions to the off-diagonal elements where the lower order operators have not given a contribution, as these lower orders should dominate the corrections. Hence, the remaining allowed combinations will not be considered for the sake of simplicity. If we do this we are left a matrix of the form:

$$M_D = \begin{pmatrix} y_0 va & z_3 v d_2 b & z_2 v d_3 b \\ z_1 v d_2 b & y_1 va & y_9 bv \\ z_4 v d_3 b & y_8 bv & y_1 va \end{pmatrix}. \tag{3.20}$$

The right-handed neutrinos admit Majorana operators of the type $\theta_c \cdot \theta_c \cdot (\theta_d)^n$, with $n \in \{0, 1, \dots\}$. The $n = 0$ operator will fill out the diagonal of the mass matrix, while the $n = 1$ operator fills the off-diagonal. Higher order operators can again be taken as dominated by these first two, lower order operators. The Majorana mass matrix can then be used along with the Dirac mass matrix in

order to generate light effective neutrino masses via a see-saw mechanism,

$$M_R = M \begin{pmatrix} 1 & 0 & 0 \\ 0 & 1 & 0 \\ 0 & 0 & 1 \end{pmatrix} + y \begin{pmatrix} 0 & d_3 & d_2 \\ d_3 & 0 & d_1 \\ d_2 & d_1 & 0 \end{pmatrix}. \tag{3.21}$$

The Dirac mass matrix can be summarised as in equation (3.20). This matrix is rank 3, with a clear large mixing between two generations, which we expect to generate a large θ_{23}. In order to reduce the parameters involved in the effective mass matrix, we will simplify the problem by searching only for solutions where $z_1 = z_3$ and $z_2 = z_4$, which significantly narrows the parameter space. We will then define some dimensionless parameters that will simplify the matrix:

$$Y_1 = \frac{y_1}{y_0} \leq 1 \tag{3.22}$$

$$Y_{2,3} = \frac{y_{8,9} b}{y_0 a} \tag{3.23}$$

$$Z_1 = \frac{z_1 d_2 b}{y_0 a} \tag{3.24}$$

$$Z_2 = \frac{z_2 d_3 b}{y_0 a} \tag{3.25}$$

If we implement these definitions, we find the Dirac mass matrix becomes:

$$M_D = y_0 v a \begin{pmatrix} 1 & Z_1 & Z_2 \\ Z_1 & Y_1 & Y_3 \\ Z_2 & Y_2 & Y_1 \end{pmatrix} \tag{3.26}$$

The Right-handed neutrino Majorana mass matrix can be approximated if we take only the $\theta_c \cdot \theta_c$ operator, since this should give a large mass scale to the right-handed neutrinos and dominate the matrix. This will leave the Weinberg

	Central value	Min → Max
$\theta_{12}/^\circ$	33.57	32.82→34.34
$\theta_{23}/^\circ$	41.9	41.5→42.4
$\theta_{13}/^\circ$	8.73	8.37→9.08
$\Delta m^2_{21}/10^{-5}\text{eV}$	7.45	7.29 → 7.64
$\Delta m^2_{31}/10^{-3}\text{eV}$	2.417	2.403 → 2.431
$R = \frac{\Delta m^2_{31}}{\Delta m^2_{21}}$	32.0	31.1 → 33.0

Table 3.6: Summary of neutrino parameters, using best fit values as found at nu-fit.org, the work of which relies upon [89] .

operator for effective neutrino mass, $M_{eff} = M_D M_R^{-1} M_D^{\mathrm{T}}$, as:

$$M_{eff} = m_0 \begin{pmatrix} 1 + Z_1^2 + Z_2^2 & Y_1 Z_1 + Y_3 Z_2 + Z_1 & Y_2 Z_1 + Y_1 Z_2 + Z_2 \\ Y_1 Z_1 + Y_3 Z_2 + Z_1 & Y_1^2 + Y_3^2 + Z_1^2 & Y_1(Y_2 + Y_3) + Z_1 Z_2 \\ Y_2 Z_1 + Y_1 Z_2 + Z_2 & Y_1(Y_2 + Y_3) + Z_1 Z_2 & Y_1^2 + Y_2^2 + Z_2^2 \end{pmatrix}, \tag{3.27}$$

Where we have also defined a mass parameter:

$$m_0 = \frac{y_0^2 v^2 a^2}{M}, \tag{3.28}$$

We then proceed to diagonalise this matrix computationally in terms of three mixing angles as is the standard procedure [90], before attempting to fit the result to experimental inputs.

3.2.5 Analysis

We shall focus on the ratio of the mass squared differences:

$$R = \left| \frac{m_3^2 - m_2^2}{m_2^2 - m_1^2} \right|, \tag{3.29}$$

which is known due to the well measured mass differences, Δm^2_{32} and Δm^2_{21} [89]. These give us a value of $R \approx 32$, which we may solve for numerically in our model using Mathematica or another suitable maths package. If we then fit the optimised values to the mass scales measured by experiment, we may predict absolute neutrino masses and further compare them with cosmological

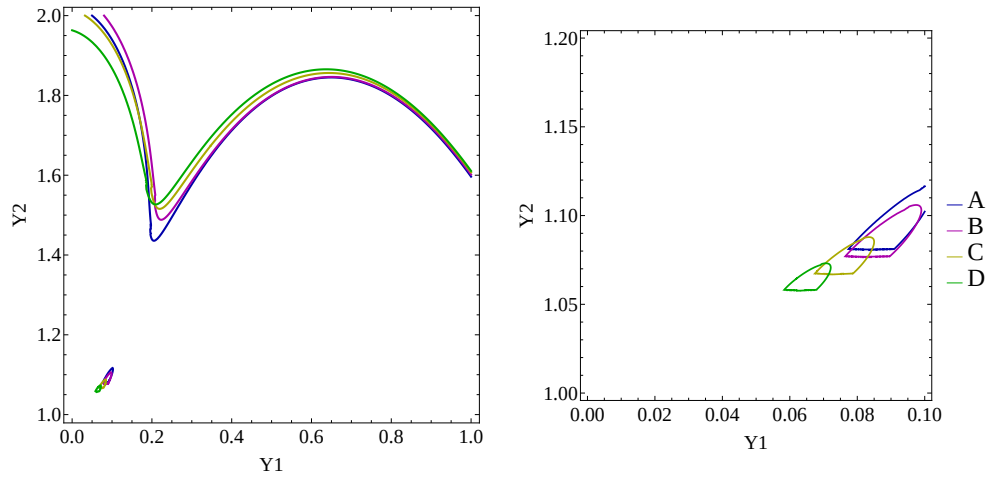

Figure 3.1: Plots of lines with the best fit value of $R = 32$ in the parameter space of (Y_1, Y_2). Left: The full range of the space examined. Right: A close plot of a small portion of the parameter space taken from the full plot. The curves have (Y_3, Z_1, Z_2) values set as follows: $A = (1.08, 0.05, 0.02)$, $B = (1.08, 0.0, 0.08)$, $C = (1.07, 0.002, 0.77)$, and $D = (1.06, 0.01, 0.065)$.

constraints.

The fit depends on a total of six coefficients, as can be seen from examining the undiagonalised effective mass matrix. Optimising R, we should also attempt to find mixing angles in line with those known to parameterize the neutrino sector - i.e. large θ_{23} and θ_{12}, with a comparatively small (but non-zero) θ_{13}. This is necessary to obtain results compatible with neutrino oscillation experiments. Table 3.6 summarises the neutrino parameters the model must be in keeping with in order to be acceptable [89]. We should note that the parameter m_0 will be trivially matched up with the mass differences shown in Table 3.6.

If we take some choice values of three of our five free parameters, we can construct a contour plot for curves with constant R using the other two. Figure 3.1 shows this for a series of fixed parameters. Each of the lines is for $R = 32$, so we can see that there is a deal of flexibility in the parameter space for finding allowed values of the ratio.

In order to further determine which parts of the broad parameter space are most suitable for returning phenomenologically acceptable neutrino parameters, we can plot the value of $\sin^2(\theta_{12})$ or $\sin^2(\theta_{23})$ in the same parameter space as

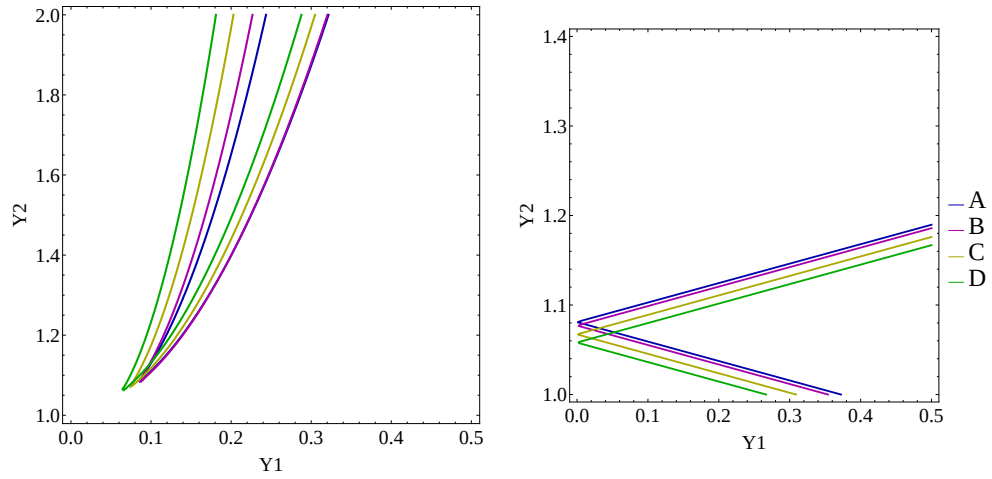

Figure 3.2: The figures show plots of two large neutrino mixing angles at their current best fit values. Left: Plot of $\sin^2(\theta_{12}) = 0.306$, Right: Plot of $\sin^2(\theta_{23}) = 0.446$. The curves have (Y_3, Z_1, Z_2) values set as follows: $A = (1.08, 0.05, 0.02)$, $B = (1.08, 0.0, 0.08)$, $C = (1.07, 0.002, 0.77)$, and $D = (1.06, 0.01, 0.065)$.

Figure 3.1 - (Y_1, Y_2). The first plot in Figure 3.2 shows that the angle θ_{12} constraints are best satisfied at lower values of Y_1, while there are the each line spans a large part of the Y_2 space. The second plot of Figure 3.2 suggests a preference for comparatively small values of Y_2 based on the constraints on θ_{23}. As such, we might expect that for this corner of the parameter space there will be some solutions that satisfy all the constraints.

Figure 3.3 also shows a plot for contours of best fitting values of R, with the free variables chosen as Y_3 and Z_1. As before, this shows that for a range of the other parameters, we can usually find suitable values of (Y_3, Z_1) that satisfy the constraints on R. This being the case, we expect that it should be possible to find benchmark points that will allow for the other constraints to also be satisfied.

This flexibility in the parameter space translates to the other experimental parameters, such that the points that allow experimentally allowed solutions are abundant enough that we can fit all the parameters quite well. Table 3.7 shows a collection of so-called benchmark points, which are points in the parameter space where all constraints are satisfied within current experimental errors - see Table 3.6. The table only shows values where θ_{23} is in the first octant. We might expect that the model should also admit solutions for second octant θ_{23}, however

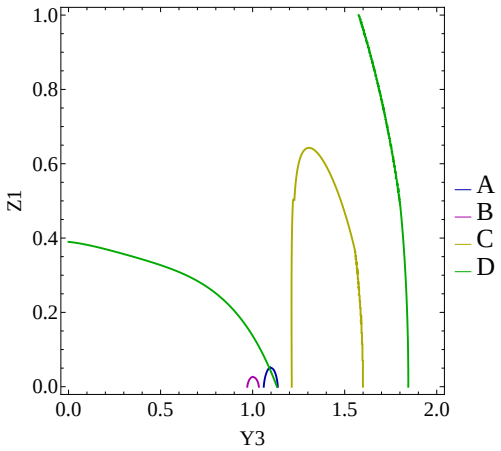

Figure 3.3: Plots of lines with the best fit value of $R = 32$ in the parameter space of (Y_3, Z_1). The curves have (Y_1, Y_2, Z_2) values set as follows: $A = (\frac{1}{5}, 1.4, 0.02)$, $B = (0.05, 1.5, 0.01)$, $C = (\frac{1}{2}, 1.6, 0.01)$, and $D = (\frac{2}{3}, 1.8, 0.5)$.

Inputs				
Y_1	0.08	0.09	0.09	0.10
Y_2	1.09	1.10	1.10	1.11
Y_3	1.07	1.08	1.08	1.09
Z_1	0.01	0.01	0.00	0.01
Z_2	0.07	0.08	0.08	0.08
m_0	54.0meV	51.6meV	50.3meV	47.8meV
Outputs				
θ_{12}	33.5	33.2	33.1	32.8
θ_{13}	8.70	8.82	9.05	9.05
θ_{23}	41.9	41.7	41.7	41.5
m_1	53.4meV	51.1meV	49.8meV	47.3meV
m_2	54.1meV	51.8meV	50.5meV	48.1meV
m_3	73.2meV	71.5meV	70.8meV	69.1meV

Table 3.7: Table of Benchmark values in the Parameter space, where all experimental constraints are satisfied within errors. These point are samples of the space of all possible points, where we assume θ_{23} is in the first octant. All inputs are given to two decimal places, while the outputs are given to 3s.f.

attempts as numerical solution indicate this possibility is strongly disfavoured. We also note that current Planck data [91] puts the sum of neutrino masses to be $\Sigma m_\nu \leq 0.23$eV, which the bench mark points are also consistent with.

3.2.6 Proton decay

As mentioned in the introduction to this thesis, proton decay is a feature of generic supersymmetric SU(5) GUTs. Within the context of the $SU(5) \times A_4 \times U(1)$ in

F-theory, these operators arise from effective operators of the type:

$$10 \cdot 10 \cdot 10 \cdot \bar{5}\,, \tag{3.30}$$

where the $\bar{5}$ contains the $SU(2)$ Lepton doublet and the d^c, and the quark doublet, u^c and e^c arise from 10 of $SU(5)$. The interaction will be mediated by the H_u and H_d doublets.

In the model under consideration, two matter curves are in the 10 representation of the GUT group: T_3 containing the third generation, and T containing the lighter two generations. In general these can be expressed as:

$$\begin{gathered} T^i \cdot T_3^j \cdot F \\ i + j = 3 \text{ and } i, j \in \{0, 1, 2, 3\} \end{gathered} \tag{3.31}$$

Here, the role of R-symmetry in the model becomes important, since due to the assignment of this symmetry, these operators are all disallowed. Further more, the operators which have $i \neq 0$ will have net charge due to the $U(1)_\perp$, requiring them to have flavons to balance the charge. This would offer further suppression in the event that R-symmetry were not enforced.

There are also proton decay operators mediated by D-Higgs triplets and their anti-particles, which arise from the same operators, but in a similar way, these will be disallowed by R-symmetry thus preventing proton decay via dimension-six operators.

The dimension-four operators, which are mediated by superpartners of the Standard Model, will also be prevented by R-symmetry. However, even in the absence of this symmetry, the need to balance the charge of the $U(1)_\perp$ would lead to the presence of additional GUT group singlets in the operators, leading to further, strong suppression of the operator.

3.2.7 Unification

The spectrum in Table 4 is equivalent to three families of quarks and leptons plus three families of $5 + \overline{5}$ representations which include the two Higgs doublets that get VEVs. Such a spectrum does not by itself lead to gauge coupling unification at the field theory level, and the splittings which may be present in F-theory cannot be sufficiently large to allow for unification, as discussed in [54]. However, as discussed in [54], where the low energy spectrum is identical to this model (although achieved in a different way) there may be additional bulk exotics which are capable of restoring gauge coupling unification and so unification is certainly possible in this mode. We refer the reader to the literature for a full discussion.

3.3 Conclusions

In this chapter we considered the phenomenological implications of F-theory $SU(5)$ models with non-Abelian discrete family symmetries. We discussed the physics of these constructions in the context of the spectral cover, which, in the elliptical fibration and under the specific choice of $SU(5)$ GUT, implies that the discrete family symmetry must be a subgroup of the permutation symmetry S_5. Furthermore, we exploited the topological properties of the associated 5-degree polynomial coefficients (inherited from the internal manifold) to derive constraints on the effective field theory models. Since we dealt with discrete gauge groups, we also proposed a discrete version of the flux mechanism for the splitting of representations. We started our analysis splitting appropriately with the spectral cover in order to implement the A_4 discrete symmetry as a subgroup of S_4. Hence, using Galois Theory techniques, we studied the necessary conditions on the discriminant in order to reduce the symmetry from S_4 to A_4. Moreover, we derived the properties of the matter curves accommodating the massless spectrum and the constraints on the Yukawa sector of the effective models. Then, we first made a choice of our flux parameters and picked up a suitable combination of trivial and non-trivial A_4 representations to accommodate the three generations so that a hierarchical mass spectrum for the charged fermion sector is guaranteed.

Next, we focused on the implications of the neutrino sector. Because of the rich structure of the effective theory emerging from the covering E_8 group, we found a considerable number of Yukawa operators contributing to the neutrino mass matrices. Despite their complexity, it is remarkable that the F-theory constraints and the induced discrete symmetry organise them in a systematic manner so that they accommodate naturally the observed large mixing effects and the smaller θ_{13} angle of the neutrino mixing matrix.

In conclusion, F-theory $SU(5)$ models with non-Abelian discrete family symmetries provide a promising theoretical framework within which the flavour problem may be addressed. The present chapter presents the first such realistic example based on A_4, which is amongst the most popular discrete symmetries used in the field theory literature in order to account for neutrino masses and mixing angles. By formulating such models in the framework of F-theory $SU(5)$, a deeper understanding of the origin of these discrete symmetries is obtained.

Chapter 4

Phenomenological implications of a D_4 monodromy and geometric matter parity

In this chapter we review the basic mechanisms responsible for the origin of both non-Abelian discrete family symmetry and Abelian continuous family symmetry, as well as matter parity, from F-theory SUSY GUTs, before piecing together the first realistic example model of its kind which includes all three types of symmetries.

F-theory effective models are endowed with Abelian and discrete symmetries, which may arise either as a subgroup of the non-Abelian symmetry or from a non-trivial Mordell-Weil group associated to rational sections of the elliptic fibration. It is well known that the discrete symmetries in particular are extremely important in suppressing undesired proton decay operators and generating a hierarchical fermion mass spectrum [1]. Furthermore, non-Abelian discrete groups were introduced to interpret the mixing properties of the neutrino sector [84–86, 94].

In the present work, then, we will focus on non-Abelian discrete symmetries emerging in the context of the spectral cover, accompanied by continuous Abelian symmetry. We continue to investigate the discrete symmetries emerging

[1] For discussions in a wider framework of discrete symmetries in String Theory see references [92]- [93].

as subgroups of the $SU(5)_\perp$ spectral cover symmetry. Motivated by the successful implementation of a class of such symmetries to the neutrino sector, we focus on the subgroups of S_4. We also show how a geometric discrete Z_2 symmetry can additionally emerge, leading to matter parity which can control proton decay operators. However, due to the basic feature of F-theory constructions with flux breaking of the GUT group yielding doublet-triplet splitting and incomplete GUT representations, the matter parity is necessarily of a new kind. In the particular example we develop, based on $D_4 \times U(1)$ family symmetry, with an $SU(5)$ GUT group, broken by fluxes, the geometric Z_2 matter parity, while suppressing proton decay, allows neutron-antineutron oscillations, providing a distinctive signature of the set-up. To be precise, while QLd^c is forbidden, the operator $u^c d^c d^c$ is present leading to $n\bar{n}$ oscillations at a calculable rate.

The layout of the remainder of the chapter is as follows. In Section 4.2 we show how a D_4 discrete symmetry subgroup of the S_4 can emerge. The structure of this non-Abelian discrete symmetry seems promising, so can be used to illustrate in the simplest setting many of the features of interest, and can be used as the basis for constructing a realistic model, which we do in Section 4.3. In Section 4.4 we investigate the physics of baryon number violation in this model, showing how the combination of symmetries can suppress proton decay, but allows baryon number violating operators which can yield neutron-antineutron oscillations, providing a distinctive signature of our scheme.

4.1 Discrete symmetries from the spectral cover

There are various phenomenological reason suggestive for a non-Abelian discrete symmetry. In the context of F-theory in particular, the D_4 symmetry was suggested in [14] for a successful implementation of a consistent effective model. This was considered in the context of a model where all Yukawa hierarchies emerge from a single E_8 enhancement point. It was further shown that the D_4 symmetry is one of the few possible monodromy groups accommodating only the minimal matter, and at the same time being compatible with viable right-handed neu-

trino scenarios. In this chapter, we will try to exploit the non-abelian nature of this discrete group in order to construct viable fermion mass textures, interpret neutrino data, and make possible predictions for other interesting processes of our effective model.

As already pointed out in the introduction, guided by reasons of phenomenology, we will analyse the $\mathcal{C}_4 \times \mathcal{C}_1$ case, as per the case of Equation (2.24). For this case the splitting of the five-degree polynomial is given in Equation (2.24), where the coefficients a_i of the new polynomials are related to b_k in a straightforward manner. We have already explained how these relations determine the homologies of the new coefficients from those of b_k's and discussed their implications on the effective theory in the previous sections. However, there are additional interesting features of these coefficients with respect to the monodromy groups which we now analyse. For our case of interest, the non-trivial part is related to the fourth order polynomial so that the maximal symmetry group S_5 reduces down to S_4, (i.e. the permutation of four objects), or to some of its subgroups.

The precise determination of the Galois group depends solely on the specific structure of the coefficients $a_n, n = 1, \ldots, 5$. Leaving the details for the appendix, we only state here that they can be classified in terms of symmetric functions of the roots. Concerning the particular symmetry groups we are dealing with, it suffices to examine the Discriminant Δ_4 and the resolvent of the corresponding fourth-degree polynomial.

The discriminant Δ_4 is a symmetric function of the roots $t_{1,2,3,4}$ and as such it can always be expressed as a function of the coefficients a_i, hence $\Delta_4 = \Delta_4(a_i)$. For generic coefficients a_i the symmetry is S_4 unless Δ_4 can be written as a square of a quantify $\delta(a_i)$ which is invariant under the S_4-even permutations which constitute the group A_4.

The resolvent is the cubic polynomial

$$f(x) \;=\; a_5^{\frac{3}{2}}(x - x_1)(x - x_2)(x - x_3) \sim x^3 + c_1 x^2 + c_2 x + c_3. \qquad (4.1)$$

where the roots $x_{1,2,3}$ are the three t_i-combinations

$$x_1 = t_1t_2 + t_3t_4, \quad x_2 = t_1t_3 + t_2t_4, \quad x_3 = t_3t_2 + t_1t_4 \tag{4.2}$$

These are invariant under the group D_4 which is the symmetry of the square. It can be seen that all coefficients c_k of the polynomial are symmetric functions of t_i and therefore they can also be expressed as functions of a_i, $c_k(a_i)$. Depending on the specific properties of the two quantities Δ_4 and $f(x)$, the Galois group may be any of the S_5 subgroups.

From the point of view of the low energy effective theory, there is a clear distinction between the two categories of discrete groups. As is well known, non-Abelian discrete groups are endowed with non-trivial (non-singlet) representations. In effect, ordinary GUT representations transform non-trivially under such symmetries. This way, additional restrictions might be imposed on superpotential terms while specific forms of mass textures may arise at the same time. In the subsequent, we will focus on the particular discrete symmetry of D_4.

4.2 The discrete group D_4 as a Family Symmetry

In a realistic F-theory effective model a superpotential should emerge containing all necessary interaction terms. In particular it should distinguish the three families and provide correct masses to all fermion fields and at the same time should exclude all other undesired ones. In the previous sections, it has become evident that the imperative distinction of the three fermion families, in F-theory should be related to possible additional symmetries and geometric properties carried by the $SU(5)$ matter curves.

In this section we will continue to explore the origin of such symmetries in the context of the spectral cover equation, Equation (2.24), which is split as $C_4 \times C_1$ splitting. With respect to the corresponding gauge group, we may turn on suitable Abelian and non-Abelian fluxes which result in the breaking of the $SU(5)_\perp$ symmetry. Hence, in the present case for example one can turn on a

$SU(4)$	$\subset$	$SU(3)$	$\subset$	S_4
4	$\to$	$3+1$	$\to$	$3+1$
6	$\to$	$3+\bar{3}$	$\to$	$3+3$
15	$\to$	$8+1+3+\bar{3}$	$\to$	$3+3'+2+1$

Table 4.1: The embedding of S_4 representations in the $\mathcal{C}_4$ spectral cover symmetry

flux along a non-trivial line bundle of the corresponding Cartan $U(1)$ so that the group originally breaks to $SU(4)_\perp \times U(1)_\perp$. Furthermore, one may assume the reduction of the $SU(4)_\perp$ part to some discrete group, as a consequence of a suitable non-Abelian flux or appropriate Higgsing. The case of $D_4 \subset S_4$ in particular can be reached from our initial maximal symmetry of $\mathcal{C}_4$ under the following chain $SU(4) \to SU(3) \to S_4$. Indeed, we may invoke the one-to-one correspondence [95] of the S_4 representations to those of $SU(3)$, and decompose the $SU(4)$ ones according to the pattern shown in Table 4.1.

An analogous symmetry reduction could be attained through the Higgs bundle description and in particular the spectral cover of the fundamental and anti-symmetric representations of our GUT gauge group. In this local picture we may exploit the fact that the geometric singularities essentially correspond to particular symmetries of the effective theory model. Hence, in accordance with the choice of the family group in our previous discussion, we will appeal to local geometry and assume the non-Abelian discrete group D_4 acting on the $SU(5)_{GUT}$ representations. To study its implications in our particular construction we start by splitting the five roots t_i into two sets

$$C_4 \leftrightarrow \{t_1, t_2, t_3, t_4\}, \quad C_1 \leftrightarrow \{t_5\}$$

in accordance with our choice of spectral cover splitting. Because $SU(5)_{GUT}$ representations are characterised by the weights t_i, as a result they fall into appropriate orbits. Hence, the matter curves accommodating the tenplets of

$SU(5)_{GUT}$ are

$$\begin{aligned} 10_a &: \{t_1, t_2, t_3, t_4\} \\ 10_b &: \{t_5\} \end{aligned}$$

In the same way, if no other restrictions are imposed, the matter curves for the fiveplets of $SU(5)$ also fall into two categories

$$\begin{aligned} \bar{5}_c &: \{t_1+t_2, t_2+t_3, t_3+t_4, t_4+t_1, t_1+t_3, t_2+t_4\} \\ \bar{5}_d &: \{t_1+t_5, t_2+t_5, t_3+t_5, t_4+t_5\} \end{aligned}$$

We can readily observe that the orbits are 'closed' under the action of the elements of the S_4 group. The $SU(5)$ superpotential couplings are subject to constraints in accordance with the above classification. Hence, for example the $10_a 10_b 5_d$ coupling is allowed while $10_a 10_b 5_c$ is incompatible with the S_4 rules.

The invariance of the orbits under the action of the whole set of S_4 elements reflects the fact that the polynomial coefficients a_k of the corresponding spectral cover fourth-order polynomial are quite generic. On the contrary, if specific restrictions are imposed on a_k the discrete group will be a subgroup of S_4, while further splitting of the orbits will occur. We will now be more specific and consider the case of the dihedral group, $D_4 \subset S_4$.

In the context of F-theory with an $SU(5)$ GUT group, if the left-over discrete group is D_4, then the four of the roots of the original $SU(5)_\perp$ group are permuted in accordance to the specific D_4 rules and the overall symmetry structure is:

$$\begin{aligned} E_8 \to & SU(5)_{\rm GUT} \times SU(5)_\perp \\ \to & SU(5)_{\rm GUT} \times D_4 \times U(1)_\perp \,. \end{aligned}$$

In order to have a D_4 symmetry relating the four roots, rather than an S_4, we must appeal to Galois theory. From Table B.2 in the Appendix, we can see that this means the discriminant of the quartic part of Equation (2.24) must not

be a square, while the cubic resolvent of the polynomial must be reducible.

If we assume the roots $t_{i=1,2,3,4}$, then the quartic part of Equation (2.24) has a cubic resolvent of the form given in (4.1) where the roots x_i are the symmetric polynomials of the weights t_i given in (4.2).

It can be shown that the discriminant (Δ_f) of Equation (4.1) is:

$$27\Delta_f = 4\left(a_3^2 - 3a_2a_4 + 12a_1a_5\right)^3 - \left(2a_3^3 - 9\left(a_2a_4 + 8a_1a_5\right)a_3 + 27\left(a_5a_2^2 + a_1a_4^2\right)\right)^2, \tag{4.3}$$

which is also equal to the discriminant of the quartic polynomial relating the four roots - this is a standard property of all cubic resolvents[2].

By computing the coefficients as functions of the a_i coefficients, the cubic takes the form

$$f(s) = a_5^{-\frac{3}{2}}[(a_5s)^3 - a_3(a_5s)^2 + (a_2a_4 - 4a_1a_5)a_5s + (4a_1a_3a_5 - a_2^2a_5 - a_1a_4^2)]\,. \tag{4.4}$$

The simplest way to make this polynomial reducible, is to demand the zero order term to vanish, $f(0) = 0$. This means that one of the roots equals to zero. By setting $f(0) = 0$ and using the SU(5) tracelessness constraint [3] we take the following known condition [50] between the a_i's :

$$a_2^2a_7 = a_1(a_0a_6^2 + 4a_3a_7)\,, \tag{4.5}$$

If we then substitute this into the equation for the fiveplets of the GUT group, Equation (2.27), we get an equation factorised into 3 parts,

$$P_5 = a_3(a_2a_6 + 4a_1a_7)(a_3a_6^2 + a_7(a_2a_6 + a_1a_7))\,, \tag{4.6}$$

which indicates that we have at least 3 distinct matter curves by the usual interpretation.

The so obtained splittings of the non-trivial $SU(5)$ representations are collected in Table 2. The first column indicates the $SU(5)$ representation, while the defining

[2] An alternative cubic resolvent is presented in the Appendix.

[3] Tracelessness constraint: $b_1 = 0$. Note that $b_1 = a_5a_6 + a_4a_7 = 0$

$SU(5)$ Rep.	Equation	Homology
10_a	a_1	$\eta - 5c_1 - \chi$
10_b	a_6	χ
5_a	a_3	$\eta - 3c_1 - \chi$
5_b	$a_2a_6 + 4a_1a_7$	$\eta - 4c_1$
5_c	$a_3a_6^2 + a_7(a_2a_6 + a_1a_7)$	$\eta - 3c_1 + \chi$

Table 4.2: Summary of the default matter curve splitting from spectral cover equation in the event of a D_4 symmetry accompanying an SU(5) GUT group in the case of the symmetric polynomials $x_{i=1,2,3}$ as discussed in text.

equation of each corresponding matter curve is shown in column 2. In the third column we designate the associated homologies. These are readily determined from the known Chern classes of the b_k coefficients through the equations $b_k = b_k(a_i)$ given in (2.24), using well known procedures [49, 51]. These are expressed in terms of the known classes [4] η, c_1 and an arbitrary one designated by χ.

4.2.1 Irreducible Representations

Thus far we have largely ignored how the group theory must be applied to matter curves in this construction. We shall now examine this side of the problem, with a particular view being taken to find the irreducible representations where possible. Given the earlier conjecture that *non-Abelian fluxes* can break $SU(5)_\perp$ to D_4, which acts as a family symmetry group in the low energy effective theory, it then follows that the low energy states must transform according to irreducible representations of D_4. In the Appendix we show how reducible 4 and 6 dimensional representations of D_4 decompose into irreducible representations. The argument is summarised as follows.

Knowing that we have four weights $t_{i=1,2,3,4}$, which are related by a D_4 symmetry, we might exploit the nature of D_4. Specifically, since D_4 can be physically interpreted as a square, we might label the corner of such a square with our weights and see how they must transform based on this. It is then clear that there should be two generators for this symmetry: a rotation about the centre by $\frac{\pi}{2}$ and a reflection along one of the lines of symmetry, which we will call a and b

[4] The Chern class of b_k is $[b_k] = (6-k)c_1 - t = \eta - kc_1$ where c_1 is the first Chern class of the GUT "divisor" S and $-t$ the corresponding one of the normal bundle [17].

Curve	D_4 rep.	t_5
10_α	1_{++}	0
10_β	1_{+-}	0
10_γ	2	0
10_δ	1_{++}	1

Table 4.3: Table summarising the representations of the tens of $SU(5)_{\text{GUT}}$

respectively. This is in keeping with the presentation of D_4:

$$a^4 = e, \;\; b^2 = e, \;\; bab = a^{-1}\,, \tag{4.7}$$

where e is the identity.

It can be shown that this quadruplet of weights can be rotated into a basis with irreducible representations of D_4 - see Appendix - by use of appropriate unitary transformations. It transpires that the irreducible basis includes a trivial singlet, a non-trivial singlet and a doublet, as summarised in Table 4.3. Note that we also have an extra singlet that is charged under the fifth weight (10_δ), which must logically be a trivial singlet since it is uncharged under the D_4 symmetry.

The $\bar{5}/5$ representations of the GUT group have a maximum of 10 weights before the reduction of the $SU(4) \to D_4$ symmetry. These have weights related to the 10s of the GUT group: $\pm(t_i + t_j)$. By consistency these must transform in the same manner as the weights of the 10s, allowing us to unambiguously write down the generators a and b.

By the same process as before, we may decompose this tenplet under D_4 into irreducible representations of the group. Referring to the Appendix once again, we may obtain a total of eight representations, as shown in Table 4.4. However, we note that three of the representations[5] are entirely indistinguishable as they are trivial singlets with only charges under $t_{i=1,2,3,4}$.

4.2.2 Reconciling Interpretations

It is clear at this point that there is some tension between the two angles of attack for this problem. Obviously we must be able to describe both the non-

[5] $\bar{5}_\delta$, $\bar{5}_\epsilon$, and $\bar{5}_\zeta$

Curve	D_4 rep.	t_5 charge	weight relation
$\bar{5}_\alpha$	1_{++}	1	$\sum_{i=1}^4 t_i$
$\bar{5}_\beta$	1_{+-}	1	$(t_1+t_3)-(t_2+t_4)$
$\bar{5}_\gamma$	2	1	$\begin{pmatrix} t_1-t_3 \\ t_2-t_4 \end{pmatrix}$
$\bar{5}_\delta$	1_{++}	0	$\sum_{i=1}^4 t_i$
$\bar{5}_\epsilon$	1_{++}	0	$\sum_{i=1}^4 t_i$
$\bar{5}_\zeta$	1_{++}	0	$\sum_{i=1}^4 t_i$
$\bar{5}_\eta$	1_{+-}	0	$(t_1+t_3)-(t_2+t_4)$
$\bar{5}_\theta$	2	0	$\begin{pmatrix} t_1-t_3 \\ t_2-t_4 \end{pmatrix}$

Table 4.4: Table summarising the representations of the fives of $SU(5)_{\rm GUT}$

Abelian discrete group representations of the matter curves, while also being able to obtain them in some manner from the spectral cover approach. In order to achieve this, we shall attempt some form of multifurcation of the spectral cover by definition of new sections in a consistent manner.

Let us begin by defining two new sections κ, λ such that

$$a_3 \to \kappa a_7, \quad a_2 \to \lambda\, a_6\,. \tag{4.8}$$

It is clear that this approach has some similarity with the tracelessness constraint solution usually employed ($b_1 = a_4 a_7 + a_5 a_6 = 0$). Furthermore, these definitions do not generate new unwanted sections. For example, the b_k's

$$b_0 = -a_0 a_7^2, b_1 = 0, b_2 = a_7^2\kappa + a_0 a_6^2, b_3 = (\kappa+\lambda) a_6 a_7, b_4 = \lambda a_6^2 + a_1 a_7, b_5 = a_1 a_6\,, \tag{4.9}$$

do not acquire an overall common factor, while the discriminant

$$\Delta = 108 a_0 \left(\lambda a_6^2 + 4 a_1 a_7\right) \left(\kappa^2 a_7^2 + a_0 \left(\lambda a_6^2 + 4 a_1 a_7\right)\right)^2 \neq \delta^2 \tag{4.10}$$

is not a square - as required for the case of a D_4 monodromy group. On the contrary, substitution to Equation (2.27) gives

$$P_a = a_6^2 \left((\kappa+\lambda)\lambda a_7 - a_0 a_1\right) \tag{4.11}$$

Constraints	P_a	P_b	P_{10}
$a_1 = \kappa a_2$ $a_3 = \lambda a_7$ $a_6 = \mu a_2$	$a_2^2\left(a_7 + \lambda\mu a_7 - \alpha_0\kappa\mu^2 a_2\right)$	$a_2 a_7\left(\kappa a_7 + (\lambda\mu + 1)\mu a_2\right)$	$\kappa\mu a_2^2$

Table 4.5: A viable splitting option of the matter curves, respecting the constraint $\Delta \neq \delta^2$ as required for D_4 symmetry.

and

$$P_b = a_7\left((\kappa + \lambda)a_6^2 + a_1 a_7\right) . \tag{4.12}$$

This appears to generate extra matter curves by increasing the number of factors available, with the added advantage that we can easily find the homologies of our matter curves and know the flux restraints for each. We can interpret these results as a multifurcation to irreducible representations of the D_4 group.

If we further assume $a_1 \to \mu a_6$, then

$$P_b = a_6 a_7\left(a_6(\kappa + \lambda) + \mu a_7\right) , \tag{4.13}$$

and the tens of the GUT group now become:

$$P_{10} \to b_5 = \mu\, a_6 a_6 . \tag{4.14}$$

So we add extra curves here as well.

This is not a unique choice of splitting, and in fact we have a number of possible options that would be compatible with the requirement to prevent unwanted overall factors. A second option is the splitting:

$$a_1 \to \lambda a_2, \quad a_3 \to \kappa a_7 . \tag{4.15}$$

With this choice, the fives are now

$$P_a = a_2\left(a_7\left(a_6\kappa + a_2\right) - a_0 a_6^2\lambda\right) \tag{4.16}$$

$P_{10} = \kappa\mu a_2^2$		
Curve	factor	Homology
10_1	κ	$-c_1$
10_2	a_2	$\eta - 4c_1 - \chi$
10_3	a_2	$\eta - 4c_1 - \chi$
10_4	μ	$-\eta + 4c_1 + 2\chi$

Table 4.6: Distribution of the tens according to the new factorisation, $P_{10} = \kappa\mu a_2^2$.

and

$$P_b = a_7 \left(a_6^2\kappa + a_2 \left(a_7\lambda + a_6\right)\right) . \tag{4.17}$$

The tens now reads $P_{10} = a_1 a_6 \to \lambda a_2 a_6$.

In the same way we can find a number of combinations that leads in suitable splits. In Table 4.5 we show the most interesting case

$$a_1 \to \kappa a_2, \quad a_3 \to \lambda a_7, \quad \text{and} \quad a_6 \to \mu a_2. \tag{4.18}$$

As we can see (4.18) leads in a maximal factorisation for the fives (six factors) and the tens (four factors). The homologies of the new coefficients are

$$[\kappa] = -c_1, \quad [\mu] = -[\lambda] = 4c_1 + 2\chi - \eta. \tag{4.19}$$

Using the above, we can calculate the homologies of the all new factors of tenplets and fives. This case is of particular interest because we have seen that we have four tens of the GUT group, while we will also have six of the fives provided we interpret the trivial singlets as one representation. This last assumption seems reasonable given that they are otherwise indistinguishable.

Flux Restrictions

In order to finally marry the two understandings present in this work, we must appeal to flux restrictions. We summarise the homologies of the various matter curves in Table 4.6 and Table 4.7 with this in mind. Let us assume the usual flux restriction rules. We denote with $\mathcal{F}_Y$ the $U(1)_Y$ flux that breaks $SU(5)$ to the Standard Model and at the same time generates chirality for the fermions. In

$P_b = a_2 a_7 \left(\kappa a_7 + (\lambda\mu + 1)\mu a_2\right)$			
Curve	t_5 charge	factor	Homology
$\bar{5}_a$	1	a_2	$\eta - 4c_1 - \chi$
$\bar{5}_b$	1	a_7	$c_1 + \chi$
$\bar{5}_c$	1	$\kappa a_7 + (\lambda\mu + 1)\mu a_2$	χ
$P_a = a_2^2 \left(a_7 + \lambda\mu a_7 - \alpha_0 \kappa \mu^2 a_2\right)$			
Curve	t_5 charge	factor	Homology
$\bar{5}_d$	0	a_2	$\eta - 4c_1 - \chi$
$\bar{5}_e$	0	a_2	$\eta - 4c_1 - \chi$
$\bar{5}_f$	0	$a_7 + \lambda\mu a_7 - \alpha_0 \kappa \mu^2 a_2$	$c_1 + \chi$

Table 4.7: Distribution of the fives into P_a and P_b. As we can see P_b are related with the t_5 charge.

order to avoid a Green-Schwarz mass for the corresponding gauge boson we must require $\mathcal{F}_Y \cdot \eta = \mathcal{F}_Y \cdot c_1 = 0$. For the unspecified homology χ we parametrise the corresponding flux restriction with an arbitrary integer $N = \mathcal{F}_Y \cdot \chi$, hence we have the constraints:

$$\mathcal{F}_Y \cdot \chi = N,\ \mathcal{F}_Y \cdot c_1 = \mathcal{F}_Y \cdot \eta = 0\,. \tag{4.20}$$

We shall also assume the doublet-triplet splitting mechanism to be powered by this flux. Indeed, assuming N units of hyperflux piercing a given matter curve, the $5/\bar{5}$ split according to:

$$\begin{aligned} n(3,1)_{-1/3} - n(\bar{3},1)_{+1/3} &= M_5\,, \\ n(1,2)_{+1/2} - n(1,2)_{-1/2} &= M_5 + N\,. \end{aligned} \tag{4.21}$$

Thus, as long as $N \neq 0$, for the fives residing on a given matter curved the number of doublets differs from the number of triplets in the effective theory. Choosing $M_5 = 0$ for a Higgs matter curve the coloured triplet-antitriplet fields appear only in pairs which under certain conditions [15, 18] form heavy massive states. On the other hand, the difference of the doublet-antidoublet fields is non-zero and is determined solely from the hyperflux integer parameter N. Similarly, on a matter curve accommodating fermion generations, Equation (4.21) implies different numbers of lepton doublets and down quarks on this particular matter

GUT rep	Def. Eqn.	Parity:	Matter content
10_1	κ	$-$	$M_1 Q_L + u_L^c M_1 + e_L^c M_1$
10_2	a_2	a	$M_2 Q_L + u_L^c (M_2 + N) + e_L^c (M_2 - N)$
10_3	a_2	a	$M_3 Q_L + u_L^c (M_3 + N) + e_L^c (M_3 - N)$
10_4	μ	$\frac{parity(a_6)}{a}$	$M_4 Q_L + u_L^c (M_4 - 2N) + e_L^c (M_4 + 2N)$
5_a	a_2	a	$M_a \bar{d}_L^c + (M_a - N)\bar{L}$
5_b	a_7	b	$M_d D_u + (M_d + N) H_u$
5_c	κa_7	$-b$	$M_c \bar{d}_L^c + (M_c + N)\bar{L}$
5_d	a_2	a	$M_b \bar{D}_d + (M_b - N)\bar{H}_d$
5_e	a_2	a	$M_e \bar{d}_L^c + (M_e - N)\bar{L}$
5_f	a_7	b	$M_f \bar{d}_L^c + (M_f + N)\bar{L}$

Table 4.8: The Generalized matter spectrum for the model before marrying D_4 representations and the matter curves from the spectral cover.

curve. As a consequence, the corresponding mass matrices are expected to differ.

Similarly, the 10s decompose under the influence of N hyperflux units to the following SM-representations:

$$\begin{aligned} n(3,2)_{+1/6} - n(\bar{3},2)_{-1/6} &= M_{10}\,, \\ n(\bar{3},1)_{-2/3} - n(3,1)_{+2/3} &= M_{10} - N\,, \\ n(1,1)_{+1} - n(1,1)_{-1} &= M_{10} + N\,. \end{aligned} \tag{4.22}$$

Hence, as in the case of fives above, the flux effects have analogous implications for the tenplets. The first line in (4.22) in particular, generates the required up-quark chirality since for $M_{10} \neq 0$ the number of $Q = (3,2)_{1/6}$ differs from $\bar{Q} = (\bar{3},2)_{-1/6}$ representations. Moreover, from the second line it is to be observed that $N \neq 0$ leads to further splitting between the $Q = (3,2)_{1/6}$ and $u^c = (\bar{3},1)_{-2/3}$ multiplicities. This fact as we will see provides interesting non-trivial quark mass matrix textures.

4.3 Constructing An $N = 1$ Model

Referring to the aforementioned geometric symmetry discussed at length in the Appendix, we may start out by assigning a Z_2 symmetry to our matter curves, Table 4.9. We shall demand some doublet-triplet splitting in our model, so we take the liberty of setting $N = 1$, motivated by a desire to produce a spectrum

GUT rep	Def. Eqn.	Parity:	$(-,-)$	$(+,-)$	$(-,+)$	$(+,+)$	$N=1$ Matter spectrum
10_1	κ	$-$	$-$	$-$	$-$	$-$	$M_1 Q_L + u_L^c M_1 + e_L^c M_1$
10_2	a_2	a	$-$	$+$	$-$	$+$	$M_2 Q_L + u_L^c (M_2+1) + e_L^c (M_2-1)$
10_3	a_2	a	$-$	$+$	$-$	$+$	$M_3 Q_L + u_L^c (M_3+1) + e_L^c (M_3-1)$
10_4	μ	$\frac{parity(a_6)}{a}$	$-$	$+$	$+$	$-$	$M_4 Q_L + u_L^c (M_4-2) + e_L^c (M_4+2)$
5_a	a_2	a	$-$	$+$	$-$	$+$	$M_a \bar{d}_L^c + (M_a-1)\bar{L}$
5_b	a_7	b	$-$	$-$	$+$	$+$	$M_d D_u + (M_d+1) H_u$
5_c	κa_7	$-b$	$+$	$+$	$-$	$-$	$M_c \bar{d}_L^c + (M_c+1)\bar{L}$
5_d	a_2	a	$-$	$+$	$-$	$+$	$M_b \bar{D}_d + (M_b-1)\bar{H}_d$
5_e	a_2	a	$-$	$+$	$-$	$+$	$M_e \bar{d}_L^c + (M_e-1)\bar{L}$
5_f	a_7	b	$-$	$-$	$+$	$+$	$M_f \bar{d}_L^c + (M_f+1)\bar{L}$

Table 4.9: Parity options are $(a = \pm, b = \pm)$. Any matter curve that has a D_4-doublet must produce doublets - i.e. split twice as fast. $a = parity(a_2)$ and $b = parity(a_7)$, by convention.

free of Higgs colour triplets.

The Z_2 parity has arbitrary phases connecting the coefficients in two cycles: $a_{1,\ldots,5}$ and $a_{6,7}$, which we must choose so that we can best fit the standard matter parity. If we start with a handful of basic requirements it becomes quickly apparent how to do this and guides our assignments of the D_4 irreducible representations.

1. We must have a tree-level Top Yukawa coupling and no other tree-level Yukawas

2. We wish to forbid Dimension-4 proton decay - which may be achieved if our Higgs have + parity and our matter − parity

3. We want a spectrum that resembles the MSSM

If we examine Table 4.9, we can see that in order to be free from $D_{u,d}$ matter, we should choose the parity option $a = b = +$. The subtlety here is that the H_u and H_d must be on matter curves that have different homologies so that if we set the multiplicity for those curves to zero (preventing the $D_{u,d}$ matter), the flux naturally pushes the H_u to be on a 5 of the GUT group, while it pushes the H_d to be a $\bar{5}$.

GUT rep	Def. Eqn.	Parity	Matter content	D_4 rep.	t_5 charge
10_1	κ	$-$	$Q_L + u_L^c + e_L^c$	1_{+-}	0
10_2	a_2	$+$	$u_L^c - e_L^c$	1_{++}	0
10_3	a_2	$+$	$u_L^c - e_L^c$	1_{++}	1
10_4	μ	$-$	$2Q_L + 4e_L^c$	2	0
5_a	a_2	$+$	$2\bar{d}_L^c$	2	0
5_b	a_7	$+$	H_u	1_{++}	0
5_c	κa_7	$-$	$-4\bar{d}_L^c - 3\bar{L}$	1_{+-}	0
5_d	a_2	$+$	$-\bar{H}_d$	1_{++}	-1
5_e	a_2	$+$	$\bar{d}_L^c$	1_{+-}	-1
5_f	a_7	$+$	$-2\bar{d}_L^c$	2	-1

Table 4.10: Full spectrum for an $SU(5)\times D_4\times U(1)_{t_5}$ model from an F-theory construct. Note that the $-t_5$ charge corresponds to the 5, while any representations that are a $\bar{5}$ will instead have t_5.

Singlet	Parity	D_4 rep.	t_5 charge	Vacuum Expectation
θ_α	$+$	1_{++}	-1	$\langle\theta_\alpha\rangle = \alpha$
θ_β	$-$	1_{+-}	-1	$\langle\theta_\beta\rangle = \beta$
θ_γ	$+$	2	-1	$\langle\theta_\gamma\rangle = (\gamma_1, \gamma_2)$
θ_a	$+$	2	0	$\langle\theta_a\rangle = (a_1, a_2)$
ν_r	$-$	1_{+-}	0	$-$
ν_R	$-$	2	0	$-$

Table 4.11: Spectrum of the required singlets to construct full Yukawa matrices with the model outlined in Table 4.10.

We now select our multiplicities M_i as follows:

$$M_2 = M_3 = M_b = M_d = 0$$

$$M_1 = M_a = -M_f = 1$$

$$M_4 = 2$$

$$M_c = -4$$

This provides us with a spectrum that has only a Top Yukawa at tree-level, the correct number of matter generations, and only $u^c d^c d^c$ type dimension 4 parity violating operators, which should shield us from the most dangerous proton decay operators. The spectrum is summarized in Table 4.10.

Low Energy Spectrum	D_4 rep	$U(1)_{t_5}$	Z_2
Q_3, u_3^c, e_3^c	1_{+-}	0	$-$
u_2^c	1_{++}	1	$+$
u_1^c	1_{++}	0	$+$
$Q_{1,2}, e_{1,2}^c$	2	0	$-$
L_i, d_i^c	1_{+-}	0	$-$
ν_3^c	1_{+-}	0	$-$
$\nu_{1,2}^c$	2	0	$-$
H_u	1_{++}	0	$+$
H_d	1_{++}	-1	$+$

Table 4.12: A summary of the low energy spectrum of the model considered. The charges include the Standard Model matter content, the D_4 family symmetry, the remaining $U(1)_{t_5}$ from the commutant SU(5) descending from E_8 orthogonally to the GUT group, and finally the geometric Z_2 symmetry.

4.3.1 Operators

Models of the form presented here taken at face-value allow a large number of GUT operators, however we must ensure that all symmetries are respected. This being the case, we find that the tree-level operators found in Table 4.13, and constructed from the low energy spectrum summarised in Table 4.12, form the basis for our model, assuming the D_4 algebra rules:

$$\begin{aligned} 2{\times}2 &= 1_{++} + 1_{+-} + 1_{-+} + 1_{--}\,, \\ 1_{a,b}{\times}1_{c,d} &= 1_{ac,bd}\,, \\ \text{with: } & \; a,b,c,d = \pm \end{aligned}$$

As well as the expected Yukawas for the quarks and charged leptons, there are also a number of parity violating operators that could lead to dangerous and unacceptable rates of proton decay. However, provided the singlet spectrum is aligned correctly it is possible to avoid unacceptable proton decay rates via dimension-4 operators. It will not be possible to remove all parity violating operators from the spectrum though, and we will be left with $u^c d^c d^c$ operators that may facilitate neutron-antineutron oscillations.

Operator→ type	D_4 irrep.	t_5 charge	Z_2 parity
$10_1 10_1 5_b \to QUH$	1_{++}	0	1
$10_1 10_2 5_b \to QUH$	1_{+-}	0	-1
$10_1 10_3 5_b \to QUH$	1_{+-}	1	-1
$10_4 10_1 5_b \to QUH$	2	0	1
$10_4 10_2 5_b \to QUH$	2	0	-1
$10_4 10_3 5_b \to QUH$	2	1	-1
$10_1 \bar{5}_c \bar{5}_d \to QDH$	1_{++}	1	1
$10_4 \bar{5}_c \bar{5}_d \to QDH$	2	1	1
$10_1 \bar{5}_c \bar{5}_d \to LEH$	1_{++}	1	1
$10_4 \bar{5}_c \bar{5}_d \to LEH$	2	1	1
$10_1 \bar{5}_c \bar{5}_c \to UDD$	1_{+-}	0	-1
$10_2 \bar{5}_c 5_c \to UDD$	1_{++}	0	1
$10_3 \bar{5}_c \bar{5}_c \to UDD$	1_{++}	1	1
$10_1 \bar{5}_c \bar{5}_c \to QLD$	1_{+-}	0	-1
$10_4 \bar{5}_c \bar{5}_c \to QLD$	2	0	-1
$10_1 \bar{5}_c 5_c \to ELL$	1_{+-}	0	-1
$10_4 \bar{5}_c 5_c \to ELL$	2	0	-1

Table 4.13: List of all trilinear couplings available in the SU(5) $\times D_4 \times U(1)$ model presented. At tree-level, these operators are not all immediately allowed, since the D_4 and t_5 symmetries must be respected.

Quark sector

The up-type quarks have four operators that contribute to the Yukawa matrix. Firstly, we have a tree level top quark coming from the operator $10_1 10_1 5_b$, which is the only tree level Yukawa operator found in the Quark and Charged Lepton sectors. The remaining three operators are non-renormalisable operators subject to suppression. We shall assume that the up-type Higgs gets a vacuum expectation value, $\langle H_u \rangle = v_u$. The singlets involved get vacuum expectations: $\langle \theta_a \rangle = (a_1, a_2)^T$ and $\langle \theta_\beta \rangle = \beta$. The following mass terms are generated

$$10_1 10_1 5_b \to y_1 v_u Q_3 u_3^c$$

$$10_4 10_1 5_b \theta_a \to y_2 v_u (Q_2 a_2 + Q_1 a_1) u_3^c$$

$$10_4 10_3 5_b \theta_a \theta_\beta \to y_3 v_u \beta (Q_2 a_2 + Q_1 a_1) u_2^c$$

$$10_1 10_3 5_b \theta_\beta \to y_4 v_u \beta Q_3 u_2^c$$

giving rise to the up-quark mass texture

$$M_{u,c,t} = v_u \begin{pmatrix} 0 & y_3 a_1 \beta & y_2 a_1 \\ 0 & y_3 a_2 \beta & y_2 a_2 \\ 0 & y_4 \beta & y_1 \end{pmatrix}. \tag{4.23}$$

The lightest generation does not get an explicit mass from this mechanism, but we can expect a small correction to come from non-commutative fluxes or instantons [33, 35, 37], thus generating a small mass for the first generation.

The down-type quarks contribute a further two operators to the model. These will be symmetric across the right-handed d^c since all three generations are found on the 5_c matter curve. We once again assume the Higgs to get a vacuum expectation, $\langle H_d \rangle = v_d$. As before, we also give the singlets a vacuum expectation value: $\langle \theta_\alpha \rangle = \alpha$ and $\langle \theta_\gamma \rangle = (\gamma_1, \gamma_2)^T$. As a result, we get the Yukawa contributions

$$\begin{aligned} 10_1 \bar{5}_c \bar{5}_d \theta_\alpha &\to y_{4,i} v_d Q_3 d_i^c \alpha \\ 10_4 \bar{5}_c \bar{5}_d \theta_\gamma &\to y_{5,i} v_d (Q_2 \gamma_2 + Q_1 \gamma_1) d_i^c \end{aligned}$$

and consequently, the down quark mass matrix form

$$M_{d,s,b} = v_d \begin{pmatrix} y_{5,1}\gamma_1 & y_{5,2}\gamma_1 & y_{5,3}\gamma_1 \\ y_{5,1}\gamma_2 & y_{5,2}\gamma_2 & y_{5,3}\gamma_2 \\ y_{4,1}\alpha & y_{4,2}\alpha & y_{4,3}\alpha \end{pmatrix}. \tag{4.24}$$

However, this mass matrix will be subject to the rank theorem, requiring that there be some suppression factor between the copies of the operator, which we indicate by the second index, $y_{i,j}$.

Charged Leptons

The Charged Lepton Yukawas are determined by the same operators as the Down-type quarks, subject to a transpose. As such their mass matrix is as follows:

$$
\begin{aligned}
&10_1\bar{5}_c\bar{5}_d\theta_\alpha \to y_{6,i}v_d L_i e_3^c \alpha \\
&10_4\bar{5}_c\bar{5}_d\theta_\gamma \to y_{7,i}v_d L_i (e_2^c\gamma_2 + e_1^c\gamma_1) \\
&M_{e,\mu,\tau} = v_d \begin{pmatrix} y_{7,1}\gamma_1 & y_{7,1}\gamma_2 & y_{6,1}\alpha \\ y_{7,2}\gamma_1 & y_{7,2}\gamma_2 & y_{6,2}\alpha \\ y_{7,3}\gamma_1 & y_{7,3}\gamma_2 & y_{6,3}\alpha \end{pmatrix}
\end{aligned} \tag{4.25}
$$

The mass relations between charged leptons and down-type quarks will not be constrained to be exact as the operators can be assumed to be localized to different parts of the GUT surface. Once again this is subject to the rank theorem, but will be able to produce a light first generation through other mechanisms.

Neutrinos

As already explained in the introduction, neutrino masses may admit both Dirac and Majorana masses, which can be used to create a seesaw mechanism and make the effective neutrino masses suitably small, which we shall exploit in this model. In order to obtain sharp predictions for lepton mixing angles along with these small masses, the relevant Yukawa coupling ratios need to be fixed, for example using vacuum alignment of family symmetry breaking flavons (for reviews see e.g. [84–86, 94]).

Any Dirac-type mass comes from an operator of the form $m_D \sim \theta_\nu 5_b \bar{5}_c$, while the right-handed Majorana mass terms are of the form $M\theta_\nu\theta_\nu$. Although we have a non-Abelian D_4 family symmetry, the lepton doublets L are in singlet representations (see Table 4.12), so the model offers no opportunity to make predictions for the lepton mixing angles.

The singlet representations and parities, as detailed in the Appendix, allow us up to nine singlets in this model. Let us then match our right-handed neutrinos

to the representations 1_{+-} and a doublet, as allowed from our spectrum. This will then give the operators for the Dirac mass:

$$\begin{aligned}
\theta_{\nu_r} 5_b \bar{5}_c &\to y_{8,i} v_u \nu_3^c L_i \\
\theta_{\nu_R} 5_b \bar{5}_c \theta_a &\to y_{9,i} v_u (\nu_1^c a_1 + \nu_2^c a_2) L_i \\
m_D &= v_u \begin{pmatrix} y_{9,1}a_1 & y_{9,1}a_2 & y_{8,1} \\ y_{9,2}a_1 & y_{9,2}a_2 & y_{8,2} \\ y_{9,3}a_1 & y_{9,3}a_2 & y_{8,3} \end{pmatrix}.
\end{aligned} \tag{4.26}$$

This Dirac matrix can be shown to be rank two, which will cause our lightest neutrino to be massless. While this is not explicitly ruled out by experiment, a small mass can be generated through some higher order operators from other singlets in the spectrum if required - for example a singlet of the type 1_{--} with + parity. This will allow an explicit Dirac type mass, however similar analysis has been done elsewhere (for example [2]), so we omit in depth discussion here.

The Majorana terms corresponding to this choice of neutrino spectrum are simply calculated, as one might expect:

$$\begin{aligned}
\theta_{\nu_r}\theta_{\nu_r} &\to m\nu_3^c\nu_3^c \\
\theta_{\nu_R}\theta_{\nu_R} &\to M\nu_1^c\nu_2^c \\
\theta_{\nu_r}\theta_{\nu_R}\theta_a &\to y\nu_3^c\nu_2^c a_2 + y\nu_3^c\nu_1^c a_1 \\
M_R &= \begin{pmatrix} 0 & M & ya_1 \\ M & 0 & ya_2 \\ ya_1 & ya_2 & m \end{pmatrix}
\end{aligned} \tag{4.27}$$

This may also be allowed corrections via extra singlets, though it will not be needed for this work.

The effective neutrino mass can be calculated from the seesaw mechanism via $m_\nu = -m_D M_R^{-1} m_D^T$. The resulting mass matrix appears complicated, with

elements given in full as:

$$\begin{aligned}
m_{11} =& M{y_{8,1}}^2 + 2a_1a_2y_{9,1}(my_{9,1} - 2y_{8,1}y) \\
m_{12} = m_{21} =& My_{8,1}y_{8,2} - 2a_1a_2(y_{8,2}yy_{9,1} - my_{9,2}y_{9,1} + y_{8,1}yy_{9,2}) \\
m_{13} = m_{31} =& My_{8,1}y_{8,3} - 2a_1a_2(y_{8,3}yy_{9,1} - my_{9,3}y_{9,1} + y_{8,1}yy_{9,3}) \\
m_{22} =& M{y_{8,2}}^2 + 2a_1a_2y_{9,2}(my_{9,2} - 2y_{8,2}y) \\
m_{23} = m_{32} =& My_{8,2}y_{8,3} - 2a_1a_2(y_{8,3}yy_{9,2} - my_{9,3}y_{9,2} + y_{8,2}yy_{9,3}) \\
m_{33} =& M{y_{8,3}}^2 + 2a_1a_2y_{9,3}(my_{9,3} - 2y_{8,3}y)
\end{aligned} \tag{4.28}$$

with an overall scaling of $m_0 = v_u^2(Mm - 2a_1a_2y^2)^{-1}$.

In order to extract mixing parameters and mass scales, we will parameterize the matrix in the following way:

$$X_i = \frac{y_{8,i}}{y_{8,1}},\ Z_i = \frac{y_{9,i}}{y_{8,1}},\ G = \frac{2a_1a_2}{M} \tag{4.29}$$

with $i = 1, 2, 3$, and trivially $X_1 = 1$. Note that $X_{2,3}$ and Z_j are not required to be order one due to the parametrization choice. Let us go a step further, approximating $m \approx M$ and setting $Z_3 = 0$, then the mass matrix is given by:

$$m_\nu \approx m_0 \begin{pmatrix} GZ_1(Z_1 - 2y) + 1 & -GyZ_1X_2 + X_2 + G(Z_1 - y)Z_2 & X_3 - GX_3yZ_1 \\ -GyZ_1X_2 + X_2 + G(Z_1 - y)Z_2 & X_2^2 - 2GyZ_2X_2 + GZ_2^2 & X_3(X_2 - GyZ_2) \\ X_3 - GX_3yZ_1 & X_3(X_2 - GyZ_2) & X_3^2 \end{pmatrix} \tag{4.30}$$

where:

$$m_0 = \frac{v_u^2 M x_1^2}{M^2 - Gy^2}\,. \tag{4.31}$$

This parametrization allows for comparatively straightforward extraction of mixing parameters. Using Mathematica, we fit the Ratio of mass squared differences in this model to experimental constraints, allowing us to extract a mass scale for the neutrinos while fitting parameters to allow acceptable mixing angles.

Figure 4.1 shows plots of the 3σ ranges of $\sin^2\theta_{12}$, $\sin^2\theta_{23}$ and $R = \left|\frac{m_3^2 - m_2^2}{m_2^2 - m_1^2}\right|$ in the parameter space of (X_2, X_3). This shows that while there are some sharp

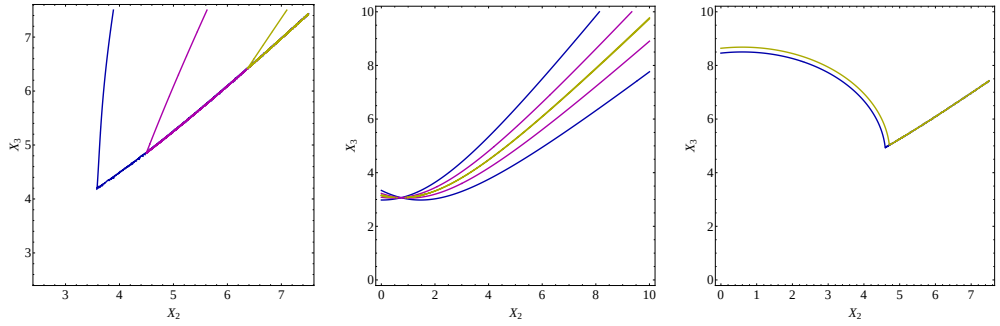

Figure 4.1: Left: Plot of $\sin^2\theta_{12}$ across its 3σ range (blue-0.270, pink-0.304, yellow-0.344), Center: Plot of $\sin^2\theta_{23}$ across its 3σ range (blue-0.382, pink-0.452, yellow-0.5). Note that the upper bound of $\sin^2\theta_{23}$ is 0.643, but this is not allowed by the model, which permits a maximum of 0.5 for these parameters. Right: Plot of the mass squared difference ratio, R, for its upper and lower bounds of 31.34 (blue) and 34.16 (yellow). For all three plots the parameter space (X_2, X_3) is plotted since these terms should lead the mixing. The remaining parameters are set at values that yield consistent mixing parameters: $(Z_1 \approx 2.4, Z_2 \approx 4.1, G \approx 0.6, y \approx 0.3)$.

cutoffs in the parameter space, the key variables can still be allowed. A full simulation of parameters gives, for example:

$$\text{Inputs: } (X_2 = 4.5,\ X_3 = 5.7,\ Z_1 = 2.4,\ Z_2 = 4.1,\ G = 0.6,\ y = 0.3) \tag{4.32}$$

$$\text{Outputs: } (R = 33.2,\ \theta_{12} = 32.4,\ \theta_{13} = 9.07,\ \theta_{23} = 39.2)$$

This also allows us to extract the neutrino masses using the mass differences, which are an implicit input parameter used in calculation of R. We know from the Dirac matrix rank that at this order of operator one neutrino is massless, so then the remaining two masses are (within experimental errors) equal to the square root of the mass differences:

$$m_1 = 0 \text{ meV}\,,\ m_2 = 8.66 \text{ meV}\,,\ m_3 = 50.3 \text{ meV}\,. \tag{4.33}$$

Being at the absolute minimum scale for the neutrino masses, this is automatically compatible with cosmological constraints.

4.3.2 μ-Terms

In this set-up the standard Higgs sector μ-term requires coupling to a singlet in order to cancel the charges under $U(1)_{t_5}$. The most suitable coupling allowed by the singlet sector is a term of the type:

$$\lambda_1 \theta_\alpha H_u H_d \,. \tag{4.34}$$

As such the μ term is proportional to the vacuum expectation of the singlet θ_α:

$$\mu = \lambda_1 \langle \theta_\alpha \rangle. \tag{4.35}$$

Since this singlet couples to the charged lepton and the bottom quark Yukawa matrices, the resulting vacuum expectation should allow a TeV scale μ-term while not affecting these Yukawas too strongly. Note that since the operators in the charged lepton and bottom quark sectors are non-renormalisable, the coupling should be suppressed by a large mass scale, making this possible. It is also shown in the D-flatness conditions (provided in the appendix) that we have a deal of freedom when choosing the vacuum expectation value for θ_α.

A second term of the type:

$$\lambda_2 \theta_a \theta_\gamma H_u H_d \,. \tag{4.36}$$

will also contribute to the μ terms, which is non-renormalisable and should be suppressed by some large mass scale. Refering to the F-flatness conditions and a cursory calculation of this coupling, we see that this contributes proportionally to the product of the vacuum expectations of the θ_a and θ_γ singlets. This again seems acceptable.

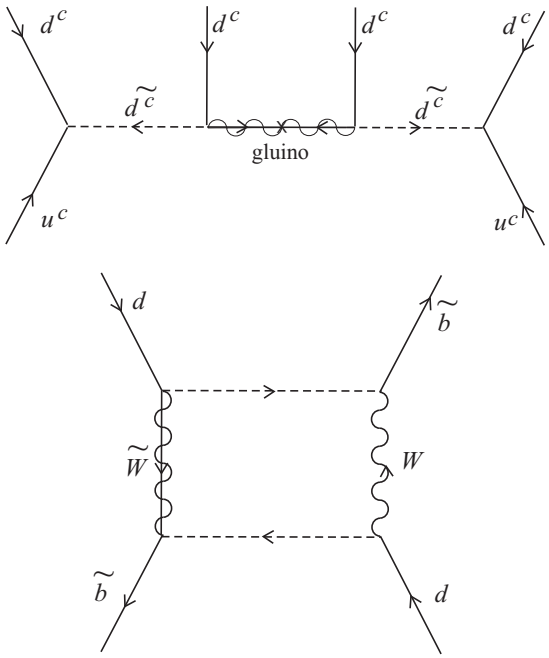

Figure 4.2: Feynman graphs for $n - \bar{n}$ oscillation processes. Top: oscillation via a gluino, Bottom: box-graph process.

4.4 Baryon number violation

4.4.1 Neutron-antineutron oscillations

As mention in the previous section, the model presented is free from proton decay at the lowest orders. However, it is subject to operators which are classically considered to be parity violating. Since these operators are all of the type $u^c d^c d^c$, they will instead facilitate neutron-antineutron oscillations. While this is a seldom considered property of GUT models, work has been done to calculate transmission amplitudes of such processes by Mohapatra and Marshak [96] and later on by Goity and Sher [97] among others. The contributions to the process are generated from tree-level and box type graphs (see [97], the reviews [98, 99] and references therein), with typical cases shown in Figure 4.2.

In the paper of Goity and Sher, they argue that one can identify a competitive mechanism, with a fully calculable transition amplitude, which sets a bound on λ_{dbu}. This mechanism is based on the sequence of reactions $u_R d_R + d_L \rightarrow \tilde{b}^*_R + d_L \rightarrow (\tilde{b}^*_L + d_L \rightarrow \bar{d}_L + \tilde{b}_L) \rightarrow \bar{d}_L + \bar{u}_R \bar{d}_R$, where the intermediate transition in the parentheses, $\tilde{b}^*_L + d_L \rightarrow \bar{d}_L + \tilde{b}_L$, is due to a W boson and gaugino

exchange box diagram. The choice of intermediate bottom squarks is the most favourable one in order to maximise factors such as m_b^2/m_W^2, which arise from the electroweak interactions of d-quarks in the box diagram (Figure 3).

Calculation of the diagram gives the following relation for the decay rate,

$$\Gamma = -\frac{3g^4\lambda_{dbu}^2 M_{\tilde{b}_{LR}}^2 m_{\tilde{w}}}{8\pi^2 M_{\tilde{b}_L}^4 M_{\tilde{b}_R}^4}|\psi(0)|^2 \sum_{j,j'}^{u,c,t} \xi_{jj'} J(M_{\tilde{w}}^2, M_W^2, M_{u_j}^2, M_{\tilde{u}_{j'}}^2) \tag{4.37}$$

where the mass term $M_{\tilde{b}_{LR}}$, which mixes $\tilde{b}_L$ and $\tilde{b}_R$, is given by $M_{\tilde{b}_{LR}} = Am_b$. Here A is the soft SUSY breaking parameter with $A = m_{\tilde{w}} = 200GeV$, and $\xi_{jj'}$ is a combination of CKM matrix parameters,

$$\xi_{jj'} = V_{bu_j} V_{u_j d}^\dagger V_{bu_{j'}} V_{u_{j'} d}^\dagger \tag{4.38}$$

and the J functions are given by:

$$J(m_1, m_2, m_3, m_4) = \sum_{i=1}^{4} \frac{m_i^4 \ln(m_i^2)}{\prod_{k\neq i}(m_i^2 - m_k^2)}\,. \tag{4.39}$$

The n-$\bar{n}$ oscillation time is $\tau = 1/\Gamma$ and the current experimental limits is $\tau \gtrsim 10^8 sec.$ [98]. Finally $|\psi(0)|$ is the baryonic wave function matrix element for three quarks inside a nucleon. This parameter was calculated to be $|\psi(0)|^2 = 10^{-4}$ and $0.8 \times 10^{-4} GeV^{-6}$ in MIT Bag models[6]. From the experimental limit on the neutron oscillation time we can obtain the bound on λ_{dbu}. The results depend on CKM parameters and the squarks masses. In Figure 4.3 we reproduce the results of Goity and Sher. As we can see the upper bound on λ_{dbu} is between 0.005 and 0.1.

Next we use the Equation (4.37) to recalculate the bounds on λ_{dbu} with the latest experimental results for the SUSY mass parameters. In Figure 4.4 the curves correspond to squark masses of 800, 1000 and 1200GeV (Blue, dashed and dotted accordingly). As we can see the value of λ_{dbu} lies between 0.1 and ~ 0.5 for stop mass between 500 and 1600GeV, neglecting GIM effects.

[6]Goity and Sher used a slightly more stringent bound, $\tau > 1.2 \times 10^8 sec.$ and for the matrix element they took $|\psi(0)|^2 = 3 \times 10^{-4} GeV^6$.

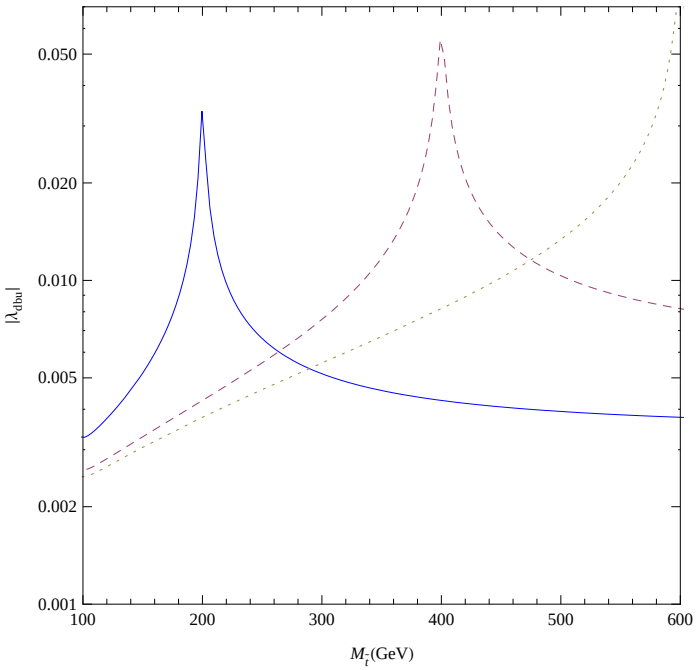

Figure 4.3: Goity and Sher bounds on λ_{dbu}. They assumed that up and bottom squark masses are degenerate. Blue: $M_{\tilde{u}} = M_{\tilde{c}} = 200GeV$, Dashed: $M_{\tilde{u}} = M_{\tilde{c}} = 400GeV$, Dotted: $M_{\tilde{u}} = M_{\tilde{c}} = 600GeV$. Also we took $M_{\tilde{b}_L} = M_{\tilde{b}_R} = 350GeV$. The peaks corresponds to GIM mechanism effects.

In F-theory there is an associated wavefunction [59] [34] to the state residing on each matter curve and it can be determined by solving the corresponding equations of motion [18]. The solutions show that each wavefunction is peaked along the corresponding matter curve. Yukawa couplings are formed at the point of intersection of three matter curves where the corresponding wavefunctions overlap. To estimate the corresponding Yukawa coupling we need to perform an integration over the three overlapping wavefunctions of the corresponding states participating in the trilinear coupling. Taking into account mixing effects this particular coupling is estimated to be of the order $\lambda_{dbu} \leq 10^{-1}$. From the figure it can be observed that recent $n - \bar{n}$ oscillation bounds on λ_{dbu} are compatible with such values.

4.5 Conclusions

In this chapter an F-theory derived SU(5) model was constructed [2], with the implications of the arising non-Abelian familiy symmetry being considered, fol-

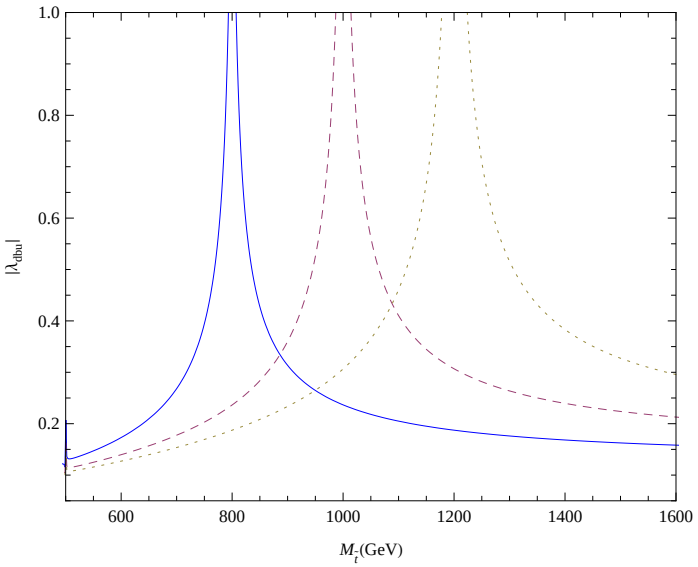

Figure 4.4: New bounds on λ_{dbu} using the latest experimental limits. Blue: $M_{\tilde{u}} = M_{\tilde{c}} = 800GeV$, Dashed: $M_{\tilde{u}} = M_{\tilde{c}} = 1000GeV$, Dotted: $M_{\tilde{u}} = M_{\tilde{c}} = 1200GeV$. Also we use the following values for the other parameters: $M_{\tilde{b}_L} = M_{\tilde{b}_R} = 500GeV$, $\tau = 10^8 sec.$ and $|\psi(0)| = 0.9 \times 10^{-4} GeV^{-6}$.

lowing from work in [50] and [2]. Using the spectral cover formalism, assuming a point of E_8 enhancement descending to an SU(5) GUT group, the corresponding maximal symmetry (also SU(5)) should reduce down to a subgroup of the Weyl group, S_5. In this chapter we derived the conditions on the spectral cover equation in the case of the non-abelian discrete group D_4, which was assumed to play the role of a family symmetry. A novel geometric symmetry was also employed to produce an R-parity-like Z_2 symmetry. The combined effect of this framework on the effective field theory has been examined, and the resulting model shown to exhibit R-parity violation in the form of neutron-antineutron oscillations, while being free from dangerous proton decay operators. The experimental constraints on this interesting process have been calculated, using current data on the masses of supersymmetric partners. Detection of such baryon-violating processes, without proton decay, would serve as a potential smoking gun for this type of model.

The physics of the neutrino was also considered, and it was shown that at lowest orders this model predicts a massless first generation neutrino. Correspondingly, the masses of the two other generations then equate to the mass

differences from experiment, with the hierarchy being normal ordered. The mixing angles were also probed numerically, with results that are consistent with large mixing in the neutrino sector and a non-zero reactor mixing angle.

In conclusion F-theory model building predicts in a natural way the coexistence of GUT models with non-Abelian discrete symmetry extensions. The rich symmetry content following from the decomposition of the E_8 covering group and the geometric symmetries emerging from the internal manifold structure are sufficient to incorporate successful non-Abelian groups which have already been proposed in phenomenological constructions during the last decade. The distinct role of the discrete groups as family symmetries occurs naturally in the F-theory constructions. Moreover, the theory provides powerful tools to get an effective field theory with definite predictions.

Chapter 5

F-theory, E_6, and the 750GeV resonance

Recently ATLAS and CMS experiments have reported an excess of 14 and 10 diphoton events at an invariant mass around 750 GeV and 760 GeV from gathering data at LHC Run-II with pp collisions at the center of mass energy of 13 TeV [100, 101]. The local significance of the ATLAS events is 3.9 σ while that of the CMS events is 2.6 σ, corresponding to cross sections $\sigma(pp \to \gamma\gamma) = 10.6$ fb and $\sigma(pp \to \gamma\gamma) = 6.3$ fb. ATLAS favours a width of $\Gamma \sim 45$ GeV, while CMS, while not excluding such a broad resonance, prefers a narrow width. The Landau-Yang theorem implies spin 0 or 2 are the only possibilities for a resonance decaying into two photons. The only modest diphoton excesses observed by ATLAS and CMS at this mass scale may be (at least partially) understood by the factor of 5 gain in cross-section due to gluon production. However there is no evidence for any coupling of the resonance into anything except gluons and photons (no final states such as $t\bar{t}$, $b\bar{b}$, $l\bar{l}$, ZZ, WW, etc., with missing E_T or jets have been observed).

If these facts are confirmed by future data, it will be the first indication for new physics at the TeV scale and possibly a harbinger of more exciting discoveries in the future. These findings also pose a challenging task for theoretical extensions of the Standard Model (SM) spectrum. Several interpretations have been suggested

based in what now constitutes an extensive literature base: [102–216]

Many of these papers suggest a spinless singlet coupled to vector-like fermions. Indeed, the observed resonance could be interpreted as a Standard Model scalar or pseudoscalar singlet state X with mass $m_X \sim 750 - 760$ GeV. The process of generating the two photons can take place by the gluon-gluon fusion mechanism according to the process

$$gg \to X \to \gamma\gamma$$

hence it requires production and decay of the particle X. In a renormalisable theory this interaction can be realised assuming vector-like multiplets $f + \bar{f}$ at the TeV scale, where f carry electric charge and colour. Such vector like pairs have not been observed at the LHC, hence the mass of the fermion pair M_f is expected roughly to be at or above the TeV scale, $M_f \gtrsim 1$ TeV.

If this theoretical interpretation is adopted, effective field theory models derived in the context of String Theory are excellent candidates to accommodate the required states. Indeed, singlet scalar fields are the most common characteristic of String Theory effective models. These can be either scalar components of supermultiplets or of pseudoscalar nature such as axion fields having direct couplings to gluons and photons and therefore relevant to the observed process. However another aspect of string theory interests us here, namely that in the low energy spectrum of a wide class of string models vector-like supemultiplets either with the quantum numbers of ordinary matter or with exotic charges are generically present. Moreover, in specific constructions they can remain in the low energy spectrum and get a mass at the TeV scale. A particularly elegant possibility is that the low energy spectrum consists of the matter content of three complete 27-dimensional representations of E_6, as in the E_6SSM [12,217], or minimal E_6SSM [218], minus the three right-handed neutrinos which have zero charge under the low energy gauged $U(1)_N$, and hence may get large masses. In both versions additional singlet and vector-like states from E_6 reside at the TeV scale, together with a Z'. In the original version [12, 217] extra vector-like Higgs states are added for the purposes of unification, while in the minimal E_6SSM [218] they

are not.

In this paper we will revisit an F-theory E_6 GUT model that has the TeV spectrum of the minimal E$_6$SSM, namely three complete 27-dimensional representations of E_6 minus the right-handed neutrinos [52, 53] plus additional bulk exotics which provide the necessary states for unification [54]. Unification is achieved since the matter content is that of the MSSM supplemented by four families of SU(5) $5 + \bar{5}$ states, although in the present model all the extra states are incomplete $SU(5)$ multiplets and crucially there are three additional TeV scale singlet states (in addition to the three high mass right-handed neutrinos which are sufficient to realise the see-saw mechanism). Moreover some of the low energy singlets couple to three families of TeV scale vector-like matter with the quantum numbers of down-type quarks [53] called here $D, \bar{D}$. Unlike the E$_6$SSM, the extra gauged $U(1)_N$ may be broken at the GUT scale, leading to an NMSSM-like theory without an extra Z', but with extra vector-like matter, as in the NMSSM+ [219]. However, here we focus exclusively on the model in [54] where one of the three low energy singlets is responsible for the Higgs μ term, and acquires an electroweak scale vacuum expectation value (VEV), while the other two singlets do not couple to Higgs but do couple to vector-like quarks $D, \bar{D}$, acquiring a TeV scale VEV. These latter candidates are therefore candidates for the 750 GeV mass resonance, able to account for the ATLAS and CMS data, since they have couplings to $D, \bar{D}$, and may have the couplings required to generate the process $pp \to X \to \gamma\gamma$ via loops of $D, \bar{D}$ and inert Higgsinos. We emphasise that these models were proposed before the recent ATLAS and CMS data, so the interpretation that we discuss is not based on *ad hoc* modifications to the Standard Model, but rather represents a genuine consequence of well motivated theoretical considerations.

The layout of the remainder of this chapter is as follows. In the next section we review the basic features of the specific E_6 F-theory model focusing mainly on its spectrum and in particular on the properties of the predicted exotics. We start section 5.2 by writing down the Yukawa interactions related to the processes

that interest us in this work. Next, we compute the corresponding cross sections and compare our findings with the recent experimental results, before we finally present our conclusions.

5.1 The F-theory model with extra vector-like matter

In F-theory constructions SM-singlets and vector-like quark or lepton type fields are ubiquitous. Many such pairs are expected to receive masses at a high scale, but it is possible that several of them initially remain massless, later acquiring TeV scale masses. To set the stage, we start with a short description on the origin of the SM spectrum and bulk vector-like states in F-theory GUTs in general. We choose E_6 as a working example where it was shown sometime ago [52–54] that scalars as well as vector-like fermion fields at the TeV scale are naturally accommodated. We start with the decomposition of the E_8-adjoint under the breaking $E_8 \supset E_6 \times SU(3)$

$$248 \to (78,1) + (1,8) + (27,3) + (\overline{27},\bar{3})$$

and label with t_i the $SU(3)$ weights (subject to the tracelessness condition $t_1 + t_2 + t_3 = 0$). Along the $SU(3)$ Cartan subalgebra, $(1,8)$ decomposes to singlets $\theta_{ij}, i,j = 1,2,3$ whilst the 27's are characterised by the three charges t_i. We impose a Z_2 monodromy $t_1 = t_2$ thus, we have the correspondence

$$(1,8) \to \theta_{13}, \theta_{31}, \theta_0; \quad (27,3) \to 27_{t_1}, 27_{t_3}; \quad (\overline{27},\bar{3}) \to \overline{27}_{-t_1}, \overline{27}_{-t_3}. \tag{5.1}$$

Notice that because of the Z_2 monodromy we get the identifications $\theta_{12} = \theta_{21} \equiv \theta_0$, as well as $\theta_{23} = \theta_{13}$ and $\theta_{32} = \theta_{31}$ and analogously for the $27_{t_1} = 27_{t_2}$. Additional bulk singlets θ_{kl} and vector-like pairs are obtained under further breaking of the symmetry down to $SU(5)$.

The $SU(5)$ breaking is realised by a non-trivial hypercharge flux. Hence, assuming M_{10}, M_5 the number of flux units determining the chiral $SU(5)$ representations and N_Y hypercharge flux units, for given tenplet and fiveplet we get

the following splittings:

$$10_{t_i} = \begin{cases} \text{Representation} & \text{flux units} \\ \#Q - \#\bar{Q} & = M_{10}^i \\ \#u^c - \#\bar{u}^c & = M_{10}^i - N_Y^i \\ \#e^c - \#\bar{e}^c & = M_{10}^i + N_Y^i \end{cases} \tag{5.2}$$

$$5_{t_i} = \begin{cases} \text{Representation} & \text{flux units} \\ \#d^c - \#\bar{d}^c & = M_5^i \\ \#\bar{\ell} - \#\ell & = M_5^i + N_Y^i \end{cases} \tag{5.3}$$

We observe that a non-trivial flux differentiates the SM content on a given matter curve. The various flux parameters are subject to restrictions coming from anomaly cancellation conditions and flux conservation [87, 88].

The detailed derivation of the particular F-theory model we are interested in can be found in reference [54]. In the present note, we only present the E_6 origin of the low energy spectrum and the corresponding $SU(5) \times U(1)_N$ multiplets, which are summarised in Table 5.1. The last column shows the 'charge' Q_N of the $U(1)_N$ Abelian gauge factor contained in E_6, under which the right-handed neutrinos are singlets as in the E$_6$SSM [12, 217]. Due to hypercharge flux conservation, the Standard Model massless states must assemble into complete $SU(5)$ multiplets. Indeed, referring to Table 5.1, the matter in the 27_{t_1} representation $(3D + 2H_u)$ together with the H_u from the 27_{t_3} form three complete fiveplets. Similarly, the $3(\overline{D} + H_d)$ matter from 27_{t_1} forms three complete anti-fiveplets.

Without the bulk exotics the spectrum has the matter equivalent of three families of E_6 27-dimensional representations as in the minimal E$_6$SSM [218], which form an anomaly free set by themselves. Such a model was realised in F-theory context [53] while it was shown that unification can be successfully achieved with the inclusion of the bulk exotics [54] relevant to our present discussion. The total low energy spectrum, including bulk exotics, then has the matter content of the MSSM plus four extra vector-like $5 + \overline{5}$ families plus three extra singlets, which do not affect the unification scale. Three right-handed neutrinos are present at

E_6	$SU(5)$	Weights	TeV spectrum	$\sqrt{10}Q_N$
27_{t_1}	$\overline{5}$	t_1+t_5	$3(d^c+L)$	1
27_{t_1}	10	t_1	$3(Q+u^c+e^c)$	$\frac{1}{2}$
27_{t_1}	5	$-t_1-t_3$	$3D+2H_u$	-1
27_{t_1}	$\overline{5}$	t_1+t_4	$3(\overline{D}+H_d)$	$-\frac{3}{2}$
27_{t_1}	1	t_1-t_4	θ_{14}	$\frac{5}{2}$
27_{t_3}	5	$-2t_1$	H_u	$-\frac{1}{2}$
27_{t_3}	1	t_3-t_4	$2\,\theta_{34}$	$\frac{5}{2}$
78	$\overline{5}$	0	$2\,X_{H_d}+X_{d^c}$	$-\frac{3}{2}$
78	5	0	$2\overline{X}_{\overline{H}_d}+\overline{X}_{\overline{d^c}}$	$\frac{3}{2}$
1	1	$\pm(t_1-t_3)$	$\theta_{13},\theta_{31},\theta_0$	0

Table 5.1: The low energy spectrum for the F-theory E_6SSM-like model with TeV scale bulk exotics taken without change from [54]. The fields Q, u^c, d^c, L, e^c represent quark and lepton SM superfields in the usual notation. In this spectrum there are three families of H_u and H_d Higgs superfields, as compared to a single one in the MSSM. There are also three families of exotic D and $\overline{D}$ colour triplet superfields, where $\overline{D}$ has the same SM quantum numbers as d^c, and D has opposite quantum numbers. We have written the bulk exotics as X with a subscript that indicates the SM quantum numbers of that state. The superfields θ_{ij} are SM singlets, with the two θ_{34} singlets containing spin-0 candidates for the 750 GeV resonance.

high energies. Renormalisation Group analysis shows [54] that perturbative unification can be achieved as shown in Fig.5.1. With this in mind, next we focus on the characteristic properties of the model that are required to accommodate the recent experimental data.

5.1.1 Proton Decay

One of the main obstacles in realising a viable $SU(5)$ model is the appearance of colour triplets $D, \bar{D}$ in the Higgs fiveplets which can mediate proton decay. In simple field theory GUT models, a doublet-triplet splitting mechanism ensures the existence of light Higgs doublets, while coloured triplets acquire a GUT mass through a term $\langle\Phi\rangle\bar{5}_{\bar{H}}5_H$. Yet, even a mass of $\langle\Phi\rangle \sim M_{GUT}$ is not adequate to suppress proton decay within the present experimental bounds.

In the present model the problem is apparently much more severe since there are colour triplets $D, \bar{D}$ at the TeV scale. However, these TeV scale colour triplets do not give rise to proton decay diagrams, due to the conserved weights t_i, which forbid the couplings required in these diagrams. The leading proton decay diagram involves string scale colour triplets, and leads to sufficiently suppressed

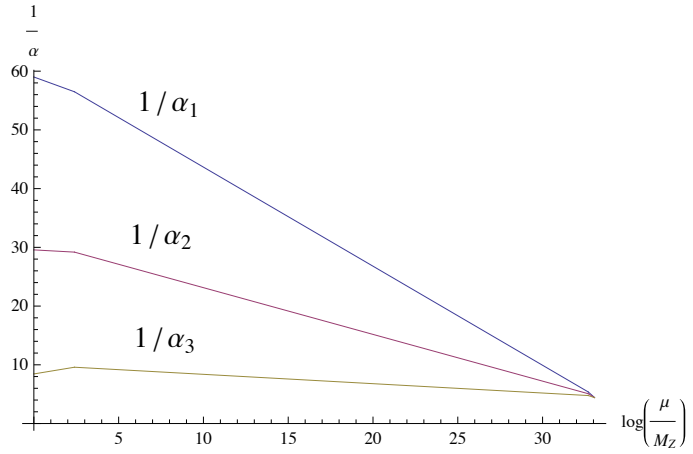

Figure 5.1: Gauge coupling unification in the model in Table 5.1 with TeV scale bulk exotics with supersymmetry. The low energy matter content is equivalent to that of the MSSM plus four extra $5 + \overline{5}$ families of $SU(5)$ at the TeV scale. Therefore we expect that the unification scale $M_{GUT} \sim 10^{16-17}$ is preserved, but the value of the coupling constant at that scale to be increased, exactly as indicated in this figure. However it is worth emphasising that the low energy matter content at the TeV scale, although equivalent to four extra $5 + \overline{5}$ families, comes from incomplete multiplets, comprising $3(D + \bar{D})$ and $2(H_u + H_d)$ distributed amongst two different matter curves, plus $2\,X_{H_d} + X_{d^c}$ and $2\overline{X}_{\overline{H}_d} + \overline{X}_{\overline{d^c}}$ from the bulk. In addition there are extra singlets responsible for the 750 GeV signal which do not affect unification.

proton decay as discussed in [53]. Furthermore, because up and down Higgs fields are accommodated in different matter curves, a tree-level proton decay diagram realised for the corresponding Kaluza-Klein modes $D_{KK}, \bar{D}_{KK}$ is also avoided.

5.2 Production and decay of the 750 GeV scalar/pseudoscalar

The terms in the superpotential which are responsible for generating the μ term and the exotic masses are [54]

$$W \sim \lambda\theta_{14}H_dH_u + \lambda_{\alpha\beta\gamma}\theta_{34}^{\alpha}H_d^{\beta}H_u^{\gamma} + \kappa_{\alpha jk}\theta_{34}^{\alpha}\overline{D}_jD_k. \tag{5.4}$$

These couplings all originate from the $27_{t_1}27_{t_1}27_{t_3}$ E_6 coupling, which is the only coupling of this type and will also give rise to the Yukawa couplings of the model. This coupling is both invariant under the E_6 GUT group and balances the charges

of the perpendicular group due to tracelessness of the SU(3) remaining from the original E_8 point. Thus two of the singlets θ_{34}^{α} couple to all three of the colour triplet charge $\mp 1/3$ vector-like fermions $D_k, \overline{D}_j$ as well as two families of inert Higgs doublets $H_d^{\beta}, H_u^{\gamma}$ (which do not get VEVs) $(\alpha, \beta, \gamma = 1, 2)$. One or both (if they are degenerate) singlet scalars may have a mass of 750 GeV and be produced by gluon fusion at the LHC, decaying into two photons as shown in Figs. 5.2 and 5.3. A third singlet θ_{14} couples to the two Higgs doublets of the MSSM, and is responsible for the effective μ term as in the NMSSM. However this singlet does not couple to coloured fermions and so cannot be strongly produced at the LHC. It should also be mentioned in passing that the E_6 singlets can generate couplings such as $\theta_0 X_d \bar{X}_{\bar{d}}$ from the E_6 invariant term $78 \cdot 78 \cdot 1$, which can give masses to bulk modes though we shall not discuss this further.

We therefore identify the 750 GeV scalar S with a spin-0 component of one of the F-theory singlets θ_{34}, which couples to three families of vector-like fermions $D_k, \overline{D}_j$ and two families of inert Higgs doublets $H_d^{\beta}, H_u^{\gamma}$. The scalar components of θ_{34} are both assumed to develop TeV scale VEVs which are responsible for generating the vector-like fermion masses for $D_k, \overline{D}_j$. Since there are two complex singlets θ_{34}, the spectrum will therefore contain two scalars, two pseudoscalars and two complex Weyl fermions. The two scalars plus two pseudoscalars are all candidates for the observed 750 GeV resonance. If two or more of them are degenerate then this may lead to an initially unresolved broad resonance. Eventually all four states may be discovered with different masses around the TeV scale, providing a smoking gun signature of the model.

5.2.1 Cross Section

We have seen that the spectrum of the F-theory derived model contains complex singlet superfields possessing scalar and pseudoscalar components. The superpotential in Eq.5.4, below the scale of the VEVs of X and the SUSY breaking scale,

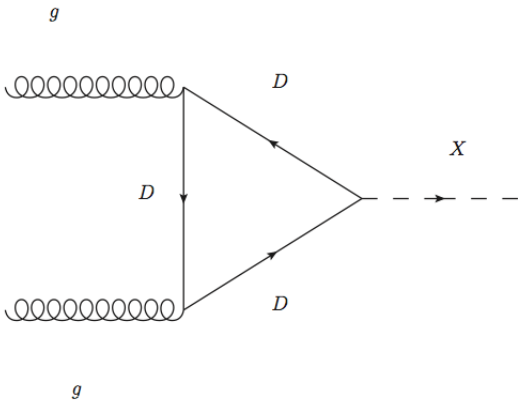

Figure 5.2: The new singlet scalar/pseudoscalar $X \equiv \theta_{34}$ with mass 750 GeV is produced by gluon fusion due to its coupling to a loop of vector-like fermions $D, \overline{D}$ which are colour triplets and have electric charge $\mp 1/3$.

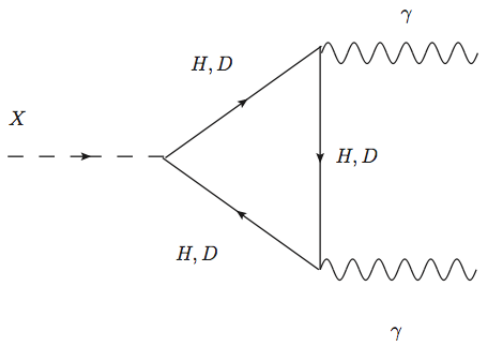

Figure 5.3: The new singlet scalar/pseudoscalar $X \equiv \theta_{34}$ with mass 750 GeV is decays into a pair of photons due to its coupling to a loop of vector-like fermions $H, \overline{H}$ which are colour singlet inert Higgsinos with electric charge ± 1 and $D, \overline{D}$ which are colour triplets and have electric charge $\mp 1/3$.

gives rise to the low energy effective Lagrangian containing the terms

$$\mathcal{L} \sim \kappa_i X \bar{D}_i D_i + \lambda_\alpha X H_u^\alpha H_d^\alpha + M_i \bar{D}_i D_i + M_{H_\alpha} H_u^\alpha H_d^\alpha + \frac{1}{2} M^2 X^2 + \cdots$$

where X is a scalar or pseudoscalar field originating from the θ_{34} coupled to a vector pair of fermions identified with the fermionic components of the three coloured triplet pairs $D_i, \bar{D}_i$, while M_i are the three masses of the triplet fermions with $M_i \sim \kappa \langle \theta_{34} \rangle$ of (5.4) and M is the mass of the singlet field originating from a combination of soft SUSY breaking masses and the VEVs of the singlets. Similar couplings are also shown to the two families of vector-like inert Higgsinos, labeled by $\alpha = 1, 2$. Note that the aforementioned soft SUSY breaking is assumed to

occur above the TeV scale.

The vector-like fermions generate loops diagrams which give rise to Effective Field Theory dimension-5 operators. For the scalar component $X \to S$

$$\mathcal{L}_{eff} \propto -\frac{1}{4} S \left(g_{S\gamma} F_{\mu\nu} F^{\mu\nu} + g_{Sg} G_{\mu\nu} G^{\mu\nu} \right) \tag{5.5}$$

and analogously for pseudoscalar $X \to A$,

$$\mathcal{L}_{eff} \propto -\frac{1}{4} A \left(g_{A\gamma} F_{\mu\nu} \tilde{F}^{\mu\nu} + g_{Ag} G_{\mu\nu} \tilde{G}^{\mu\nu} \right) . \tag{5.6}$$

A related mechanism has been already suggested as a plausible scenario in string derived models [182,206,208], where pseudoscalar fields such as axions and scalar fields such as the dilaton field have couplings of the above form. Here, instead, we regard the scalar and pseudoscalar as originating from a 27-dimensional matter superfield, coupling to vector-like extra quarks that appear in the 27-rep of E_6.

We consider a scalar/pseudoscalar particle X originating from one of the two θ_{34} fields, coupling to three families of colour triplet charge $\mp 1/3$ extra vector-like quarks $D_i, \bar{D}_i$ and two families of Higgsinos $H^{\alpha}_{u/d}$ - as per Equation 5.4. The cross section for production of this scalar/pseudoscalar from gluon fusion, $\sigma(pp \to X \to \gamma\gamma)$, where X is an uncoloured boson with mass M and spin $J = 0$, can be written as [103]

$$\sigma(pp \to X \to \gamma\gamma) = \frac{1}{M\Gamma s} C_{gg} \Gamma(X \to gg) \Gamma(X \to \gamma\gamma) \tag{5.7}$$

where C_{gg} is the dimensionless partonic integral for gluon production, which at $\sqrt{s} = 13$ TeV is $C_{gg} = 2137$. Here $\Gamma = \Gamma(X \to gg) + \Gamma(X \to \gamma\gamma)$ since no other interactions contribute to the effect.

For the case in which a scalar/pseudoscalar resonance is produced from gluon fusion, mediated by extra vector-like fermions $D_i, \bar{D}_i$ with mass M_i and charges Q_i, decaying into two photons by a combination of the same vector-like fermions and Higgsinos H^{α}_{d} and H^{α}_{u}, the corresponding decay widths read [103]:

$$\frac{\Gamma(X \to gg)}{M} = \frac{\alpha_3^2}{2\pi^3} \left| \sum_i C_{r_i} \kappa_i \frac{2M_i}{M} \mathcal{X}\left(\frac{4M_i^2}{M^2}\right) \right|^2 , \tag{5.8}$$

$$\frac{\Gamma(X \to \gamma\gamma)}{M} = \frac{\alpha^2}{16\pi^3} \left| \sum_i d_{r_i} Q_i^2 \kappa_i \frac{2M_i}{M} \mathcal{X}\left(\frac{4M_i^2}{M^2}\right) + \sum_\alpha d_{r_\alpha} Q_\alpha^2 \lambda_\alpha \frac{2M_{H_\alpha}}{M} \mathcal{X}\left(\frac{4M_{H\alpha}^2}{M^2}\right) \right|^2 . \tag{5.9}$$

The function $\mathcal{X}(t)$ takes a different form, depending on whether the particle is a scalar or a pseudoscalar - $\mathcal{S}$ or $\mathcal{P}$ respectively [220]:

$$\mathcal{P}(t) = \arctan^2(1/\sqrt{t-1}), \tag{5.10}$$

$$\mathcal{S}(t) = 1 + (1-t)\mathcal{P}(t)\,. \tag{5.11}$$

In the case in question with colour triplets of mass M_i mediating the process, $Q_i = 1/3$, $C_{r_i} = 1/2$, and $d_{r_i} = 3$, while the Higgsinos have $Q_i = d_{r_i} = 1$ and a mass of M_k. Combining the equations above we calculate the cross section for a scalar of mass $M = 750$ GeV at $\sqrt{s} = 13$ TeV. While the 750 GeV mass scale arises from an assumed soft, SUSY-breaking singlet scalar mass at that scale, the mass scale of the vector-like exotics in this model arise from singlet scalar VEVs, also assumed to be around the TeV scale. For simplicity we set all the masses of the vector-like fermions to be equal (likewise for the Higgsinos), and all the couplings of the scalar singlet to the fermions to be equal to y_f. The results are presented in Figure 5.4 and Figure 5.5. Note also that the $\Gamma(X \to gg)/M$ take values in the region of 10^{-4} and 10^{-5}, which is not excluded by searches for dijet resonances at Run 1.

In the computations of the cross sections presented above we have considered only the fermionic contributions while we have ignored the scalar ones. Masses of the scalar partners are related to SUSY breaking. Although the details of the SUSY breaking are not known, given the present experimental bounds on squark masses from the LHC, we assume that the scalar components of the exotic coloured fermions to be above $\mathcal{O}(1)$ TeV, whilst the corresponding coloured

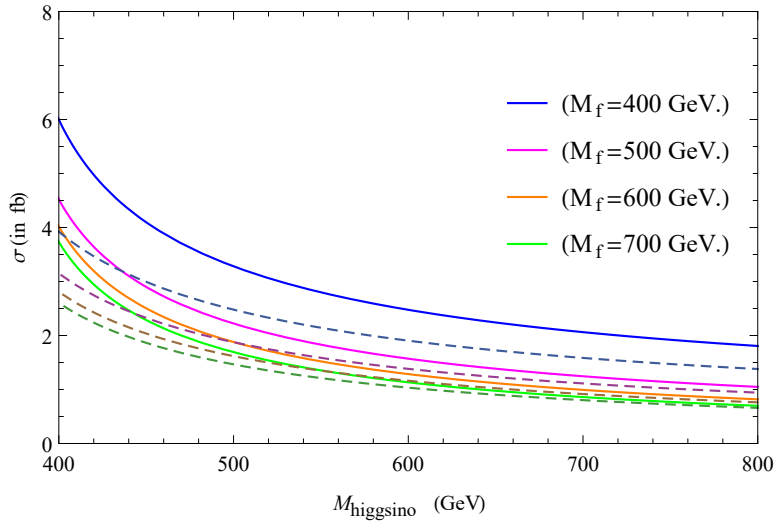

Figure 5.4: The cross section $\sigma(pp \to X \to \gamma\gamma)$ (in fb units) in the parametric space of the Higgsinos H_u^β / H_d^γ, for a selection of masses of the vector-like $D_i/\overline{D}_i$ with all masses M_i set equal to M_f and the coupling y_f, with $y_f = 1$. The solid lines correspond to the Pseudoscalar candidate state, while the dashed lines of the same hue correspond to the Scalar option.

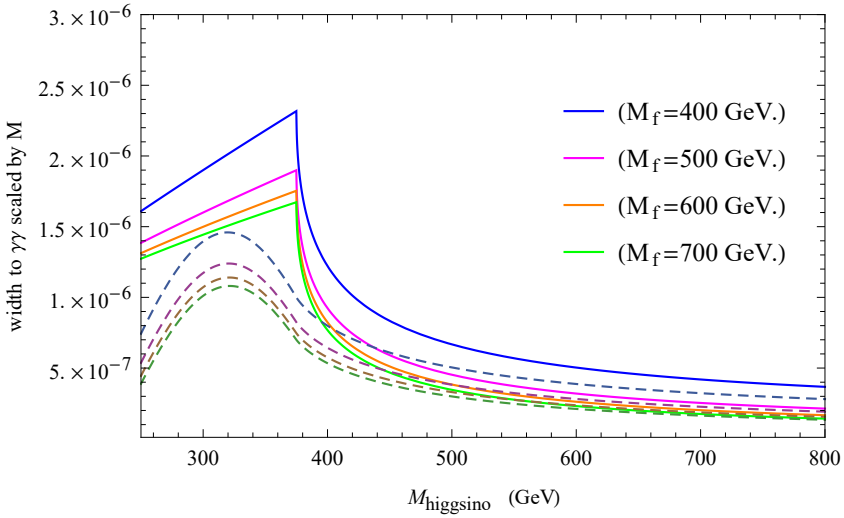

Figure 5.5: The mass weighted width $\Gamma(X \to \gamma\gamma)$ in the parametric space of the Higgsinos H_u^β / H_d^γ, for a selection of masses of the vector-like $D_i/\overline{D}_i$ with masses M_f and the coupling y_f, with $y_f = 1$. The solid lines correspond to the Pseudoscalar candidate state, while the dashed lines of the same hue correspond to the Scalar option.

fermions are assumed to be somewhat lighter. Furthermore we know that loops of scalar bosons give smaller contributions to the anomalous loop amplitudes than do fermions of the same mass. (see also similar reasoning in [221]). Given also that fermion components are lighter, we anticipate that the contribution of the

latter dominates the cross section.

5.3 Conclusions

We have interpreted the 750-760 GeV diphoton resonance as one or more of the spinless components of two singlet superfields arising from the three 27-dimensional representations of E_6 in F-theory, which also contain three copies of colour-triplet charge $\mp 1/3$ vector-like fermions $D_i, \bar{D}_i$ as well as inert Higgsino doublets H_d^β, H_u^γ to which the singlets may couple. For definiteness we have considered (without change) a model that was proposed some time ago that contains such states, as well as bulk exotics, leading to gauge coupling unification.

In order to obtain a large enough cross-section, we require the resonance to be identified with one of the two pseudoscalar (rather than scalar) states. However even in this case, a sufficiently large cross-section requires quite light colour triplets and charged Higgsinos below a TeV, even with of order unit Yukawa couplings, which is one of the predictions of the model.

The smoking gun prediction of the model is the existence of other similar spinless resonances, possibly close in mass to 750-760 GeV, decaying into diphotons, as well as the three families of vector-like fermions $D_i, \bar{D}_i$ and two families of inert Higgsino doublets H_d^β, H_u^γ.

It is possible that two or more of the singlet spinless states may be close in mass, providing nearby resonances, which could be initially mistaken for a single broad resonance in the current data. Indeed, from the 27-dimensional representations of the E_6 F-theory model there are two singlet superfields that couple to the vector-like fermions $D_i, \bar{D}_i$, so there could be up to four spinless resonances to can be searched for.

Further bulk singlets arising from the 78 reps of the E_6 F-theory model are also expected to be present in the low energy spectrum whose VEVs are responsible for the low energy exotic bulk masses of the $2X_{H_d}$, X_{d^c} and their vector partners. These bulk singlets are also candidates for the 750 GeV diphoton resonance, or may have similar masses.

In conclusion, realistic E_6 F-theory models generically contain extra low energy states, which include a plethora of spinless singlets and vector-like fermions with various charges and colours, especially colour singlet unit charged states and colour triplets with charges $\mp 1/3$, which appear to have the correct properties to provide an explanation of the 750 GeV diphoton resonance indicated by the LHC Run 2 data. We have discussed an already existing model (without change) that is perfectly capable of accounting for these data, as well as furnishing many predictions of multiple other similar resonances as well as the exotic fermions and their superpartners, which should be observable in future.

Chapter 6

R-parity violation and Yukawa couplings from local F-theory

In the previous chapters various phenomenological aspects of F-theory effective models using the spectral cover description [1–3] have been considered. While, in F-theory constructions, R-parity conservation (RPC) can emerge either as a remnant symmetry of extra $U(1)$ factors, or it can be imposed by appealing to some geometric property of the internal manifold and the flux [58], and there is no compelling reason to assume this. Moreover, experimental bounds permit R-parity violating (RPV) interactions at small but non-negligible rates.

Typically, in the absence of a suitable symmetry or displacement mechanism, the tree-level operators $QLd^c, d^cd^cu^c, e^cLL$ all appear simultaneously, which leads to Baryon and Lepton (B and L) violating processes at unacceptable rates [222]. On the other hand, in F-theory constructions, parts of GUT multiplets are typically projected out by fluxes, giving rise only to a part of the above operators, as we have seen in Chapter 4. In other cases, due to symmetry arguments, the Yukawa couplings relevant to RPV operators are identically zero. As a result, several B/L violating processes, either are completely prevented or occur at lower rates in F-theory models, providing a controllable signal of RPV. This observation motivates a general study of RPV in F-theory, which is the subject of this chapter.

In this chapter, we will consider RPV in local F-theory, trying to be as general as possible, with the goal of making a bridge between F-theory and experiment. The principal aim is to compute the strength of the RPV Yukawa couplings, which mainly depend on the topological properties of the internal space and are more or less independent of many details of a particular model, enabling us to work in a generic local F-theory setting. We focus on F-theory SU(5) constructions, where a displacement mechanism, based on non-trivial fluxes, renders several GUT multiplets incomplete. This mechanism has already been suggested to eliminate the colour triplets from the Higgs five-plets, so that dangerous dimension-5 proton decay operators are not present. However, it turns out that, in several cases, not only the Higgs but also other matter multiplets are incomplete, while the superpotential structure is such that it implies RPV terms. In this context, it is quite common that not all of the RPV operators appear simultaneously, allowing observable RPV effects without disastrous proton decay.

Our goal in this chapter is twofold. Firstly, to present a detailed analysis of all possible combinations of RPV operators arising from a generic semi-local F-theory spectral cover framework, assuming an $SU(5)$ GUT. This includes a detailed analysis of the classification of all possible allowed combinations of RPV operators, originating from the $SU(5)$ term $10 \cdot \bar{5} \cdot \bar{5}$, including the effect of $U(1)$ fluxes, with *global* restrictions, which are crucial in controlling the various possible multiplet splittings. Secondly, using F-theory techniques developed in the last few years, we perform explicit computations of the bottom/tau and RPV Yukawa couplings, assuming only *local* restrictions on fluxes, and comparing our results with the present experimental limits on the coupling for each specific RPV operator. The ingredients for this study have already appeared scattered through the literature, which we shall refer to as we go along.

We emphasise that the first goal is related to the nature of the available *global* Abelian fluxes of the particular model and their restrictions on the various matter curves, hence, on its specific geometric properties. The second goal requires the computation of the strengths of the corresponding Yukawa couplings. This in turn

requires knowledge of the wavefunctions' profiles of the particles participating in the corresponding trilinear Yukawa couplings and, as we will see, these involve the *local* flux data. Once such couplings exist in the effective Lagrangian, we wish to explore the regions of the available parameter space where these couplings are sufficiently suppressed and are compatible with the present experimental data.

Our aim in this dedicated study is to develop and extend the scope of the existing results in the literature, in order to provide a complete and comprehensive study, which makes direct contact with experimental limits on RPV, enabling F-theory models to be classified and confronted with experiment more easily and directly than previously. This is the first study in the literature that focuses exclusively on RPV in F-theory.

The remainder of the chapter divides into two parts: in the first part, we consider semi-local F-theory constructions where global restrictions are imposed on the fluxes, which imply that they take integer values. In Section 6.1 we show that RPV is a generic expectation of semi-local F-theory constructions. We start by detailing the numerous options for Abelian monodromies in semi-local F-theory, then in Section 6.1.1 we introduce the notion of flux, quantised according to global restrictions, which, when switched on, leads to incomplete $SU(5)$ multiplets in the low energy (massless) spectrum, which can lead in incomplete GUT multiplets and a subset of R-parity violating processes. Appendix C.1 details all possible sources of R-parity violating couplings for all models classified with respect to the monodromies in semi-local F-theory constructions.

In the second part of the chapter, we relax the global restrictions of the semi-local constructions, and allow the fluxes to take general values, subject only to local restrictions. In Section 6.2 we describe the calculation of a Yukawa coupling originating from an operator $10 \cdot \bar{5} \cdot \bar{5}$ at an $SO(12)$ local point of enhancement in the presence of general local fluxes, with only local (not global) flux restrictions. In Section 6.3 we apply these methods to calculate the numerical values of Yukawa couplings for bottom, tau and RPV operators, exploring the parameter space of local fluxes. In Section 6.4 we finally consider RPV coupling regions and

calculate ratios of Yukawa couplings from which the physical RPV couplings at the GUT scale can be determined and compared to limits on these couplings from experiment. Appendix C.2 details the local F-theory constructions and local chirality constraints on flux data and RPV operators.

6.1 R-parity violation in semi-local F-theory constructions

In the previous chapters of this thesis we have presented models based on the spectral cover analysis, which is a so-called semi-local approach. In particular, we have emphasised the role of monodromies in these constructions, as well as the effect this has on the physical processes of such models.

A classification of the set of models with simple monodromies (Abelian Z_N types) that retain some perpendicular $U(1)_\perp$ charges associated with the weights t_i has been put forward in [14,47,49], where we follow the notation of Dudas and Palti [49] . In the following, we categorize these models in order to assess whether tree-level, renormalisable, perturbative RPV is generic if matter is allocated in different curves. More specifically, we present four classes, characterised by the splitting of the spectral cover equation. These are:

- 2+1+1+1-splitting, which retains three independent perpendicular $U(1)_\perp$. These models represent a Z_2 monodromy ($t_1 \leftrightarrow t_2$), and as expected we are left with seven **5** curves, and four **10** curves.

- $2 + 2 + 1$-splitting, which retains two independent perpendicular $U(1)_\perp$. These models represent a $Z_2 \times Z_2$ monodromy ($t_1 \leftrightarrow t_2$, $t_3 \leftrightarrow t_4$), and as expected we are left with five **5** curves, and three **10** curves.

- $3 + 1 + 1$-splitting, which retains two independent perpendicular $U(1)_\perp$. These models represent a Z_3 monodromy ($t_1 \leftrightarrow t_2 \leftrightarrow t_3$), and as expected we are left with five **5** curves, and three **10** curves.

- $3 + 2$-splitting, which retains a single perpendicular $U(1)_\perp$. These models

represent a $Z_3 \times Z_2$ monodromy ($t_1 \leftrightarrow t_2 \leftrightarrow t_3$, $t_4 \leftrightarrow t_5$), and as expected we are left with three **5** curves, and two **10** curves.

We note also that the cases $4+1$ and 5 exist for the spectral cover, though for Abelian monodromies they are too constraining to be suitable for model building.

In Appendix C.1 we develop the above classes of models, identifying which curve contains the Higgs fields and which contains the matter fields, in order to show that RPV is a generic phenomenon in semi-local F-theory constructions. Of course, if all the RPV operators are present, then proton decay will be an inevitable consequence. In the next subsection we show that this is generally avoided in semi-local F-theory constructions when fluxes are switched on, which has the effect of removing some of the RPV operators, while leaving some observable RPV in the low energy spectrum.

6.1.1 Hypercharge flux with global restrictions and R-parity violating operators

As we have seen in the previous chapters, hypercharge flux may be used to break GUT groups to the SM in F-theory constructions. This doublet-triplet spliting principally serves to eliminate colour triplets arising from the Higgs GUT multiplet from the spectrum. This would be an alternative to the doublet-triplet scenario since only the two Higgs doublets remain and the light spectrum. The occurrence of this minimal scenario presupposes that all other matter curves are left intact by the flux.

However, this is usually not the case, with the majority of models exhibiting incomplete representations for some or all matter representations. This stands as an important feature if one does not assume some mechanism to eliminate baryon and lepton number violating operators, since it can lead to models where only a subset of the operators are allowed. In this event, one may avoid proton decay, while still having other exotic processes - a good review of these is found in [99]. In Appendix C.1 we further develop the ideas relating to these models.

6.2 Yukawa couplings in local F-theory constructions: formalism

In this section (and subsequent sections) we relax the global constraints on fluxes, and consider the calculation of Yukawa couplings, imposing only local flux restrictions. The motivation for doing this is to calculate the Yukawa couplings associated with the RPV operators in a rather model independent way, and then compare our results to the experimental limits. Flavour hierarchies and Yukawa structures in F-theory have been studied in a large number of papers [59] [57]. In this section we shall discuss Yukawa couplings in F-theory, following the approach of [32–34].

In the previous section we assessed how chirality is realised on different curves due to flux effects. These considerations take into account the global flux data and are therefore called semi-local models. The flux units considered in the examples above are integer valued as they follow from the Dirac flux quantisation

$$\frac{1}{2\pi}\int_{\Sigma\subset S} F = n \tag{6.1}$$

where n is an integer, Σ a matter curve (two-cycle in the divisor S), and F the gauge field-strength tensor, i.e. the flux. In conjugation with the index theorems, the flux units piercing different matter curves Σ will tell us how many chiral states are globally present in a model.

While the semi-local approach defines the full spectrum of a model, the computation of localised quantities, such as the Yukawa couplings, requires appropriate description of the local geometry. As we will see below, a crucial quantity in the local geometry is the notion of *local* flux density, understood as follows.

First we notice that the unified gauge coupling is related to the compactification scale through the volume of the compact space

$$\alpha_G^{-1} = m_*^4 \int_S 2\omega\wedge\omega = m_*^4 \int \mathrm{dVol}_S = \mathrm{Vol}(S) m_*^4 \tag{6.2}$$

where α_G is the unified gauge coupling, m_* is the F-Theory characteristic scale, S the GUT divisor with Kähler form

$$\omega = \frac{i}{2}(dz_1 \wedge d\bar{z}_1 + dz_2 \wedge d\bar{z}_2) \tag{6.3}$$

that defines the volume form

$$\mathrm{dVol}_S = 2\omega \wedge \omega = dz_1 \wedge dz_2 \wedge d\bar{z}_1 \wedge d\bar{z}_2. \tag{6.4}$$

As the volume of Σ is bounded by the volume of S, we assume that

$$\mathrm{Vol}(\Sigma) \simeq \sqrt{\mathrm{vol}(S)}, \tag{6.5}$$

and if we now consider that the background of F is constant, we can estimate the values that F takes in the S by

$$F \simeq 2\pi\sqrt{\alpha_G} m_*^2 n. \tag{6.6}$$

This means that, in units of m_*, the background F is a real number of order one. Since in the computation of Yukawa couplings it is the local values of F – and not the global quantisation constraints – that matter, we will from now on abuse terminology and refer to flux densities, F, as fluxes. Furthermore, as we will see later, the local values of F also define what chiral states are supported locally. This will be crucial to study the full plenitude of RPV couplings in different parts of the parameter space.

6.2.1 The local $SO(12)$ model

In F-theory matter is localised along Riemann surfaces (matter curves), which are formed at the intersections of D7-branes with the GUT surface S. Yukawa couplings are then realised when three of these curves intersect at a single point on S, while, at the same time, the gauge symmetry is enhanced. The computation relies on the knowledge of the profile of the wavefunctions of the states participat-

ing in the intersection. When a specific geometry is chosen for the internal space (and in particular for the GUT surface) these profiles are found by solving the corresponding equations of motion [32–35]. Their values are obtained by computing the integral of the overlapping wavefunctions at the triple intersections. In this chapter we focus on the $SO(12)$ point of enhancement, which corresponds to the SU(5) Yukawa coupling for the bottom and tau Yukawa couplings, as well as R-parity violating couplings. To do this we shall use the techniques presented in [34].[1]

The 4-dimensional theory can be obtained by integrating out the effective 8-dimensional action over the divisor S

$$W = m_*^4 \int_S \mathrm{Tr}(F \wedge \Phi) \tag{6.7}$$

where $F = dA - iA \wedge A$ is the field-strength of the gauge vector boson A and Φ is $(2,0)$-form on S.

From the above superpotential, the F-term equations can be computed by varying A and Φ. In conjugation with the D-term

$$D = \int_S \omega \wedge F + \frac{1}{2}[\Phi, \bar{\Phi}], \tag{6.8}$$

where ω is the Kähler form of S, a 4-dimensional supersymmetric solution for the equations of motion of F and Φ can be computed.

Both A and Φ, locally are valued in the Lie algebra of the symmetry group at the Yukawa point. In the case in hand, the fibre develops an $SO(12)$ singularity at which point couplings of the form $\mathbf{10} \cdot \bar{\mathbf{5}} \cdot \bar{\mathbf{5}}$ arise. Away from the enhancement point, the background Φ breaks $SO(12)$ down to the GUT group $SU(5)$. The rôle of $\langle A \rangle$ is to provide a 4d chiral spectrum and to break further the GUT gauge group.

More systematically, the Lie-Algebra of $SO(12)$ is composed of its Cartan generators H_i with $i = 1, ..., 6$, and 60 step generators E_ρ. Together, they respect

[1] For a general E_8 point of enhancement that containing both type of couplings see [36, 37]. Similar, an E_7 analysis is given in [223].

the Lie algebra

$$[H_i, E_\rho] = \rho_i E_\rho \tag{6.9}$$

where ρ_i is the i^{th} component of the root ρ. The E_ρ generators can be completely identified by their roots

$$\rho = (\underline{\pm 1, \pm 1, 0, 0, 0, 0, 0}) \tag{6.10}$$

where underline means all 60 permutations of the entries of the vector, including different sign combinations. To understand the meaning of this notation it is sufficient to consider a simpler example:

$$(0, \underline{1, 0, 0}, 0, 0, 0, 0) \equiv \{(0,1,0,0,0,0,0), (0,0,1,0,0,0,0), (0,0,0,1,0,0,0)\} \tag{6.11}$$

The background of Φ will break $SO(12)$ away from the $SO(12)$ singular point. In order to see this consider that it takes the form

$$\Phi = \Phi_{z_1 z_2} dz_1 \wedge dz_2 \tag{6.12}$$

where it's now explicit that it parameterises the transverse directions to S. The background we are considering is

$$\langle \Phi_{z_1 z_2} \rangle = m^2 \left(z_1 Q_{z_1} + z_2 Q_{z_2} \right) \tag{6.13}$$

where m is related to the slope of the intersection of 7-branes, and

$$Q_{z_1} = -H_1 \tag{6.14}$$

$$Q_{z_2} = \frac{1}{2} \sum_i H_i. \tag{6.15}$$

The unbroken symmetry group will be the commutant of $\langle \Phi_{z_1 z_2} \rangle$ in $SO(12)$. The commutator between the background and the rest of the generators is

$$[\langle \Phi_{z_1 z_2} \rangle, E_\rho] = m^2 q_\Phi(\rho) E_\rho \tag{6.16}$$

Curve	Roots	q_Φ	$SU(5)$ irrep	q_{z_1}	q_{z_2}
$\Sigma_{a^\pm}$	$(\pm 1, \underline{\mp 1, 0, 0, 0, 0})$	$\mp z_1$	$\bar{\mathbf{5}}/\mathbf{5}$	∓ 1	0
$\Sigma_{b^\pm}$	$(0, \underline{\pm 1, \pm 1, 0, 0, 0})$	$\mp z_2$	$\mathbf{10}/\bar{\mathbf{10}}$	0	± 1
$\Sigma_{c^\pm}$	$(\mp 1, \underline{\mp 1, 0, 0, 0, 0})$	$\pm(z_1 - z_2)$	$\bar{\mathbf{5}}/\mathbf{5}$	± 1	∓ 1

Table 6.1: Matter curves and respective data for an $SO(12)$ point of enhancement model with a background Higgs given by Equation 6.13. The underline represent all allowed permutations of the entries with the signs fixed

where $q_\Phi(\rho)$ are holomorphic functions of the complex coordinates z_1, z_2. The surviving symmetry group is composed of the generators that commute with $\langle\Phi\rangle$ on every point of S. With our choice of background, the surviving step generators are identified to be

$$E_\rho : (0, \underline{1, -1, 0, 0, 0}), \tag{6.17}$$

which, together with H_i, trivially commute with $\langle\Phi\rangle$, generating $SU(5) \times U(1) \times U(1)$.

When $q_\Phi(\rho) = 0$ in certain loci we have symmetry enhancement, which accounts for the presence of matter curves. This happens as at these loci, extra step generators survive and furnish a representation of $SU(5) \times U(1) \times U(1)$. For the case presented we identify three curves joining at the $SO(12)$ point, these are

$$\Sigma_a = \{z_1 = 0\} \tag{6.18}$$

$$\Sigma_b = \{z_2 = 0\} \tag{6.19}$$

$$\Sigma_c = \{z_1 = z_2\}, \tag{6.20}$$

and defining a charge under a certain generator as

$$[Q_i, E_\rho] = q_i(\rho) E_\rho \tag{6.21}$$

all the data describing these matter curves are presented in Table 6.1. Since the bottom and tau Yukawas come from such an $SO(12)$ point, in order to have such a coupling the point must have the a^+, b^+, and c^+.

In order to both induce chirality on the matter curves and break the two $U(1)$ factors, we have to turn on fluxes on S valued along the two Cartan generators that generate the extra factors.

We first consider the flux

$$\langle F_1 \rangle = i(M_{z_1} dz_1 \wedge d\bar{z_1} + M_{z_2} dz_2 \wedge d\bar{z_2}) Q_F, \tag{6.22}$$

with

$$Q_F = -Q_{z_1} - Q_{z_2} = \frac{1}{2}(H_1 - \sum_{j=2}^{6} H_j). \tag{6.23}$$

It's easy to see that the $SU(5)$ roots are neutral under Q_F, and therefore this flux does not break the GUT group. On the other hand, the roots on a, b sectors are not neutral. This implies that this flux will be able to differentiate $\bar{\mathbf{5}}$ from $\mathbf{5}$ and $\mathbf{10}$ from $\bar{\mathbf{10}}$

$$\int_{\Sigma_a,\ \Sigma_b} F_1 \neq 0 \Rightarrow \text{ Induced Chirality.} \tag{6.24}$$

This flux does not induce chirality in $c^{\pm}$ curves as $q_F = 0$ for all roots in $c^{\pm}$. To induce chirality in $c^{\pm}$ one needs another contribution to the flux

$$\langle F_2 \rangle = i(dz_1 \wedge d\bar{z_2} + dz_2 \wedge d\bar{z_1})(N_a Q_{z_1} + N_b Q_{z_2}) \tag{6.25}$$

that does not commute with the roots on the $c^{\pm}$ sectors for $N_a \neq N_b$.

Breaking the GUT down to the SM gauge group requires flux along the Hypercharge. In order to avoid generating a Green-Schwarz mass for the Hypercharge gauge boson, this flux has to respect global constraints. Locally we may define it as

$$\langle F_Y \rangle = i[(dz_1 \wedge d\bar{z_2} + dz_2 \wedge d\bar{z_1}) N_Y + (dz_2 \wedge d\bar{z_2} - dz_1 \wedge d\bar{z_1}) \tilde{N}_Y] Q_Y \tag{6.26}$$

and the Hypercharge is embedded in our model through the linear combination

$$Q_Y = \frac{1}{3}(H_2 + H_3 + H_4) - \frac{1}{2}(H_5 + H_6). \tag{6.27}$$

Since this contribution to the flux does not commute with all elements of $SU(5)$, only with its SM subgroup, distinct SM states will feel this flux differently. This fact is used extensively in semi-local models as a mechanism to solve the doublet-triplet splitting problem. As we will see bellow, it can also be used to locally prevent the appearance of certain chiral states and therefore forbid some RPV in subregions of the parameter space.

The total flux will then be the sum of the three above contributions. It can be expressed as

$$\begin{aligned}\langle F\rangle =& i(dz_2\wedge d\bar{z_2}-dz_1\wedge d\bar{z_1})Q_P\\ &+i(dz_1\wedge d\bar{z_2}+dz_2\wedge d\bar{z_1})Q_S\\ &+i(dz_2\wedge d\bar{z_2}+dz_1\wedge d\bar{z_1})M_{z_1z_2}Q_F\end{aligned} \tag{6.28}$$

with the definitions

$$Q_P = MQ_F+\tilde{N}_YQ_Y \tag{6.29}$$

$$Q_S = N_aQ_{z_1}+N_bQ_{z_2}+N_YQ_Y \tag{6.30}$$

and

$$M = \frac{1}{2}(M_{z_1}-M_{z_2}) \tag{6.31}$$

$$M_{z_1z_2} = \frac{1}{2}(M_{z_2}+M_{z_1}). \tag{6.32}$$

As the Hypercharge flux will affect SM states differently, breaking the GUT group, we will be able to distinguishing them inside each curve. The full split of the states present in the different sectors and all relevant data are presented in Table 6.2.

6.2.2 Wavefunctions and the Yukawa computation

In general, the Yukawa strength is obtained by computing the integral of the overlapping wavefunctions. More precisely, according to the discussion in the

Sector	Root	SM	q_F	q_{z_1}	q_{z_2}	q_S	q_P
a_1	$(1,\underline{-1,0,0},0,0)$	$(\bar{\mathbf{3}},\mathbf{1})_{-\frac{1}{3}}$	1	-1	0	$-N_a-\frac{1}{3}N_Y$	$M-\frac{1}{3}\tilde{N}_Y$
a_2	$(1,0,0,0,\underline{-1,0})$	$(\mathbf{1},\mathbf{2})_{\frac{1}{2}}$	1	-1	0	$-N_a+\frac{1}{2}N_Y$	$M+\frac{1}{2}\tilde{N}_Y$
b_1	$(0,\underline{1,1,0},0,0)$	$(\overline{\mathbf{3}},\mathbf{1})_{\frac{2}{3}}$	-1	0	1	$N_b+\frac{2}{3}N_Y$	$-M+\frac{2}{3}\tilde{N}_Y$
b_2	$(0,\underline{1,0,0},\underline{1,0})$	$(\mathbf{3},\mathbf{2})_{-\frac{1}{6}}$	-1	0	1	$N_b-\frac{1}{6}N_Y$	$-M-\frac{1}{6}\tilde{N}_Y$
b_3	$(0,0,0,0,1,1)$	$(\mathbf{1},\mathbf{1})_{-1}$	-1	0	1	N_b-N_Y	$-M-\tilde{N}_Y$
c_1	$(-1,\underline{-1,0,0},0,0)$	$(\bar{\mathbf{3}},\mathbf{1})_{-\frac{1}{3}}$	0	1	-1	$N_a-N_b-\frac{1}{3}N_Y$	$-\frac{1}{3}\tilde{N}_Y$
c_2	$(-1,0,0,0,\underline{-1,0})$	$(\mathbf{1},\mathbf{2})_{\frac{1}{2}}$	0	1	-1	$N_a-N_b+\frac{1}{2}N_Y$	$\frac{1}{2}\tilde{N}_Y$

Table 6.2: Complete data of sectors present in the three curves crossing in an $SO(12)$ enhancement point considering the effects of non-vanishing fluxes. The underline represent all allowed permutations of the entries with the signs fixed

previous section, one has to solve for the zero mode wavefunctions for the sectors a, b and c presented in Table (6.2). The physics of the D7-Branes wrapping on S can be described in terms of a twisted 8-dimensional $\mathcal{N}=1$ gauge theory on $R^{1,3}\times S$, where S is a Kähler submanifold of elliptically fibered Calabi-Yau 4-fold, X. One starts with the action of the effective theory, which was given in [19]. The next step is to obtain the equations of motion for the 7-brane fermionic zero modes. This procedure has been performed in several papers [33, 34, 36] and we will not repeat it here in detail. In order for this chapter to be self-contained we highlight the basic computational steps.

The equations for a 4-dimensional massless fermionic field are of the Dirac form:

$$\mathcal{D}_A\Psi=0 \tag{6.33}$$

where

$$\mathcal{D}_A=\begin{pmatrix} 0 & D_1 & D_2 & D_3 \\ -D_1 & 0 & -D_{\bar{3}} & D_{\bar{2}} \\ -D_2 & -D_{\bar{3}} & 0 & -D_{\bar{1}} \\ -D_3 & -D_{\bar{2}} & D_{\bar{1}} & 0 \end{pmatrix} \quad , \quad \Psi=\Psi E_\rho=\begin{pmatrix} -\sqrt{2}\eta \\ \psi_{\bar{1}} \\ \psi_{\bar{2}} \\ \chi_{12} \end{pmatrix}. \tag{6.34}$$

The indices here are a shorthand notation instead of the coordinates z_1, z_2, z_3. The components of Ψ represent 7-brane degrees of freedom. Also the covariant derivatives are defined as $D_i = \partial_i - i[\langle A_i \rangle, \ldots]$ for $i = 1, 2, \bar{1}, \bar{2}$ and as $D_{\bar{3}} = -i[\langle \Phi_{12} \rangle, \ldots]$ for the coordinate z_3. It is clear from equations (6.33,6.34) that we have to solve the equations for each sector. According to the detailed solutions in [34] the wavefunctions for each sector have the general form

$$\Psi \sim f(az_1 + bz_2) e^{M_{ij} z_i z_j} \tag{6.35}$$

where $f(az_1 + bz_2)$ is a holomorphic function and M_{ij} incorporates flux effects. In an appropriate basis this holomorphic function can be written as a power of its variables $f_i \sim (az_1 + bz_2)^{3-i}$ and in the case where the generations reside in the same matter curve, the index-i can play the rôle of a family index. Moreover the Yukawa couplings as a triple wavefunction integrals have to respect geometric $U(1)$ selection rules. The coupling must be invariant under geometric transformations of the form: $z_{1,2} \to e^{i\alpha} z_{1,2}$. In this case the only non-zero tree level coupling arises for $i = 3$ and by considering that, the index in the holomorphic function f_i indicates the fermion generation we obtain. Hierarchical couplings for the other copies on the same matter curve can generated in the presence of non commutative fluxes [35] or by incorporating non-perturbative effects [33] [223].

The RPV couplings under consideration emerge from a tree level interaction. Hence, its strength is given by computing the integral where now the rôle of the Higgs $\bar{5}_H$ is replaced by $\bar{5}_M$. We consider here the scenario where the generations are accommodated on different matter curves. In this case the two couplings, the bottom/tau Yukawa and the tree level RPV, are localised at different $SO(12)$ points on $\mathcal{S}_{GUT}$, (see Figure 6.1). In this approach, at first approximation we can take the holomorphic functions f as constants absorbed in the normalization factors.

As a first approach, our goal is to calculate the bottom Yukawa coupling as well as the coupling without hypercharge flux and compare the two values. So, at this point we write down the wavefunctions and the relevant parameters in a

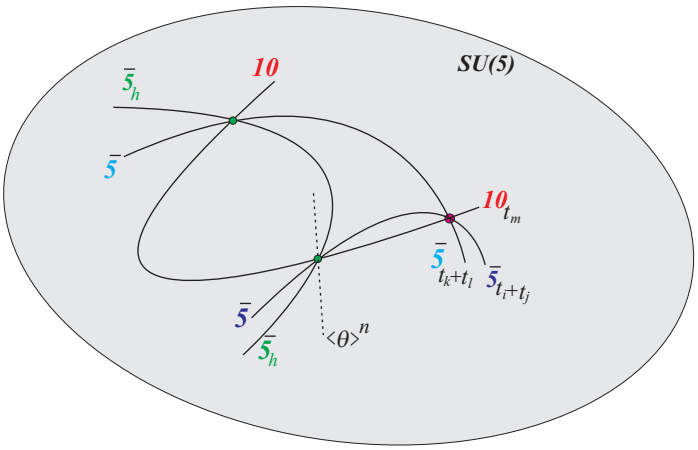

Figure 6.1: Intersecting matter curves, Yukawa couplings and the case of RPV .

more detailed form as given in [34] but without the holomorphic functions. The wavefunctions in the holomorphic gauge have the following form

$$\vec{\psi}^{(b)hol}_{10_M} = \vec{v}^{(b)}\chi^{(b)hol}_{10_M} = \vec{v}^{(b)}\kappa^{(b)}_{10_M} e^{\lambda_b z_2(\bar{z}_2-\zeta_b\bar{z}_1)} \tag{6.36}$$

$$\vec{\psi}^{(a)hol}_{5_M} = \vec{v}^{(a)}\chi^{(a)hol}_{5_M} = \vec{v}^{(a)}\kappa^{(a)}_{5_M} e^{\lambda_a z_1(\bar{z}_1-\zeta_a\bar{z}_2)} \tag{6.37}$$

$$\vec{\psi}^{(c)hol}_{5_H} = \vec{v}^{(c)}\chi^{(c)hol}_{5_H} = \vec{v}^{(c)}\kappa^{(c)}_{5_H} e^{(z_1-z_2)(\zeta_c\bar{z}_1-(\lambda_c-\zeta_c)\bar{z}_2)} \tag{6.38}$$

$$\vec{\psi}^{(c)hol}_{5_M} = \vec{v}^{(c)}\chi^{(c)hol}_{5_H} = \vec{v}^{(c)}\kappa^{(c)}_{5_M} e^{(z_1-z_2)(\zeta_c\bar{z}_1-(\lambda_c-\zeta_c)\bar{z}_2)} \tag{6.39}$$

where

$$\zeta_a = -\frac{q_S(a)}{\lambda_a - q_P(a)} \tag{6.40}$$

$$\zeta_b = -\frac{q_S(b)}{\lambda_b + q_P(b)} \tag{6.41}$$

$$\zeta_c = \frac{\lambda_c(\lambda_c - q_P(c) - q_S(c)}{2(\lambda_c - q_S(c))} \tag{6.42}$$

and λ_ρ is the smallest eigenvalue of the matrix

$$m_\rho = \begin{pmatrix} -q_P & q_S & im^2 q_{z_1} \\ q_S & q_P & im^2 q_{z_2} \\ -im^2 q_{z_1} & -im^2 q_{z_2} & 0 \end{pmatrix}. \tag{6.43}$$

To compute the above quantities we make use of the values of q_i from Table

6.2. It is important to note that the values of the flux densities in this table depend on the $SO(12)$ enhancement point. This means that one can in principle have different numerical values for the strength of the interactions at different points.

The column vectors are given by

$$\vec{v}^{(b)} = \begin{pmatrix} -\frac{i\lambda_b}{m^2}\zeta_b \\ \frac{i\lambda_b}{m^2} \\ 1 \end{pmatrix}, \vec{v}^{(a)} = \begin{pmatrix} -\frac{i\lambda_a}{m^2} \\ \frac{i\lambda_a}{m^2}\zeta_a \\ 1 \end{pmatrix}, \vec{v}^{(c)} = \begin{pmatrix} -\frac{i\zeta_c}{m^2} \\ \frac{i(\zeta_c-\lambda_c)}{m^2} \\ 1 \end{pmatrix}. \tag{6.44}$$

Finally, the κ coefficients in equations (6.36-6.37) are normalization factors. These factors are fixed by imposing canonical kinetic terms for the matter fields. More precisely, for a canonically normalized field χ_i supported in a certain sector (e), the normalization condition for the wavefunctions in the real gauge is

$$1 = 2m_*^4 ||\vec{v}^{(e)}||^2 \int (\chi^{(e)real})_i^* \chi_i^{(e)real} \mathrm{dVol}_S \tag{6.45}$$

where $\chi_i^{(e)real}$ are now in the real gauge, and in our convention $\mathrm{Tr} E_\alpha^\dagger E_\beta = 2\delta_{\alpha\beta}$. The wavefunctions in real and holomorphic gauge are related by

$$\psi^{real} = e^{i\Omega}\psi^{hol} \tag{6.46}$$

where

$$\Omega = \frac{i}{2}\left[\left(M_{z_1}|z_1|^2 + M_{z_2}|z_2|^2\right) Q_F - \tilde{N}_Y\left(|z_1|^2 - |z_2|^2\right) Q_Y + \left(z_1\bar{z}_2 + z_2\bar{z}_1\right) Q_S\right], \tag{6.47}$$

which only transforms the scalar coefficient of the wavefunctions, χ, leaving the $\vec{v}$ part invariant.

With the above considerations, one can find the normalization factors to be

$$|\kappa_{5_M}^{(a)}|^2 = -4\pi g_s \sigma^2 \cdot \frac{q_P(a)(2\lambda_a + q_P(a)(1+\zeta_a^2))}{\lambda_a(1+\zeta_a^2) + m^4}, \tag{6.48}$$

$$|\kappa^{(b)}_{10_M}|^2 = -4\pi g_s\sigma^2 \cdot \frac{q_P(b)(-2\lambda_b + q_P(b)(1+\zeta_b^2))}{\lambda_b(1+\zeta_b^2)+m^4}, \tag{6.49}$$

$$|\kappa^{(c)}_{5_H}|^2 = -4\pi g_s\sigma^2 \cdot \frac{2(q_P(c)+\zeta_c)(q_P(c)+2\zeta_c-2\lambda_c)+(q_S(c)+\lambda_c)^2}{\zeta_c^2+(\lambda_c-\zeta_c)^2+m^4}, \tag{6.50}$$

$$|\kappa^{(c)}_{5_M}|^2 = -4\pi g_s\sigma^2 \cdot \frac{2(q_P(c)+\zeta_c)(q_P(c)+2\zeta_c-2\lambda_c)+(q_S(c)+\lambda_c)^2}{\zeta_c^2+(\lambda_c-\zeta_c)^2+m^4}, \tag{6.51}$$

where we used the relation $\left(\frac{m}{m_*}\right)^2 = (2\pi)^{3/2} g_s^{1/2}\sigma$, making use of the dimensionless quantity $\sigma = (m/m_{st})^2$, where m_{st} the string scale. The expressions (6.48-6.51) above can be shown numerically to be always positive.

The superpotential trilinear couplings can be taken to be in the holomorphic gauge. For the bottom Yukawa, we consider that ψ_{10_M} and ψ_{5_M} contain the heaviest down-type quark generations. In this case the bottom and tau couplings can be computed:

$$\begin{aligned} y_{b,\tau} =& m_*^4\, t_{abc} \int_S \det(\vec{\psi}^{(b)hol}_{10_M}, \vec{\psi}^{(a)hol}_{5_M}, \vec{\psi}^{(c)hol}_{5_H}) \mathrm{dVol}_S \\ =& m_*^4\, t_{abc}\ \det(\vec{v}^{(b)}, \vec{v}^{(a)}, \vec{v}^{(c)}) \int_S \chi^{(b)hol}_{10_M} \chi^{(a)hol}_{5_M} \chi^{(c)hol}_{5_H} \mathrm{dVol}_S. \end{aligned} \tag{6.52}$$

The bottom and tau Yukawa couplings differ since they have different SM quantum numbers and arise from different sectors, leading to different q_S and q_P as shown in Table 6.2.

A similar formula can be written down for the RPV coupling

$$\begin{aligned} y_{RPV} =& m_*^4\, t_{abc} \int_S \det(\vec{\psi}^{(b)hol}_{10_M}, \vec{\psi}^{(a)hol}_{5_M}, \vec{\psi}^{(c)hol}_{5'_M}) \mathrm{dVol}_S \\ =& m_*^4\, t_{abc}\ \det(\vec{v}^{(b)}, \vec{v}^{(a)}, \vec{v}^{(c)}) \int_S \chi^{(b)hol}_{10_M} \chi^{(a)hol}_{5_M} \chi^{(c)hol}_{5_M} \mathrm{dVol}_S. \end{aligned} \tag{6.53}$$

Here this RPV Yukawa coupling can in principle refer to any generation of squarks and sleptons, and may have arbitrary generation indices (suppressed here for simplicity).The factor t_{abc} represents the structure constants of the $SO(12)$ group. The integral in the last term can be computed by applying standard Gaussian

techniques. Computing the determinant and the integral, the combined result of the two is a flux independent factor and the final result reads:

$$y_{b,\tau} = \pi^2 \left(\frac{m_*}{m}\right)^4 t_{abc} \kappa^{(b)}_{10_M} \kappa^{(a)}_{5_M} \kappa^{(c)}_{5_H}. \tag{6.54}$$

This is a standard result for the heaviest generations. As we observe the flux dependence is hidden in the normalization factors.

We turn now our attention to the case of a tree-level RPV coupling of the form $10_M \cdot \bar{5}_M \cdot \bar{5}_M$. This coupling can be computed at a different $SO(12)$ enhancement point p. As a first approach we consider that the hypercharge flux parameters are zero in the vicinity of p. From a different point of view, $\bar{5}_M$ replace the Higgs matter curve in the previous computation. The new wavefunction ($\psi^{(c)}_{5_M}$) can be found by setting all the Hypercharge flux parameters on $\psi^{(c)}_{5_H}$, equal to zero. The RPV coupling will be given by an equation similar to that of the bottom coupling:

$$y_{RPV} = \pi^2 \left(\frac{m_*}{m}\right)^4 t_{abc} \kappa^{(b)}_{10_M} \kappa^{(a)}_{5_M} \kappa^{(c)}_{5_M}. \tag{6.55}$$

Notice that the κ's in equations (6.54, 6.55) are the modulus of the normalization factors defined in equations (6.48-6.51).

In the next section, using equations (6.54) and (6.55), we perform a numerical analysis for the couplings presented above with emphasis on the case of the RPV coupling. We notice that in our conventions for the normalization of the $SO(12)$ generators, the gauge invariant coupling supporting the above interactions has $t_{abc} = 2$.

6.3 Yukawa couplings in local F-theory constructions: numerics

Using the mathematical machinery developed in the previous section, we can study the behaviour of $SO(12)$ points in F-theory - including both the bottom-tau point of enhancement and RPV operators. The former has been well studied in [34] for example. The coupling is primarily determined by five parameters -

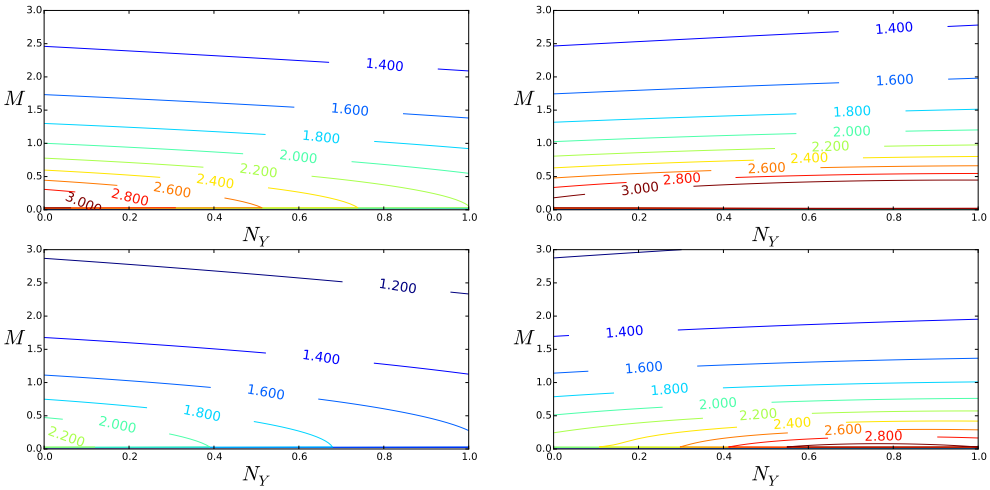

Figure 6.2: Ratio between bottom and tau Yukawa couplings, shown as contours in the plane of local fluxes. The requirement for chiral matter and absence of coloured Higgs triplets fixes $N_b = N_a - \frac{1}{3}N_Y$

N_a, N_b, M, N_Y and $\tilde{N_Y}$. The parameters N_a and N_b give net chirality to the c-sector, while N_Y and $\tilde{N_Y}$ are components of hypercharge flux, parameterising the doublet triplet splitting. M is related to the chirality of the a and b-sectors. There is also the $N_b = N_a - \frac{1}{3}N_Y$ constraint, which ensures the elimination of Higgs colour triplets at the Yukawa point. This can be seen by examining the text of the previous section, based on the work found in [34].

For a convenient and comprehensive presentation of the results we make the following redefinitions. In Eq. (6.54) and (6.55), one can factor out $4\pi g_s \sigma^2$ from inside Eq. (6.48),(6.49), and (6.50). In addition by noticing that $\left(\frac{m}{m_*}\right)^2 = (2\pi)^{3/2} g_s^{1/2} \sigma$, we obtain

$$y_{b,\tau} = 2 g_s^{1/2} \sigma \; y'_{b,\tau} \tag{6.56}$$

$$y_{RPV} = 2 g_s^{1/2} \sigma \; y'_{RPV} \tag{6.57}$$

where $y'_{b,\tau}$ and y'_{RPV} are functions of the flux parameters. Furthermore, we set the scale $m = 1$ and as such the remainder mass dimensions are given in units of m. The presented values for the strength of the couplings are then in units of $2 g_s^{1/2} \sigma$.

Figure 6.2 shows the ratio of the bottom and tau Yukawa couplings at a point of $SO(12)$ in a region of the parameter space with reasonable values. These results are consistent with those in [34]. Note that the phenomenological desired ratio of the couplings at the GUT scale is $Y_\tau/Y_b = 1.37 \pm 0.1 \pm 0.2$ [224], which can be achieved within the parameter ranges shown in Figure 6.2. Having shown that this technique reproduces the known results for the bottom- tau ratio, we now go on to study the behaviour of an RPV coupling point in $SO(12)$ models.

6.3.1 Behaviour of $SO(12)$ points

The simplest scenario for an $SO(12)$ enhancement generating RPV couplings, would be the case where all three of the types of operator, QLD, UDD, and LLE arise with equal strengths, which would occur in a scenario with vanishing hypercharge flux, leading to an entirely "unsplit" scenario. This assumption sets N_Y and $\tilde{N_Y}$ to vanish, and we may also ignore the condition $N_b = N_a - \frac{1}{3}N_Y$. The remaining parameters determining are then N_a, N_b and M. Figure 6.3 shows the coupling strength in the N_a plane for differing N_b and M values. The general behaviour is that coupling strength is directly related to M, while the coupling vanishes at the point where $N_a = N_b$. This latter point is due to the flip in net chirality for the c-sector at this point in the parameter space - $N_a > N_b$ gives the c^+ part of the spectrum.

Figure 6.4 and Figure 6.5 also demonstrate this set of behaviours, but for contours of the coupling strength. Figure 6.4, showing all combinations of the three non-zero parameters, shows that in the $N_a - N_b$ plane there is a line of vanishing coupling strength about the $N_a = N_b$, chirality switch point for the c-sector. The figure also reinforces the idea that small values of M correspond to small values of the coupling strength, as close to the point of $M = 0$ the coupling again reduces to zero. Figure 6.5 again shows this behaviour, with the smallest values of M giving the smallest values of the coupling. From this we can infer that an RPV $SO(12)$ point is most likely to be compatible with experimental constraints if M takes a small value.

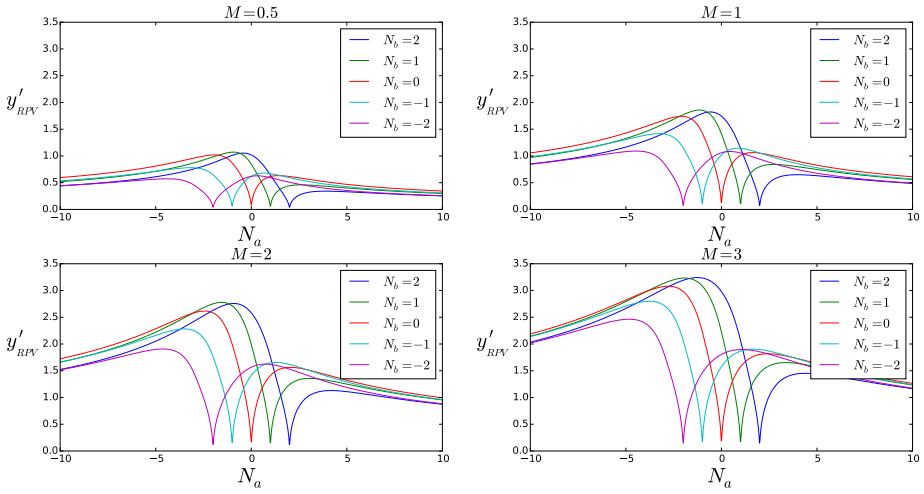

Figure 6.3: Dependency of the RPV coupling (in units of $2g_s^{1/2}\sigma$) on N_a in the absence of hypercharge fluxes, for different values of M and N_b.

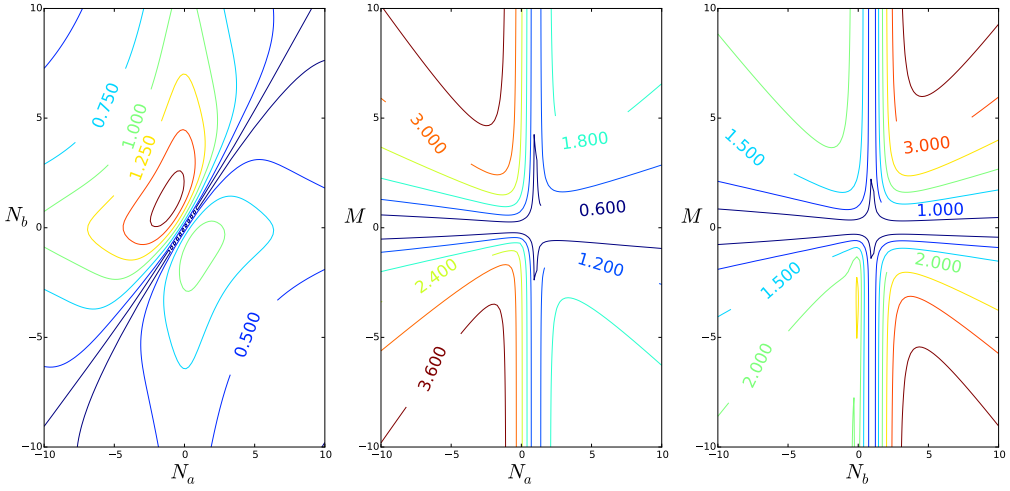

Figure 6.4: Dependency of the RPV coupling (in units of $2g_s^{1/2}\sigma$) on different flux parameters, in absence of Hypercharge fluxes. Any parameter whose dependency is not shown is set to zero.

Figure 6.6a (and Figure 6.6b) shows the RPV coupling strength in the absence of flux for the N_a (N_b) plane, along with the "bottom" coupling strength for corresponding values. The key difference is that the Hypercharge flux is switched on at the bottom $SO(12)$ point, with values of $N_Y = 0.1$ and $\tilde{N}_Y = 3.6$. The figures show that for the bottom coupling, the fluxes always push the coupling higher, similarly to increasing the M values.

Figure 6.6c plots out the two couplings in the M-plane, showing that the bottom Yukawa goes to zero for two values of M, while the RPV point has only

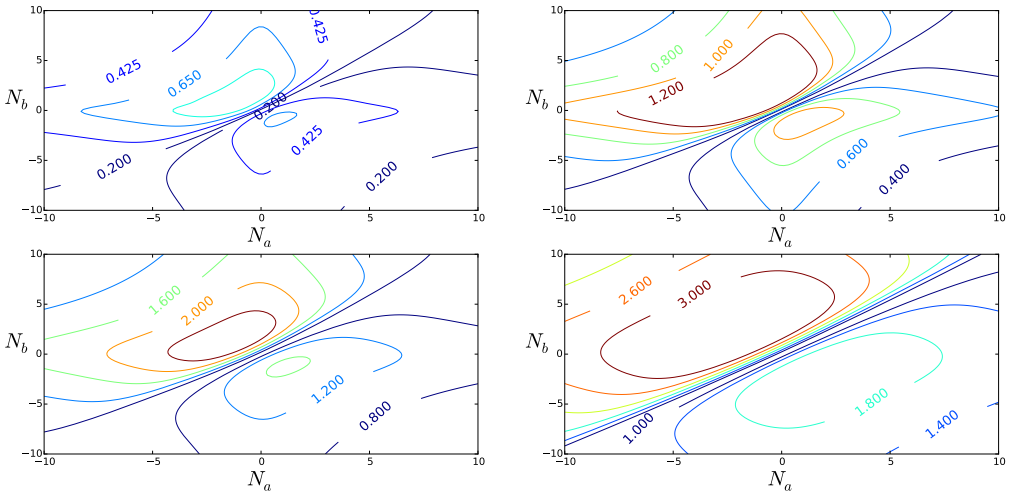

Figure 6.5: Dependency of the RPV coupling (in units of $2g_s^{1/2}\sigma$) on the (N_a, N_b)-plane, in absence of hypercharge fluxes and for different values of M. Top: left $M = 0.5$, right $M = 1.0$. Bottom: left $M = 2.0$, right $M = 3.0$.

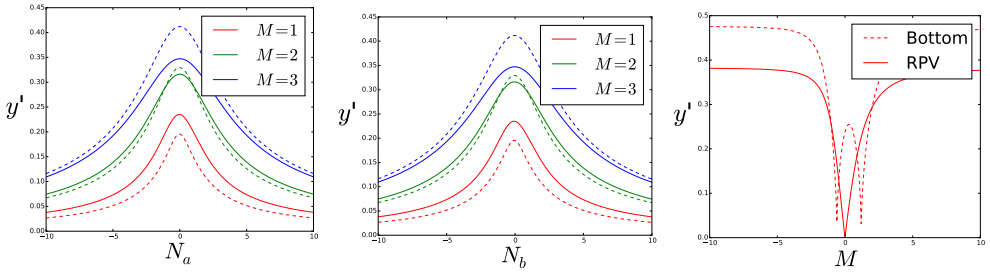

(a) Varying N_a with fixed M (b) Varying N_b with fixed M (c) Varying M with fixed N_a=1, $N_b = 29/30$, $N_Y = 0.1$, $\tilde{N}_Y = 3.6$

Figure 6.6: Dependency of the RPV and bottom Yukawa couplings (in units of $2g_s^{1/2}\sigma$) on different parameters at different regions of the parameter space

one. Considering the form of Equation (6.54), we can see that the factors κ_{5_M} and κ_{10_M} are proportional to the parameter q_p. Referring to Table 6.2, one can see which values these take for each sector - namely, $q_p(a_1) = M - \frac{1}{3}\tilde{N}_Y$ and $q_p(b_2) = -M - \frac{1}{6}\tilde{N}_Y$. Solving these two equations shows trivially that zeros should occur when $M = \frac{1}{3}\tilde{N}_Y$ and $-\frac{1}{6}\tilde{N}_Y$, which is the exact behaviour exhibited in Figure 6.6c.

6.4 R-parity violating Yukawa couplings: allowed regions and comparison to data

In this section we focus on calculating the RPV Yukawa coupling constant at the GUT scale, which may be directly compared to the experimental limits, using the methods and results of the previous two sections. As a point of notation, we have denoted the RPV Yukawa coupling at the GUT scale to be generically y_{RPV}, independently of flavour or operator type indices. This coupling may be directly compared to the phenomenological RPV Yukawa couplings at the GUT scale λ_{ijk}, λ'_{ijk} and λ''_{ijk} as defined below.

Recall that, in the weak/flavour basis, the superpotential generically includes RPV couplings, in particular:

$$W \supset \frac{1}{2}\lambda_{ijk}L_iL_je^c_k + \lambda'_{ijk}L_iQ_jd^c_k + \frac{1}{2}\lambda''_{ijk}u^c_id^c_jd^c_k \tag{6.58}$$

In the local F-theory framework, each of the above Yukawa couplings (generically denoted as y_{RPV}) is computable through Eq. (6.55). What distinguishes different RPV couplings, say λ from λ', are the values of the flux densities, namely the hypercharge flux. This is because the normalization of matter curves depends on the hypercharge flux density. As such, different SM states will have different hypercharges and consequently different respective normalization coefficient.

Even though a given $SO(12)$ enhancement point can in principle support different types of trilinear RPV interactions, the actual effective interactions arising at such point depend on the local chiral spectrum present at each curve. For example, in order to have an LLe^c interaction, both Σ_a and Σ_c curves need to have chiral L states, and the Σ_b curve an e^c state at the enhancement point. In Figure 6.7 we show contours on the (N_a,N_b) plane for the different types of trilinear RPV couplings.

The local spectrum is assessed by local chiral index theorems [36]. In Appendix C.2 we outline the results for the constraints on flux densities such that different RPV points are allowed at a given $SO(12)$ enhancement point. These

results are graphically presented in Figure 6.8. Thus, the green coloured region is associated with the $10_3\bar{5}_1\bar{5}_1$ operator of this Table, the blue colour with $10_1\bar{5}_3\bar{5}_3$, the pink with $10_2\bar{5}_4\bar{5}_4$ and so on. Thus different regions of the parameter space can support different types of RPV interactions at a given enhancement point. We can then infer that in F-theory the allowed RPV interactions can, in principle, be only a subset of all possible RPV interactions.

In the limiting cases where only one coupling is turned on, one can derive bounds on its magnitude at the GUT scale from low-energy processes [225]. In order to do so, one finds the bounds at the weak scale in the mass basis, performs a rotation to the weak basis and then evaluates the couplings at the GUT scale with the renormalisation group equation. Since the effects of the rotation to the weak basis in the RPV couplings requires a full knowledge of the Yukawa matrices, we assume that the mixing only happens in the down-quark sector as we are not making any considerations regarding the up-quark sector in this work. Table 6.3 shows the upper bounds for the trilinear RPV couplings at the GUT scale.

The bounds presented in Table 6.3 have to be understood as being derived under certain assumptions regarding mixing and points of the parameter space [99, 226]. For example, the bound on λ_{12k} can be shown to have an explicit dependence on

$$\frac{\tilde{m}_{e_{k,R}}}{100 \text{ GeV}} \tag{6.59}$$

where $\tilde{m}_{e_{k,R}}$ refers to a 'right-handed' selectron soft-mass. The values presented in Table 6.3, as found in [225], were obtained by setting the soft-masses to 100 GeV, which are ruled out by more recent LHC results [227–232] . By assuming heavier scalars, for example around 1 TeV, we would then get the bounds in Table 6.3 to be relaxed by one order of magnitude.

The results show that the λ type of coupling, corresponding to the LLe^c interactions, is constrained to be < 0.05 regardless of the indices taken. The red regions of Figures 6.11a and 6.9 show the magnitude of the coupling where it is allowed. A similar analysis can be carried out for the remaining couplings. The

ijk	λ_{ijk}	λ'_{ijk}	λ''_{ijk}
111	-	1.5×10^{-4}	-
112	-	6.7×10^{-4}	4.1×10^{-10}
113	-	0.0059	1.1×10^{-8}
121	0.032	0.0015	4.1×10^{-10}
122	0.032	0.0015	-
123	0.032	0.012	1.3×10^{-7}
131	0.041	0.0027	1.1×10^{-8}
132	0.041	0.0027	1.3×10^{-7}
133	0.0039	4.4×10^{-4}	-
211	0.032	0.0015	-
212	0.032	0.0015	(1.23)
213	0.032	0.016	(1.23)
221	-	0.0015	(1.23)
222	-	0.0015	-
223	-	0.049	(1.23)
231	0.046	0.0027	(1.23)
232	0.046	0.0028	(1.23)
233	0.046	0.048	-
311	0.041	0.0015	-
312	0.041	0.0015	0.099
313	0.0039	0.0031	0.015
321	0.046	0.0015	0.099
322	0.046	0.0015	-
323	0.046	0.049	0.015
331	-	0.0027	0.015
332	-	0.0028	0.015
333	-	0.091	-

Table 6.3: Upper bounds of RPV couplings (ijk refer to flavour/weak basis) at the GUT scale under the assumptions: 1) Only mixing in the down-sector, none in the Leptons; 2) Scalar masses $\tilde{m} = 100$ GeV; 3) $\tan\beta(M_Z) = 5$; and 4) Values in parenthesis refer to non-perturbative bounds, when these are stronger than the perturbative ones. This Table is reproduced from [225].

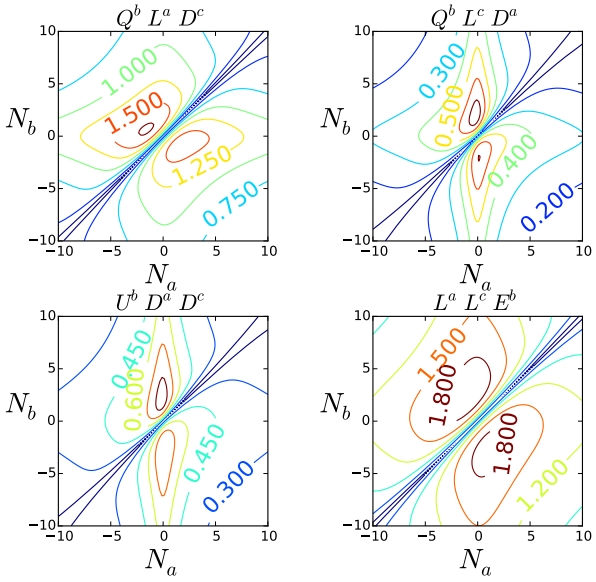

Figure 6.7: Strength of different RPV couplings (in units of $2g_s^{1/2}\sigma$) in the (N_a, N_b)-plane in the presence of Hypercharge fluxes $N_Y = 0.1$, $\tilde{N}_Y = 3.6$, and with $M = 1$. The scripts a, b, c refer to which sector each state lives.

λ' coupling, which measures the strength of the LQd^c type of interactions, can be seen in the yellow regions of Figure 6.10. Finally, the derived values for λ'' coupling, related to the $u^c d^c d^c$ type of interactions, are shown in the blue regions of Figures 6.10 and 6.11b. However these couplings shown are all expressed in units of $2g_s^{1/2}\sigma$, and so cannot yet be directly compared to the experimental limits.

In order to make contact with experiment we must eliminate the $2g_s^{1/2}\sigma$ coefficient. We do this by taking ratios of the couplings computed in this framework where the $2g_s^{1/2}\sigma$ coefficient cancels in the ratio. The ratio between any RPV coupling and the bottom Yukawa at the GUT scale is given by

$$r = \frac{y_{RPV}}{y_b} = \frac{y'_{RPV}}{y'_b}, \tag{6.60}$$

as defined in Equation (6.56) and Equation (6.57). This ratio can be used to assess the absolute strength of the RPV at the GUT scale as follows.

First we assume that the RPV interaction is localised in an $SO(12)$ point far away from the bottom Yukawa point. This allows us to use different and independent flux densities at each point. We can then compute y'_b at a point in

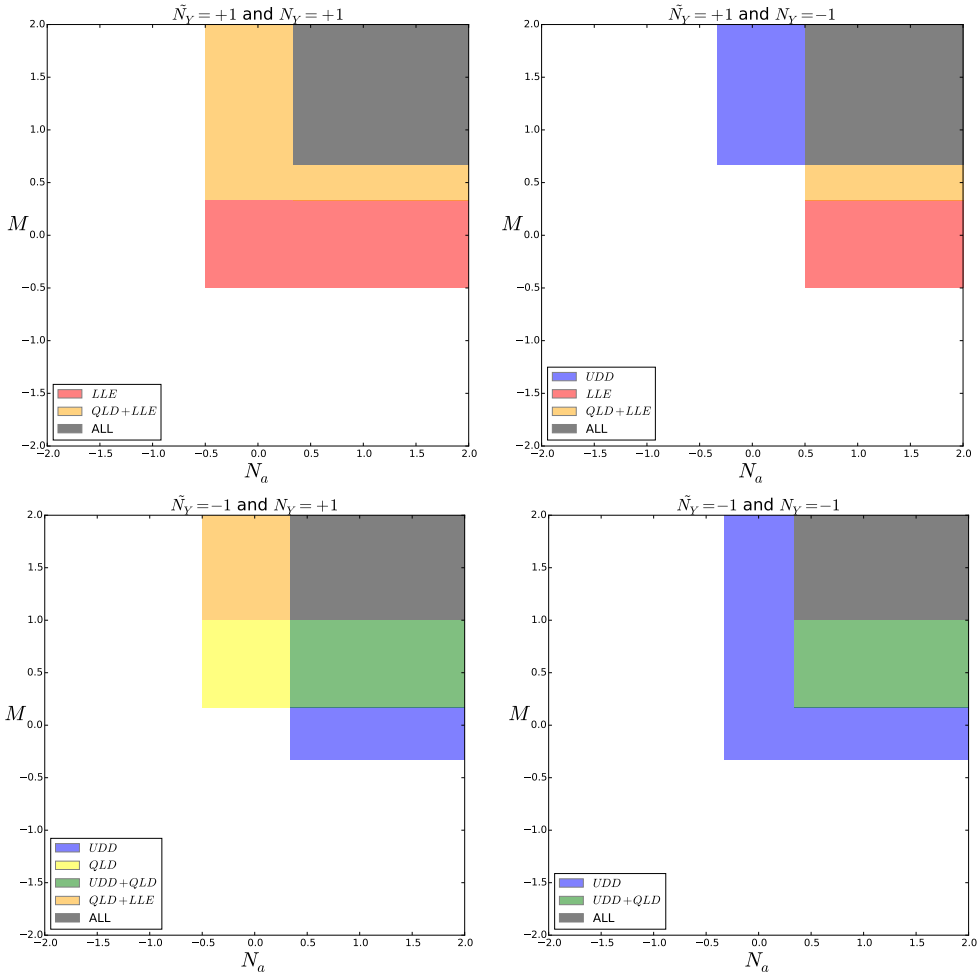

Figure 6.8: Allowed regions in the parameter space for different RPV couplings. These figures should be seen in conjunction with the allowed combinations of R-parity violating operators.

the parameter space where the ratio y_b/y_τ takes reasonable values, following [34]. Finally we take the ratio, r. In certain regions of the parameter space, r is naturally smaller than 1. This suppression of the RPV coupling in respect to the bottom Yukawa is shown in Figures 6.12a, 6.12b, 6.12c, and 6.12d, for different regions of the parameter space that allows for distinct types of RPV interactions.

Since r is the ratio of both primed and unprimed couplings, respectively unphysical and physical, at the GUT scale, we can extend the above analysis to find the values of the physical RPV couplings at the GUT scale. To do so, we use low-energy, experimental, data to set the value of the bottom Yukawa at the weak scale for a certain value of $\tan\beta$. Next, we follow the study in [224] to assess

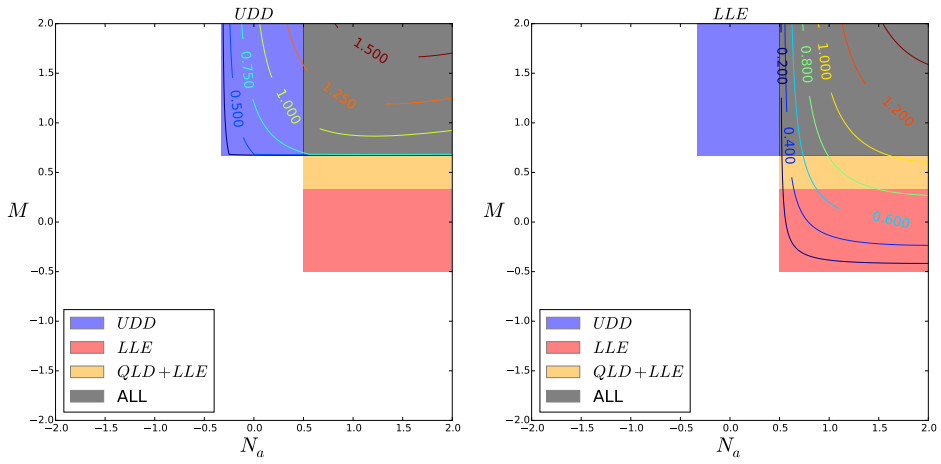

Figure 6.9: Allowed regions in the parameter space for different RPV couplings with $\tilde{N_Y} = -N_Y = 1$. We have also include the corresponding contours for the $u^c d^c d^c$ operator (left) and LLe^c (right).

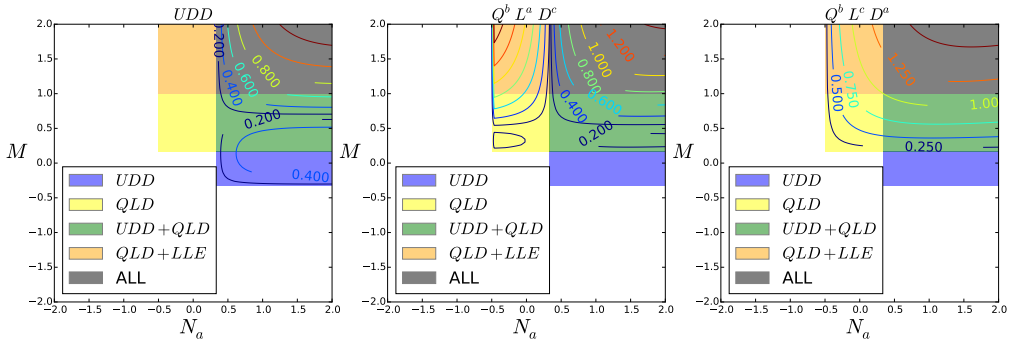

Figure 6.10: Allowed regions in the parameter space for different RPV couplings with $N_Y = -\tilde{N_Y} = 1$. We have also include the corresponding contours for the $u^c d^c d^c$ operator (left) and QLd^c (middle and right). The scripts a, b and c refer to which sector each state lives.

the value of the bottom Yukawa at the GUT scale through RGE runnings.

In order to make a connection with the bounds in Table 6.3, we pick $\tan\beta = 5$ and we find $y_b(M_{GUT}) \simeq 0.03$. The results for the value of the RPV couplings in different regions in the parameter space at the GUT scale are presented in Figures 6.13a, 6.13b, 6.13c, and 6.13d. These results show that, for any set of flavour indices, the strength of the coupling λ related to an LLe^c interaction is within the bounds. This means that this purely leptonic RPV operator, which

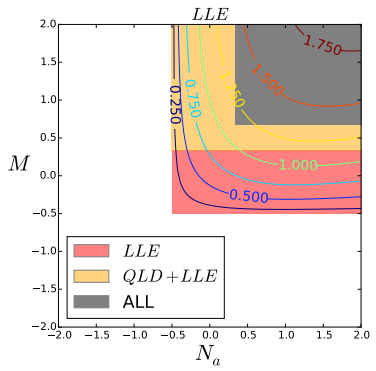

(a) LLe^c regions with $\tilde{N_Y} = N_Y = 1$

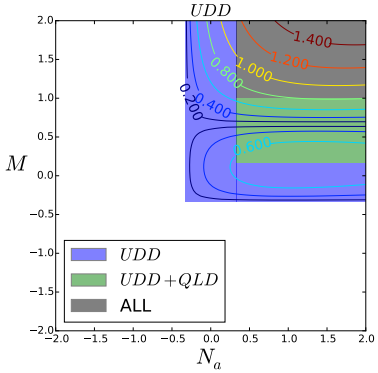

(b) $u^c d^c d^c$ regions with $\tilde{N_Y} = N_Y = -1$

Figure 6.11: Allowed regions in the parameter space for different RPV couplings.

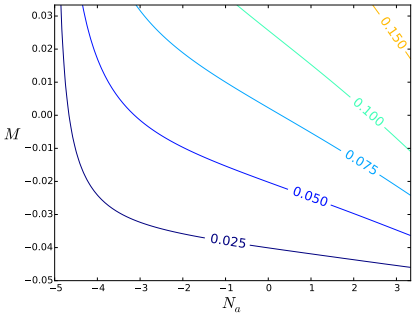

(a) LLe^c region: $N_Y = 10$, $\tilde{N_Y} = 0.1$

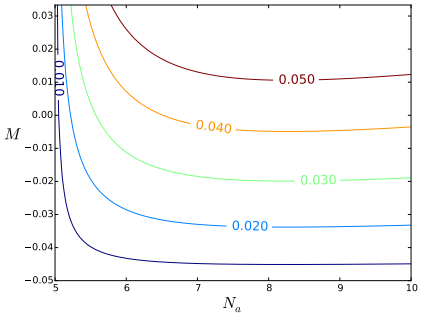

(b) LLe^c region: $N_Y = -10$, $\tilde{N_Y} = 0.1$

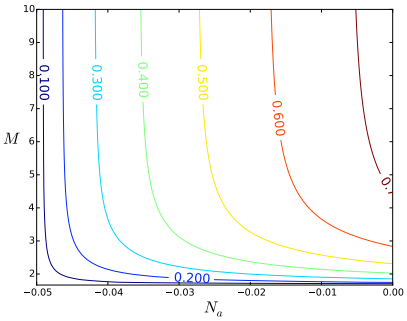

(c) QLd^c region: $N_Y = 0.1$, $\tilde{N_Y} = -10$

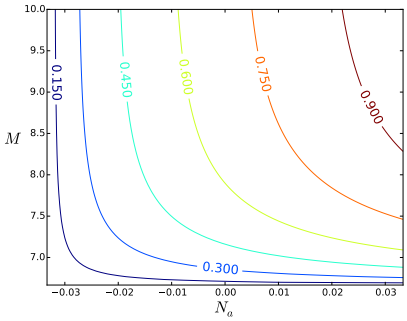

(d) $u^c d^c d^c$ region: $N_Y = -0.1$, $\tilde{N_Y} = -10$

Figure 6.12: y_{RPV}/y_b ratio. The bottom Yukawa was computed in a parameter space point that returns a reasonable y_b/y_τ ratio [34]

violates lepton number but not baryon number, may be present with a sufficiently suppressed Yukawa coupling, according to our calculations. Therefore in the future lepton number violating processes could be observed.

By contrast, only for a subset of possible flavour index assignments for baryon

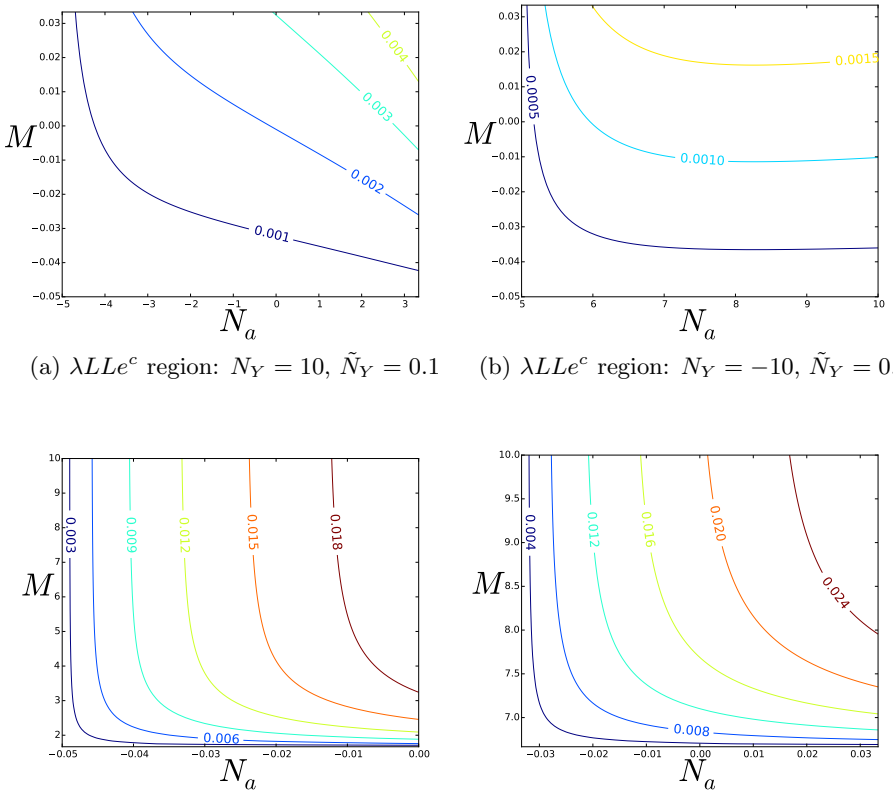

(a) λLLe^c region: $N_Y = 10$, $\tilde{N}_Y = 0.1$ (b) λLLe^c region: $N_Y = -10$, $\tilde{N}_Y = 0.1$

(c) $\lambda' QLd^c$ region: $N_Y = 0.1$, $\tilde{N}_Y = -10$ (d) $\lambda'' u^c d^c d^c$ region: $N_Y = -0.1$, $\tilde{N}_Y = -10$

Figure 6.13: y_{RPV} at GUT scale for $\tan\beta = 5$. The values here can be compared directly to the bounds presented in Table 6.3.

number violating (but lepton number conserving) $u^c d^c d^c$ couplings are within the bounds in Table 6.3. The constraint on the first family up quark coupling λ''_{1jk} for the $u_1^c d_j^c d_k^c$ interaction is so stringent, that this operator must only be permitted for the cases $u_2^c d_j^c d_k^c$ and $u_3^c d_j^c d_k^c$ (corresponding to the two heavy up-type quarks c^c, t^c), assuming no up-type quark mixing. However, if up-type quark mixing is allowed, then such operators could lead to an effective $u_1^c d_j^c d_k^c$ operator suppressed by small mixing angles, in which case it could induce $n - \bar{n}$ oscillations [3].

Finally the LQd^c operator with Yukawa coupling λ' apparently must be avoided, since according to our calculations, the value of λ' that we predict exceeds the experimental limit by about an order of magnitude for all flavour indices, apart from λ'_{333} coupling corresponding to the $L_3 Q_3 d_3^c$ operator. This implies that we should probably eliminate such operators which violate both baryon number and lepton number, using the flux mechanism that we have de-

scribed. However in some parts of parameter space, for certain flavour indices, such operators may be allowed leading to lepton number violating processes such as $K^+ \to \pi^- e^+ e^+$ and $D^+ \to K^- e^+ e^+$.

6.5 Conclusions

In this chapter we have provided the first dedicated study of R-parity violation (RPV) in F-theory semi-local and local constructions based on the $SU(5)$ grand unified theory (GUT) contained in the maximal subgroup $SU(5)_{GUT} \times SU(5)_\perp$ of an E_8 singularity associated with the elliptic fibration. Within this framework, we have tried to be as general as possible, with the primary aim of making a bridge between F-theory and experiment.

We have focused on semi-local and local F-theory $SU(5)$ constructions, where a non-trivial hypercharge flux breaks the GUT symmetry down to the Standard Model and in addition renders several GUT multiplets incomplete. Acting on the Higgs curves this novel mechanism can be regarded as the surrogate for the doublet-triplet splitting of conventional GUTs. However, from a general perspective, at the same time the hyperflux may work as a displacement mechanism, removing certain components of GUT multiplets while accommodating fermion generations on other matter curves.

In the first part of the chapter we considered semi-local constructions, focusing on F-theory $SU(5)_{GUT}$ models which are classified according to the discrete symmetries – acting as identifications on the $SU(5)_\perp$ representations – and appearing as a subgroup of the maximal $SU(5)_\perp$ Weyl group S_5. Furthermore, we considered phenomenologically appealing scenarios with the three fermion generations distributed on different matter curves and showed that RPV couplings are a generic feature of such models. Upon introducing the flux breaking mechanism, we classified all possible cases of incomplete GUT multiplets and examined the implications of their associated RPV couplings. Then we focused on the induced MSSM plus RPV Yukawa sector which involves only part of the MSSM allowed RPV operators as a consequence of the missing components of the multiplets

projected out by the flux. Next, we tabulated all distinct cases and the type of physical process that can arise from particular operators involving different types of incomplete multiplets.

In the second part of the chapter we computed the strength of the RPV Yukawa couplings, which mainly depend on the topological properties of the internal space and are more or less independent of many details of a particular model, enabling us to work in a generic local F-theory setting. Due to their physical relevance, we paid special attention to those couplings originating from the $SU(5)$ operator $10 \cdot \bar{5} \cdot \bar{5}$ in the presence of general fluxes, which is realised at an $SO(12)$ point of enhancement. Then, we applied the already developed F-theory techniques to calculate the numerical values of Yukawa couplings for bottom, tau and RPV operators. Taking into account flux restrictions, which limit the types of RPV operators that may appear simultaneously, we then calculated ratios of Yukawa couplings, from which the physical RPV couplings at the GUT scale can be determined. We have explored the possible ranges of the Yukawa coupling strengths of the $10 \cdot \bar{5} \cdot \bar{5}$-type operators in a five-dimensional parameter space, corresponding to the number of the distinct flux parameters/densities associated with this superpotential term. Varying these densities over a reasonable range of values, we have observed the tendencies of the various Yukawa strengths with respect to the flux parameters and, to eliminate uncertainties from overall normalization constants, we have computed the ratios of the RPV couplings to the bottom Yukawa one. This way, using the experimentally determined mass of the bottom quark, we compared our results to limits on these couplings from experiment.

The results of this paper show firstly that, in semi-local F-theory constructions based on $SU(5)$ GUTs, RPV is a generic feature, but may occur without proton decay, due to flux effects. Secondly, our calculations based on local F-theory constructions show that the value of the RPV Yukawa couplings at the GUT scale may be naturally suppressed over large regions of parameter space. Furthermore, we found that the existence of LLe^c type of RPV interactions from F-Theory are

expected to be within the current bounds. This implies that such lepton number violating operators could be present in the effective theory, but simply below current experimental limits, and so lepton number violation could be observed in the future. Similarly, the baryon number violating operators $c^c d_j^c d_k^c$ and $t^c d_j^c d_k^c$ could also be present, leading to $n - \bar{n}$ oscillations. Finally some QLd^c operators could be present leading to lepton number violating processes such as $K^+ \to \pi^- e^+ e^+$ and $D^+ \to K^- e^+ e^+$. In conclusion, our results suggest that RPV SUSY consistent with proton decay and current limits may be discovered in the future, shedding light on the nature of F-theory constructions.

Chapter 7

Conclusions

In this thesis, semi-local F-theory GUT models have been examined, using an SU(5) GUT group. Developing existing ideas in the literature, non-Abelian monodromy groups were considered, with particular interest in a few particular subgroups of the S_4 Weyl group of the split spectral cover. In chapter 2, the Klein monodromy group was discussed as a candidate monodromy, leading to a model similar to the MSSM [1]. The model was endowed with a geometric parity arising from the spectral cover equation, which eliminated the usual dimension-4 R-parity violating terms known to facilitate proton decay. This parity mechanism added extra constraints when considering model building, meaning not all models in the literature would be compatible with it, as we showed.

Chapter 3 features an SU(5) GUT model with an A_4 monodromy, where the focus of the work was to utilise the irreducible representation of the monodromy group to generate large mixings for the neutrinos of the model [2]. This was achieved using singlets of the GUT group, which allowed effective operators that were invariant under the requisite symmetries. By numerically fitting the ratio of the mass differences in the model against those from experiment, it was also possible to predict an absolute mass scale for the neutrinos in this model, with a prediction for the lightest neutrino being in the region of 50meV. This was compatible with constraints from cosmology on the sum of the neutrino masses.

In keeping with this train of thought, considering subgroups of S_4, in chap-

ter 4 a D_4 monodromy was applied to an SU(5) GUT [3]. Pairing this with implementation of the geometric parity discussed in chapter 2, a model was constructed with a number of novel features. In particular, the geometric parity does not eliminate the complete spectrum of R-parity violating operators, allowing the UDD operators to remain in the model. Consequently, while proton decay cannot occur due to the absence of the QLD operator, the model will exhibit baryon number violating. This manifests in the form of neutron-antineutron oscillations, which are a seldom considered R-parity violating process. The neutrino sector of the model also has interesting features, requiring a massless lightest neutrino, essentially setting the neutrino masses exactly.

In chapter 5 we discussed the LHC diphoton excess, which indicated a 750GeV scalar or pseudoscalar [4]. This was shown to be compatible with an F-theory E_6 mode, based on [52–54]l, where the new particle would be identified with bulk singlets, which arise from breaking the E_6 symmetry to SU(5). The model appears to favour a psuedoscalar to be compatible with the excess, however, the production and decay are mediated by a combination of higgs colour triplets and higgsinos, which would need to be below 1TeV in mass. This prediction of the model would require the discovery of these mediating particles in order to remain viable. More recently, new data greatly reduced the significance of the excess.

The final chapter provides an examination of the potential strength of R-parity violating couplings in F-theory [5]. Using a local approach, the interactions are reduced to a point of enhanced symmetry on the assumed SU(5) GUT surface. The enhancement to a point of SO(12), previously used to calculate the bottom and tau Yukawa couplings, was reinterpreted and reused to describe R-parity violating couplings, which must also be an SO(12) point. An exhaustive discussion of the behaviour of the coupling was then offered, with a set of conditions for single-coupling regions of R-parity violation. This special case is important, since in scenarios where one coupling type is isolated, the experimental bounds are less strict. It was shown that single R-parity couplings from F-theory can then be within the experimental limits, with some couplings on the edge of the

natural parameter space, indicating that R-parity violation should be discovered by experiment if the parameter space is not to be pushed to unnatural limits.

Non-Abelian monodromies have been shown to provide interesting platforms for building models in semi-local F-theory, which has been very much under-utilised by model builders in the literature. These monodromies should now be explored in the context of global constructions, which may prove a challenge for future research. The direction of the F-theory community seems to be geared towards realising global models, so it is not a stretch to imagine that work will be done on this matter.

Another key finding of this thesis is that R-parity violation in F-theory should be considered a generic feature of all SU(5) models. Previously such operators have been eliminated by *ad hoc* methods and assumptions that can only be justified by the anthropic principle. While we present a mechanism for removing such operators from the spectrum, the problem should be addressed in more depth, with the option to consider that such operators may be accommodated without issue in the appropriate parameter space as shown in chapter 6. In the case that R-parity is discovered by experimentalists at future experiments, F-theory would certainly provide for such an outcome, whether or not a single coupling is detected or a more generic spectrum of effects.

In conclusion, F-theory GUTs are an intriguing prospect for model building, with a host of novel features that could be sought by experiment, ranging form absolute predictions of neutrino masses to R-parity violation.

Appendices

Appendix A

Appendix: chapter 3

A.1 Block diagonalisation of A_4

A.1.1 Four dimensional case

From considering the symmetry properties of a regular tetrahedron, we can see quite easily that it can be parameterised by four coordinates and its transformations can be decomposed into a mere two generators. If we write these coordinates as a basis for A_4, which is the symmetry group of the tetrahedron, it would be of the form $(t_1, t_2, t_3, t_4)^{\mathrm{T}}$. The two generators can then be written in matrix form explicitly as:

$$S = \begin{pmatrix} 0 & 0 & 0 & 1 \\ 0 & 0 & 1 & 0 \\ 0 & 1 & 0 & 0 \\ 1 & 0 & 0 & 0 \end{pmatrix} \text{ and } T = \begin{pmatrix} 1 & 0 & 0 & 0 \\ 0 & 0 & 0 & 1 \\ 0 & 1 & 0 & 0 \\ 0 & 0 & 1 & 0 \end{pmatrix} . \tag{A.1}$$

However, it is well known that A_4 has an irreducible representation in the form of a singlet and triplet under these generators. If we consider the tetrahedron again, this can be physically interpreted by observing that under any rotation through one of the vertices of the tetrahedron the vertex chosen remains unmoved under the transformation.[1] In order to find the irreducible representation, we must note

[1] This is a trivial notion for the T generator, but slightly more difficult for the S generator. In the latter case, consider fixing one vertex in place and performing the transformation about

some conditions that this decomposition will satisfy.

In order to obtain the correct basis, we must find a unitary transformation V that block diagonalises the generators of the group. As such, we have the following conditions:

$$
\begin{aligned}
VSV^{\mathrm{T}} = S' &= \begin{pmatrix} 1 & 0 & 0 & 0 \\ 0 & - & - & - \\ 0 & - & - & - \\ 0 & - & - & - \end{pmatrix}, \\
VTV^{\mathrm{T}} = T' &= \begin{pmatrix} 1 & 0 & 0 & 0 \\ 0 & - & - & - \\ 0 & - & - & - \\ 0 & - & - & - \end{pmatrix}, \\
VV^{\mathrm{T}} &= \mathrm{I}_{4x4} \ ,
\end{aligned}
\tag{A.2}
$$

as well as the usual conditions that must be satisfied by the generators: $S^2 = T^3 = (ST)^3 = \mathrm{I}$. It will also be useful to observe three extra conditions, which will expedite finding the solution. Namely that the block diagonal of one of the two generators must have zeros on the diagonal to insure the triplet changes within itself.

If we write an explicit form for V,

$$
V = \begin{pmatrix} v_{11} & v_{12} & v_{13} & v_{14} \\ v_{21} & v_{22} & v_{23} & v_{24} \\ v_{31} & v_{32} & v_{33} & v_{34} \\ v_{41} & v_{42} & v_{43} & v_{44} \end{pmatrix}, \tag{A.3}
$$

we can extract a set of quadratic equations and attempt to solve for the elements of the matrix. Note that we have assumed as a starting point that $v_{ij} \in \mathbb{R} \forall i, j$.

it.

The complete list is included in the appendix. The problem is quite simple, but at the same time would be awkward to solve numerically, so we shall attempt to simplify the problem analytically first. If we start be using:

$$\begin{aligned} v_{11}^2 + v_{12}^2 + v_{13}^2 + v_{14}^2 &= 1\,, \\ \&\;\; 2v_{12}v_{13} + 2v_{11}v_{14} &= 1\,, \end{aligned} \tag{A.4}$$

we can trivially see two quadratics,

$$(v_{11} - v_{14})^2 + (v_{12} - v_{13})^2 = 0\,. \tag{A.5}$$

Since we assume that all our elements or V are real numbers, it must be true then that:

$$v_{11} = v_{14} \;\text{ and }\; v_{12} = v_{13}\,. \tag{A.6}$$

We may now substitute this result into a number of equations. However, we chose to focus on the following two:

$$\begin{aligned} v_{11}v_{21} + v_{12}v_{23} + v_{13}v_{24} + v_{14}v_{22} \to v_{11}(v_{21} + v_{22}) + v_{12}(v_{23} + v_{24}) \;\text{ and} \\ v_{11}v_{21} + v_{12}v_{24} + v_{13}v_{22} + v_{14}v_{23} \to v_{11}(v_{21} + v_{23}) + v_{12}(v_{22} + v_{24})\,. \end{aligned} \tag{A.7}$$

Taking the difference of these two equations, we can easily see there is a solution where $v_{11} = v_{12}$, and as such by the previous result:

$$v_{11} = v_{12} = v_{13} = v_{14} = \pm\frac{1}{2}\,. \tag{A.8}$$

We are free to choose whichever sign for these four elements we please, provided they all have the same sign. This outcome reduces the number of useful equations to twelve, as nine of them can be summarised as

$$\sum_i v_{2i} = \sum_i v_{3i} = \sum_i v_{4i} = 0\,. \tag{A.9}$$

Let us consider the first of these three derived conditions, along with the condi-

tions:

$$\begin{aligned} v_{21}^2 + v_{22}^2 + v_{23}^2 + v_{24}^2 &= 1\,, \\ v_{21}^2 + v_{22}v_{23} + v_{22}v_{24} + v_{23}v_{24} &= 0\,. \end{aligned} \tag{A.10}$$

Squaring the condition $\sum_i v_{2i} = 0$ and using these relations, we can derive easily that $v_{21} = \pm\frac{1}{2}$. Likewise we can derive the same for v_{31} and v_{41}. As before, we might chose either sign for each of these elements, with each possibility yielding a different outcome for the basis, though our choices will constrain the signs of the remaining elements in V.

Let us make a choice for the signs of our known coefficients in the matrix and choose them all to be positive for simplicity. We are now left with a much smaller set of conditions:

$$\begin{aligned} \sum_{i=2}^{4} v_{ji} &= -\frac{1}{2}\ , \\ \sum_{i=2}^{4} v_{ji}^2 &= \frac{3}{4}\ \text{ and} \\ \sum_{i=2}^{4} v_{ji}v_{ki} &= \frac{1}{4}\ , \end{aligned} \tag{A.11}$$

$$j, k \in \{2, 3, 4\}\ \text{ and }\ k \neq j\ \ .$$

After a few choice rearrangements, these coefficients can be calculated numerically in Mathematica. This yields a unitary matrix,

$$V = \frac{1}{2}\begin{pmatrix} 1 & 1 & 1 & 1 \\ 1 & -1 & -1 & 1 \\ 1 & -1 & 1 & -1 \\ 1 & 1 & -1 & -1 \end{pmatrix}\ , \tag{A.12}$$

up to exchanges of the bottom three rows, which arises due to the fact the triplet arising in this representation may be ordered arbitrarily. There is also a degree of choice involved regarding the sign of the rows. However, this is again largely unimportant as the result would be equivalent.

If we apply this transformation to our original basis t_i, we find that we have a singlet and a triplet in the new basis,

$$\begin{aligned} t_{singlet} &= t_1 + t_2 + t_3 + t_4 \\ t_{triplet} &= (t_1 - t_2 - t_3 + t_4,\, t_1 - t_2 + t_3 - t_4\,, t_1 + t_2 - t_3 - t_4)\ , \end{aligned} \tag{A.13}$$

and that our generators become block-diagonal:

$$\begin{aligned} S' &= \begin{pmatrix} 1 & 0 & 0 & 0 \\ 0 & 1 & 0 & 0 \\ 0 & 0 & -1 & 0 \\ 0 & 0 & 0 & -1 \end{pmatrix} \\ T' &= \begin{pmatrix} 1 & 0 & 0 & 0 \\ 0 & 0 & 1 & 0 \\ 0 & 0 & 0 & 1 \\ 0 & 1 & 0 & 0 \end{pmatrix}\ . \end{aligned} \tag{A.14}$$

List of Conditions

$$
\begin{aligned}
&0)\ \ v_{ij} \in \mathbb{R} \forall i,j \\
&1\text{-}4)\ \ \sum_{j=1}^{4} v_{ij}^2 = 1 \ \ i \in \{1,2,3,4\} \\
&5)\ \ v_{11}v_{21} + v_{12}v_{22} + v_{13}v_{23} + v_{14}v_{24} = 0 \\
&6)\ \ v_{11}v_{31} + v_{12}v_{32} + v_{13}v_{33} + v_{14}v_{34} = \\
&7)\ \ v_{11}v_{41} + v_{12}v_{42} + v_{13}v_{43} + v_{14}v_{44} = 0 \\
&8)\ \ v_{21}v_{31} + v_{22}v_{32} + v_{23}v_{33} + v_{24}v_{34} = 0 \\
&9)\ \ v_{21}v_{41} + v_{22}v_{42} + v_{23}v_{43} + v_{24}v_{44} = 0 \\
&10)\ \ v_{31}v_{41} + v_{32}v_{42} + v_{33}v_{43} + v_{34}v_{44} = 0 \\
&11)\ \ 2v_{12}v_{13} + 2v_{11}v_{14} = 1 \\
&12)\ \ v_{11}v_{24} + v_{12}v_{23} + v_{13}v_{22} + v_{14}v_{21} = 0 \\
&13)\ \ v_{11}v_{34} + v_{12}v_{33} + v_{13}v_{32} + v_{14}v_{31} = 0 \\
&14)\ \ v_{11}v_{44} + v_{12}v_{43} + v_{13}v_{42} + v_{14}v_{41} = 0 \\
&15)\ \ v_{11}^2 + v_{12}v_{13} + v_{12}v_{14} + v_{13}v_{14} = 1 \\
&16)\ \ v_{11}v_{21} + v_{12}v_{24} + v_{13}v_{22} + v_{14}v_{23} = 0 \\
&17)\ \ v_{11}v_{31} + v_{12}v_{34} + v_{13}v_{32} + v_{14}v_{33} = 0 \\
&18)\ \ v_{11}v_{41} + v_{12}v_{44} + v_{13}v_{42} + v_{14}v_{43} = 0 \\
&19)\ \ v_{11}v_{21} + v_{12}v_{23} + v_{13}v_{24} + v_{14}v_{22} = 0 \\
&20)\ \ v_{11}v_{31} + v_{12}v_{33} + v_{13}v_{34} + v_{14}v_{32} = 0 \\
&21)\ \ v_{11}v_{41} + v_{12}v_{43} + v_{13}v_{44} + v_{14}v_{42} = 0 \\
&22)\ \ v_{21}^2 + v_{22}v_{23} + v_{22}v_{24} + v_{23}v_{24} = 0 \\
&23)\ \ v_{31}^2 + v_{32}v_{33} + v_{32}v_{34} + v_{33}v_{34} = 0 \\
&24)\ \ v_{41}^2 + v_{42}v_{43} + v_{42}v_{44} + v_{43}v_{44} = 0
\end{aligned}
\tag{A.15}
$$

A.2 Yukawa coupling algebra

Table 3.5 specifies all the allowed operators for the $N = 0$ $SU(5) \times A_4 \times U(1)$ model discussed in the main text. Here we include the full algebra for calculation

of the Yukawa matrices given in the text. All couplings must have zero t_5 charge, respect R-symmetry and be A_4 singlets. In the basis derived in Appendix A.1, we have the triplet product:

$$3_a \times 3_b = 1 + 1' + 1'' + 3_1 + 3_2$$

$$1 = a_1 b_2 + a_2 b_2 + a_3 b_3$$

$$1' = a_1 b_2 + \omega a_2 b_2 + \omega^2 a_3 b_3$$

$$1'' = a_1 b_2 + \omega^2 a_2 b_2 + \omega a_3 b_3$$

$$3_1 = (a_2 b_3,\, a_3 b_1,\, a_1 b_2)^{\mathrm{T}}$$

$$3_2 = (a_3 b_2,\, a_1 b_3,\, a_2 b_1)^{\mathrm{T}}$$

where $3_a = (a_1,\, a_2,\, a_3)^{\mathrm{T}}$ and $3_b = (b_1,\, b_2,\, b_3)^{\mathrm{T}}$.

A.2.1 Top-type quarks

The top-type quarks have four non-vanishing couplings, while the $T \cdot T_3 \cdot H_u \cdot \theta_a \cdot \theta_a$ and $T \cdot T \cdot H_u \cdot \theta_a \cdot \theta_a \cdot \theta_b$ couplings vanishings due to the chosen vacuum expectations: $\langle H_u \rangle = (v, 0, 0)^{\mathrm{T}}$ and $\langle \theta_a \rangle = (a, 0, 0)^{\mathrm{T}}$.

The contribution to the heaviest generation self-interaction is due to the $T_3 \cdot T_3 \cdot H_u \cdot \theta_a$ operator:

$$(1 \times 1) \times (3 \times 3) \to 1 \times 1$$

$$\to 1$$

$$(T_3 \times T_3) \times H_u \times \theta_a \to (T_3 \times T_3) v a$$

We note that this is the lowest order operator in the top-type quarks, so should dominate the hierarchy.

The interaction between the third generation and the lighter two generations

is determined by the $T \cdot T_3 \cdot H_u \cdot \theta_a \cdot \theta_b$ operator:

$$(1 \times 1) \times (3 \times 3) \times 1 \to 1 \times 1 \times 1$$
$$\to 1$$
$$T \times T_3 \times H_u \times \theta_a \times \theta_b \to vab$$

The remaining, first-second generation operators give contributions, in brief:

$$T \times T \times H_u \times \theta_a \times (\theta_b)^2 \to vab^2$$
$$T \times T \times H_u \times (\theta_a)^3 \to va^3$$

These will be subject to Rank Theorem arguments, so that only one of the generations directly gets a mass from the Yukawa interaction. However the remaining generation will gain a mass due to instantons and non-commutative fluxes, as in [35] [33].

A.2.2 Charged leptons

The charged Leptons and Bottom-type quarks come from the same operators in the GUT group, though in this exposition we shall work in terms of the Charged Leptons. The complication for Charged leptons is that the Left-handed doublet is an A_4 triplet, while the right-handed singlets of the weak interaction are singlets of the monodromy group. There are a total of six contributions to the Yukawa matrix, with the third generation right-handed types being generated by two operators.

The operators giving mass to the interactions of the right-handed third generation are dominated by the tree level operator $F \cdot H_d \cdot T_3$, which gives a contribution

as:

$$3 \times 3 \times 1 \to 1 \times 1 \to 1$$
$$F \times H_d \times T_3 \to y_1 \begin{pmatrix} 0 & 0 & v_1 \\ 0 & 0 & v_2 \\ 0 & 0 & v_3 \end{pmatrix}$$

Clearly this should dominated the next order operator, however when we choose a vacuum expectation for the H_d field, we will have contributions from $F \cdot H_d \cdot T_3 \cdot \theta_d$:

$$3 \times 3 \times 3 \times 1 \to 3 \times 3 \times 1 \to 1$$
$$F \times H_d \times \theta_d \times T_3 \to \begin{pmatrix} 0 & 0 & y_2 v_2 d_3 + y_3 v_3 d_2 \\ 0 & 0 & y_2 v_3 d_1 + y_3 v_1 d_3 \\ 0 & 0 & y_2 v_1 d_2 + y_3 v_2 d_1 \end{pmatrix}$$

The generation of Yukawas for the lighter two generations comes, at leading order, from the operators $F \cdot H_d \cdot T \cdot \theta_b$ and $F \cdot H_d \cdot T \cdot \theta_a$:

$$F \times H_d \times T \times \theta_b \to y_4 b \begin{pmatrix} v_1 & v_1 & 0 \\ v_2 & v_2 & 0 \\ v_3 & v_3 & 0 \end{pmatrix}$$
$$F \times H_d \times T \times \theta_a \to y_5 a \begin{pmatrix} 0 & 0 & 0 \\ v_3 & v_3 & 0 \\ v_2 & v_2 & 0 \end{pmatrix},$$

where the vacuum expectations for θ_a and θ_b are as before. The next order of operator take the same form, but with corrections due to the flavon triplet, θ_d.

$$F \times H_d \times T \times \theta_b \times \theta_d \to \begin{pmatrix} y_6 v_2 d_3 + y_7 v_3 d_2 & y_6 v_2 d_3 + y_7 v_3 d_2 & 0 \\ y_6 v_3 d_1 + y_7 v_1 d_3 & y_6 v_3 d_1 + y_7 v_1 d_3 & 0 \\ y_6 v_1 d_2 + y_7 v_2 d_1 & y_6 v_1 d_2 + y_7 v_2 d_1 & 0 \end{pmatrix}$$

$$F \times H_d \times T \times \theta_a \times \theta_d \to a \begin{pmatrix} y_8 v_1 d_1 + y_{10} v_2 d_2 + y_{11} v_3 d_3 & y_8 v_1 d_1 + y_{10} v_2 d_2 + y_{11} v_3 d_3 & 0 \\ y_{12} v_1 d_2 & y_{12} v_1 d_2 & 0 \\ y_9 v_1 d_3 & y_9 v_1 d_3 & 0 \end{pmatrix}$$

A.2.3 Neutrinos

The neutrino sector admits masses of both Dirac and Majorana types. In the A_4 model, the right-handed neutrino is assigned to a matter curve constituting a singlet of the GUT group. However it is a triplet of the A_4 family symmetry, which along with the $SU(2)$ doublet will generate complicated structures under the group algebra.

Dirac Mass Terms

The Dirac mass terms coupling left and right-handed neutrinos comes from a maximum of four operators. The leading order operators are $\theta_c \cdot F \cdot H_u \cdot \theta_b$ and $\theta_c \cdot F \cdot H_u \cdot \theta_a$, where as we have already seen the GUT singlet flavons θ_a and θ_b are used to cancel t_5 charges. The right-handed neutrino is presumed to live on the GUT singlet θ_d .

The first of the operators, $\theta_c \cdot F \cdot H_u \cdot \theta_b$, contributes via two channels:

$$3 \times 3 \times 3 \times 1 \to 3 \times 3_a \times 1 \to 1 \times 1$$
$$\to \begin{pmatrix} c_1 \\ c_2 \\ c_3 \end{pmatrix} \times \begin{pmatrix} F_2 v_3 \\ F_3 v_1 \\ F_1 v_2 \end{pmatrix} \times b \to y_8 b \begin{pmatrix} 0 & 0 & v_2 \\ v_3 & 0 & 0 \\ 0 & v_1 & 0 \end{pmatrix}$$
$$3 \times 3 \times 3 \times 1 \to 3 \times 3_b \times 1 \to 1 \times 1$$
$$\to \begin{pmatrix} c_1 \\ c_2 \\ c_3 \end{pmatrix} \times \begin{pmatrix} F_3 v_2 \\ F_1 v_3 \\ F_2 v_1 \end{pmatrix} \times b \to y_9 b \begin{pmatrix} 0 & v_3 & 0 \\ 0 & 0 & v_1 \\ v_2 & 0 & 0 \end{pmatrix}$$

With the VEV alignments $\langle \theta_a \rangle = (a, 0, 0)^{\mathrm{T}}$ and $\langle H_u \rangle = (v, 0, 0)^{\mathrm{T}}$, we have a total matrix for the op

$$\to \begin{pmatrix} 0 & 0 & 0 \\ 0 & 0 & y_9 b v \\ 0 & y_8 b v & 0 \end{pmatrix}$$

The second leading order operator, $\theta_c \cdot F \cdot H_u \cdot \theta_a$, is more cimplicated due to the presence of four A_4 triplet fields. The simpelst contribution to the operator is:

$$(3 \times 3) \times (3 \times 3) \to 1 \times 1$$
$$\to \begin{pmatrix} y_1(v_1 a_1 + v_2 a_2 + v_3 a_3) & 0 & 0 \\ 0 & y_1(v_1 a_1 + v_2 a_2 + v_3 a_3) & 0 \\ 0 & 0 & y_1(v_1 a_1 + v_2 a_2 + v_3 a_3) \end{pmatrix},$$

which only contributes to the diagonal. This is accompanied by two similar

operators in the way of:

$$
\begin{aligned}
(3\times 3)\times(3\times 3) &\to 1'\times 1'' \\
&\to (c_1F_1+\omega c_2F_2+\omega^2 c_3F_3)\times(v_1a_1+\omega^2 v_2a_2+\omega v_3a_3) \\
&\to y_2\begin{pmatrix} v_1a_1 & 0 & 0 \\ 0 & v_2a_2 & 0 \\ 0 & 0 & v_3a_3 \end{pmatrix} \\
(3\times 3)\times(3\times 3) &\to 1''\times 1' \\
&\to (c_1F_1+\omega^2 c_2F_2+\omega c_3F_3)\times(v_1a_1+\omega v_2a_2+\omega^2 v_3a_3) \\
&\to y_3\begin{pmatrix} v_1a_1 & 0 & 0 \\ 0 & v_2a_2 & 0 \\ 0 & 0 & v_3a_3 \end{pmatrix}.
\end{aligned}
$$

The remaining contribtuions are the complicated four-triplet products. However, upon retaining to our previous vacuum expectation values, these will all vanish, leaving an overall matrix of:

$$
\to \begin{pmatrix} y_0va & 0 & 0 \\ 0 & y_1va & 0 \\ 0 & 0 & y_1va \end{pmatrix}
$$

Where $y_0 = y_1 + y_2 + y_3$ as before. These contributions will produce a large mixing between the second and third generations, however they do not allow for mixing with the first generation.

Corrections from the next order operators will give a weaker mixing with the first generation. These correcting terms are $\theta_c \cdot F \cdot H_u \cdot \theta_d \cdot \theta_b$ and $\theta_c \cdot F \cdot H_u \cdot \theta_d \cdot \theta_a$, though we choose to only consider the first of these two operators, since the flavon θ_a will generate a very complicated structure, hindering computations with little obvious benefit in terms of model building. The $\theta_c \cdot F \cdot H_u \cdot \theta_d \cdot \theta_b$ operator has

of diagonal contributions as:

$$(3 \times 3) \times (3 \times 3) \times 1 \to 3_a \times 3_x \times 1 \to 1$$

$$\theta_c \times F \times H_u \times \theta_d \times \theta_b \to \begin{pmatrix} c_2 F_3 \\ c_3 F_1 \\ c_1 F_2 \end{pmatrix} \times \begin{pmatrix} 0 \\ 0 \\ v d_2 \end{pmatrix} \times b$$

$$\to \begin{pmatrix} 0 & 0 & 0 \\ z_1 v d_2 b & 0 & 0 \\ 0 & 0 & 0 \end{pmatrix}.$$

This is mirrored by similar combinations from the other 3 triplet-triplet combinations allowed by the algebra. Overall, this gives:

$$\to \begin{pmatrix} 0 & z_3 v d_2 b & z_2 v d_3 b \\ z_1 v d_2 b & 0 & 0 \\ z_4 v d_3 b & 0 & 0 \end{pmatrix}.$$

Due to the choice of Higgs vacuum expectation, the diagonal contributions will only correct the first generation mass, giving a contribution to it $\sim v d_1 b$.

Majorana operators

The right-handed neutrinos are also given a mass by Majorana terms. These are as it transpires relatively simple. The leading order term $\theta_c \cdot \theta_c$, gives a diagonal contribtuion:

$$3 \times 3 \to 1$$

$$\theta_c \cdot \theta_c \to M \mathrm{I}_{3\times 3}$$

There may also be corrections to the off diagonal, due to operators such as $\theta_c \cdot \theta_c \cdot \theta_d$. These yield:

$$3 \times 3 \times 3 \to 3 \times 3 \to 1$$
$$\theta_c \times \theta_c \times \theta_d \to \begin{pmatrix} 0 & d_3 & d_2 \\ d_3 & 0 & d_1 \\ d_2 & d_1 & 0 \end{pmatrix},$$

Higher orders of the flavon θ_d are also permitted, but should be suppressed by the coupling.

A.3 Flux mechanism

For completeness, we discribe here in a simple manner the flux mechanism introduced to break symmetries and generate chirality.

- We start with the $U(1)_Y$-flux inside of $SU(5)_{GUT}$.

The **5**'s and **10**'s reside on matter curves $\Sigma_{5_i}, \Sigma_{10_j}$ while are characterised by their defining equations. From the latter, we can deduce the corresponding homologies χ_i following the standard procedure. If we turn on a $U(1)_Y$-flux $\mathcal{F}_Y$, we can determine the flux restrictions on them which are expressed in terms of integers through the "dot product"

$$N_{Y_i} = \mathcal{F}_Y \cdot \chi_i$$

The flux is responsible for the $SU(5)$ breaking down to the Standard Model and this can happen in such a way that the $U(1)_Y$ gauge boson remains massless [15, 18]. On the other hand, flux affects the multiplicities of the SM-representations carrying non-zero $U(1)_Y$-charge.

Thus, on a certain Σ_{5_i} matter curve for example, we have

$$\mathbf{5} \in SU(5) \Rightarrow \begin{cases} n_{(3,1)_{-\frac{1}{3}}} - n_{(\bar{3},1)_{\frac{1}{3}}} &= M_5 \\ n_{(1,2)_{\frac{1}{2}}} - n_{(1,2)_{-\frac{1}{2}}} &= M_5 + N_{Y_i} \end{cases} \tag{A.16}$$

where $N_{Y_i} = \mathcal{F}_Y \cdot \chi_i$ as above. We can arrange for example $M_5 + N_{Y_i} = 0$ to eliminate the doublets or $M_5 = 0$ to eliminate the triplet.

• Let's turn now to the $SU(5) \times S_3$. The S_3 factor is associated to the three roots $t_{1,2,3}$ which can split to a singlet and a doublet

$$\mathbf{1}_{S_3} = t_s = t_1 + t_2 + t_3,\ \mathbf{2}_{S_3} = \{t_1 - t_2,\ t_1 + t_2 - 2t_3\}^T$$

It is convenient to introduce the two new linear combinations

$$t_a = t_1 - t_3,\ t_b = t_2 - t_3$$

and rewrite the doublet as follows

$$\mathbf{2}_{S_3} = \begin{pmatrix} t_a - t_b \\ t_a + t_b \end{pmatrix} \rightarrow \begin{pmatrix} -t_b \\ +t_b \end{pmatrix}_{t_a} \tag{A.17}$$

Under the whole symmetry the $SU(5)_{GUT}$ $\mathbf{10}_{t_i}, i = 1, 2, 3$ representations transform

$$(\mathbf{10}, \mathbf{1}_{S_3}) + (\mathbf{10}, \mathbf{2}_{S_3})$$

Our intention is to turn on fluxes along certain directions. We can think of the following two different choices:

1) We can turn on a flux N_a along t_a[2]. The singlet $(\mathbf{10}, \mathbf{1}_{S_3})$ does not transform under t_a, hence this flux will split the multiplicities as follows

$$\mathbf{10}_{t_i} \Rightarrow \begin{cases} (\mathbf{10}, \mathbf{1}_{S_3}) &= M \\ (\mathbf{10}, \mathbf{2}_{S_3}) &= M + N_a \end{cases} \tag{A.18}$$

This choice will also break the S_3 symmetry to Z_3.

2) Turning on a flux along the singlet direction t_s will preserve S_3 symmetry.

[2]In the old basis we would require $N_{t_1} = \frac{2}{3}N_a$ and $N_{t_2} = N_{t_3} = -\frac{1}{3}N_a$.

The multiplicities now read

$$\mathbf{10}_{t_i} \Rightarrow \begin{cases} (\mathbf{10}, \mathbf{1}_{S_3}) &= M + N_s \\ (\mathbf{10}, \mathbf{2}_{S_3}) &= M \end{cases} \tag{A.19}$$

To get rid of the doublets we choose $M = 0$ while because flux restricts non-trivially on the matter curve, the number of singlets can differ by just choosing $N_s \neq 0$.

A.4 The $b_1 = 0$ constraint

To solve the $b_1 = 0$ constraint we have repeatidly introduced a new section a_0 and assumed factorisation of the involved a_i coefficients. To check the validity of this assumption, we take as an example the $S_3 \times Z_2$ case, where $b_1 = a_2 a_6 + a_3 a_5 = 0$. We note first that the coefficients b_k are holomorphic functions of z, and as such they can be expressed as power series of the form $b_k = b_{k,0} + b_{k,1} z + \cdots$ where $b_{k,m}$ do not depend on z. Hence, the coefficients a_k have a z-independent part

$$a_k = \sum_{m=0} a_{k,m} z^m$$

while the product of two of them can be cast to the form

$$a_l \, a_k = \sum_{p=0} \beta_p \, z^p, \;\; \text{with} \;\; \beta_p = \sum_{n=0}^{p} a_{ln} a_{k,p-n}$$

Clearly the condition $b_1 = a_2 a_6 + a_3 a_5 = 0$ has to be satisfied term-by-term. To this end, at the next to zeroth order we define

$$\lambda = \frac{a_{3,1} a_{5,0} + a_{2,1} a_{6,0}}{a_{5,1} a_{6,0} - a_{5,0} a_{6,1}} \tag{A.20}$$

The requirement $a_{5,1} a_{6,0} \neq a_{5,0} a_{6,1}$ ensures finiteness of λ, while at the same time excludes a relation of the form $a_5 \propto \kappa a_6$ where κ would be a new section.

We can write the expansions for a_2, a_3 as follows

$$\begin{aligned} a_2 &= \lambda a_{5,0} + a_{2,1} z + \mathcal{O}(z^2) \\ a_3 &= -\lambda a_{6,0} + a_{3,1} z + \mathcal{O}(z^2) \end{aligned} \tag{A.21}$$

The $b_1 = 0$ condition is now

$$b_1 = 0 + 0 \, z + \mathcal{O}(z^2)$$

i.e., satified up to second order in z. Hence, locally we can set $z = 0$ and simply

write

$$a_2 = \lambda\, a_5,\ a_3 = -\lambda\, a_6$$

Appendix B

Appendix: chapter 4

B.1 Irreducible representations of D_4

Since we have four weights related, the representation of the 10s of the GUT group will be quadruplets of D_4: $(t_1, t_2, t_3, t_4)^{\mathrm{T}}$. Physically we may take each of these weights to represent a corner of a square (or an equivalent interpretation). These weights will transform in this representation such that the two generators required to describe all possible transformations are equivalent to a rotation about the center of the square of $\frac{\pi}{2}$ and a reflection about a line passing through the center - say the diagonal running between the top right and bottom left corners (see Figure B.1).

The two generators are:

$$a = \begin{pmatrix} 0 & 0 & 0 & 1 \\ 1 & 0 & 0 & 0 \\ 0 & 1 & 0 & 0 \\ 0 & 0 & 1 & 0 \end{pmatrix}, \tag{B.1}$$

$$b = \begin{pmatrix} 1 & 0 & 0 & 0 \\ 0 & 0 & 0 & 1 \\ 0 & 0 & 1 & 0 \\ 0 & 1 & 0 & 0 \end{pmatrix}. \tag{B.2}$$

These generators must obey the general conditions for dihedral groups, which for D_4 are:

$$a^4 = b^2 = \mathrm{I} \tag{B.3}$$

$$b \cdot a \cdot b = a^{-1} \tag{B.4}$$

It is trivial to see that these conditions are obeyed by our generators. In order to obtain the irreducible representations we should put this basis into block-diagonal form, which is achieved by applying the appropriate unitary matrices.

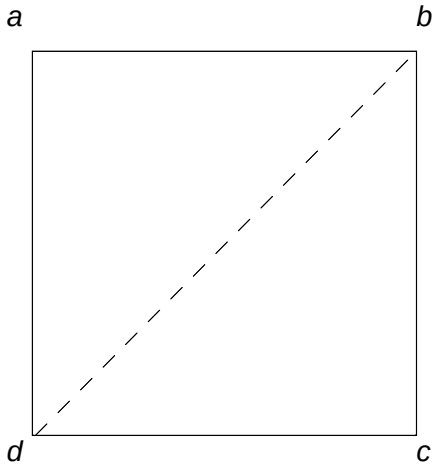

Figure B.1: A physical representation of the symmetry group D_4. The dashed line shows a possible reflection symmetry, while it also has a rotational symmetry if rotated by $\frac{n\pi}{2}$.

Since D_4 is known to have a two-dimensional irreducible representation, we might assume that our four-dimensional case can be taken to a block diagonal form including either a doublet and two singlets or two doublets via a unitary transformation.

If we initially assume two doublets, then we may put some conditions on our unitary matrix:

$$A' = U \cdot A \cdot U^{\mathrm{T}} = \begin{pmatrix} - & - & 0 & 0 \\ - & - & 0 & 0 \\ 0 & 0 & - & - \\ 0 & 0 & - & - \end{pmatrix} \tag{B.5}$$

$$B' = U \cdot B \cdot U^{\mathrm{T}} = \begin{pmatrix} - & - & 0 & 0 \\ - & - & 0 & 0 \\ 0 & 0 & - & - \\ 0 & 0 & - & - \end{pmatrix} \tag{B.6}$$

$$\mathrm{I} = U \cdot U^{\mathrm{T}} \,. \tag{B.7}$$

If we make use of these conditions, there are a number of equivalent solutions for U, one of which is:

$$U = \frac{1}{\sqrt{2}} \begin{pmatrix} 1 & 0 & 1 & 0 \\ 0 & 1 & 0 & 1 \\ 1 & 0 & -1 & 0 \\ 0 & 1 & 0 & -1 \end{pmatrix} . \tag{B.8}$$

This matrix will give a block diagonal form for the generators. Explicitly this is:

$$A' = \begin{pmatrix} 0 & 1 & 0 & 0 \\ 1 & 0 & 0 & 0 \\ 0 & 0 & 0 & -1 \\ 0 & 0 & 1 & 0 \end{pmatrix}, \tag{B.9}$$

$$B' = \begin{pmatrix} 1 & 0 & 0 & 0 \\ 0 & 1 & 0 & 0 \\ 0 & 0 & 1 & 0 \\ 0 & 0 & 0 & -1 \end{pmatrix}, \tag{B.10}$$

$$\begin{pmatrix} t_1 \\ t_2 \\ t_3 \\ t_4 \end{pmatrix} \to \frac{1}{\sqrt{2}} \begin{pmatrix} t_1 + t_3 \\ t_2 + t_4 \\ t_1 - t_3 \\ t_2 - t_4 \end{pmatrix}. \tag{B.11}$$

A cursory examination reveals that the conditions for D_4 are still fulfilled by this new basis, and it would seem that at a minimum we have two doublets of the group. However we shall now examine if one of the doublets decomposes to two singlets.

B.1.1 D_4 representations for GUT group antisymmetric representation

The upper block of the B' generator takes the form of the identity, so we might suppose that the first of our two doublets could decompose into two singlets. Using the same conditions as for the four-dimensional starting point, which can

be enforced on the two-dimensional case, we can find easily that:

$$V = \frac{1}{\sqrt{2}} \begin{pmatrix} 1 & 1 \\ 1 & -1 \end{pmatrix} \tag{B.12}$$

$$A'' = \begin{pmatrix} 1 & 0 \\ 0 & -1 \end{pmatrix} \tag{B.13}$$

$$B'' = \begin{pmatrix} 1 & 0 \\ 0 & 1 \end{pmatrix} \tag{B.14}$$

$$\frac{1}{\sqrt{2}} \begin{pmatrix} t_1 + t_3 \\ t_2 + t_4 \end{pmatrix} \to \frac{1}{2} \begin{pmatrix} t_1 + t_2 + t_3 + t_4 \\ t_1 - t_2 + t_3 - t_4 \end{pmatrix} \tag{B.15}$$

It would seem then in this case that the four-dimensional representation of D_4 can be reduced to a doublet and two singlets forming an irreducible representation. The type of the singlets can be determined by examination of the conjugacy classes of the group, which reveals that the upper singlet is of the type 1_{++}, while the lower is 1_{+-}. Table 2 summarising the representations of the tens.

B.1.2 D_4 representations for GUT group fundamental representation

The roots of the five-curves can also be described in terms of the roots:

$$t_i + t_j = 0 \, \forall i \neq j \, . \tag{B.16}$$

which gives a total of ten solutions, though these will be related by the discrete group. Under the D_4 symmetry, we can see trivially that since the weight t_5 is chosen to be the invariant root, all the roots corresponding to the fives of the form $t_i + t_5$ will transform separately to the $i, j \neq 5$ roots. In fact, these will form a doublet and two singlets: 1_{++} and 1_{+-}.

The remaining six roots of P_5 can be constructed into a sextet:

$$R_6 = \begin{pmatrix} t_1 + t_3 \\ t_2 + t_4 \\ t_1 + t_2 \\ t_3 + t_4 \\ t_1 + t_4 \\ t_2 + t_3 \end{pmatrix} . \tag{B.17}$$

By construction, we have arranged that the array manifestly has block diagonal generators, A and B, such that the first two lines have generators:

$$A = \begin{pmatrix} 0 & 1 \\ 1 & 0 \end{pmatrix} \quad B = \begin{pmatrix} 1 & 0 \\ 0 & 1 \end{pmatrix} . \tag{B.18}$$

We can again refer to the previous results to see that this reduces to two singlets: 1_{++} and 1_{+-}.

The remaining quadruplet has generators:

$$A = \begin{pmatrix} 0 & 0 & 1 & 0 \\ 0 & 0 & 0 & 1 \\ 0 & 1 & 0 & 0 \\ 1 & 0 & 0 & 0 \end{pmatrix} \quad B = \begin{pmatrix} 0 & 0 & 0 & 1 \\ 0 & 0 & 1 & 0 \\ 0 & 1 & 0 & 0 \\ 1 & 0 & 0 & 0 \end{pmatrix} , \tag{B.19}$$

which we can block diagonalise using the unitary matrix:

$$U = \frac{1}{\sqrt{2}} \begin{pmatrix} 1 & 1 & 0 & 0 \\ 0 & 0 & 1 & 1 \\ -1 & 1 & 0 & 0 \\ 0 & 0 & 1 & -1 \end{pmatrix} . \tag{B.20}$$

This gives two blocks, which are distiniguished principally by their A generators:

$$A' = \begin{pmatrix} 0 & 1 & 0 & 0 \\ 1 & 0 & 0 & 0 \\ 0 & 0 & 0 & -1 \\ 0 & 0 & 1 & 0 \end{pmatrix} \quad B' = \begin{pmatrix} 0 & 1 & 0 & 0 \\ 1 & 0 & 0 & 0 \\ 0 & 0 & 0 & 1 \\ 0 & 0 & 1 & 0 \end{pmatrix} . \tag{B.21}$$

The upper block can be further diagonalised to yield two singlets, using the unitary matrix:

$$V_u = \frac{1}{\sqrt{2}} \begin{pmatrix} 1 & 1 \\ 1 & -1 \end{pmatrix} , \tag{B.22}$$

$$A''_u = B''_u = \begin{pmatrix} 1 & 0 \\ 0 & 1 \end{pmatrix} , \tag{B.23}$$

which, after consulting a character table for the group, returns two singlets of the type 1_{++}.

The lower block can be rotated into the usual doublet basis by the matrix:

$$V_d = \frac{1}{\sqrt{2}} \begin{pmatrix} 1 & 1 \\ -1 & 1 \end{pmatrix} . \tag{B.24}$$

The full set of states arising from the five-curves is given in Table 4.4.

B.1.3 D_4 representations for GUT group singlet spectrum

The singlets in F-theory correspond to differences of weights of the perpendicular group:

$$\pm(t_i - t_j) \;\; \forall i \neq j \, .$$

As such in the case of an $SU(5)$ GUT group we have a total of 20 possible singlets allowed on the GUT surface. Note that four of the singlets have no weight. In the

case where four of the roots are related by a D_4, the singlets can be considered to split into two different sets:

$$\pm(t_i - t_j) = 0\,,$$
$$\pm(t_i - t_5) = 0\,,$$
$$i \neq j\,.$$

This is obvious given that we consider t_5 not to transform with the D_4 action.

$\pm(t_i - t_5)$

In the event $\mathbf{t_i - t_5}$ is considered we can essentially ignore the t_5 weight, since it doesn't transform. Then we can immediately refer to the known result for decomposing the 10s of the GUT group:

$$\begin{pmatrix} t_1 - t_5 \\ t_2 - t_5 \\ t_3 - t_5 \\ t_4 - t_5 \end{pmatrix} \rightarrow 1^{-t_5}_{++} + 1^{-t_5}_{+-} + 2^{-t_5}$$

The diagonalising matrix is:

$$U = \frac{1}{2}\begin{pmatrix} 1 & 1 & 1 & 1 \\ 1 & -1 & 1 & -1 \\ \sqrt{2} & 0 & -\sqrt{2} & 0 \\ 0 & \sqrt{2} & 0 & -\sqrt{2} \end{pmatrix}$$

For $\mathbf{t_5 - t_i}$, we expect a similar decomposition by symmetry. However, if we decompose to the same generators as the $\mathbf{t_i - t_5}$ case, then the t_i charges are negative.

$\pm(t_i - t_j)$

The t_5-free singlet combinations fill out 12 combinations. In the "traditional " interpretation of a monodromy group in F-theory, these would all be weightless. I.e. because we identify t_i (with $i = 1, 2, 3, 4$) under our monodromy group action they would all have $t_i - t_i = 0$.

However, in the case that we have a non-Abelian group such as D_4 the weights are not directly identified. In this case the irreducible representations appear to be important. We can treat these in a few "clusters", which will simplify block diagonalising. Firstly:

$$\begin{pmatrix} t_1 - t_3 \\ t_2 - t_4 \\ t_3 - t_1 \\ t_4 - t_2 \end{pmatrix} \rightarrow \begin{pmatrix} t_4 - t_2 \\ t_1 - t_3 \\ t_1 + t_3 \\ t_2 + t_4 \end{pmatrix}$$

The upper-block is manifestly a doublet of the type already encountered in other part of the spectrum, while the lower part can be rotate into a basis with a trivial singlet and a non trivial singlet: 1_{++} and 1_{+-}.

The remaining weight combinations have a symmetry under exchange of $i \rightarrow -i$ that allows them to be decomposed into two sets:

$$\pm \begin{pmatrix} t_1 - t_2 \\ t_2 - t_3 \\ t_3 - t_4 \\ t_4 - t_1 \end{pmatrix} \tag{B.25}$$

D_4 rep.	t_5	t_i	Type
1_{++}	-1	$t_1+t_2+t_3+t_4$	θ_α
1_{+-}	-1	$t_1-t_2+t_3-t_4$	θ_β
2	-1	$\begin{pmatrix} t_4-t_2 \\ t_1-t_3 \end{pmatrix}$	θ_γ
1_{++}	$+1$	$-t_1-t_2-t_3-t_4$	θ'_α
1_{+-}	$+1$	$-t_1+t_2-t_3+t_4$	θ'_β
2	$+1$	$\begin{pmatrix} t_2-t_4 \\ t_3-t_1 \end{pmatrix}$	θ'_γ
1_{++}	0	$t_1+t_2+t_3+t_4$	θ_1
1_{+-}	0	$t_1-t_2+t_3-t_4$	θ_2
1_{+-}	0	$-t_1+t_2-t_3+t_4$	θ_2
1_{--}	0	$-t_1-t_2-t_3-t_4$	θ_3
2	0	$\begin{pmatrix} t_2-t_4 \\ t_3-t_1 \end{pmatrix}$	θ_4
1_{+-}	0	$t_1-t_2+t_3-t_4$	θ_2
1_{--}	0	$t_1+t_2+t_3+t_4$	θ_3
2	0	$\begin{pmatrix} t_4-t_2 \\ t_1-t_3 \end{pmatrix}$	θ_4

Table B.1: The complete list of the irreducible representations of D_4 obtained by block diagonalizing the singlets of the GUT group. Each of these GUT singlets is duly labeled θ_i to classify them, since some appear to be in some sense degenerate.

These can be decomposed into a doublet and two singlets by:

$$U = \frac{1}{2}\begin{pmatrix} 0 & \sqrt{2} & 0 & -\sqrt{2} \\ -\sqrt{2} & 0 & \sqrt{2} & 0 \\ 1 & -1 & 1 & -1 \\ 1 & 1 & 1 & 1 \end{pmatrix} \tag{B.26}$$

The interesting result here is that the singlets are of the types: 1_{+-} and 1_{--}, which is unique to our singlet sector. A complete list of the singlet spectrum is given in Table B.1

B.1.4 Basic galois theory

According to Galois theory if $\mathcal{L}$ is the splitting field of a separable polynomial $P \in \mathcal{F}[x]$, then the Galois group $Gal(\mathcal{L}/\mathcal{F})$ is associated with the permutations of the roots of P. Let P has degree n. Then in $\mathcal{L}[x]$ we can write the P as the

product

$$P(x) = c(x - t_1) \dots (x - t_n) \tag{B.27}$$

where $c \neq 0$ and the roots $t_1, \dots t_n \in \mathcal{L}$ are distinct. In this situation we get a map

$$Gal(\mathcal{L}/\mathcal{F}) \to S_n$$

which is a one-to-one group homomorphism. Important rôle in the determination of the Galois group of a polynomial plays the discriminant, which is a symmetric function of the roots t_i. The discriminant $\Delta(P) \in \mathcal{F}$ of a (monic) polynomial $P \in \mathcal{F}[x]$ with $P = (x - t_1) \dots (x - t_n)$ in a splitting field $\mathcal{L}$ of P is

$$\Delta(P) = \prod_{i<j} (t_i - t_j)^2. \tag{B.28}$$

Another useful object is the square root of the discriminant:

$$\sqrt{\Delta(P)} = \prod_{i<j} (t_i - t_j) \quad \in \mathcal{L}. \tag{B.29}$$

Note that while Δ is uniquely determined by P, the above square root depends on how the roots are labeled. It is obvious that the $\sqrt{\Delta(P)}$ controls the relation between $Gal(\mathcal{L}/\mathcal{F})$ and the alternating group $A_n \subset S_n$. More precisely, the image of $Gal(\mathcal{L}/\mathcal{F})$ lies in A_n if and only if $\sqrt{\Delta(P)} \in \mathcal{F}$ (i.e., $\Delta(P)$ is the square of an element of $\mathcal{F}$). In our case we deal with a fourth degree polynomial corresponding to the spectral surface C_4, hence our starting point is S_4 and A_4.

To reduce further the S_4/A_4 down to their subgroups (D_4, Z_4 and V_4) we need the service of the so called *resolvent cubic* of P

$$R_3 = (x - x_1)(x - x_2)(x - x_3) \tag{B.30}$$

where now the x_i's are symmetric polynomials of the roots with

$\Delta(P)$	R_3 in $\mathcal{F}$	$Gal(\mathcal{L}/\mathcal{F})$
$\neq \square$	irreducible	S_4
$= \square$	irreducible	A_4
$\neq \square$	reducible	D_4 or Z_4
$= \square$	reducible	V_4

Table B.2: The Galois groups for the various cases of the discriminant and the reducibility of the cubic resolvent R_3.

$$x_1 = t_1t_2 + t_3t_4, \quad x_2 = t_1t_3 + t_2t_4, \quad x_3 = t_3t_2 + t_1t_4 \tag{B.31}$$

A permutation of the indices carries x_1 to one of the three polynomials x_i, i=1,2,3. Since S_4 has order 24, the stabilizer of x_1 is of order 8, it is one of the three dihedral groups D_4. Also, $\Delta(R_3) = \Delta(P)$, so when P is separable so is R_3. Using the discriminant and the reducibility of the cubic resolvent we can correlate the groups S_4, D_4, Z_4, A_4 and V_4 with the Galois group of a quartic irreducible polynomial. The analysis above with respect to $\Delta(P)$ and R_3 is summarized in Table B.2.

B.2 Flatness conditions

In order to obtain a realistic model we use the SU(5) singlets which acquire VEV's . Any such VEV's should be consistent with F and D flatness conditions. Singlets spectrum in F-Theory is described by the equation

$$\prod_{i\neq j}(t_i - t_j) = 0$$

where the product is the discriminant of the spectral cover polynomial. By calculating the discriminant using the $b_1 = 0$ constraint as well as the splitting options we end up with the following equation

$$\begin{aligned}
&a_0 a_2^3 a_7^2 \left(-a_7^3\kappa - a_2 a_7^2\lambda\mu^2 + 2a_0 a_2^3\mu^4 + a_2 a_7^2\mu\right)^2 \\
&\left(256a_0^2 a_7^3 a_2^2\kappa^3 + 128a_0 a_7^4 a_2\kappa^2\lambda^2 + 144a_0^2 a_7^2 a_2^3\kappa^2\lambda\mu^2 + 27a_0^3 a_2^5\kappa^2\mu^4 + 192a_0^2 a_7^2 a_2^3\kappa^2\mu + 16a_7^5\kappa\lambda^4\right. \\
&+4a_0 a_7^3 a_2^2\kappa\lambda^3\mu^2 - 18a_0^2 a_7 a_2^4\kappa\lambda\mu^3 - 144a_0 a_7^3 a_2^2\kappa\lambda - 6a_0^2 a_7 a_2^4\kappa\mu^2 - 4a_7^4 a_2\lambda^3 - a_0 a_7^2 a_2^3\lambda^2\mu^2 \\
&\left.+18a_0 a_7^2 a_2^3\lambda\mu - 80a_0 a_7^3 a_2^2\kappa\lambda^2\mu + 4a_0^2 a_2^5\mu^3 + 27a_0 a_7^2 a_2^3\right) = 0
\end{aligned} \tag{B.32}$$

As we can see we have nine factors, four of which correspond to a negative parity (the a_0 factor, the double factor $\left(-a_7^3\kappa - a_2 a_7^2\lambda\mu^2 + 2a_0 a_2^3\mu^4 + a_2 a_7^2\mu\right)$ and $256a_0^2 a_7^3 a_2^2\kappa^3 + \dots$).

B.2.1 *F*-flatness

In general the Superpotential for the massless singlet fields ($\theta_{ij} \equiv \theta_{t_i - t_j}$) is given by

$$\mathcal{W} = \mu_{ijk}\theta_{ij}\theta_{jk}\theta_{ki} \tag{B.33}$$

and the F-flatness conditions are given by :

$$\frac{\partial\mathcal{W}}{\partial\theta_{ij}} = \mu_{ijk}\theta_{jk}\theta_{ki} = 0. \tag{B.34}$$

$$\begin{aligned}\mathcal{W}_\theta = &\mu_1\theta_1\theta_\alpha\theta'_\alpha + \mu_2\theta_1\theta_\beta\theta'_\beta + \mu_3\theta_1\theta_\gamma\theta'_\gamma + \mu_4\theta_3\theta_\gamma\theta'_\gamma \\ &+ \lambda_1\theta_4\theta_\gamma\theta'_\alpha + \lambda_2\theta_4\theta'_\gamma\theta_\alpha + \lambda_3\theta'_4\theta'_\gamma\theta_\beta + \lambda_4\theta'_4\theta_\gamma\theta'_\beta \\ &+ \lambda_5\theta_2\theta_\alpha\theta'_\beta + \lambda_6\theta_2\theta'_\alpha\theta_\beta + \lambda_7\theta_2\theta_4\theta'_4 \end{aligned} \tag{B.35}$$

where all the singlets have positive parity except the θ_β, θ'_β, θ_2 and θ'_4. Here with θ_4 we mean the θ_a (θ'_4*corresponds to* ν_R).

Minimization of the superpotential leads to the following equations:

$$\begin{aligned}
\frac{\partial\mathcal{W}}{\partial\theta_1} &= \mu_1\theta_\alpha\theta'_\alpha + \mu_2\theta_\beta\theta'_\beta + \mu_3\theta_\gamma\theta'_\gamma = 0 \\
\frac{\partial\mathcal{W}}{\partial\theta_2} &= \lambda_5\theta_\alpha\theta'_\beta + \lambda_5\theta'_\alpha\theta_\beta + \lambda_7\theta_4\theta'_4 = 0 \\
\frac{\partial\mathcal{W}}{\partial\theta_3} &= \mu_4\theta_\gamma\theta'_\gamma = 0 \\
\frac{\partial\mathcal{W}}{\partial\theta_4} &= \lambda_1\theta_\gamma\theta'_\alpha + \lambda_2\theta'_\gamma\theta'_\alpha + \lambda_7\theta_2\theta'_4 = 0 \\
\frac{\partial\mathcal{W}}{\partial\theta'_4} &= \lambda_3\theta'_\gamma\theta_\beta + \lambda_4\theta_\gamma\theta'_\beta + \lambda_7\theta_2\theta_4 = 0 \\
\frac{\partial\mathcal{W}}{\partial\theta_\alpha} &= \mu_1\theta_1\theta'_\alpha + \lambda_2\theta_4\theta'_\gamma + \lambda_5\theta_2\theta'_\beta = 0 \\
\frac{\partial\mathcal{W}}{\partial\theta'_a} &= \mu_1\theta_1\theta_\alpha + \lambda_1\theta_4\theta_\gamma + \lambda_6\theta_\beta\theta_2 = 0 \\
\frac{\partial\mathcal{W}}{\partial\theta_\beta} &= \mu_2\theta_1\theta'_\beta + \lambda_3\theta'_4\theta'_\gamma + \lambda_6\theta_2\theta'_\alpha = 0 \\
\frac{\partial\mathcal{W}}{\partial\theta'_\beta} &= \mu_2\theta_1\theta_\beta + \lambda_4\theta'_4\theta_\gamma + \lambda_5\theta_2\theta_\alpha = 0 \\
\frac{\partial\mathcal{W}}{\partial\theta_\gamma} &= \mu_3\theta_1\theta'_\gamma + \mu_4\theta_3\theta'_\gamma + \lambda_1\theta_4\theta'_\alpha + \lambda_4\theta'_4\theta'_\beta = 0 \\
\frac{\partial\mathcal{W}}{\partial\theta'_\gamma} &= \mu_3\theta_1\theta_\gamma + \mu_4\theta_3\theta_\gamma + \lambda_2\theta_4\theta_\alpha + \lambda_3\theta'_4\theta_b = 0
\end{aligned}$$

As we can see we have a system of 11-equations. Solving the system with the requirements $\langle\theta'_4\rangle = 0 \rightarrow \langle\nu_1\rangle = \langle\nu_2\rangle = 0$ and $\langle\theta_2\rangle = 0$ we end up with a number of solutions. The most palatable solution gives the following relations between the VEV's,

$$\langle\theta_\alpha\rangle^2 \equiv \alpha^2 = 2\frac{\lambda_1\mu_3}{\lambda_2\mu_1}\gamma_1\gamma_2 \tag{B.36}$$

$$a_1^2 = \frac{\mu_1\mu_3}{2\lambda_1\lambda_2}\frac{\gamma_1\langle\theta_1\rangle}{\gamma_2} \quad and \quad a_2^2 = \frac{\mu_1\mu_3}{2\lambda_1\lambda_2}\frac{\gamma_2\langle\theta_1\rangle}{\gamma_1} \tag{B.37}$$

$$\langle\theta_3\rangle = \frac{\mu_2}{\mu_3}\langle\theta_1\rangle \tag{B.38}$$

with all the other singlet VEV's equal to zero, except the $\langle\theta_\beta\rangle$ which will be designated by D-flatness condition. Notice that equation (B.36) gives $\alpha^2 = 2\gamma_1\gamma_2$ for $\lambda_1\mu_3 = \lambda_2\mu_1$. We should also observe that combining the equations in (B.37) we have $a_1\gamma_2 = \pm a_2\gamma_1$.

B.2.2 D-flatness

The D-flatness condition for an anomalous $U(1)$ is given by

$$\sum_{i,j} Q_{ij}^A \left(|\langle\theta_{ij}\rangle|^2 - |\langle\theta_{ji}\rangle|^2\right) = -\frac{TrQ^A}{192\pi^2}g_s^2M_s^2 \tag{B.39}$$

where Q_{ij}^A are the singlet charges and the trace TrQ^A is over all singlet and non-singlet states. The D-flatness conditions must be checked for each the $U(1)'s$. In our case we have a D_4 symmetry and one $U(1)$. The trace in the $SU(5)$ case has the general form

$$TrQ^A = 5\sum n_{ij}(t_i - t_j) + 10\sum n_k t_k + \sum m_{ij}(t_i - t_j) \tag{B.40}$$

The coefficients n_{ij}, n_k and m_{ij} corresponds to the $M_{U(1)}$ multiplicities. Only the curves with a t_5 charge contributes to the relation since the $t_{l=1,2,3,4}$ are subject to the D_4 rules. Using this information, the computation of the trace gives:

$$TrQ = (m'_\alpha + m'_\beta + 2m'_\gamma - m_\alpha - m_\beta - 2m_\gamma - 5)t_5 \tag{B.41}$$

where the m_i, m'_i are the (unknown) multiplicities of the singlets θ_i and θ'_i, with

$i = \alpha, \beta, \gamma$. Inserting the trace in the relation (B.39) we end up with the following equation

$$|\theta'_\alpha|^2 - |\theta_\alpha|^2 + |\theta'_\beta|^2 - |\theta_\beta|^2 + |\theta'_\gamma|^2 - |\theta_\gamma|^2 = (5 - \tilde{m}_\alpha - \tilde{m}_\beta - 2\tilde{m}_\gamma)\mathcal{X} \quad \text{(B.42)}$$

where $\tilde{m}_i \equiv m'_i - m_i$ and $\mathcal{X} = \frac{g_s^2 M_s^2}{192\pi^2}$. By using the results of the F-flatness conditions the last relation takes the form

$$\alpha^2 + \beta^2 + 2\gamma_1\gamma_2 = (\tilde{m}_\alpha + \tilde{m}_\beta + 2\tilde{m}_\gamma - 5)\mathcal{X} \quad \text{(B.43)}$$

which gives an estimation for the β VEV ,

$$\beta^2 = \tilde{\mathcal{M}}\mathcal{X} - \left(1 + \frac{\mu_1\lambda_2}{\mu_3\lambda_1}\right)\alpha^2 \approx \tilde{\mathcal{M}}\mathcal{X} - 2\alpha^2 \quad \text{(B.44)}$$

where we make use of the equation (B.36) and the approach $\lambda_1\mu_3 \approx \lambda_2\mu_1$ in the last step. Finally for shorthand we have set $\tilde{\mathcal{M}} \equiv \tilde{m}_\alpha + \tilde{m}_\beta + 2\tilde{m}_\gamma - 5$. Checking equation (B.44) we see that $\tilde{M}$ is a positive number and as a result $\tilde{m}_\alpha + \tilde{m}_\beta + 2\tilde{m}_\gamma > 5$.

Summarizing, equations (B.36,B.37,B.38) and (B.44) show us that controlling the scale of $\gamma_{1,2}$ and $\langle\theta_1\rangle$ we can have an estimation of the scale of all the singlets participating in the model.

B.3 An alternative polynomial

Another resolvent cubic that shares its discriminant with the quartic polynomial can be built using the following three roots:

$$z_1 = (t_1 + t_2)(t_3 + t_4), \quad z_2 = (t_1 + t_3)(t_2 + t_4), \quad z_3 = (t_1 + t_4)(t_2 + t_3) \quad \text{(B.45)}$$

with the two symmetric polynomial set-ups related as follows :

$$z_1 = x_2 + x_3, \quad z_2 = x_1 + x_3, \quad z_3 = x_1 + x_2. \tag{B.46}$$

To see that the two discriminants coincide, note that the differences for each set of symmetric polynomials are related as:

$$x_i - x_j = -(z_i - z_j) \tag{B.47}$$

and since the discriminant can be expressed as products of these difference it is trivial to see that the two must coincide:

$$\Delta = \prod_{i \neq j} (z_i - z_j) = \prod_{i \neq j} (x_i - x_j)\,. \tag{B.48}$$

In this case the cubic resolvent polynomial has the form:

$$g(s) = a_5^{-3/2}[(a_5 s)^3 - 2a_3(a_5 s)^2 + (a_3^2 + a_2 a_4 - 4a_1 a_5)a_5 s + (a_2^2 a_5 - a_2 a_3 a_4 + a_1 a_4^2)]\,. \tag{B.49}$$

And we can see that by setting $g(0) = 0$ we obtain the following condition:

$$a_2^2 a_5 - a_2 a_3 a_4 + a_1 a_4^2 = 0\,. \tag{B.50}$$

Substituting the above condition in the equation of the fives the result is zero, which is not a surprising result since the three symmetric functions of the roots, z_i, can be used to rewrite the equation of the GUT fives as:

$$P_5 = \prod_{i,j} (t_i + t_j) = z_1 z_2 z_3 \prod_i^4 (t_i + t_5) = -g(0) \prod_i^4 (t_i + t_5). \tag{B.51}$$

If we substitute this new condition into the discriminant we find that it now reads:

$$\Delta \propto 4\,(4a_1 a_5 - a_2 a_4)\left(a_3^2 + a_2 a_4 - 4a_1 a_5\right)^2 \tag{B.52}$$

Combined with the constraint for tracelessness of the GUT group[1], $b_1 = 0$, the condition becomes:

$$g(0) = 0 \to a_7 a_2^2 + a_3 a_6 a_2 = a_0 a_1 a_6^2 \,. \tag{B.53}$$

Correspondingly the fives of the GUT group now have an equation that factors into only two parentheses,

$$P_5 = \left(a_7 a_2^2 + a_3 a_6 a_2 - a_0 a_1 a_6^2\right)\left(a_3 a_6^2 + a_7\left(a_2 a_6 + a_1 a_7\right)\right) \to P_a P_b \,, \tag{B.54}$$

where, the first factor vanishes due to the constraint and corresponds to the roots $z_1 z_2 z_3 = 0$.

In this relation it is clear that the trivial condition $g(0) = 0$ automatically leads to $P_5 = 0$. So we need a more general factorisation for the cubic polynomial. In general a cubic is reducible if it can be factorised as a linear and a quadratic part.

B.4 Matter parity from geometric symmetry

One of the major issues in supersymmetric GUT model building is the appearance of dimension four violating operators leading to proton decay at unacceptable rates. The problem is usually solved by introducing the concept of R-parity which is a suitable discrete symmetry preventing the appearance of baryon and lepton four-dimensional non-conserving operators in the Lagrangian. R-parity is equivalent to a Z_2 symmetry, which is the simplest possibility. However, other discrete symmetries in more involved models may be useful as well. The implementation of such a scenario in String and F-theory models in particular has been the subject of considerable recent work.

In our present approach we have constantly dealt with non-Abelian discrete symmetries which were used to organise the fermion mass hierarchies and in par-

[1] $\{a_4 \to a_0 a_6, a_5 \to -a_0 a_7\}$

ticular the neutrino mass textures aiming to reconcile the current experimental data. At the same time, they are also expected to suppress flavour changing operators. Phenomenological investigations however, have shown that additional discrete symmetries may account for the rare flavour decays in a more elegant manner. This fact could be used as an inspiration to search for discrete symmetries of different origin in the present constructions.

Indeed, a thorough study of the effective F-theory models the last few years has uncovered a plentiful source of such symmetries which may arise from the internal geometry and the fluxes. We will present such a mechanism (firstly proposed in [58] and implemented on specific GUT constructions in [55]) in what follows.

In constructing models in F-theory the relevant data originate form the geometric properties of the Calabi-Yau four-fold X and the G_4-flux. Therefore, if we wish to obtain a Z_2 (or some other discrete) symmetry of geometric origin, in principle we need to impose it on the (X, G_4) pair. It is not easy to prove the existence of such symmetries globally. Nevertheless for the local model constructions we are interested in it is sufficient to work out such a symmetry in the local geometry around the GUT divisor S_{GUT}, which in our case corresponds to an $SU(5)$ singularity. This incorporates the concept of the spectral surface.

Indeed, in the weakly coupled limit of F-theory, the supersymmetric configurations of the effective theory can be described in terms of the adjoint scalars and the gauge fields. A convenient simplification is based on the spectral cover description where the Higgs is replaced by its eigenvalues and the bundle by the corresponding eigenvectors. Since our primary interest is the reduction of E_8 to $SU(5) \times SU(5)_\perp$ we focus in $SU(5)$ group where the spectral surface is described by the equation:

$$\sum_{k=0}^{5} b_k s^{5-k} = 0\,. \tag{B.55}$$

We consider the GUT divisor S_{GUT} and three open patches S, T, U covering S_{GUT}; we define a phase $\phi_N = \frac{2\pi}{N}$ and a map σ_N such that:

$$\sigma_N : [S : T : U] \ \rightarrow \ [e^{i\phi_N} S : e^{i\phi_N} T : U] \,. \tag{B.56}$$

For a Z_2 symmetry discussed in [58] one requires a Z_2 background configuration, with a Z_2 action so that the mapping is:

$$\sigma_2 : [S : T : U] \rightarrow [-S : -T : U] \text{ or } [S : T : -U] \,. \tag{B.57}$$

To see if this is a symmetry of the local geometry for a given divisor, we take local coordinates for the three trivialization patches. These can be defined as $(t_1, u_1) = (T/S, U/S)$, $(s_2, u_2) = (S/T, U/T)$ and $(s_3, t_3) = (S/U, T/U)$. Assuming that $\sigma_2(p)$, is the map of a point p under σ_2 transformation, the corresponding local coordinates are mapped according to

$$\begin{aligned} (t_1, u_1, \xi_s)|_{\sigma_2(p)} &= (t_1, -u_1, -\xi_s)|_p \\ (s_2, u_2, \xi_t)|_{\sigma_2(p)} &= (s_2, -u_2, -\xi_t)|_p \\ (s_3, t_3, \xi_u)|_{\sigma_2(p)} &= (-s_3, -t_3, \xi_u)|_p \end{aligned} \tag{B.58}$$

This is an $SU(3)$ rotation on the three complex coordinates which acts on the spinors in the same way. Hence, starting from a Z_2 symmetry of the three-fold we conclude that a Z_2 transformation is also induced on the spinors. The required discrete symmetry must be a symmetry of the local geometry. This can happen if the defining equation of the spectral surface is left invariant under the corresponding discrete transformation. Consequently we expect non-trivial constraints on the polynomial coefficients b_k which carry the information of local geometry.

In order to extract these constraints we focus on a single trivialization patch and take s to be the coordinate along the fiber. Under the mapping of points

$p \to \sigma(p)$ we consider the phase transformation

$$s(\sigma(p)) = s(p)\, e^{i\phi}, \;\; b_k(\sigma(p)) \;=\; b_k(p)\, e^{i(\chi-(6-k)\phi)}\,. \tag{B.59}$$

Under this action, each term in the spectral cover equation transforms the same way,

$$b_k s^{5-k} \to e^{i(\chi-\phi)} b_k s^{5-k}\,. \tag{B.60}$$

We observe that the spectral surface equation admits a continuous symmetry. A trivial solution arises for $\phi = 0$ where all b_k pick up a common phase:

$$s \to s,\; b_k \to b_k\, e^{i\chi} \tag{B.61}$$

In the general case however, the non-trivial solution accommodates a Z_N symmetry for

$$\phi = \frac{2\pi}{N} \tag{B.62}$$

Thus, for $N = 2$, we have $\phi = \pi$ and the trasformation reduces to

$$s \to -s,\; b_k \to (-1)^k e^{i\chi}\, b_k \tag{B.63}$$

B.4.1 Extension to $C_5 \to C_4 \times C_1$

In the event that the spectral cover is taken to split down to products of factors, for example $C_5 \to C_4 \times C_1$, this symmetry is conveyed to the matter curves by consistency with the original spectral cover equation. It is trivial to determine that the coefficients of C_5 are related to the $C_4 \times C_1$ coefficients by:

$$b_k = \sum_{n+m=12-k} a_i a_j \tag{B.64}$$

where $i \neq j$. As such, we can directly write that if

$$a_n \to \mathrm{e}^{i\psi_n} \mathrm{e}^{i(3-n)\phi} a_n \tag{B.65}$$

a_n	$N=2$	$N=3$	$N=4$	$N=5$
a_1	$-$	α^2	β^2	γ^2
a_2	$+$	α	β	γ
a_3	$-$	1	1	1
a_4	$+$	α^2	β^3	γ^4
a_5	$-$	α	β^2	γ^3
a_6	$+$	1	β	γ^2
a_7	$-$	α^2	1	γ

Table B.3: Z_N parities coming from geometric symmetry of the spectral cover. In the case of $C_5 \to C_4 \times C_1$, a general phase relates the parities of $a_{1,2,3,4,5}$, such that if we flip the parity of a_1 all the other a_i in this chain must also change. A similar rule applies to $a_{6,7}$.

so that the product $a_n a_m$ picks up a total phase:

$$a_n a_m \to \mathrm{e}^{i(\psi_n+\psi_m)}\mathrm{e}^{i(6-n-m)\phi} a_n a_m = \mathrm{e}^{i(\psi_n+\psi_m)}\mathrm{e}^{-i(6-k)\phi} a_n a_m \tag{B.66}$$

then provided the phases of the a_n coefficients satisfy $\chi = \psi_n + \psi_m$, the symmetry is handed down to the split spectral cover. This is trival to enforce since the phases are independent of the index k. It can also be demonstrated that this consistency requires the coefficients of $C_4 \times C_1$ to have phases in two cycles: $\psi_i = \psi_1 = \psi_2 = \cdots = \psi_5$ and $\psi_j = \psi_6 = \psi_7$, in order to be consistent with the C_5 phase.

Table B.3 shows some examples of possible parities we might assign to the $C_4 \times C_1$ coefficients. In most cases, the minimal $N = 2$ scenario will be the most appealing and manageable choice, though this mechanism is not confined to it.

Appendix C

Appendix: chapter 6

C.1 Semi-local F-theory constructions: R-Parity violating couplings for the various monodromies

In this Appendix we examine the semi-local F-theory models in detail in order to demonstrate that RPV couplings are generic or at least common. To this end we note that:

1. We want models with matter being distributed on different curves. This setup we call multi-curve models, in contrast to the models presented section 4 of [49] and usually considered in other papers that compute Yukawa couplings.

2. The models defined in this framework "choose" the H_u assignment for us, since a tree-level, renormalizable, perturbative top-Yukawa requires the existence of the coupling

$$\mathbf{10}_a\mathbf{10}_a\mathbf{5}_b \tag{C.1}$$

such that the perpendicular charges cancel out. As such, all the models listed above will have a definite assignment for the curve supporting H_u, and we do not assign the remaining MSSM states to curves, i.e. all the remaining $\mathbf{5}$ curves will be called $\overline{\mathbf{5}}_a$, making clear that they are either supporting some $\overline{\mathbf{5}}_M$ or H_d. Furthermore, we will refer to the $\mathbf{10}$ curve

containing the top quark as $\mathbf{10}_M$.

3. The indication for existence of tree-level, renormalizable, perturbative RPV is given by the fact we can find two couplings of the form

$$\mathbf{10}_a\overline{\mathbf{5}}_b\overline{\mathbf{5}}_c \tag{C.2}$$

$$\mathbf{10}_d\overline{\mathbf{5}}_e\overline{\mathbf{5}}_f \tag{C.3}$$

for $(b,c) \neq (e,f)$, and a,d unconstrained. This happens as H_d cannot be both supported in one of the $\overline{\mathbf{5}}_b$, $\overline{\mathbf{5}}_c$ and at the same in one of the $\overline{\mathbf{5}}_e$, $\overline{\mathbf{5}}_f$.

4. We do not make any comment on flux data. The above criteria can be evaded by switching off the fluxes such that the RPV coupling (once the assignment of H_d to a curve is realised) disappears.

With this in mind we study the possible RPV realisations in multi-curve models.

C.1.1 $2+1+1+1$

In this case the spectral cover polynomial splits into four factors, three linear terms and a quadratic one. Also, due to the quadratic factor we impose a Z_2 monodromy. The bestiary of matter curves and their perpendicular charges (t_i) is given in the Table 6.

Curve :	5_{H_u}	5_1	5_2	5_3	5_4	5_5	5_6	10_M	10_2	10_3	10_4
Charge :	$-2t_1$	$-t_1-t_3$	$-t_1-t_4$	$-t_1-t_5$	$-t_3-t_4$	t_3-t_5	$-t_4-t_5$	t_1	t_3	t_4	t_5

Table C.1: Matter curves and the corresponding $U(1)$ charges for the case of a $2+1+1+1$ spectral cover split. Note that because of the Z_2 monodromy we have $t_1 \longleftrightarrow t_2$.

In this model RPV is expected to be generic as we have the following terms

$$\mathbf{10}_4\overline{\mathbf{5}}_1\overline{\mathbf{5}}_2,\ \mathbf{10}_3\overline{\mathbf{5}}_1\overline{\mathbf{5}}_3,\ \mathbf{10}_M\overline{\mathbf{5}}_1\overline{\mathbf{5}}_6,\ \mathbf{10}_2\overline{\mathbf{5}}_2\overline{\mathbf{5}}_3,\ \mathbf{10}_M\overline{\mathbf{5}}_2\overline{\mathbf{5}}_5,\ \mathbf{10}_M\overline{\mathbf{5}}_3\overline{\mathbf{5}}_4 \tag{C.4}$$

C.1.2 $2+2+1$

Here the spectral cover polynomial splits into three factors, it is the product of two quadratic terms and a linear one. We can impose a $Z_2 \times Z_2$ monodromy which leads to the following identifications between the weights,$(t_1 \leftrightarrow t_2)$ and $(t_3 \leftrightarrow t_4)$. In this case there are two possible assignments for H_u (and $\mathbf{10}_M$), as we can see in Table 7.

				case 1				
Curve	5_{H_u}	5_1	5_2	5_3	5_4	10_M	10_2	10_3
Charge	$-2t_1$	$-t_1-t_3$	$-t_1-t_5$	$-t_3-t_5$	$-2t_3$	t_1	$-t_3$	t_5
				case 2				
Curve	5_{H_u}	5_1	5_2	5_3	5_4	10_M	10_2	10_3
Charge	$-2t_3$	$-t_1-t_3$	$-t_1-t_5$	$-t_3-t_5$	$-2t_1$	t_3	$-t_1$	t_5

Table C.2: The scenario of a $2+2+1$ spectral cover split with the corresponding matter curves and $U(1)$ charges. Note that we have two possible cases.

$2+2+1$ **case 1**

The bestiary of matter curves and their perp charges is given in the upper half table of Table 7.

In this model RPV is expected to be generic as we have the following terms

$$\mathbf{10}_2\overline{\mathbf{5}}_1\overline{\mathbf{5}}_2,\ \mathbf{10}_M\overline{\mathbf{5}}_1\overline{\mathbf{5}}_3,\ \mathbf{10}_M\overline{\mathbf{5}}_2\overline{\mathbf{5}}_4,\ \mathbf{10}_3\overline{\mathbf{5}}_1\overline{\mathbf{5}}_1 \tag{C.5}$$

Notice that if $\overline{\mathbf{5}}_1$ contains only one state, then the last coupling is absent due to anti-symmetry of SU(5) contraction.

$2+2+1$ **case 2**

The bestiary of matter curves and their perp charges is given in the lower half table of Table 7.

In this model RPV is expected to be generic as we have the following terms

$$\mathbf{10}_M\overline{\mathbf{5}}_1\overline{\mathbf{5}}_2,\ \mathbf{10}_2\overline{\mathbf{5}}_1\overline{\mathbf{5}}_3,\ \mathbf{10}_M\overline{\mathbf{5}}_3\overline{\mathbf{5}}_4,\ \mathbf{10}_3\overline{\mathbf{5}}_1\overline{\mathbf{5}}_1 \tag{C.6}$$

Notice that if $\overline{\mathbf{5}}_1$ contains only one state, then the last coupling is absent due to anti-symmetry of SU(5) contraction.

C.1.3 $3+1+1$

In this scenario the splitting of the spectral cover leads to a cubic and two linear factors. We can impose a Z_3 monodromy for the roots of the cubic polynomial. The bestiary of matter curves and their perpendicular charges is given in Table 8:

Curve	5_{H_u}	5_1	5_2	5_3	10_M	10_2	10_3
Charge	$-2t_1$	$-t_1-t_4$	$-t_1-t_5$	$-t_4-t_5$	t_1	t_4	t_5

Table C.3: Matter curves and the corresponding $U(1)$ charges for the case of a $3+1+1$ spectral cover split. Note that we have impose a Z_3 monodromy.

In this model R-parity violation is not immediately generic as we only have

$$\mathbf{10}_2\overline{\mathbf{5}}_1\overline{\mathbf{5}}_2,\ \mathbf{10}_M\overline{\mathbf{5}}_1\overline{\mathbf{5}}_3 \tag{C.7}$$

and as such assigning H_d to $\overline{\mathbf{5}}_1$ avoids tree-level, renormalizable, perturbative RPV.

C.1.4 $3+2$

These type of models are in general very constrained because of the large monodromies which leads to a low number of matter curves.

In this case there are two possible assignments for H_u (and $\mathbf{10}_M$), as described in Table 9.

		case 1			
Curve	5_{H_u}	5_2	5_3	10_M	10_2
Charge	$-2t_1$	$-t_1-t_3$	$-2t_3$	t_1	t_3
		case 2			
Curve	5_{H_u}	5_2	5_3	10_M	10_2
Charge	$-2t_3$	$-t_1-t_3$	$-2t_1$	t_3	t_1

Table C.4: The two possible cases in the scenario of a $3+2$ spectral cover split, the matter curves and the corresponding $U(1)$ charges.

$3+2$ **case 1**

The matter curves content is given in the upper half of Table 9 (case 1).

Possible RPV couplings are

$$\mathbf{10}_M\overline{\mathbf{5}}_2\overline{\mathbf{5}}_3\,,\,\mathbf{10}_2\overline{\mathbf{5}}_2\overline{\mathbf{5}}_2 \tag{C.8}$$

Notice that if $\overline{\mathbf{5}}_2$ contains only one state, then the last coupling is absent due to anti-symmetry of SU(5) contraction.

$3+2$ **case 2**

This second scenario is referred as case 2 in the lower half of Table 9.

Only one coupling

$$\mathbf{10}_M\overline{\mathbf{5}}_2\overline{\mathbf{5}}_2 \tag{C.9}$$

which is either RPV or is absent. Notice that if $\overline{\mathbf{5}}_2$ contains only one state, then the last coupling is absent due to anti-symmetry of SU(5) contraction.

C.2 Local F-theory constructions: local chirality constraints on flux data and R-Parity violating operators

The chiral spectrum of a matter curve is locally sensitive to the flux data. This is happens as there is a notion of local chirality due to local index theorems [36,39]. The presence of a chiral state in a sector with root ρ is given if the matrix

$$m_\rho = \begin{pmatrix} -q_P & q_S & im^2 q_{z_1} \\ q_S & q_P & im^2 q_{z_2} \\ -im^2 q_{z_1} & -im^2 q_{z_2} & 0 \end{pmatrix}$$

with q_i presented in Table 6.2, has positive determinant

$$\det m_\rho > 0. \tag{C.10}$$

As such, if we want a certain RPV coupling to be present, then the above condition has to be satisfied for the three states involved in the respective interaction at the $SO(12)$ enhancement point. For example, in order for the emergence of an QLd^c type of RPV interaction, locally the spectrum has to support a Q, a L, and a d^c states. The requirement that at a single point Equation (C.10) hold for each of these states imposes constraints on the values of the flux density parameters.

Therefore, while RPV effects in general include all three operators - QLd^c, $u^cd^cd^c$, LLe^c - there are regions of the parameter space that allow for the elimination of some or all of the couplings. These are in principle divided into four regions, depending on the sign of the parameters $\tilde{N}_Y$ and N_Y. In this appendix we present the resulting regions of the parameter space and which operators are allowed in each.

These regions are graphically represented in the main text, see Figure 6.8 and related figures.

C.2.1 Parameter space regions for $\tilde{N}_Y \leq 0$

For $\tilde{N}_Y \leq 0$, the conditions on the flux density parameters for which each RPV interaction is turned on are

$$\begin{aligned} QLd^c: \; & M > \frac{-\tilde{N}_Y}{6} \\ & N_a - N_b > \frac{-N_Y}{2} \\ u^cd^cd^c: \; & M > \frac{\tilde{N}_Y}{3} \\ & N_a - N_b > -\frac{N_Y}{3} \\ LLe^c: \; & M > -\tilde{N}_Y \\ & N_a - N_b > \frac{-N_Y}{2} \end{aligned}$$

Depending on the sign of N_Y, the above conditions define different regions of the flux density parameter space. These are presented in Tables C.5 and C.6.

The case of $N_Y > 0$

–	$M < \frac{\tilde{N}_Y}{3}$	$\frac{\tilde{N}_Y}{3} < M < \frac{-\tilde{N}_Y}{6}$	$\frac{-\tilde{N}_Y}{6} < M < -\tilde{N}_Y$	$-\tilde{N}_Y < M$
$(N_a - N_b) < \frac{-N_Y}{2}$	None	None	None	None
$\frac{-N_Y}{2} < (N_a - N_b) < \frac{N_Y}{3}$	None	None	QLd^c	QLd^c, LLe^c
$\frac{N_Y}{3} < (N_a - N_b)$	None	$u^c d^c d^c$	QLd^c, $u^c d^c d^c$	All

Table C.5: Regions of the parameter space and the respective RPV operators supported for $\tilde{N}_Y \leq 0$, $N_Y > 0$

The case of $N_Y < 0$

–	$M < \frac{\tilde{N}_Y}{3}$	$\frac{\tilde{N}_Y}{3} < M < \frac{-\tilde{N}_Y}{6}$	$\frac{-\tilde{N}_Y}{6} < M < -\tilde{N}_Y$	$-\tilde{N}_Y < M$
$(N_a - N_b) < \frac{N_Y}{3}$	None	None	None	None
$\frac{N_Y}{3} < (N_a - N_b) < \frac{-N_Y}{2}$	None	$u^c d^c d^c$	$u^c d^c d^c$	$u^c d^c d^c$
$\frac{-N_Y}{2} < (N_a - N_b)$	None	$u^c d^c d^c$	QLd^c, $u^c d^c d^c$	All

Table C.6: Regions of the parameter space and the respective RPV operators supported for $\tilde{N}_Y \leq 0$, $N_Y < 0$

C.2.2 Parameter space regions for $\tilde{N}_Y > 0$

For $\tilde{N}_Y > 0$, the conditions on the flux density parameters for which each RPV interaction is turned on are

$$\begin{aligned} QLd^c: \; & M > \frac{\tilde{N}_Y}{3} \\ & N_a - N_b > \frac{-N_Y}{2} \\ u^c d^c d^c: \; & M > \frac{2\tilde{N}_Y}{3} \\ & N_a - N_b > -\frac{N_Y}{3} \\ LLe^c: \; & M > \frac{-\tilde{N}_Y}{2} \\ & N_a - N_b > \frac{-N_Y}{2} \end{aligned}$$

Depending on the sign of N_Y, the above conditions define different regions of the flux density parameter space. These are presented in Tables C.7 and C.8.

–	$M < -\frac{-\tilde{N}_Y}{2}$	$-\frac{-\tilde{N}_Y}{2} < M < \frac{\tilde{N}_Y}{3}$	$\frac{\tilde{N}_Y}{3} < M < \frac{2\tilde{N}_Y}{3}$	$\frac{2\tilde{N}_Y}{3} < M$
$(N_a - N_b) < \frac{-N_Y}{2}$	None	None	None	None
$\frac{-N_Y}{2} < (N_a - N_b) < \frac{N_Y}{3}$	None	LLe^c	QLd^c, LLe^c	QLd^c, LLe^c
$\frac{N_Y}{3} < (N_a - N_b)$	None	LLe^c	QLd^c, LLe^c	All

Table C.7: Regions of the parameter space and the respective RPV operators supported for $\tilde{N}_Y > 0$, $N_Y > 0$

The case of $N_Y > 0$

The case of $N_Y < 0$

–	$M < -\frac{-\tilde{N}_Y}{2}$	$-\frac{-\tilde{N}_Y}{2} < M < \frac{\tilde{N}_Y}{3}$	$\frac{\tilde{N}_Y}{3} < M < \frac{2\tilde{N}_Y}{3}$	$\frac{2\tilde{N}_Y}{3} < M$
$(N_a - N_b) < \frac{N_Y}{3}$	None	None	None	None
$\frac{N_Y}{3} < (N_a - N_b) < \frac{-N_Y}{2}$	None	None	None	$u^c d^c d^c$
$\frac{-N_Y}{2} < (N_a - N_b)$	None	LLe^c	QLd^c, LLe^c	All

Table C.8: Regions of the parameter space and the respective RPV operators supported for $\tilde{N}_Y > 0$, $N_Y < 0$

Bibliography

[1] Miguel Crispim Romo, Athanasios Karozas, Stephen F. King, George K. Leontaris, and Andrew K. Meadowcroft. MSSM from F-theory SU(5) with Klein Monodromy. *Phys. Rev.*, D93(12):126007, 2016, 1512.09148.

[2] Athanasios Karozas, Stephen F. King, George K. Leontaris, and Andrew Meadowcroft. Discrete Family Symmetry from F-Theory GUTs. *JHEP*, 09:107, 2014, 1406.6290.

[3] Athanasios Karozas, Stephen F. King, George K. Leontaris, and Andrew K. Meadowcroft. Phenomenological implications of a minimal F-theory GUT with discrete symmetry. *JHEP*, 10:041, 2015, 1505.00937.

[4] Athanasios Karozas, Stephen F. King, George K. Leontaris, and Andrew K. Meadowcroft. 750 GeV diphoton excess from E_6 in F-theory GUTs. *Phys. Lett.*, B757:73–78, 2016, 1601.00640.

[5] Miguel Crispim Romo, Athanasios Karozas, Stephen F. King, George K. Leontaris, and Andrew K. Meadowcroft. R-Parity violation in F-Theory. 2016, 1608.04746.

[6] B. P. Abbott et al. GW151226: Observation of Gravitational Waves from a 22-Solar-Mass Binary Black Hole Coalescence. *Phys. Rev. Lett.*, 116(24):241103, 2016, 1606.04855.

[7] Georges Aad et al. Observation of a new particle in the search for the Standard Model Higgs boson with the ATLAS detector at the LHC. *Phys. Lett.*, B716:1–29, 2012, 1207.7214.

[8] Serguei Chatrchyan et al. Observation of a new boson at a mass of 125 GeV with the CMS experiment at the LHC. *Phys. Lett.*, B716:30–61, 2012, 1207.7235.

[9] H. Georgi and S. L. Glashow. Unity of All Elementary Particle Forces. *Phys. Rev. Lett.*, 32:438–441, 1974.

[10] Stephen M. Barr. A New Symmetry Breaking Pattern for SO(10) and Proton Decay. *Phys. Lett.*, B112:219–222, 1982.

[11] Jogesh C. Pati and Abdus Salam. Lepton Number as the Fourth Color. *Phys. Rev.*, D10:275–289, 1974. [Erratum: Phys. Rev.D11,703(1975)].

[12] S. F. King, S. Moretti, and R. Nevzorov. Theory and phenomenology of an exceptional supersymmetric standard model. *Phys. Rev.*, D73:035009, 2006, hep-ph/0510419.

[13] Cumrun Vafa. Evidence for F theory. *Nucl. Phys.*, B469:403–418, 1996, hep-th/9602022.

[14] Jonathan J. Heckman, Alireza Tavanfar, and Cumrun Vafa. The Point of E(8) in F-theory GUTs. *JHEP*, 08:040, 2010, 0906.0581.

[15] Ron Donagi and Martijn Wijnholt. Model Building with F-Theory. *Adv. Theor. Math. Phys.*, 15(5):1237–1317, 2011, 0802.2969.

[16] Ron Donagi and Martijn Wijnholt. Breaking GUT Groups in F-Theory. *Adv. Theor. Math. Phys.*, 15(6):1523–1603, 2011, 0808.2223.

[17] Ron Donagi and Martijn Wijnholt. Higgs Bundles and UV Completion in F-Theory. *Commun. Math. Phys.*, 326:287–327, 2014, 0904.1218.

[18] Chris Beasley, Jonathan J. Heckman, and Cumrun Vafa. GUTs and Exceptional Branes in F-theory - I. *JHEP*, 01:058, 2009, 0802.3391.

[19] Chris Beasley, Jonathan J. Heckman, and Cumrun Vafa. GUTs and Exceptional Branes in F-theory - II: Experimental Predictions. *JHEP*, 01:059, 2009, 0806.0102.

[20] Jonathan J. Heckman. Particle Physics Implications of F-theory. *Ann. Rev. Nucl. Part. Sci.*, 60:237–265, 2010, 1001.0577.

[21] Timo Weigand. Lectures on F-theory compactifications and model building. *Class. Quant. Grav.*, 27:214004, 2010, 1009.3497.

[22] Ralph Blumenhagen, Thomas W. Grimm, Benjamin Jurke, and Timo Weigand. Global F-theory GUTs. *Nucl. Phys.*, B829:325–369, 2010, 0908.1784.

[23] Mirjam Cvetic, Inaki Garcia-Etxebarria, and James Halverson. Global F-theory Models: Instantons and Gauge Dynamics. *JHEP*, 01:073, 2011, 1003.5337.

[24] Mirjam Cvetic, Denis Klevers, Damin Kaloni Mayorga Pea, Paul-Konstantin Oehlmann, and Jonas Reuter. Three-Family Particle Physics Models from Global F-theory Compactifications. *JHEP*, 08:087, 2015, 1503.02068.

[25] Thomas W. Grimm, Sven Krause, and Timo Weigand. F-Theory GUT Vacua on Compact Calabi-Yau Fourfolds. *JHEP*, 07:037, 2010, 0912.3524.

[26] Thomas W. Grimm and Timo Weigand. On Abelian Gauge Symmetries and Proton Decay in Global F-theory GUTs. *Phys. Rev.*, D82:086009, 2010, 1006.0226.

[27] Thomas W. Grimm. The N=1 effective action of F-theory compactifications. *Nucl. Phys.*, B845:48–92, 2011, 1008.4133.

[28] Christoph Mayrhofer, Eran Palti, Oskar Till, and Timo Weigand. Discrete Gauge Symmetries by Higgsing in four-dimensional F-Theory Compactifications. *JHEP*, 12:068, 2014, 1408.6831.

[29] Ching-Ming Chen, Johanna Knapp, Maximilian Kreuzer, and Christoph Mayrhofer. Global SO(10) F-theory GUTs. *JHEP*, 10:057, 2010, 1005.5735.

[30] G. K. Leontaris and G. G. Ross. Yukawa couplings and fermion mass structure in F-theory GUTs. *JHEP*, 02:108, 2011, 1009.6000.

[31] A. Font and L. E. Ibanez. Yukawa Structure from U(1) Fluxes in F-theory Grand Unification. *JHEP*, 02:016, 2009, 0811.2157.

[32] A. Font and L. E. Ibanez. Matter wave functions and Yukawa couplings in F-theory Grand Unification. *JHEP*, 09:036, 2009, 0907.4895.

[33] Luis Aparicio, Anamaria Font, Luis E. Ibanez, and Fernando Marchesano. Flux and Instanton Effects in Local F-theory Models and Hierarchical Fermion Masses. *JHEP*, 08:152, 2011, 1104.2609.

[34] Anamaria Font, Luis E. Ibanez, Fernando Marchesano, and Diego Regalado. Non-perturbative effects and Yukawa hierarchies in F-theory SU(5) Unification. *JHEP*, 03:140, 2013, 1211.6529. [Erratum: JHEP07,036(2013)].

[35] Sergio Cecotti, Miranda C. N. Cheng, Jonathan J. Heckman, and Cumrun Vafa. Yukawa Couplings in F-theory and Non-Commutative Geometry. 2009, 0910.0477.

[36] Eran Palti. Wavefunctions and the Point of E_8 in F-theory. *JHEP*, 07:065, 2012, 1203.4490.

[37] Fernando Marchesano, Diego Regalado, and Gianluca Zoccarato. Yukawa hierarchies at the point of E_8 in F-theory. *JHEP*, 04:179, 2015, 1503.02683.

[38] Pablo G. Camara, Emilian Dudas, and Eran Palti. Massive wavefunctions, proton decay and FCNCs in local F-theory GUTs. *JHEP*, 12:112, 2011, 1110.2206.

[39] Anamaria Font, Fernando Marchesano, Diego Regalado, and Gianluca Zoccarato. Up-type quark masses in SU(5) F-theory models. *JHEP*, 11:125, 2013, 1307.8089.

[40] David R. Morrison and Daniel S. Park. F-Theory and the Mordell-Weil Group of Elliptically-Fibered Calabi-Yau Threefolds. *JHEP*, 10:128, 2012, 1208.2695.

[41] Sven Krippendorf, Sakura Schafer-Nameki, and Jin-Mann Wong. Froggatt-Nielsen meets Mordell-Weil: A Phenomenological Survey of Global F-theory GUTs with U(1)s. *JHEP*, 11:008, 2015, 1507.05961.

[42] Sven Krippendorf, Damian Kaloni Mayorga Pena, Paul-Konstantin Oehlmann, and Fabian Ruehle. Rational F-Theory GUTs without exotics. *JHEP*, 07:013, 2014, 1401.5084.

[43] Christoph Mayrhofer, Eran Palti, Oskar Till, and Timo Weigand. On Discrete Symmetries and Torsion Homology in F-Theory. *JHEP*, 06:029, 2015, 1410.7814.

[44] Mirjam Cvetic, Denis Klevers, Hernan Piragua, and Peng Song. Elliptic fibrations with rank three Mordell-Weil group: F-theory with U(1) x U(1) x U(1) gauge symmetry. *JHEP*, 03:021, 2014, 1310.0463.

[45] Mirjam Cvetic, Denis Klevers, and Hernan Piragua. F-Theory Compactifications with Multiple U(1)-Factors: Constructing Elliptic Fibrations with Rational Sections. *JHEP*, 06:067, 2013, 1303.6970.

[46] Volker Braun, Thomas W. Grimm, and Jan Keitel. Geometric Engineering in Toric F-Theory and GUTs with U(1) Gauge Factors. *JHEP*, 12:069, 2013, 1306.0577.

[47] Joseph Marsano, Natalia Saulina, and Sakura Schafer-Nameki. Monodromies, Fluxes, and Compact Three-Generation F-theory GUTs. *JHEP*, 08:046, 2009, 0906.4672.

[48] Emilian Dudas and Eran Palti. Froggatt-Nielsen models from E(8) in F-theory GUTs. *JHEP*, 01:127, 2010, 0912.0853.

[49] Emilian Dudas and Eran Palti. On hypercharge flux and exotics in F-theory GUTs. *JHEP*, 09:013, 2010, 1007.1297.

[50] I. Antoniadis and G. K. Leontaris. Neutrino mass textures from F-theory. *Eur. Phys. J.*, C73:2670, 2013, 1308.1581.

[51] S. F. King, G. K. Leontaris, and G. G. Ross. Family symmetries in F-theory GUTs. *Nucl. Phys.*, B838:119–135, 2010, 1005.1025.

[52] James C. Callaghan, Stephen F. King, George K. Leontaris, and Graham G. Ross. Towards a Realistic F-theory GUT. *JHEP*, 04:094, 2012, 1109.1399.

[53] James C. Callaghan and Stephen F. King. E6 Models from F-theory. *JHEP*, 04:034, 2013, 1210.6913.

[54] James C. Callaghan, Stephen F. King, and George K. Leontaris. Gauge coupling unification in E_6 F-theory GUTs with matter and bulk exotics from flux breaking. *JHEP*, 12:037, 2013, 1307.4593.

[55] I. Antoniadis and G. K. Leontaris. Building SO(10) models from F-theory. *JHEP*, 08:001, 2012, 1205.6930.

[56] Hirotaka Hayashi, Teruhiko Kawano, Yoichi Tsuchiya, and Taizan Watari. More on Dimension-4 Proton Decay Problem in F-theory – Spectral Surface, Discriminant Locus and Monodromy. *Nucl. Phys.*, B840:304–348, 2010, 1004.3870.

[57] Arthur Hebecker and James Unwin. Precision Unification and Proton Decay in F-Theory GUTs with High Scale Supersymmetry. *JHEP*, 09:125, 2014, 1405.2930.

[58] Hirotaka Hayashi, Teruhiko Kawano, Yoichi Tsuchiya, and Taizan Watari. Flavor Structure in F-theory Compactifications. *JHEP*, 08:036, 2010, 0910.2762.

[59] Jonathan J. Heckman and Cumrun Vafa. Flavor Hierarchy From F-theory. *Nucl. Phys.*, B837:137–151, 2010, 0811.2417.

[60] S. F. King. Neutrino mass. *Contemp. Phys.*, 48:195, 2007, 0712.1750.

[61] S. L. Adler. Axial-Vector Vertex in Spinor Electrodynamics. *Physical Review*, 177:2426–2438, January 1969.

[62] J. S. Bell and R. Jackiw. A PCAC puzzle: $\pi^0 \to \gamma\gamma$ in the σ-model. *Nuovo Cimento A Serie*, 60:47–61, March 1969.

[63] Sidney R. Coleman and J. Mandula. All Possible Symmetries of the S Matrix. *Phys. Rev.*, 159:1251–1256, 1967.

[64] Stephen P. Martin. A Supersymmetry primer. 1997, hep-ph/9709356. [Adv. Ser. Direct. High Energy Phys.18,1(1998)].

[65] J. Patera and R. T. Sharp. On the Triangle Anomaly Number of SU(N) Representations. *J. Math. Phys.*, 22:2352, 1981.

[66] K. A. Olive et al. Review of Particle Physics. *Chin. Phys.*, C38:090001, 2014.

[67] David Tong. String Theory. 2009, 0908.0333.

[68] David R. Morrison and Cumrun Vafa. Compactifications of F theory on Calabi-Yau threefolds. 2. *Nucl. Phys.*, B476:437–469, 1996, hep-th/9603161.

[69] Jonathan J. Heckman, Joseph Marsano, Natalia Saulina, Sakura Schafer-Nameki, and Cumrun Vafa. Instantons and SUSY breaking in F-theory. 2008, 0808.1286.

[70] Ralph Blumenhagen, Volker Braun, Thomas W. Grimm, and Timo Weigand. GUTs in Type IIB Orientifold Compactifications. *Nucl. Phys.*, B815:1–94, 2009, 0811.2936.

[71] R. Ahl Laamara, M. Miskaoui, and E. H. Saidi. Building SO 10 -models with D4 symmetry. *Nucl. Phys.*, B901:59–75, 2015, 1511.03166.

[72] George K. Leontaris. Aspects of F-Theory GUTs. *PoS*, CORFU2011:095, 2011, 1203.6277.

[73] K. Kodaira. On compact complex analytic surfaces, i. *Annals of Mathematics*, 71(1):111–152, 1960.

[74] K. Kodaira. On compact analytic surfaces: Ii. *Annals of Mathematics*, 77(3):563–626, 1963.

[75] J. Tate. *Algorithm for determining the type of a singular fiber in an elliptic pencil*, pages 33–52. Springer Berlin Heidelberg, Berlin, Heidelberg, 1975.

[76] M. Bershadsky, Kenneth A. Intriligator, S. Kachru, David R. Morrison, V. Sadov, and Cumrun Vafa. Geometric singularities and enhanced gauge symmetries. *Nucl. Phys.*, B481:215–252, 1996, hep-th/9605200.

[77] Joseph Marsano and Sakura Schafer-Nameki. Yukawas, G-flux, and Spectral Covers from Resolved Calabi-Yau's. *JHEP*, 11:098, 2011, 1108.1794.

[78] Renato M. Fonseca. Calculating the renormalisation group equations of a SUSY model with Susyno. *Comput. Phys. Commun.*, 183:2298–2306, 2012, 1106.5016.

[79] Peter Minkowski. $\mu \to e\gamma$ at a Rate of One Out of 10^9 Muon Decays? *Phys. Lett.*, B67:421–428, 1977.

[80] S. F. King. Large mixing angle MSW and atmospheric neutrinos from single right-handed neutrino dominance and U(1) family symmetry. *Nucl. Phys.*, B576:85–105, 2000, hep-ph/9912492.

[81] Stephen F. King. Littlest Seesaw. *JHEP*, 02:085, 2016, 1512.07531.

[82] Luis E. Ibanez and Graham G. Ross. Discrete gauge symmetry anomalies. *Phys. Lett.*, B260:291–295, 1991.

[83] M. Berasaluce-Gonzalez, P. G. Camara, F. Marchesano, D. Regalado, and A. M. Uranga. Non-Abelian discrete gauge symmetries in 4d string models. *JHEP*, 09:059, 2012, 1206.2383.

[84] Guido Altarelli and Ferruccio Feruglio. Discrete Flavor Symmetries and Models of Neutrino Mixing. *Rev. Mod. Phys.*, 82:2701–2729, 2010, 1002.0211.

[85] Stephen F. King and Christoph Luhn. Neutrino Mass and Mixing with Discrete Symmetry. *Rept. Prog. Phys.*, 76:056201, 2013, 1301.1340.

[86] Stephen F. King, Alexander Merle, Stefano Morisi, Yusuke Shimizu, and Morimitsu Tanimoto. Neutrino Mass and Mixing: from Theory to Experiment. *New J. Phys.*, 16:045018, 2014, 1402.4271.

[87] Christoph Mayrhofer, Eran Palti, and Timo Weigand. Hypercharge Flux in IIB and F-theory: Anomalies and Gauge Coupling Unification. *JHEP*, 09:082, 2013, 1303.3589.

[88] Joseph Marsano. Hypercharge Flux, Exotics, and Anomaly Cancellation in F-theory GUTs. *Phys. Rev. Lett.*, 106:081601, 2011, 1011.2212.

[89] M. C. Gonzalez-Garcia, Michele Maltoni, Jordi Salvado, and Thomas Schwetz. Global fit to three neutrino mixing: critical look at present precision. *JHEP*, 12:123, 2012, 1209.3023.

[90] S. F. King. Neutrino mass models. *Rept. Prog. Phys.*, 67:107–158, 2004, hep-ph/0310204.

[91] P. A. R. Ade et al. Planck 2013 results. XVI. Cosmological parameters. *Astron. Astrophys.*, 571:A16, 2014, 1303.5076.

[92] Mikel Berasaluce-Gonzalez, Luis E. Ibanez, Pablo Soler, and Angel M. Uranga. Discrete gauge symmetries in D-brane models. *JHEP*, 12:113, 2011, 1106.4169.

[93] Mirjam Cveti, Ron Donagi, Denis Klevers, Hernan Piragua, and Maximilian Poretschkin. F-theory vacua with $\mathbb{Z}_3$ gauge symmetry. *Nucl. Phys.*, B898:736–750, 2015, 1502.06953.

[94] Hajime Ishimori, Tatsuo Kobayashi, Hiroshi Ohki, Yusuke Shimizu, Hiroshi Okada, and Morimitsu Tanimoto. Non-Abelian Discrete Symmetries in Particle Physics. *Prog. Theor. Phys. Suppl.*, 183:1–163, 2010, 1003.3552.

[95] Christoph Luhn, Salah Nasri, and Pierre Ramond. Simple Finite Non-Abelian Flavor Groups. *J. Math. Phys.*, 48:123519, 2007, 0709.1447.

[96] Rabindra N. Mohapatra and R. E. Marshak. Local B-L Symmetry of Electroweak Interactions, Majorana Neutrinos and Neutron Oscillations. *Phys. Rev. Lett.*, 44:1316–1319, 1980. [Erratum: Phys. Rev. Lett.44,1643(1980)].

[97] J. L. Goity and Marc Sher. Bounds on $\Delta B = 1$ couplings in the supersymmetric standard model. *Phys. Lett.*, B346:69–74, 1995, hep-ph/9412208. [Erratum: Phys. Lett.B385,500(1996)].

[98] D. G. Phillips, II et al. Neutron-Antineutron Oscillations: Theoretical Status and Experimental Prospects. *Phys. Rept.*, 612:1–45, 2016, 1410.1100.

[99] R. Barbier et al. R-parity violating supersymmetry. *Phys. Rept.*, 420:1–202, 2005, hep-ph/0406039.

[100] The ATLAS collaboration. Search for resonances decaying to photon pairs in 3.2 fb^{-1} of pp collisions at $\sqrt{s} = 13$ TeV with the ATLAS detector. 2015.

[101] CMS Collaboration. Search for new physics in high mass diphoton events in proton-proton collisions at 13TeV. 2015.

[102] Stefano Di Chiara, Luca Marzola, and Martti Raidal. First interpretation of the 750 GeV diphoton resonance at the LHC. *Phys. Rev.*, D93(9):095018, 2016, 1512.04939.

[103] Roberto Franceschini, Gian F. Giudice, Jernej F. Kamenik, Matthew McCullough, Alex Pomarol, Riccardo Rattazzi, Michele Redi, Francesco Riva, Alessandro Strumia, and Riccardo Torre. What is the $\gamma\gamma$ resonance at 750 GeV? *JHEP*, 03:144, 2016, 1512.04933.

[104] Andrei Angelescu, Abdelhak Djouadi, and Grgory Moreau. Scenarii for interpretations of the LHC diphoton excess: two Higgs doublets and vector-like quarks and leptons. *Phys. Lett.*, B756:126–132, 2016, 1512.04921.

[105] Mihailo Backovic, Alberto Mariotti, and Diego Redigolo. Di-photon excess illuminates Dark Matter. *JHEP*, 03:157, 2016, 1512.04917.

[106] Yann Mambrini, Giorgio Arcadi, and Abdelhak Djouadi. The LHC diphoton resonance and dark matter. *Phys. Lett.*, B755:426–432, 2016, 1512.04913.

[107] John Ellis, Sebastian A. R. Ellis, Jrmie Quevillon, Veronica Sanz, and Tevong You. On the Interpretation of a Possible $\sim$ 750 GeV Particle Decaying into $\gamma\gamma$. *JHEP*, 03:176, 2016, 1512.05327.

[108] Simon Knapen, Tom Melia, Michele Papucci, and Kathryn Zurek. Rays of light from the LHC. *Phys. Rev.*, D93(7):075020, 2016, 1512.04928.

[109] Brando Bellazzini, Roberto Franceschini, Filippo Sala, and Javi Serra. Goldstones in Diphotons. *JHEP*, 04:072, 2016, 1512.05330.

[110] Rick S. Gupta, Sebastian Jger, Yevgeny Kats, Gilad Perez, and Emmanuel Stamou. Interpreting a 750 GeV Diphoton Resonance. *JHEP*, 07:145, 2016, 1512.05332.

[111] Samuel D. McDermott, Patrick Meade, and Harikrishnan Ramani. Singlet Scalar Resonances and the Diphoton Excess. *Phys. Lett.*, B755:353–357, 2016, 1512.05326.

[112] Matthew Low, Andrea Tesi, and Lian-Tao Wang. A pseudoscalar decaying to photon pairs in the early LHC Run 2 data. *JHEP*, 03:108, 2016, 1512.05328.

[113] Christoffer Petersson and Riccardo Torre. 750 GeV Diphoton Excess from the Goldstino Superpartner. *Phys. Rev. Lett.*, 116(15):151804, 2016, 1512.05333.

[114] Emiliano Molinaro, Francesco Sannino, and Natascia Vignaroli. Minimal Composite Dynamics versus Axion Origin of the Diphoton excess. 2015, 1512.05334.

[115] Tetsutaro Higaki, Kwang Sik Jeong, Naoya Kitajima, and Fuminobu Takahashi. The QCD Axion from Aligned Axions and Diphoton Excess. *Phys. Lett.*, B755:13–16, 2016, 1512.05295.

[116] Apostolos Pilaftsis. Diphoton Signatures from Heavy Axion Decays at the CERN Large Hadron Collider. *Phys. Rev.*, D93(1):015017, 2016, 1512.04931.

[117] Yuichiro Nakai, Ryosuke Sato, and Kohsaku Tobioka. Footprints of New Strong Dynamics via Anomaly and the 750 GeV Diphoton. *Phys. Rev. Lett.*, 116(15):151802, 2016, 1512.04924.

[118] Keisuke Harigaya and Yasunori Nomura. Composite Models for the 750 GeV Diphoton Excess. *Phys. Lett.*, B754:151–156, 2016, 1512.04850.

[119] Bhaskar Dutta, Yu Gao, Tathagata Ghosh, Ilia Gogoladze, and Tianjun Li. Interpretation of the diphoton excess at CMS and ATLAS. *Phys. Rev.*, D93(5):055032, 2016, 1512.05439.

[120] Qing-Hong Cao, Yandong Liu, Ke-Pan Xie, Bin Yan, and Dong-Ming Zhang. A Boost Test of Anomalous Diphoton Resonance at the LHC. 2015, 1512.05542.

[121] Archil Kobakhidze, Fei Wang, Lei Wu, Jin Min Yang, and Mengchao Zhang. 750 GeV diphoton resonance in a top and bottom seesaw model. *Phys. Lett.*, B757:92–96, 2016, 1512.05585.

[122] Peter Cox, Anibal D. Medina, Tirtha Sankar Ray, and Andrew Spray. Diphoton Excess at 750 GeV from a Radion in the Bulk-Higgs Scenario. 2015, 1512.05618.

[123] Aqeel Ahmed, Barry M. Dillon, Bohdan Grzadkowski, John F. Gunion, and Yun Jiang. Higgs-radion interpretation of 750 GeV di-photon excess at the LHC. 2015, 1512.05771.

[124] D. Beirevi, Enrico Bertuzzo, Olcyr Sumensari, and Renata Zukanovich Funchal. Can the new resonance at LHC be a CP-Odd Higgs boson? *Phys. Lett.*, B757:261–267, 2016, 1512.05623.

[125] Jose Miguel No, Veronica Sanz, and Jack Setford. See-saw composite Higgs model at the LHC: Linking naturalness to the 750 GeV diphoton resonance. *Phys. Rev.*, D93(9):095010, 2016, 1512.05700.

[126] S. V. Demidov and D. S. Gorbunov. On sgoldstino interpretation of the diphoton excess. *JETP Lett.*, 103(4):219–222, 2016, 1512.05723. [Pisma Zh. Eksp. Teor. Fiz.103,no.4,241(2016)].

[127] Wei Chao, Ran Huo, and Jiang-Hao Yu. The Minimal Scalar-Stealth Top Interpretation of the Diphoton Excess. 2015, 1512.05738.

[128] Sylvain Fichet, Gero von Gersdorff, and Christophe Royon. Scattering light by light at 750 GeV at the LHC. *Phys. Rev.*, D93(7):075031, 2016, 1512.05751.

[129] David Curtin and Christopher B. Verhaaren. Quirky Explanations for the Diphoton Excess. *Phys. Rev.*, D93(5):055011, 2016, 1512.05753.

[130] Ligong Bian, Ning Chen, Da Liu, and Jing Shu. Hidden confining world on the 750 GeV diphoton excess. *Phys. Rev.*, D93(9):095011, 2016, 1512.05759.

[131] Joydeep Chakrabortty, Arghya Choudhury, Pradipta Ghosh, Subhadeep Mondal, and Tripurari Srivastava. Di-photon resonance around 750 GeV: shedding light on the theory underneath. 2015, 1512.05767.

[132] Csaba Cski, Jay Hubisz, and John Terning. Minimal model of a diphoton resonance: Production without gluon couplings. *Phys. Rev.*, D93(3):035002, 2016, 1512.05776.

[133] Adam Falkowski, Oren Slone, and Tomer Volansky. Phenomenology of a 750 GeV Singlet. *JHEP*, 02:152, 2016, 1512.05777.

[134] Yang Bai, Joshua Berger, and Ran Lu. 750 GeV dark pion: Cousin of a dark G -parity odd WIMP. *Phys. Rev.*, D93(7):076009, 2016, 1512.05779.

[135] R. Benbrik, Chuan-Hung Chen, and Takaaki Nomura. Higgs singlet boson as a diphoton resonance in a vectorlike quark model. *Phys. Rev.*, D93(5):055034, 2016, 1512.06028.

[136] Jong Soo Kim, Jrgen Reuter, Krzysztof Rolbiecki, and Roberto Ruiz de Austri. A resonance without resonance: scrutinizing the diphoton excess at 750 GeV. *Phys. Lett.*, B755:403–408, 2016, 1512.06083.

[137] E. Gabrielli, K. Kannike, B. Mele, M. Raidal, C. Spethmann, and H. Veerme. A SUSY Inspired Simplified Model for the 750 GeV Diphoton Excess. *Phys. Lett.*, B756:36–41, 2016, 1512.05961.

[138] Alexandre Alves, Alex G. Dias, and Kuver Sinha. The 750 GeV *S*-cion: Where else should we look for it? *Phys. Lett.*, B757:39–46, 2016, 1512.06091.

[139] Eugenio Megias, Oriol Pujolas, and Mariano Quiros. On dilatons and the LHC diphoton excess. *JHEP*, 05:137, 2016, 1512.06106.

[140] Linda M. Carpenter, Russell Colburn, and Jessica Goodman. Supersoft SUSY models and the 750 GeV diphoton excess, beyond effective operators. *Phys. Rev.*, D94(1):015016, 2016, 1512.06107.

[141] Jrmy Bernon and Christopher Smith. Could the width of the diphoton anomaly signal a three-body decay? *Phys. Lett.*, B757:148–153, 2016, 1512.06113.

[142] Wei Chao. Symmetries behind the 750 GeV diphoton excess. *Phys. Rev.*, D93(11):115013, 2016, 1512.06297.

[143] Chengcheng Han, Hyun Min Lee, Myeonghun Park, and Veronica Sanz. The diphoton resonance as a gravity mediator of dark matter. *Phys. Lett.*, B755:371–379, 2016, 1512.06376.

[144] Spencer Chang. A Simple $U(1)$ Gauge Theory Explanation of the Diphoton Excess. *Phys. Rev.*, D93(5):055016, 2016, 1512.06426.

[145] Mansi Dhuria and Gaurav Goswami. Perturbativity, vacuum stability and inflation in the light of 750 GeV diphoton excess. 2015, 1512.06782.

[146] Huayong Han, Shaoming Wang, and Sibo Zheng. Scalar Explanation of Diphoton Excess at LHC. *Nucl. Phys.*, B907:180–186, 2016, 1512.06562.

[147] Ming-xing Luo, Kai Wang, Tao Xu, Liangliang Zhang, and Guohuai Zhu. Squarkonium, diquarkonium, and octetonium at the LHC and their diphoton decays. *Phys. Rev.*, D93(5):055042, 2016, 1512.06670.

[148] Jung Chang, Kingman Cheung, and Chih-Ting Lu. Interpreting the 750 GeV diphoton resonance using photon jets in hidden-valley-like models. *Phys. Rev.*, D93(7):075013, 2016, 1512.06671.

[149] Debjyoti Bardhan, Disha Bhatia, Amit Chakraborty, Ushoshi Maitra, Sreerup Raychaudhuri, and Tousik Samui. Radion Candidate for the LHC Diphoton Resonance. 2015, 1512.06674.

[150] Tai-Fu Feng, Xue-Qian Li, Hai-Bin Zhang, and Shu-Min Zhao. The LHC 750 GeV diphoton excess in supersymmetry with gauged baryon and lepton numbers. 2015, 1512.06696.

[151] Wei Liao and Han-qing Zheng. Scalar resonance at 750 GeV as composite of heavy vector-like fermions. *Commun. Theor. Phys.*, 66(2):219–223, 2016, 1512.06741.

[152] Won Sang Cho, Doojin Kim, Kyoungchul Kong, Sung Hak Lim, Konstantin T. Matchev, Jong-Chul Park, and Myeonghun Park. 750 GeV Diphoton Excess May Not Imply a 750 GeV Resonance. *Phys. Rev. Lett.*, 116(15):151805, 2016, 1512.06824.

[153] Daniele Barducci, Andreas Goudelis, Suchita Kulkarni, and Dipan Sengupta. One jet to rule them all: monojet constraints and invisible decays of a 750 GeV diphoton resonance. *JHEP*, 05:154, 2016, 1512.06842.

[154] Ran Ding, Li Huang, Tianjun Li, and Bin Zhu. Interpreting 750 GeV Diphoton Excess with R-parity Violating Supersymmetry. 2015, 1512.06560.

[155] Xiao-Fang Han and Lei Wang. Implication of the 750 GeV diphoton resonance on two-Higgs-doublet model and its extensions with Higgs field. *Phys. Rev.*, D93(5):055027, 2016, 1512.06587.

[156] Oleg Antipin, Matin Mojaza, and Francesco Sannino. Minimal Coleman-Weinberg theory explains the diphoton excess. *Phys. Rev.*, D93(11):115007, 2016, 1512.06708.

[157] Fei Wang, Lei Wu, Jin Min Yang, and Mengchao Zhang. 750 GeV diphoton resonance, 125 GeV Higgs and muon g 2 anomaly in deflected anomaly mediation SUSY breaking scenarios. *Phys. Lett.*, B759:191–199, 2016, 1512.06715.

[158] Junjie Cao, Chengcheng Han, Liangliang Shang, Wei Su, Jin Min Yang, and Yang Zhang. Interpreting the 750 GeV diphoton excess by the singlet extension of the ManoharWise model. *Phys. Lett.*, B755:456–463, 2016, 1512.06728.

[159] Fa Peng Huang, Chong Sheng Li, Ze Long Liu, and Yan Wang. 750 GeV Diphoton Excess from Cascade Decay. 2015, 1512.06732.

[160] Jonathan J. Heckman. 750 GeV Diphotons from a D3-brane. *Nucl. Phys.*, B906:231–240, 2016, 1512.06773.

[161] Xiao-Jun Bi, Qian-Fei Xiang, Peng-Fei Yin, and Zhao-Huan Yu. The 750 GeV diphoton excess at the LHC and dark matter constraints. *Nucl. Phys.*, B909:43–64, 2016, 1512.06787.

[162] Jong Soo Kim, Krzysztof Rolbiecki, and Roberto Ruiz de Austri. Model-independent combination of diphoton constraints at 750 GeV. *Eur. Phys. J.*, C76(5):251, 2016, 1512.06797.

[163] Laure Berthier, James M. Cline, William Shepherd, and Michael Trott. Effective interpretations of a diphoton excess. *JHEP*, 04:084, 2016, 1512.06799.

[164] James M. Cline and Zuowei Liu. LHC diphotons from electroweakly pair-produced composite pseudoscalars. 2015, 1512.06827.

[165] Martin Bauer and Matthias Neubert. Flavor anomalies, the 750 GeV diphoton excess, and a dark matter candidate. *Phys. Rev.*, D93(11):115030, 2016, 1512.06828.

[166] Mikael Chala, Michael Duerr, Felix Kahlhoefer, and Kai Schmidt-Hoberg. Tricking LandauYang: How to obtain the diphoton excess from a vector resonance. *Phys. Lett.*, B755:145–149, 2016, 1512.06833.

[167] Sofiane M. Boucenna, Stefano Morisi, and Avelino Vicente. The LHC diphoton resonance from gauge symmetry. *Phys. Rev.*, D93(11):115008, 2016, 1512.06878.

[168] P. S. Bhupal Dev and Daniele Teresi. Asymmetric dark matter in the Sun and diphoton excess at the LHC. *Phys. Rev.*, D94(2):025001, 2016, 1512.07243.

[169] Jorge de Blas, Jose Santiago, and Roberto Vega-Morales. New vector bosons and the diphoton excess. *Phys. Lett.*, B759:247–252, 2016, 1512.07229.

[170] Christopher W. Murphy. Vector Leptoquarks and the 750 GeV Diphoton Resonance at the LHC. *Phys. Lett.*, B757:192–198, 2016, 1512.06976.

[171] A. E. Crcamo Hernndez and Ivan Niandi. LHC diphoton resonance at 750 GeV as an indication of $SU(3)_L \times U(1)_X$ electroweak symmetry. *Eur. Phys. J.*, C76(7):380, 2016, 1512.07165.

[172] Ujjal Kumar Dey, Subhendra Mohanty, and Gaurav Tomar. 750 GeV resonance in the dark leftright model. *Phys. Lett.*, B756:384–389, 2016, 1512.07212.

[173] Giulio Maria Pelaggi, Alessandro Strumia, and Elena Vigiani. Trinification can explain the di-photon and di-boson LHC anomalies. *JHEP*, 03:025, 2016, 1512.07225.

[174] Alexander Belyaev, Giacomo Cacciapaglia, Haiying Cai, Thomas Flacke, Alberto Parolini, and Hugo Serdio. Singlets in composite Higgs models in light of the LHC 750 GeV diphoton excess. *Phys. Rev.*, D94(1):015004, 2016, 1512.07242.

[175] Wei-Chih Huang, Yue-Lin Sming Tsai, and Tzu-Chiang Yuan. Gauged Two Higgs Doublet Model confronts the LHC 750 GeV diphoton anomaly. *Nucl. Phys.*, B909:122–134, 2016, 1512.07268.

[176] Qing-Hong Cao, Shao-Long Chen, and Pei-Hong Gu. Strong CP Problem, Neutrino Masses and the 750 GeV Diphoton Resonance. 2015, 1512.07541.

[177] Jiayin Gu and Zhen Liu. Physics implications of the diphoton excess from the perspective of renormalization group flow. *Phys. Rev.*, D93(7):075006, 2016, 1512.07624.

[178] Ketan M. Patel and Pankaj Sharma. Interpreting 750 GeV diphoton excess in SU(5) grand unified theory. *Phys. Lett.*, B757:282–288, 2016, 1512.07468.

[179] Marcin Badziak. Interpreting the 750 GeV diphoton excess in minimal extensions of Two-Higgs-Doublet models. *Phys. Lett.*, B759:464–470, 2016, 1512.07497.

[180] Sabyasachi Chakraborty, Amit Chakraborty, and Sreerup Raychaudhuri. Diphoton resonance at 750 GeV in the broken R-symmetric MSSM. *Phys. Rev.*, D94(3):035014, 2016, 1512.07527.

[181] Wolfgang Altmannshofer, Jamison Galloway, Stefania Gori, Alexander L. Kagan, Adam Martin, and Jure Zupan. 750 GeV diphoton excess. *Phys. Rev.*, D93(9):095015, 2016, 1512.07616.

[182] Mirjam Cveti, James Halverson, and Paul Langacker. String Consistency, Heavy Exotics, and the 750 GeV Diphoton Excess at the LHC. 2015, 1512.07622.

[183] B. C. Allanach, P. S. Bhupal Dev, S. A. Renner, and Kazuki Sakurai. 750 GeV diphoton excess explained by a resonant sneutrino in R-parity violating supersymmetry. *Phys. Rev.*, D93(11):115022, 2016, 1512.07645.

[184] Hooman Davoudiasl and Cen Zhang. 750 GeV messenger of dark conformal symmetry breaking. *Phys. Rev.*, D93(5):055006, 2016, 1512.07672.

[185] Kasinath Das and Santosh Kumar Rai. 750 GeV diphoton excess in a U(1) hidden symmetry model. *Phys. Rev.*, D93(9):095007, 2016, 1512.07789.

[186] Kingman Cheung, P. Ko, Jae Sik Lee, Jubin Park, and Po-Yan Tseng. Higgs precision study of the 750 GeV diphoton resonance and the 125 GeV standard model Higgs boson with Higgs-singlet mixing. 2015, 1512.07853.

[187] Nathaniel Craig, Patrick Draper, Can Kilic, and Scott Thomas. Shedding Light on Diphoton Resonances. *Phys. Rev.*, D93(11):115023, 2016, 1512.07733.

[188] Jia Liu, Xiao-Ping Wang, and Wei Xue. LHC diphoton excess from colorful resonances. 2015, 1512.07885.

[189] Jue Zhang and Shun Zhou. Electroweak Vacuum Stability and Diphoton Excess at 750 GeV. *Chin. Phys.*, C40(8):081001, 2016, 1512.07889.

[190] J. A. Casas, J. R. Espinosa, and J. M. Moreno. The 750 GeV Diphoton Excess as a First Light on Supersymmetry Breaking. *Phys. Lett.*, B759:159–165, 2016, 1512.07895.

[191] Lawrence J. Hall, Keisuke Harigaya, and Yasunori Nomura. 750 GeV Diphotons: Implications for Supersymmetric Unification. *JHEP*, 03:017, 2016, 1512.07904.

[192] Jong-Chul Park and Seong Chan Park. Indirect signature of dark matter with the diphoton resonance at 750 GeV. 2015, 1512.08117.

[193] Alberto Salvio and Anupam Mazumdar. Higgs Stability and the 750 GeV Diphoton Excess. *Phys. Lett.*, B755:469–474, 2016, 1512.08184.

[194] Gang Li, Ying-nan Mao, Yi-Lei Tang, Chen Zhang, Yang Zhou, and Shouhua Zhu. Pseudoscalar Decaying Only via Loops as an Explanation for the 750 GeV Diphoton Excess. *Phys. Rev. Lett.*, 116(15):151803, 2016, 1512.08255.

[195] Minho Son and Alfredo Urbano. A new scalar resonance at 750 GeV: Towards a proof of concept in favor of strongly interacting theories. *JHEP*, 05:181, 2016, 1512.08307.

[196] Haipeng An, Clifford Cheung, and Yue Zhang. Broad Diphotons from Narrow States. 2015, 1512.08378.

[197] Fei Wang, Wenyu Wang, Lei Wu, Jin Min Yang, and Mengchao Zhang. Interpreting 750 GeV diphoton resonance as degenerate Higgs bosons in NMSSM with vector-like particles. 2015, 1512.08434.

[198] Qing-Hong Cao, Yandong Liu, Ke-Pan Xie, Bin Yan, and Dong-Ming Zhang. Diphoton excess, low energy theorem, and the 331 model. *Phys. Rev.*, D93(7):075030, 2016, 1512.08441.

[199] Jun Gao, Hao Zhang, and Hua Xing Zhu. Diphoton excess at 750 GeV: gluongluon fusion or quarkantiquark annihilation? *Eur. Phys. J.*, C76(6):348, 2016, 1512.08478.

[200] Florian Goertz, Jernej F. Kamenik, Andrey Katz, and Marco Nardecchia. Indirect Constraints on the Scalar Di-Photon Resonance at the LHC. *JHEP*, 05:187, 2016, 1512.08500.

[201] P. S. Bhupal Dev, Rabindra N. Mohapatra, and Yongchao Zhang. Quark Seesaw, Vectorlike Fermions and Diphoton Excess. *JHEP*, 02:186, 2016, 1512.08507.

[202] Junjie Cao, Liangliang Shang, Wei Su, Fei Wang, and Yang Zhang. Interpreting The 750 GeV Diphoton Excess Within Topflavor Seesaw Model. 2015, 1512.08392.

[203] Chengfeng Cai, Zhao-Huan Yu, and Hong-Hao Zhang. 750 GeV diphoton resonance as a singlet scalar in an extra dimensional model. *Phys. Rev.*, D93(7):075033, 2016, 1512.08440.

[204] Jihn E. Kim. Is an axizilla possible for di-photon resonance? *Phys. Lett.*, B755:190–195, 2016, 1512.08467.

[205] Wei Chao. Neutrino Catalyzed Diphoton Excess. 2015, 1512.08484.

[206] Luis A. Anchordoqui, Ignatios Antoniadis, Haim Goldberg, Xing Huang, Dieter Lust, and Tomasz R. Taylor. 750 GeV diphotons from closed string states. *Phys. Lett.*, B755:312–315, 2016, 1512.08502.

[207] N. Bizot, S. Davidson, M. Frigerio, and J. L. Kneur. Two Higgs doublets to explain the excesses $pp \to \gamma\gamma(750\text{ GeV})$ and $h \to \tau^{\pm}\mu^{\mp}$. *JHEP*, 03:073, 2016, 1512.08508.

[208] Luis E. Ibanez and Victor Martin-Lozano. A Megaxion at 750 GeV as a First Hint of Low Scale String Theory. *JHEP*, 07:021, 2016, 1512.08777.

[209] Xian-Jun Huang, Wei-Hong Zhang, and Yu-Feng Zhou. A 750 GeV dark matter messenger at the Galactic Center. *Phys. Rev.*, D93:115006, 2016, 1512.08992.

[210] Cheng-Wei Chiang, Masahiro Ibe, and Tsutomu T. Yanagida. Revisiting Scalar Quark Hidden Sector in Light of 750-GeV Diphoton Resonance. *JHEP*, 05:084, 2016, 1512.08895.

[211] Sin Kyu Kang and Jeonghyeon Song. Top-phobic heavy Higgs boson as the 750 GeV diphoton resonance. *Phys. Rev.*, D93(11):115012, 2016, 1512.08963.

[212] Shinya Kanemura, Kenji Nishiwaki, Hiroshi Okada, Yuta Orikasa, Seong Chan Park, and Ryoutaro Watanabe. LHC 750 GeV Diphoton excess in a radiative seesaw model. 2015, 1512.09048.

[213] Ian Low and Joseph Lykken. Implications of Gauge Invariance on a Heavy Diphoton Resonance. *Submitted to: Phys. Rev. Lett.*, 2015, 1512.09089.

[214] A. E. Crcamo Hernndez. A novel and economical explanation for SM fermion masses and mixings and its connection with the 750 GeV diphoton excess. 2015, 1512.09092.

[215] Kunio Kaneta, Subeom Kang, and Hye-Sung Lee. Diphoton excess at the LHC Run 2 and its implications for a new heavy gauge boson. 2015, 1512.09129.

[216] Arnab Dasgupta, Manimala Mitra, and Debasish Borah. Minimal Left-Right Symmetry Confronted with the 750 GeV Di-photon Excess at LHC. 2015, 1512.09202.

[217] S. F. King, S. Moretti, and R. Nevzorov. Exceptional supersymmetric standard model. *Phys. Lett.*, B634:278–284, 2006, hep-ph/0511256.

[218] R. Howl and S. F. King. Minimal E(6) Supersymmetric Standard Model. *JHEP*, 01:030, 2008, 0708.1451.

[219] Jonathan P. Hall and Stephen F. King. NMSSM+. *JHEP*, 01:076, 2013, 1209.4657.

[220] Abdelhak Djouadi. The Anatomy of electro-weak symmetry breaking. I: The Higgs boson in the standard model. *Phys. Rept.*, 457:1–216, 2008, hep-ph/0503172.

[221] Abdelhak Djouadi, John Ellis, Rohini Godbole, and Jrmie Quevillon. Future Collider Signatures of the Possible 750 GeV State. *JHEP*, 03:205, 2016, 1601.03696.

[222] Savas Dimopoulos and Lawrence J. Hall. Lepton and Baryon Number Violating Collider Signatures from Supersymmetry. *Phys. Lett.*, B207:210–216, 1988.

[223] Federico Carta, Fernando Marchesano, Wieland Staessens, and Gianluca Zoccarato. Open string multi-branched and Kahler potentials. 2016, 1606.00508.

[224] Graham Ross and Mario Serna. Unification and fermion mass structure. *Phys. Lett.*, B664:97–102, 2008, 0704.1248.

[225] B. C. Allanach, A. Dedes, and Herbert K. Dreiner. Bounds on R-parity violating couplings at the weak scale and at the GUT scale. *Phys. Rev.*, D60:075014, 1999, hep-ph/9906209.

[226] B. C. Allanach, A. Dedes, and H. K. Dreiner. R parity violating minimal supergravity model. *Phys. Rev.*, D69:115002, 2004, hep-ph/0309196. [Erratum: Phys. Rev.D72,079902(2005)].

[227] Eung Jin Chun, Sunghoon Jung, Hyun Min Lee, and Seong Chan Park. Stop and Sbottom LSP with R-parity Violation. *Phys. Rev.*, D90:115023, 2014, 1408.4508.

[228] Frank F. Deppisch, Martin Hirsch, and Heinrich Pas. Neutrinoless Double Beta Decay and Physics Beyond the Standard Model. *J. Phys.*, G39:124007, 2012, 1208.0727.

[229] H. K. Dreiner, M. Hanussek, and S. Grab. Bounds on R-parity Violating Couplings at the Grand Unification Scale from Neutrino Masses. *Phys. Rev.*, D82:055027, 2010, 1005.3309.

[230] Vardan Khachatryan et al. Searches for R-parity-violating supersymmetry in pp collisions at sqrt(s)=8 TeV in final states with 0-4 leptons. *Submitted to: Phys. Rev. D*, 2016, 1606.08076.

[231] Georges Aad et al. Summary of the searches for squarks and gluinos using $\sqrt{s} = 8$ TeV pp collisions with the ATLAS experiment at the LHC. *JHEP*, 10:054, 2015, 1507.05525.

[232] Georges Aad et al. ATLAS Run 1 searches for direct pair production of third-generation squarks at the Large Hadron Collider. *Eur. Phys. J.*, C75(10):510, 2015, 1506.08616. [Erratum: Eur. Phys. J.C76,no.3,153(2016)].